STUDYING A CONTRACTILE ACTOMYOSIN NETWORK UNDERLYING LARVAL EPITHELIAL CELL BEHAVIOUR COORDINATION DURING DROSOPHILA ABDOMINAL MORPHOGENESIS

Pau Pulido Companys

A Thesis Submitted for the Degree of PhD
at the
University of St Andrews

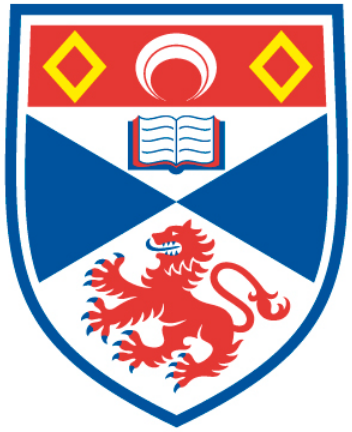

2018

Studying a contractile actomyosin network underlying larval epithelial cell behaviour coordination during *Drosophila* abdominal morphogenesis

Pau Pulido Companys

A thesis submitted for the degree of Phd

at the

University of St Andrews

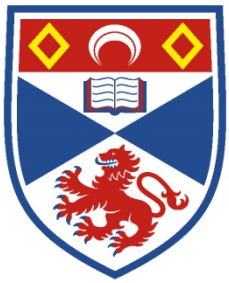

University of
St Andrews

2018

Abstract

During animal development, cells undergo various behaviours, such as migration and shape change, which need to be coordinated. How this coordination is achieved is still elusive. During morphogenesis of the adult abdominal epidermis of *Drosophila*, the larval epithelial cells (LECs) are replaced by the adult histoblasts. The LECs migrate directedly and, subsequently, cease migration, constrict apically and die. Here, I use *in vivo* 4D microscopy to study the spatial and temporal organisation of the actomyosin cytoskeleton of LECs as a potential mechanism to coordinate migration and apical constriction. The analysis of LECs apical actomyosin network shows that are planar polarized during migration, undergoing pulsed contractions in the back of the cell, while protruding at the front. During constriction, the cytoskeleton of LECs displays radial polarity with contractions localising in the centre of the cell. Behavioural change, thus, involves a change in the polarity of the contractile network. The properties of the contractile network are further studied manipulating actomyosin contractility by interfering with Rho kinase and Myosin phosphatase. The results show that the regulation of Myosin activation not only impacts on the contractility of the network but also on the network's dynamics and the cell's behaviour. A loss-of-function analysis of several Rho-GEFs, the activators of the Rho GTPases, is performed to study the molecular mechanisms that underlie the behavioural change. The depletion of individual RhoGEFs identifies 5 genes involved in the regulation of specific aspects of cell migration and the apical constriction of LECs. Altogether, the results suggest that cytoskeletal architecture and autonomous network dynamics underlie the behaviour of the contractile network. The results furthermore suggest that pulsed contractions, along with the cortical actomyosin network, underlie behavioural change, being one of the force generation mechanisms that orchestrate abdominal morphogenesis.

Candidate's declaration

I, **Pau Pulido Companys**, hereby certify that this thesis, which is approximately 47.000 words, has been written by me, and that it is the record of work carried out by me, or principally by myself in collaboration with others as acknowledged, and that it has not been submitted in any previous application for a higher degree. I was admitted as a research student in November 2013 as a candidate for the degree of Doctor Of Philosophy (PhD) in Cell Biology; the higher study for which this is a record was carried out in the University of St Andrews between 2013 and 2017.

Date ……. Signature of candidate …….

Supervisor's declaration

I hereby certify that the candidate has fulfilled the conditions of the Resolution and Regulations appropriate for the degree of Doctor of Philosophy (PhD) in Cell Biology in the University of St Andrews and that the candidate is qualified to submit this thesis in application for that degree.

Date ……Signature of supervisor ……

Dr Marcus Bischoff

Permission for publication

In submitting this thesis to the University of St Andrews I understand that I am giving permission for it to be made available for use in accordance with the regulations of the University Library for the time being in force, subject to any copyright vested in the work not being affected thereby. I also understand that the title and the abstract will be published, and that a copy of the work may be made and supplied to any bona fide library or research worker, that my thesis will be electronically accessible for personal or research use unless exempt by award of an embargo as requested below, and that the library has the right to migrate my thesis into new electronic forms as required to ensure continued access to the thesis. I have obtained any third-party copyright permissions that may be required in order to allow such access and migration, or have requested the appropriate embargo below.

The following is an agreed request by candidate and supervisor regarding the publication of this thesis:

PRINTED COPY

Embargo on all or part of print copy for a period of 2 years on the following ground:

- Publication would preclude future publication

ELECTRONIC COPY

Embargo on all or part of electronic copy for a period of 2 years on the following ground:

- Publication would preclude future publication

ABSTRACT AND TITLE EMBARGOES

a) I agree to the title and abstract being published NO
b) I require an embargo on abstract YES
c) I require an embargo on title NO

Date ……..Signature of candidate …….

Pau Pulido Companys

Date ……..Signature of supervisor…….

Dr Marcus Bischoff

Acknowledgements

There are so many people to thank and that have been essential in this. Firstly, thanks Marcus. Thanks for all the help and support during these years in the lab and during the writing of this thesis, without you none of this would have been possible. Secondly, I would like to thank the members of the Bischoff lab, Anneliese, Stefania and Jill, for your help during my time in the lab, for the discussions, advice and support. Also, thanks to Carl Donovan for providing the bootstrap code used for the statistical analysis and Claudia Faustino for helping me in using the code.

Thanks to all the people with whom I have shared offices, coffees and lunch breaks. You have made it much more fun.

Last but not least, I want to thank Fra, Malika, Mikel, Aurora, Karim, Carla and all the other members of my Dundonian family. To Lucía and Iosu, thank you for being there all these years. To my family, thank you for encouraging me and giving me the strength to continue. To Raisa, for always believing in me and helping me through the most difficult of times. I would not have made it without you. I cannot thank you enough.

Table of contents

List of figures

List of Tables

Abbreviations

Abl	Abelson
AJs	Adherens Junctions
A-P	Anterior-Posterior
Dia	Diaphanous
Dpp	Decapentaplegic
Ds	Dachsous
D-V	Dorsal-Ventral
E-cad	E-cadherin
ELC	Essential light chain
Ena	Enabled
Fog	Folded Gastrulatio
GAP	Rho GTPase activating protein
GEF	Rho Guanine nucleotide exchange factor
Hb	Histoblasts
LEC(s)	Larval Epithelial Cell (s)
MBS	Myosin binding subunit
MLCK	Myosin light chain kinase
MLCP	Myosin light chain phosphatase
PCP	Planar cell polarity
RLC	Regulatory light chain
Rok	Rho associated kinase
RP	Relative Position
Sqh	Spaghetti squash

1. General introduction

The shape of the body of an organism arises from the behavior of cells during development. Cells migrate, change their shape, divide and die in an organised and coordinated manner. Shape then, is a direct consequence of regulated and coordinated cell behaviour, always in interaction with the tissue (Lecuit and Le Goff, 2007). The mechanisms that control individual cell behaviour have been extensively studied in many different systems, although less is known about how individual cells coordinate multiple behaviours. In this context, the present thesis aims to widen the knowledge on the mechanisms that individual cells use to coordinate multiple behaviours, using the morphogenesis of the *Drosophila* abdomen as a model system.

As an introduction, the following pages highlight the importance of collective cell behaviour in morphogenesis and the known mechanisms that control individual cell behaviour, putting emphasis on cell migration and apical constriction. Then, the abdominal morphogenesis of *Drosophila* is introduced as a model system, describing the most recent and important findings on the cellular behaviours and signalling pathways that drive this morphogenetic event. Finally, this introduction presents the aims and objectives of the thesis, which focus on the study of the organisation and regulation of the cytoskeleton as a cellular mechanism that helps in coordinating cellular behaviour during the development of the *Drosophila* abdomen.

1.1 Morphogenesis: the coordination of cell group behaviour

Morphogenesis is the process by which the shape of tissues, organs and organisms emerge. This process happens through the coordination of the behaviour of cell groups (Gilmour et al., 2017). The large number of studies on the morphogenesis of many different animals and organs has identified some conserved signalling pathways, common in many different morphogenetic systems, and also the general modes of action of such pathways during pattern formation. In general, the patterning information comes in the form of signals that trigger a response in cells. Cells interpret the molecular information from these signalling pathways and mechanically respond (Lecuit and Lenne, 2007), for instance, by altering their adhesiveness or orienting in

certain directions in order to create affinity gradients or polarised tissues, participating in the organism shaping (Lawrence, 2001). Despite the large number of specific molecules and signalling pathways that participate in the different animal systems described in the literature, cell group behaviour, and thus morphogenesis, is orchestrated by a small number of modular cellular properties, such as cell-cell adhesion, cell-matrix adhesion, protrusion, and contractility (Montell, 2008). The mechanisms that modulate these properties include the contractile actomyosin network and the adherens junctions (AJs), which facilitate cell-cell contact. The proteins that form the actomyosin cytoskeleton and AJs are expressed by all cells at all times, meaning that in order to determine the outcome of the morphogenetic event, they need to be tightly regulated (Gilmour et al., 2017).

Collective cell migration and apical constriction are two of the most important group behaviours displayed by cells in developing animals (Ewald et al., 2009; Friedl and Gilmour, 2009; Sawyer et al., 2010) and of special relevance to this thesis. Next a brief description of the role of these two collective behaviours in different morphogenetic processes is presented, concluding that in order for cells to migrate or constrict collectively, the production of force and maintenance of the cohesion of cells is required.

1.2 Collective cell migration and apical constriction in morphogenesis

The following description of multicellular migration and apical constriction focuses on the mechanisms that are common across the different animal systems and that are thought to drive collective cell behaviour.

Cell migration normally occurs as a response to an extracellular signal. In response, the cell needs to polarise, creating a front and a rear, protrude in the direction of migration and attach to the substratum to generate traction (Lauffenburger and Horwitz, 1996). In contrast to migration after epithelial-to-mesenchymal (EMT) transition, in which cells migrate exhibiting little cell-cell adhesion, there are several well-studied examples of collective cell migration in which cells remain in contact with each other (Montell, 2008). One example of collective migration is observed in the

adult ovary of *Drosophila*, during egg chamber development (Montell et al., 1992). The egg chamber is composed by follicle epithelial cells surrounding the germline cells. The cells of the anterior pole of the epithelium -the border cells- actively protrude and migrate towards the oocyte together, maintaining their cell-cell contacts to form a cluster (Figure 1A). Border cell migration is crucial for the development of a functional egg. Failure of the collective migration of border cells causes improper morphogenesis of the micropyle, the egg shell structure through which the sperm enters at fertilisation (Montell et al., 1992). Collective cell migration also occurs during the tracheal branching in the *Drosophila* embryo. Upon invagination, a subset of tracheal cells actively migrates, while the rest of the cells intercalate to elongate the tube (Figure 1B). During migration, tracheal cells remain attached to one another and the absence of the signal that triggers cell migration completely blocks movement and thus branching, suggesting that the collective migration of these cells plays a decisive role in the morphogenesis of the trachea (Affolter and Caussinus, 2008). Vertebrate embryos also exhibit collective cell movements. During the migration of the lateral line in zebrafish, a group of approximately 100 cells migrates down the length of the zebrafish embryo. Although most of the cells are actively motile, migration of the lateral line is led by small group of leader cells providing direction to the followers. Periodically, the migrating mass leaves a group of cells that stops moving, being left behind to form a sensory organ(Haas and Gilmour, 2006). Hence, in many vertebrate and invertebrate systems, collective cell migration drives the morphogenesis of different tissues and organs. In general, collective migration of cells involves the migration of some or all the cells involved, in most of the cases maintaining direct contact with others.

Cell migration is not the only multicellular behaviour observed during the development of tissues and organs. Collective cell shape changes, especially the coordinated apical constriction of a group of cells, can drive morphogenesis (Sawyer et al., 2010). The apical constriction of a group of cells requires the generation of tension at each individual cell junction level to increase local surface tension and reduce the cell apical area (Lecuit and Lenne, 2007). There are well studied examples in which the collective

apical constriction of cells is observed. One of the most representative is the bending and invagination of cells during *Drosophila melanogaster* gastrulation (Sawyer et al., 2010). Two major invaginations occur during gastrulation, the ventral furrow and the posterior midgut, in which the mesodermal and the posterior endodermal precursor cells are internalised (Turner and Mahowald, 1976). In both morphogenetic processes, apical constriction of the precursor cells is crucial for the formation of the furrow and invagination of the primordium (Sweeton et al., 1991) (Figure 1C). Tissue bending is also driven by apical constriction in vertebrates (Chung and Andrew, 2008). During the formation of the neural tube, a group of cells in the neuroepithelium apically constricts to bend the neural plate. This morphogenetic event depends on apical constriction and failure in neural tube closure causes congenital birth defects (Sawyer et al., 2010).

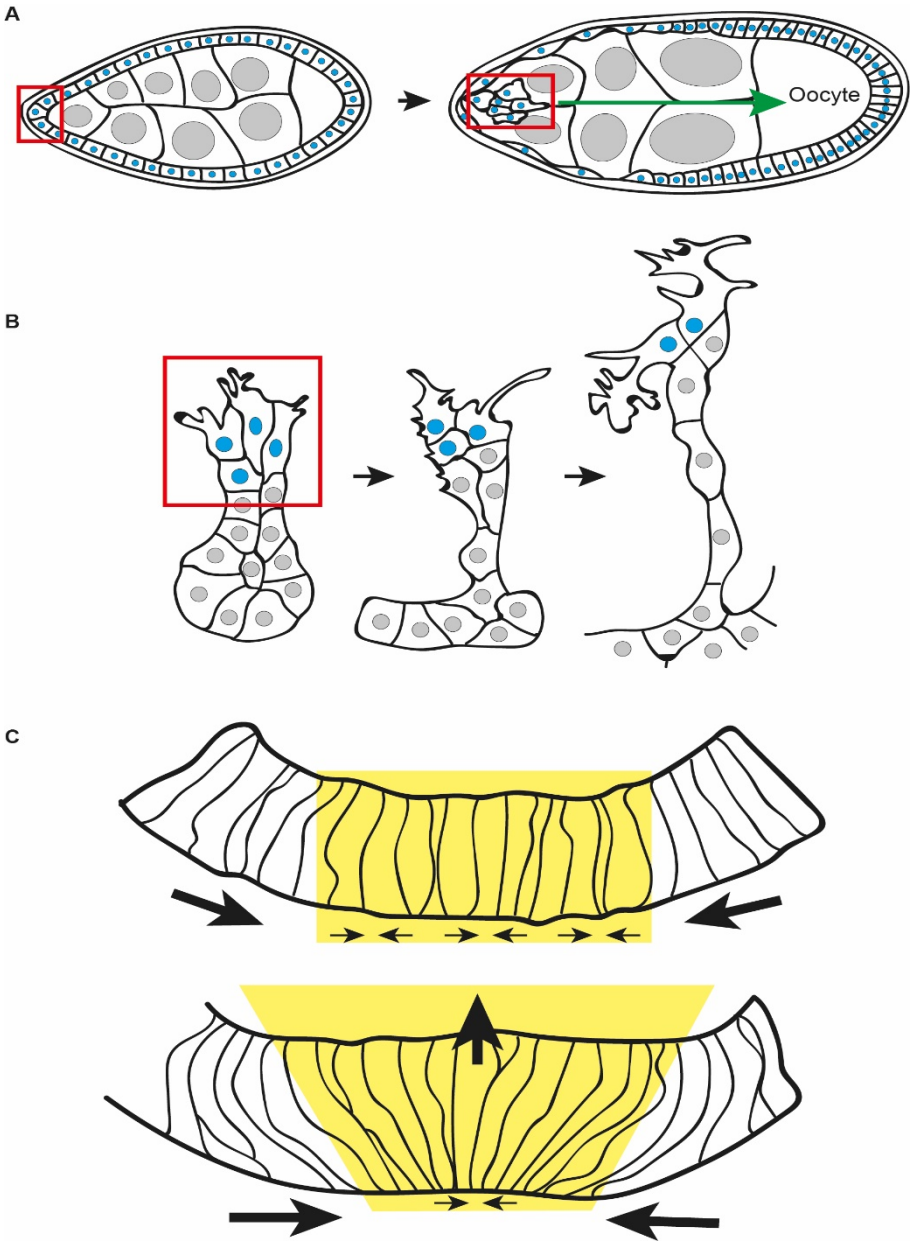

Figure 1. Collective cell behaviour drives different morphogenetic systems

Figure taken from (Montell, 2008) **A)** Schematic representation of the egg chamber development, with the posterior follicle cells (blue nuclei) surrounding the germline cells (grey nuclei). At stage 7 of development (left), follicle cells are uniformly shaped. At stage 9 (right), the anterior pole of follicle cells undergo collective migration (Montell, 2008). **B)** Schematic drawing of the developing *Drosophila* trachea at three time points. Cells at the tip (blue nuclei) exhibit membrane protrusions and migrate (Montell, 2008). **C)** Forces driving *Drosophila* ventral furrow invagination. The small arrows within the yellow box represent the vectors of forces that result from the apical constriction of cells (yellow box). Larger arrows indicate the forces that result from the combined forces of individual cells and which drive invagination (Sawyer et al., 2010).

In summary, the multicellular movements and shape changes are crucial for many morphogenetic events in different animal systems and ultimately are driven by single-cell behaviour in an interconnected tissue. Collective migration is driven by the polarised force created within the group, generated by the migration of individuals (Friedl and Gilmour, 2009). Apical constriction is driven by local forces that are transmitted between cells of a tissue through the junctions or through the extracellular matrix (Martin, 2010). Hence, multicellular movement and apical constriction depends on: (1) **force generation,** produced by the cytoskeleton, to drive single cell behaviour and (2) **cell adhesion,** relying mainly on the AJs, to transmit the local force through the tissue to combine the forces that drive morphogenesis. The following section describes the main proteins that form the cytoskeleton and the AJs as well as their common regulators across different animal systems, which are thought to control the activity of these proteins and drive collective cell migration and apical constriction.

1.3 Force generation: coordination of the cytoskeletal activity

Force generation depends on the contractile actomyosin network of cells. The actomyosin cytoskeleton of cells is mainly formed by the molecular motor type II Myosin (Myosin-II) and filamentous actin (F-actin) (Munjal and Lecuit, 2014). The regulation of the activity of the motor produces the force. The specific organisation of the supra-cellular actomyosin cytoskeleton determines the direction and extent of the force (Levayer and Lecuit, 2012). Thus, regulation of Myosin activation and control of the actomyosin network organisation are crucial for producing the different behaviours displayed by cells.

1.3.1 Molecular motors and their regulation

Myosin-II belongs to a super family of diverse proteins that all contain an actin and an ATP binding site in their catalytic head domains (Hartman and Spudich, 2012). In particular, Myosin-II is an hexamer composed of a pair of heavy chains, containing a catalytic head each, a pair of regulatory light chains (RLCs) and a pair of essential light chains (ELCs) (Bresnick, 1999) (Figure 2A). The activation of the motor activity depends

on the phosphorylation of certain residues within the RLC and is controlled by several kinases. Both Myosin Light Chain Kinase (MLCK) and Rho-associated kinase (Rok) have been shown to phosphorylate the RLC *in vitro* (Amano et al., 1996). At the same time, Myosin-II deactivation is mediated by the phosphatase (Figure 2B). Studies *in vitro* have shown that Myosin light chain phosphatase (MLCP) dephosphorylates the RLC (Hartshorne et al., 1998). The MLCP is a heterotrimer composed of the catalytic subunit, the Myosin-binding subunit (MBS) and a region of about 20 KDa whose function has not been identified (Hartshorne et al., 1998). MBS regulates the activity of the MLCP as a target of upstream signals. For instance, MBS is phosphorylated by Rok, inactivating the MLCP. *In vitro* assays also show that when Myosin-II is active, it forms bipolar filaments by the aggregation of dozens of Myosin molecules. Myosin filaments along with actin form the so-called contractile network. These bipolar Myosin filaments bind the actin filaments, pulling on them and generating force (Niederman and Pollard, 1975) (Figure 2C). The regulation of motor activity determines the magnitude of the force generated (Bendix et al., 2008).

In vivo, the impairment of Rok itself blocks morphogenetic processes during the embryonic development of invertebrates, such as ventral furrow formation in *Drosophila* (Barrett et al., 1997; Dawes-Hoang, 2005) or neural tube invagination in vertebrates (Hildebrand, 2005). MBS, the regulatory region of MLCP, has also been found to be important *in vivo* for the maintenance of the integrity of epithelial cells in *Drosophila* imaginal discs through the regulation of Myosin-II activity (Lee and Treisman, 2004; Mitonaka et al., 2007).

In summary, the experiments performed *in vivo,* which complement the in-depth studies performed *in vitro*, show that Rok and MBS are key molecules that regulate Myosin, the main motor that induces shape changes during morphogenesis (Quintin et al., 2008).

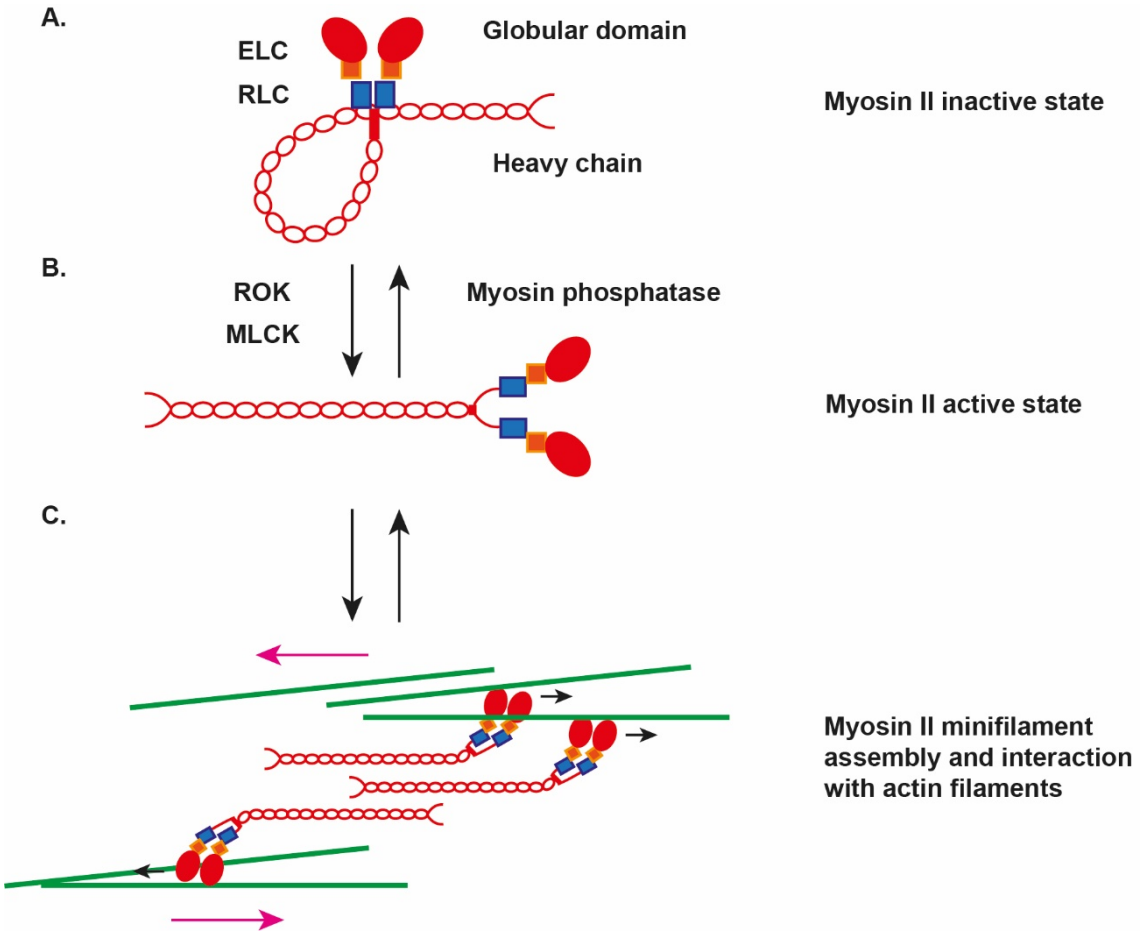

Figure 2. Biochemical pathways controlling Myosin-II activation and minifilament assembly.

Figure modified from Levayer & Lecuit 2012. **A)** Schematic representation of Myosin-II indicating the location of the regulatory light chain (RLC) and the essential light chain (ELC). **B)** The conformational change produced by the phosphorylation of RLC by the kinase Rok activates the motor. **C)** The activation induces the assembly of Myosin-II molecules into minifilaments and the association with actin filaments (green lines). When active, Myosin pulls on Actin, generating force. Pink arrows represent the sliding of the actin filaments.

1.3.2 The specific organisation of the actomyosin network

Myosin needs to be associated with a specific spatial organisation of actin in order to produce a protrusion and generate cell migration or reduce the apical area. This spatial organisation is achieved by the interplay of several proteins that regulate the organisation of the cytoskeleton. One of the most well-studied cytoskeletal regulators is the Rho GTPase family of proteins, which plays an important role as cytoskeletal regulators in polarity generation, cell shape changes or mesenchymal transitions (Aelst

and Symons, 2002). All these processes, involved in cytoskeleton reorganization and remodelling, depend on the cyclic activity of these proteins. GTPases are molecular switches that cycle between two conformational states: an active state, bound to GTP and an inactive state, bound to GDP. In the active state, GTPases recognize target proteins and generate response until GTP hydrolysis returns them to the inactive state. The proteins that regulate Rho GTPases activity are the Rho Guanine nucleotide exchange factors (RhoGEFs) and Rho GTPase activating proteins (RhoGAPs), which activate and deactivate corresponding GTPases, respectively (Etienne-Manneville and Hall, 2002) (Figure 3).

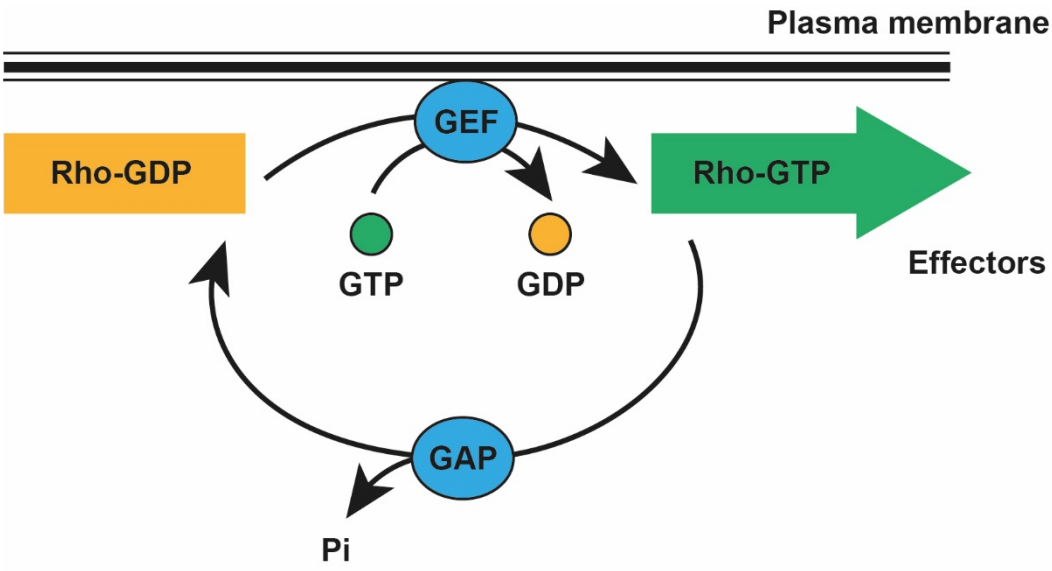

Figure 3. The Rho GTPase cycle

Figure modified from Etienne-Manneville & Hall 2002. Rho GTPases cycle between an active (GTP-bound) and an inactive (GDP-bound) conformation. In the active state, they interact with target proteins (effectors). The cycle is regulated by the nucleotide exchange factors (GEFs), which catalyse nucleotide exchange and mediate activation and the GTPase-activating proteins (GAPs), which stimulate GTP hydrolysis, leading to inactivation.

Different Rho GTPases and downstream effectors specifically organise the cytoskeleton, creating the structures required to produce a variety of cellular responses. Extensive studies using cultured tissues have shown that Rho regulates the assembly of contractile actomyosin structures (Ridley and Hall, 1992), whereas Rac and Cdc42 regulate the polymerisation and organisation of Actin to enable cell migration (Nobes and Hall, 1995; Ridley et al., 1992). All three GTPases are involved in the attachment of the cell to the extracellular matrix (Nobes and Hall, 1995). Below are described the common regulators that, downstream of Rho GTPases, organise the actomyosin network of a single cell during migration and apical constriction.

1.3.2.1 Actomyosin spatial organisation and its control during cell migration

A large number of studies *in vitro* have described the mechanism by which cells migrate and the molecules involved in the organisation of the cytoskeleton (Ridley, 2003; Ridley, 2011). In general, in response to a polarity cue, protrusion and especially lamellipodium formation are essential for cell migration. The lamellipodium, an actin projection of the leading edge of the cell, acts as a structure that pushes the cell forward during migration (Ridley, 2003). For this structure to be formed, actin polymerisation has to be regulated in order to form the actin filaments. Also, the actin filaments have to be branched and located near the leading edge. All these processes are controlled by several actin-binding proteins which interact with the Rho-GTPases to allow lamellipodium extension (Figure 4). A small protein called Profilin controls the pool of available actin for polymerisation. Profilin is responsible for polarized actin assembly, the polymerization of filaments in a specific direction and the inhibition of spontaneous filament polymerization in cultured cells (Pollard and Borisy, 2003). At the same time, actin monomer dissociation from the end of filaments is mediated by the ADF/cofilin family proteins (Pollard et al., 2000). The branch organization of the actin filaments is mediated by a complex called Arp2/3, which includes several actin related proteins (Welch and Mullins, 2002). This complex binds to existing actin filaments and induces the formation of branches. The activation of Arp2/3 is mediated by WASP/WAVE, a family of proteins responsible for the regulation of actin polymerization during the activation of the protrusive machinery. In vitro, WASP/WAVE proteins are recruited to the leading edge by Rac and Cdc42 GTPases. WASP/WAVE at the same time regulates as well the activity of Rac and Cdc42 by generating positive or negative feedback loops (Ridley, 2003; Welch and Mullins, 2002). For the formation of branches, cross-linking of the filaments is required and proteins like Filamin and α-Actinin create and stabilize the branched structure (Welch and Mullins, 2002). Other proteins are also involved in stabilising actin, such as Cortactin, which stabilizes branches by slowing actin network disassembly and increasing mechanical rigidity. Cell attachment is also crucial for migration to occur as the formed protrusions must be attached to a substratum. Attachment allows the

traction of the cell forward and involves the formation of focal adhesions, regulated by Rho, Rac and Cdc42, which serve as a mechanical linkage to the extracellular matrix (Ridley, 2003). Also, actomyosin contractility at the back of the cell, mediated by Rho, promotes movement of the body and facilitates detachment of the rear, contributing to cell migration (Mitchison and Cramer, 1996) (Figure 4).

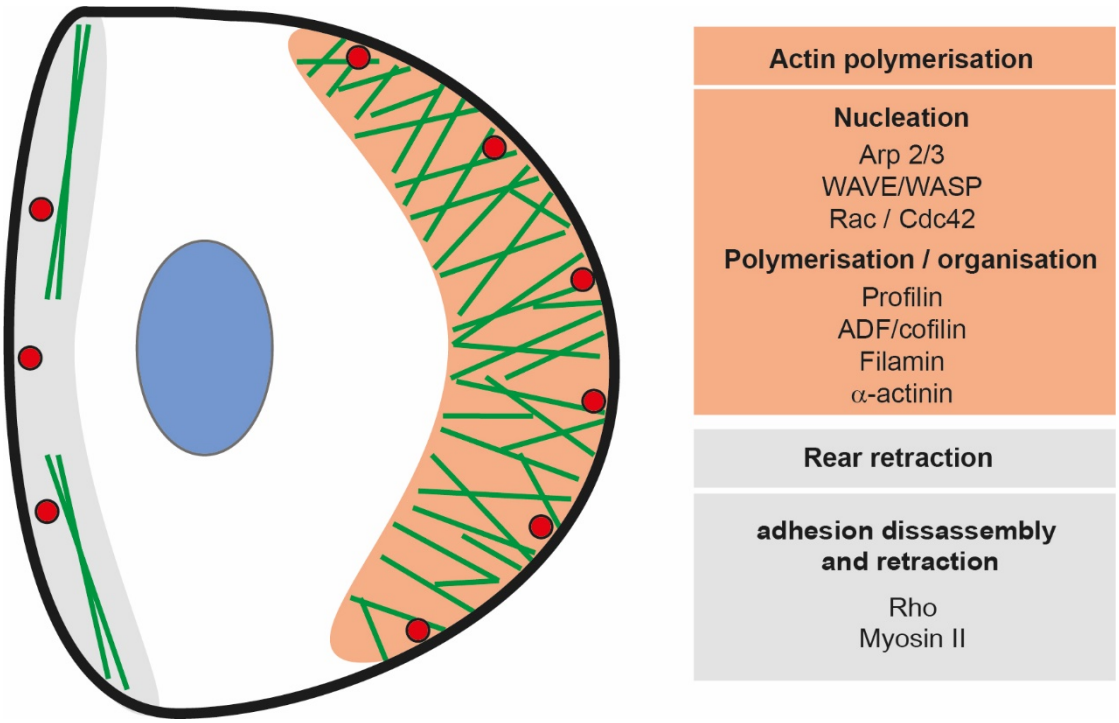

Figure 4. Schematic drawing of a migrating cell

Figure modified from Ridley 2003. In a migrating cell, WASP/ WAVE proteins are targets of Rac and Cdc42 and regulate the formation of actin branches on existing actin filaments by their action on the Arp2/3 complex. Actin polymerization (green lines), in turn, is regulated by proteins that control the availability of activated actin monomers, like Profilin, and debranching and depolymerizing proteins, like ADF/cofilin, as well proteins that stabilise the actin meshwork. Protrusions are also stabilized by the formation of adhesions (red dots). At the back of the cell, adhesions disassemble as the rear retracts.

Although the interactions at a molecular level are much more complex *in vivo*, great progress has been made in identifying the function of the Rho GTPases in both vertebrates and invertebrates during development. Border cell migration during *Drosophila* ovary development is one of the invertebrate morphogenetic systems in which the function of Rho GTPases has been extensively studied. Lamellipodium driven border cell migration requires the activation of Rac (Murphy and Montell, 1996) and, in fact, local activation of a photo-activatable analogue of Rac is sufficient to produce membrane ruffling and the migration of border cells (Wang et al., 2010). Lamellipodium formation in border cells requires cytoskeletal remodelling, which is controlled by proteins like Profilin, which promotes border cell protrusion by regulating actin polymerisation or Cofilin. The latter controls the pool of uncapped barbed ends to stimulate actin polymerisation at the leading edge (Chen et al., 2001; Knowles and Cooley, 1994; Verheyen and Cooley, 1994). The localisation of active Cofilin at the leading edge involves the interaction with Rac, although the mechanism of interaction are still elusive *in vivo* (Chen et al., 2001; Zhang et al., 2011). Crosslinkers, such as Filamin, are also required for protrusion and border cell migration (Sokol and Cooley, 2003). Cdc42 and Rho are required for maintaining the cohesion between border cells, as their knockdown causes clusters of cells to splay apart (Bastock and Strutt, 2007; Llense and Martín-Blanco, 2008). In other invertebrate systems in which individual cells can be observed migrating *in vivo*, such as the hemocytes during wound healing in *Drosophila* embryos, Cdc42 has been found to be important for chemotaxis and directed migration along with the function of Rac (Stramer et al., 2002). Rho has been found to be important for rear retraction from the matrix or cell contacts (Stramer et al., 2002; Wood et al., 2002).

In vertebrates, the study of collective cell migration *in vivo* also shows that cells maintain an intrinsically bipolar state, with the protruding leading edge oriented toward the ECM and the rear engaged with cell-cell connections to follower cells (Khalil and Friedl, 2010). During convergent extension movements during *Xenopus* gastrulation, cell movement is controlled by the cooperation of Rac and Rho to control the rate of the extension and retraction of cell protrusions (Tada and Heisenberg,

2012; Tahinci and Symes, 2003). Rac and Rho have also been found to be important to control branching during mammary gland formation, by initiating cell migration and maintaining cell cohesion, respectively (Ewald et al., 2009). Furthermore, studies in neural crest cell migration show that directional movement of cells requires the presence of higher levels of active Rac at the front of the cell and active Rho at the back (Clay and Halloran, 2013; Matthews et al., 2008; Theveneau et al., 2010). These observations show that front to back polarity linked to directional migration of neural crest cells is controlled by the localized activity of small GTPases (Mayor and Theveneau, 2014).

Rac and Cdc42 Rho GTPases also regulate individual cell migration *in vivo*. The Rac family of Rho GTPases has been found to control lamellipodial extension through the regulation of the actin cytoskeleton in mice. For instance, during neutrophil migration, different Rac molecules control the uncapping of existing actin filaments and the polymerisation of actin filaments through the activation of cofilin or ARP 2/3 (Li et al., 2018; Sun et al., 2007). Cdc42-null or Cdc42GAP-null leukocytes show alterations in recruitment to inflammatory sites *in vivo* (Szczur et al., 2018; Yang et al., 2007), but it is unknown whether these defects reflect changes to adhesion, migration or chemotaxis (Heasman and Ridley, 2008).

The function of the three main Rho isoforms - RhoA, RhoB and RhoC - present in vertebrates has been studied in mouse development and the results show that RhoB-null and RhoC-null mice are viable and have no major developmental defects in migration or cell survival. The results on RhoA-knockout mice have not been reported (Heasman and Ridley, 2008; Wheeler and Ridley, 2004).

In summary, the different Rho GTPases have conserved functions in both vertebrates and invertebrates. In general, cells migrating within a collective or on their own need to be polarised, creating a front and a rear (Khalil and Friedl, 2010; Ridley, 2003). This polarisation depends on the differential localisation of the different Rho GTPases; Rac and Cdc42 are active at the front and are important for directed migration and the formation of a lamellipodium in the direction of movement through the interaction with the cytoskeleton (Heasman and Ridley, 2008; Montell et al., 1992; Ridley, 2003;

Welch and Mullins, 2002). Rho has been shown to be essential for rear cell detachment in single migrating cells (Mitchison and Cramer, 1996), though it may be less important in cells moving together as sheets, where it is implicated in cell-cell cohesion (Raftopoulou and Hall, 2004). Many interesting questions remain unanswered and present opportunities for the future. Unravelling the crosstalk between Rho, Rac and Cdc42 and their specific localisation within the cell in this *in vivo* context may contribute significant new insights into the functions of these crucial regulators of protrusion, adhesion and contractility (Montell et al., 2012).

1.3.2.2 Actomyosin spatial organisation and its control during apical constriction

The extensive studies done *in vitro* and *in vivo* show that apical constriction requires the apical localization and activation of Myosin on an F-actin meshwork (Barrett et al., 1997; Dawes-Hoang, 2005; Nishimura and Takeichi, 2008). The commonly demonstrated mechanism involves the localisation of an actomyosin ring at cell junctions, the so called “purse string” mechanism. This tensile system increases cell surface tension through the increment of cortical tension, producing the reduction of cell apical area (Lecuit and Lenne, 2007). The contractile mechanism that drives apical constriction and its regulation appears to vary between organisms and between tissues (Sawyer et al., 2010), although this “purse string” mechanism has been shown to operate similarly in different systems (Figure 5). Next, there is a brief description of the most studied vertebrate and invertebrate systems in which this mechanism drives apical constriction and the common regulators that control it.

One of the most studied invertebrate systems used as a model for studying apical constriction is ventral furrow formation in *Drosophila*. In ventral furrow cells, as mentioned above, Rok is necessary for Myosin activation (Barrett et al., 1997; Dawes-Hoang, 2005). Rok is activated by a secreted receptor called Folded Gastrulation (Fog), which is found to be necessary to drive apical Myosin localization through the activation of RhoGEF2 and their downstream effectors Rho1 (Barrett et al., 1997; Dawes-Hoang, 2005). The transmembrane protein T48 also recruits RhoGEF2 to the apical site of ventral furrow cells to promote contractility (Kolsch et al., 2007). The

meshwork organization of actin in these cells is mediated by Abelson (Abl). Abl, a non-receptor tyrosine kinase, is required for actin to localize in the apical side of the ventral furrow cells (Fox and Peifer, 2007; Grevengoed et al., 2003). For this, Abl restricts the localization of Enabled (Ena) from the apical side of cells (Fox and Peifer, 2007), another actin regulator that binds directly to actin and allows continuous actin filament elongation (Barzik et al., 2005; Krause et al., 2002). Without Abl, Ena is inappropriately regulated and the formation of the actin contractile ring is prevented (Fox and Peifer, 2007). Diaphanous (Dia) is the only Diaphanous-related Formin in *Drosophila*, a family of actin nucleation and elongation regulators. Dia is activated by Rho in ventral furrow cells and is also implicated in the assembly of the actin filamentous network and Myosin activation at cell junctions (Homem and Peifer, 2008). Dia is proposed to be important in forming the actomyosin ring that is thought to produce apical constriction (Homem and Peifer, 2008) (Figure 5). Although presenting some differences, other morphogenetic systems in *Drosophila* share this mechanism of apical constriction. Eye morphogenetic furrow in *Drosophila* is formed by the constriction of the apical side of cells of the eye imaginal disc (Tomlinson, 1985). In this system, activation of Myosin-II is again mediated by Rok (Escudero et al., 2007). Dia is also involved in this morphogenetic event and is needed for apical accumulation of actin and Myosin stabilization, making it essential for apical constriction to take place (Corrigall et al., 2007). Rho 1 and Rok, have been shown to play an important role in other systems like *Drosophila* salivary gland morphogenesis, where cells from ectodermal placodes apically constrict and invaginate (Xu et al., 2008).

The general use of common proteins spans through many different animal systems, including vertebrates. Vertebrate neural tube formation shares some key proteins with the systems mentioned before. Studies in different vertebrate systems, including amphibians, showed that for normal neural tube formation, Rho, Rho kinase (ROCK) and the motor protein Myosin-IIB are required and localized apically (Kinoshita et al., 2008; Nishimura and Takeichi, 2008). Working together with the Rho-Rock pathway, the localisation of Myosin is mediated by Shroom, an actin binding protein that localises at apical junctions. Shroom co-localises with the apically positioned

actomyosin complex, which facilitates apical constriction during neural tube formation (Hildebrand, 2005). Other cytoskeleton regulators organise the distribution of the actin cytoskeleton, including Abl (Koleske et al., 1998) and Xena (Roffers-Agarwal et al., 2008), a homolog of Enabled, which are known to function in neural tube closure as well (Figure 5).

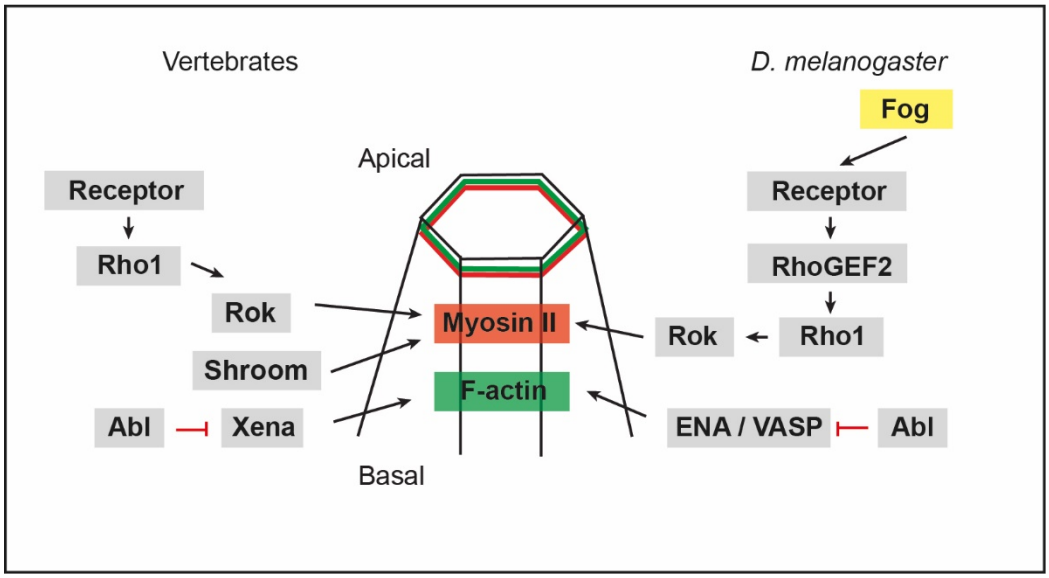

Figure 5. Apical constriction and its regulation in *Drosophila* and vertebrate neural tube morphogenesis

Figure modified from Lecuit & Lenne 2007. Apical constriction requires the formation of an apical contractile actomyosin network (red and green belt) that spans the junctional area in *Drosophila* and vertebrates. In flies, apical constriction involves the phosphorylation of Myosin-II, regulated by the activation of RhoGEF2, the Rho small GTPase Rho1 and Rho kinase (Rok). The ligand FOG activates this pathway via an unknown receptor. In vertebrates, an additional molecule Shroom acts in parallel to activate Myosin-II apically. The reorganization of actin filaments is mediated in flies and vertebrates by the kinase Abl.

Recent studies propose that, apart from the actomyosin ring underlying the AJs, other force generation mechanism contribute to apical constriction. The first study to propose this was performed during *Drosophila* gastrulation and argued that the apico-medial actomyosin pool of ventral furrow cells contributes to apical constriction by generating forces (Martin et al., 2009). This apico-medial actomyosin network, which

spans the whole apical side of cells, was found to be pulsatile, showing repeated rhythmical contractions of the actomyosin network that pull the adherens junctions (AJs) sites inwards (Martin et al., 2009). This study proposed a new model for apical constriction in which not only the cortical pool of actomyosin generates force to produce constriction, but both the medial and cortical actomyosin cytoskeleton work co-ordinately to drive apical constriction (Martin et al., 2009). Since this first study was published, pulsing of the actomyosin cytoskeleton has been observed in a great number of biological contexts and, although the mechanism that controls the pulsing of the cytoskeleton and its function in not fully understood, its appearance has been correlated with cell shape changes (Coravos et al., 2017; Gorfinkiel and Blanchard, 2011). In the third chapter of this thesis, I will review some of the most studied *in vivo* systems, in which pulsing has been observed and its proposed function during morphogenesis.

1.4 Cell-cell cohesion: Molecular basis of adhesion

If the organisation of the cytoskeleton is important for the shaping, contraction, and movement of cells, the regulation and assembly of the adherens junctions (AJs) are essential for the integrity of cells in a tissue, and thus for collective behaviour (Gumbiner, 1996; Nishimura and Takeichi, 2009). Especially important in epithelia, AJs help in translating the generated force by the cytoskeleton of singles cells into cell shape changes, maintaining at the same time the multicellular architecture, avoiding junction disruption and maintaining tissue integrity. AJs are mainly composed of cadherin adhesion receptors and associated proteins (Halbleib and Nelson, 2006; Nishimura and Takeichi, 2009). Cadherins, with epithelial E-cadherin (E-cad) the most studied, are transmembrane adhesion proteins that form bonds between adjacent cells (Cavey and Lecuit, 2009; Halbleib and Nelson, 2006). Also, the adhesions need to be stabilised to ensure tissue integrity and for that they need to interact with the actin cytoskeleton (Cavey and Lecuit, 2009). Following a model proposed by Nishimura & Takeichi 2009, the levels of adhesiveness and the interaction between AJs and the cytoskeleton are important to determine the collective behaviour of cells (Figure 6).

During collective cell migration in several in vivo systems, such as mammary gland branching in vertebrates (Ewald et al., 2009) and cancer models (Grünert et al., 2003), E-cad mediates cell interactions. To ensure cell motility but maintain tissue integrity, E-cad is downregulated during cell migration, maintaining a certain number of cell-cell junctions (Friedl and Gilmour, 2009). E-cad interaction with the cytoskeleton is mediated by members of the Armadillo-family proteins, such as p120-catenin, which plays a dual role in cell locomotion and cell-cell junction assembly. p120-catenin interacts with Cortactin, which activates Arp 2/3 to generate lamellipodium protrusions by regulating branched actin polymerisation. p120-catenin also binds cadherins to promote cell-cell junctions stability (Boguslavsky et al., 2007).

In non-migrating epithelia, the interaction of E-cad with the cytoskeleton involves proteins like β-catenin (β-cat) and α-catenin (α-cat) to facilitate the tethering of AJs with the actin filaments (Cavey and Lecuit, 2009; Cavey et al., 2008; Drees et al., 2012).

This interaction of the AJs with the actin cytoskeleton allow cadherins to transmit cortical forces generated by junctional actomyosin networks (Cavey et al., 2008; Costa et al., 1998; Martin et al., 2009). For apical constriction, actin needs to be organised into parallel actin bundles near the cell junction. Factors that promote branched actin polymerisation (Rac1, Arp 2/3) are depleted from the cell contact region (Yamada and Nelson, 2007) and regulators that promote unbranched F-actin elongation (Formins), are recruited to AJs (Kobielak et al., 2008). In *Drosophila*, Dia is recruited to cell contacts and is required for junction maintenance (Homem and Peifer, 2008). α-cat is thought to recruit Dia to the junctions (Cavey and Lecuit, 2009), as it also recruits its activator Rho 1 (Magie et al., 2002) while repressing Arp 2/3 (Drees et al., 2012), facilitating the transition to a parallel bundle meshwork. This meshwork organisation favours Myosin tension, which inhibits the formation of protrusions by alignment of actin filaments parallel to the cell membrane and stabilise junctions (Gloushankova et al., 1998). As the cell-cell contacts shrink or change during tissue morphogenesis, remodelling of the AJs is especially important for maintaining the dynamics of the epithelial monolayer. The remodelling of cell-contacts requires turnover of AJs components, achieved by the endocytosis of cadherins and recycling back to the same plasma membrane domain (Cavey and Lecuit, 2009; Souza-schorey, 2005).

Thus, the regulation of the level of the AJ components and the interplay with the actin cytoskeleton through the cadherin/catenin system provides a link to integrate the intracellular and intercellular forces that drive the different cell movements and cell shape changes required for tissue morphogenesis (Cavey and Lecuit, 2009; Nishimura and Takeichi, 2009) (Figure 6).

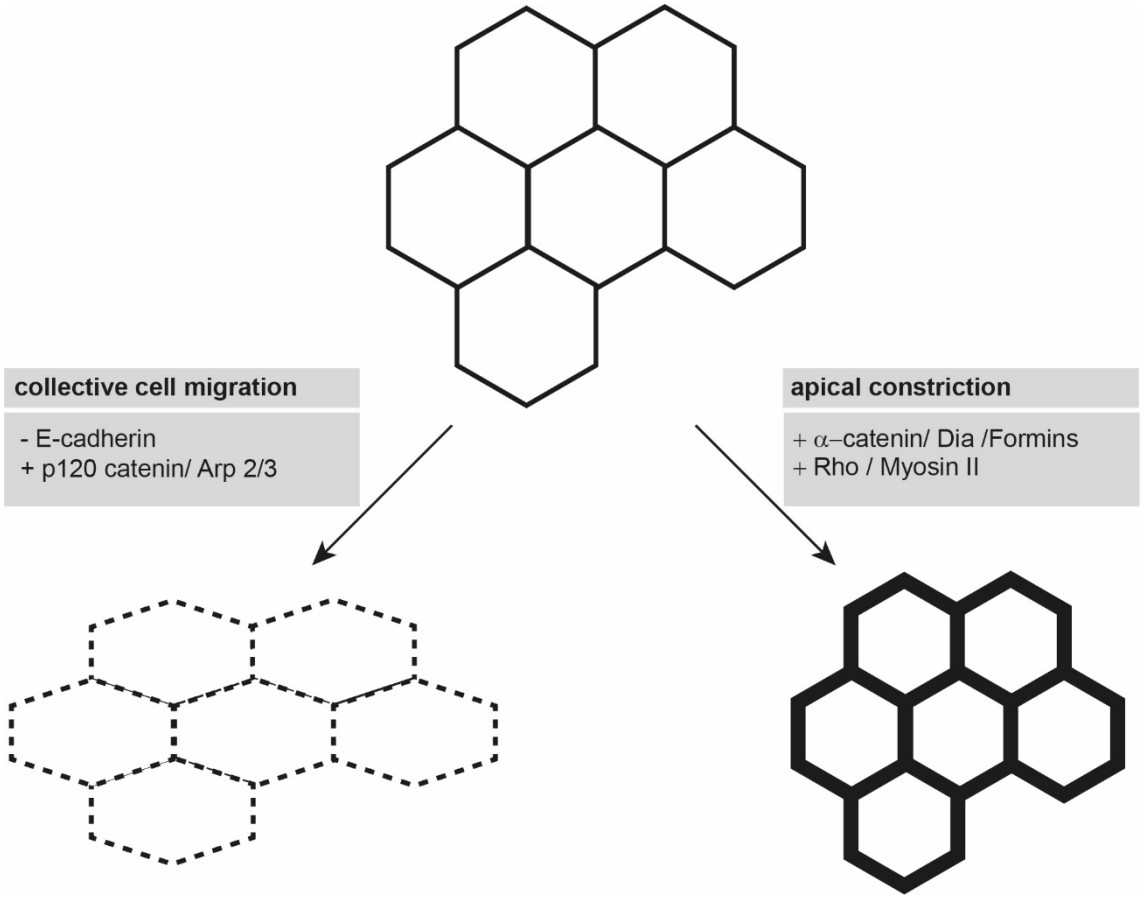

Figure 6. Collective cell behaviour depends on the interaction between the adherens junction and the cytoskeleton

Figure modified from Nishimura & Takeichi 2009. For cells to migrate collectively the levels of E-cadherin have to be down-regulated. The interaction between cadherins and the actin cytoskeleton is mediated by p120-catenin, promoting cell motility through the activation of Arp 2/3 and stabilising junctions. Apical constriction of a collective group of cells requires the stabilisation of the AJs through the interaction between the actomyosin cytoskeleton and cadherins. Mediated by α-catenin, the organisation of the actomyosin cytoskeleton into parallel bundles reinforces adhesion and maintains cortical tension.

1.5 The importance of coordinated cell behaviour in morphogenesis

As described above, a lot is known about the fundamental cell behaviours that drive the formation of organisms and the cellular mechanisms that produce them. However, during most morphogenetic events, cells display multiple behaviours that must be coordinated to shape the organism. For instance, and considering the examples introduced above, the formation of the trachea of *Drosophila* requires the coordination of invagination with cell migration and intercalation (Affolter and Caussinus, 2008) and for the morphogenesis of the lateral line in *Zebrafish*, the coordination of migration with cell shape changes, to form the adult sensory organs (Aman and Piotrowski, 2011).

Not many studies focus on the cellular mechanisms underlying behaviour coordination. Moreover, although several studies have shown the function of different cytoskeletal regulators, such as the role of Rho GTPases in developmental processes and cell behaviour, more detailed analysis of the links between the Rho GTPases and the molecules with which they interact will be crucial for understanding how different cellular processes are coordinated during morphogenesis.

To this end, the abdominal morphogenesis of *Drosophila* offers an interesting possibility to study the coordination between migration and apical constriction.

1.5.1 The strengths of *Drosophila* as a system for *in vivo* analysis

Drosophila melanogaster is a genetically tractable organism that possesses many components of mammalian signalling pathways. It is inexpensive to keep in the lab and its fast life cycle allows quick experimentation. In addition, *Drosophila* has little genetic redundancy compared with vertebrates, making it ideal for the analysis of conserved gene functions. Moreover, loss-of-function genetics is specially efficient and versatile in flies, in contrast to the costly, complex and time consuming knock-out experiments in mice, for instance (Bae et al., 2012; Bier and Bodmer, 2004). Therefore, in *Drosophila*, genetic approaches can be easily applied to study the regulation of cellular behaviours, such as migration and cell shape changes.

1.5.2 *Drosophila* abdominal morphogenesis: A system to study collective cell migration and apical constriction

The development of the adult abdominal epidermis of *Drosophila* is one of the morphogenetic systems in which multiple cell behaviours need to be coordinated within a cell type, and is the model system chosen to study in this thesis.

The adult abdomen has eight abdominal segments and the epidermis is formed by cells descending from histoblasts (hb), imaginal cells specified during embryonic stages and organized in nests. Each adult abdominal segment contains two ventral and two dorsal histoblast nests, which remain quiescent during larval life (Mandaravally Madhavan and Schneiderman, 1977). The histoblasts become active during metamorphosis. The development of the adult epidermis of the abdomen consists of three kinds of morphogenetic processes occurring in the histoblasts and larval epithelial cells (LECs): (1) Increase in the number of cells of the histoblasts nests (proliferation) (2) Extrusion and programmed cell death among the LECs and the coordinated spreading and fusion of the histoblasts nests, replacing the dying LECs. (3) Differentiation of the histoblasts resulting in the formation of hairs, bristles, tendons for muscle attachment and secretion of the cuticle (Madhavan and Madhavan, 1980; Roseland and Schneiderman, 1979). Further studies have shown that LECs extrude from the epithelia by apical constriction and that interfering with both histoblast extension or LECs extrusion produce abnormal abdominal morphogenesis, suggesting that both processes are non-autonomous and coordinated (Ninov et al., 2007).

Recent studies have described in detail the behaviour of LECs during abdominal morphogenesis and found that their replacement is associated with cell movements and cell shape changes, making LECs optimal for studying the coexistence and coordination of cell migration and apical constriction (Bischoff 2012). In particular, throughout larval life, LECs are stationary epithelial cells. During metamorphosis LECs undergo a transition from stationary to migratory behaviour, changing their shape and becoming mobile (Figure 7A)(Bischoff 2012). LECs collectively migrate posteriorly by apical lamellipodia-like protrusions in the direction of movement. When approached by the histoblasts, some LECs turn and move dorsally towards the midline (Figure 7B).

LECs also constrict apically while they move towards the midline (Figure 7C). Thus, while the histoblast nests expand, the LECs undergo a coordination of collective cell movement, first posterior and then dorsal, while their apical surface shrinks to give space to the histoblasts, which meet at the midline at the end of the process, when LECs have delaminated and died (Figure 7D) (Bischoff 2012).

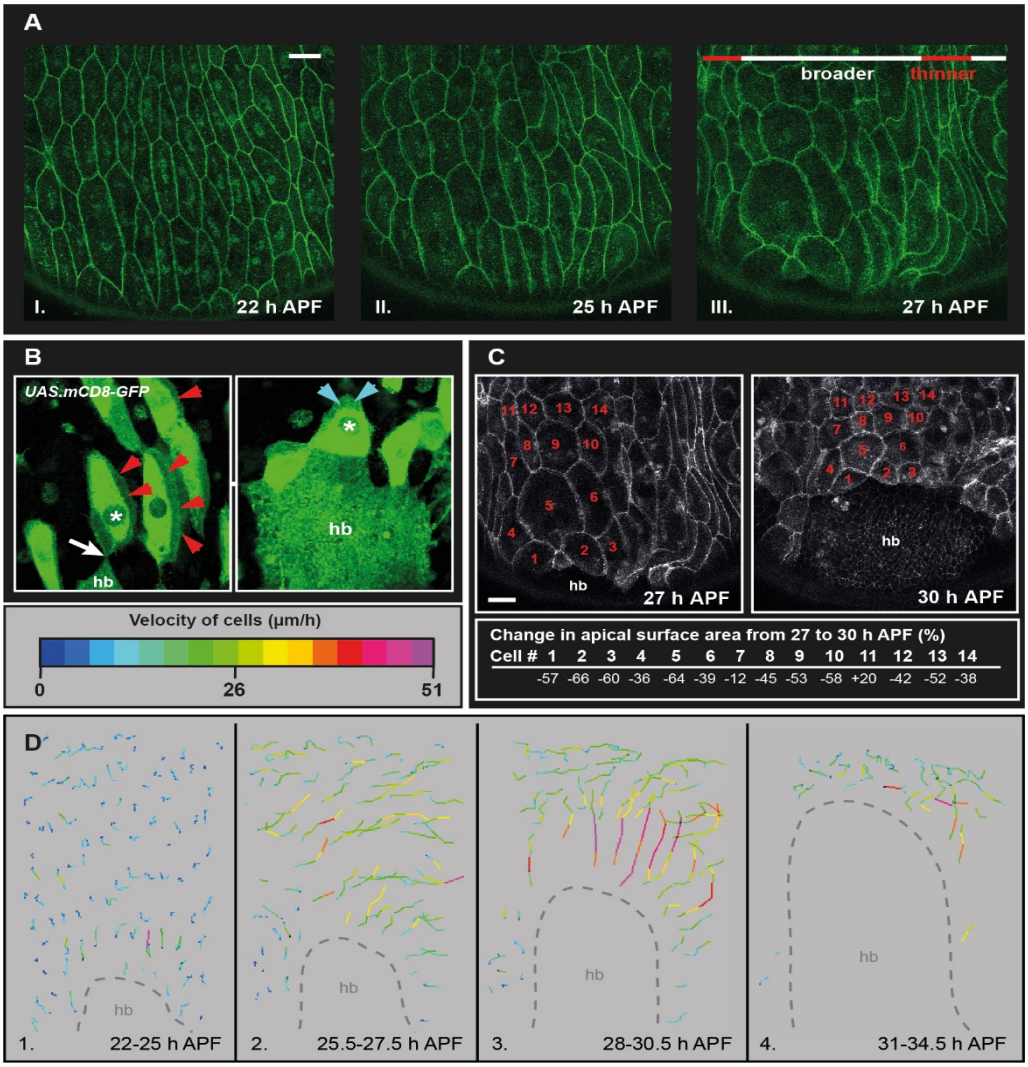

Figure 7. Shape changes and migrations of LECs.

Figure taken and modified from Bischoff 2012, published under CC BY license (https://creativecommons.org/licenses/by/3.0/). Pictures from Figures 1 and 2 were arranged to create one single figure. In all images, a hemisegment of segment A2 is shown. Anterior is to the left. Scale bars, 25 µm. Timing is calculated in hours after puparium formation (APF). **A)** LECs change shape before the onset of migration. LECs initially are more or less hexagonally shaped (I). Shortly before (II) and after the onset of migration (III) most cells in the centre of the segment become wider, whereas those at the segment boundaries become narrower. **B)** The LECs generate their protrusions in the direction of movement. Red arrow heads show posterior, blue arrowheads dorsal protrusions. The LEC marked with an asterisk repolarises when it is approached by the hb. **C)** While migrating, LECs also constrict apically. The pattern of LEC constriction is shown by displaying the change in surface area of some cells. **D)** Trajectories of LECs migration plotted by connecting the coordinates of a cell in 30-minute intervals with a line. The colour represents the velocity of the cells. 1. Beginning of hb spreading. 2. LECs move posteriorly. 3. LECs repolarise and move dorsally. 4. Final apical constriction of LECs before the hb of both hemisegments meet at the midline.

Histoblast nest expansion has been shown to be triggered by Decapentaplegic (Dpp) (Ninov et al., 2007). The migratory behaviour of LECs is also induced by Dpp signalling (Bischoff 2012). Planar cell polarity (PCP) signalling is involved in the directionality of migration in development, like in *Xenopus* neural crest cells (Carmona-Fontaine et al., 2008). LECs use the existing planar cell polarity (PCP) of the epithelium, which is mediated by the atypical cadherin Dachsous (Ds), to orient their posterior migrations (Bischoff 2012; Arata et al. 2017). How migratory cells stop protruding and start constricting seems to involve the activation of the small GTPase Rho1. Altering levels of Rho1 GTPase can bias the cell to display one behaviour or another, whereas Rho1 activation induces constriction, its down-regulation increases migratory behaviour (Figure 8) (Bischoff 2012). LEC migration together with apical constriction are required for normal closure of the adult epithelium (Bischoff 2012).

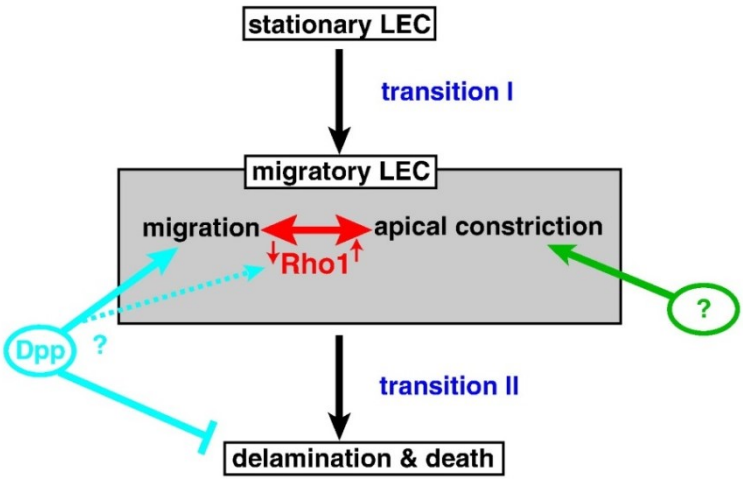

Figure 8. Model of the regulation of LEC behaviour during abdominal closure.

Figure taken from Bischoff 2012, published under CC BY license (https://creativecommons.org/licenses/by/3.0/). Signalling map of the regulation of LEC behaviour during abdominal closure. LECs undergo two transitions: I) transition from stationary to migratory behaviour, showing some aspects of EMT such as the down-regulation of cell–cell adhesion. II) After migration and constriction, the LECs undergo a second transition which leads to their delamination and death. Rho1 levels can bias cells towards migratory or constrictive behaviour. Dpp signalling stimulates migratory behaviour and promotes cell survival. The observation that both Rho1 and Dpp signalling can affect LEC motility might suggest that at least some aspects of Dpp-stimulated LEC motility might be mediated by Rho1.

1.6 Research aims and objectives

The goal of this thesis is to gain insights into the cellular mechanisms that allow the coordination of migration and apical constriction of LECs. As previously introduced in this first chapter, the collective behaviour of cells relies on the generation of local forces by the actomyosin cytoskeleton of cells. The cytoskeleton of LECs must be highly dynamic and tightly controlled to produce the specific organisation to coordinate multiple cellular behaviours. The dynamic control of LEC behaviour seems to depend on the levels of Rho1. Hence, the downstream cytoskeletal regulators in the Rho1 signalling pathway among others must play a crucial role in controlling the organisation of the actomyosin cytoskeleton in order to coordinate migration and apical constriction. Also, Rho GAPs and GEFs must be involved in the dynamic regulation of the levels of Rho and are the candidate upstream regulators of the signalling pathway that controls the organisation of the cytoskeleton and thus, the behaviour of the cell. In order to tackle this question, in the present thesis, I sought to address the regulation and organisation of the actomyosin contractile network that underlies the coordination of multiple cellular behaviours in LECs during the development of the abdomen in *Drosophila*.

The main aims of the thesis are as follows:

- To characterise the spatial and temporal organisation of the actomyosin cytoskeleton of LECs using 4D microscopy, while they migrate and apically constrict during abdominal morphogenesis.
- To evaluate the role of Rho associated Kinase (Rok) and Myosin phosphatase, as members of the conserved Rho1 signalling pathway, in regulating the dynamic activation of Myosin and the effect on cytoskeletal organisation and cell behaviour coordination.
- To analyse the effects of the loss of function of several Rho GEFs in the behaviour of LECs. The screen aims to identify candidate molecules that regulate the activity of Rho1 and other GTPases, observing and quantifying their effect on specific aspects of cell migration and apical constriction.

2 Materials and Methods

2.1 Genetic tools

2.1.1 Gal4/UAS system

This widely used genetic tool allows the expression of target genes selectively in a tissue of interest. To do that, this expression system has two parts: the GAL4 gene, encoding the yeast transcriptional factor, and the UAS (Upstream Activation Sequence), an enhancer to which GAL4 specifically binds to activate gene transcription. Both parts are kept in separate fly lines, so GAL4 only activates the transcription of the gene of interest, in which UAS has been previously introduced, in the progeny from mated lines. Having GAL4 under the control of a selected endogenous promoter allows the expression of the gene of interest in the specific cells in where the promoter is expressed (Brand and Perrimon, 1993).

2.1.2 Temporal control of Gal4 expression

The temporal expression of the UAS enhancer can be controlled using temperature sensitive promoters. Gal80 is an inhibitor of Gal4 that when expressed ubiquitously is able to inhibit Gal4 activity in *Drosophila* and exhibits no deleterious phenotypic effects (Lee and Luo, 1999). Gal80ts is a temperature sensitive mutant of Gal80. Gal80ts represses the expression of Gal4 in flies raised at the restrictive temperature (18 °C). The repression ceases when flies are shifted to the permissive temperature (29 °C) and the levels of expression of Gal4 can be comparable to the non Gal80ts controls (McGuire, 2003). Gal80ts was used to express genes of interest that are lethal when being expressed at embryonic and larval stages.

2.1.3 Generation of clones in the larval epithelial cells (LECs)

To express a gene of interest in the LECs during the pupal stage, clones were induced using the FLP-out technique (Struhl and Basler, 1993). This technique uses a site-specific recombinase, the yeast protein Flp, and the homologous target sites (FRTs) from the 2µ circle genome from yeast. The recombinase catalyses recombination between the FRTs in the 2µ mini-chromosome (Broach and Hicks, 1980). This flp-out-cassette is placed between the promoter and the sequence of interest. If the FRTs are

arranged as direct repeats, Flp-mediated recombination leads to excision of the DNA sequence lying between them and joining of the sequences on either side (Figure 9).

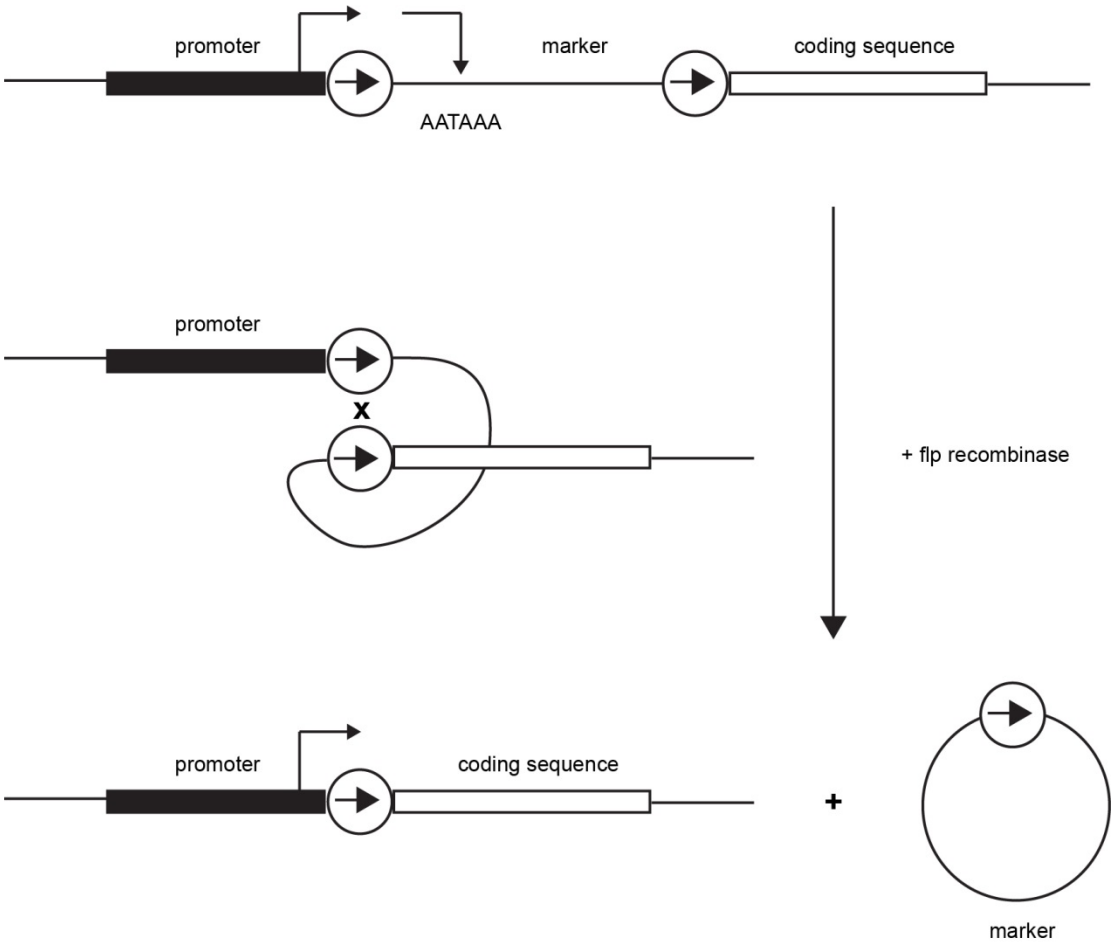

Figure 9. Flp-out technique

Image modified from Struhl & Basler 1993. To drive the expression of any coding sequence, a constitutive promoter is placed upstream of the coding sequence of interest. The coding sequence and the promoter are separated by a segment of DNA bounded to two direct FRT sites, the flp-out cassette. A transcriptional terminator is placed between the FRTs. Prior to recombination, the promoter drives expression of transcripts that terminate within the transcriptional terminator (AATAAA). After the activation of flp and recombination, the promoter now drives constitutive expression of the coding sequence.

A recombinase under the control of a heat shock promoter is used to trigger the flp-out event by heat shock. To express the sequence of interest only in the LECs, 3rd instar larvae were heat shocked for 10-15 min, 30 hours prior to recording. This heat shock gives enough time for the recombination event to happen in the polyploid larval epithelial cells (LECs), but not in the diploid histoblasts (Ninov et al., 2007).

2.1.4 RNA interference

RNA interference (RNAi) is an evolutionary conserved mechanism for knocking down gene expression. RNAi suppresses gene expression by, among other mechanisms, targeted sequence specific degradation of messenger RNA (mRNA) (Montgomery et al., 1998). The effector molecules that guide mRNA degradation are small double stranded RNA (dsRNA) molecules, called small interfering RNAs (siRNAs). These are produced by the cleavage of long dsRNAs. The cleavage is mediated by the cytoplasmic Dicer family of RNAase III-like enzymes (Bernstein et al., 2001). The siRNAs are taken up into a multi-subunit ribonucleoprotein complex called RISC (RNA-induced silencing complex) (Hammond et al., 2000). The anti-sense strand of the siRNA will direct RISC to the homologous site on the messenger RNA, resulting in mRNA cleavage and degradation (Hammond et al., 2000; Zamore et al., 2000).

First tested in animal cells, injection of dsRNA into *C.elegans* proved to be an efficient sequence-specific gene silencing technique and a powerful tool for reverse genetic experiments(Fire et al., 1998). In *Drosophila*, there are fly lines containing RNAi constructs against hundreds of genes whose phenotypes can be identified either from the published literature or in the *Drosophila* database Flybase (http://flybase.bio.indiana.edu/). These lines contain UAS-constructs that contain hairpin RNAs, which form dsRNA once expressed.

2.2 4D microscopy: Imaging of pupae

Specimens were staged approximately between 18 and 42 hours after pupa formation (APF) in order to record LEC migration, apical constriction and cell death. Reliable estimation of the stage of the pupae is possible based on external features that become apparent during pupal life (Figure 10). Specimens could be used for experiments when showing a pair of white Malpighian tubules visible in the abdomen until the Malpighian tubules were prominent and green, not showing the presence of the black body between them (Bainbridge and Bownes, 1981).

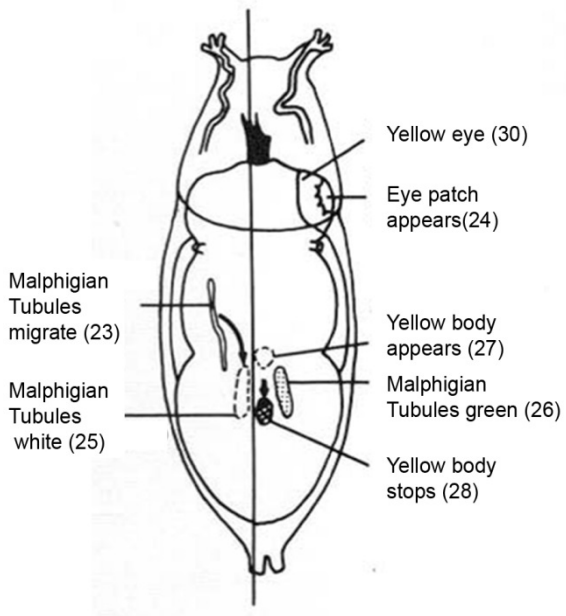

Figure 10. External features used to stage pupae between 18 and 42 hours AFP.

Figure modified from Bainbridge & Bownes 1981 showing an scheme of a pupa in stage P5 (i) & (ii). During this stage, the initial segments of the anterior pair of Malpighian tubules move from the thorax into the abdomen (23) and a translucent patch becomes discernible in the middle of the eye region (24). Then, the pair of white Malpighian tubules becomes visible dorsally in the abdomen when looked under a microscope light (25) and they become prominent and green (26), indicating that the pupa is approximately between 13-48 hours APF. Later on, the dark green "yellow body" appears between the two Malpighian tubules (27) and moves towards the posterior (28), staging the pupa between 34-50 hours APF.

The selected specimens for overnight imaging were placed in a slide with double sided sticky tape dorsal side up. A window on the pupal case was opened using a pair of forceps. Pupae were removed from the sticky tape using water and placed in a chamber made of metal (Figure 11). Pupae were covered with water and the openings of the chamber were filled with voltalef oil to prevent water evaporation and ensure oxygen supply. For shorter experiments, pupae were placed on a slide and mounted

between three bands of Parafilm, arranged in a U-shape. Each band, made of five layers of Parafilm, ensured minimal squashing. Water was used to surround the pupa. A coverslip was placed over the sample and sealed with melted paraffin. The open part of the chamber was filled with voltalef oil (Escudero et al., 2007).

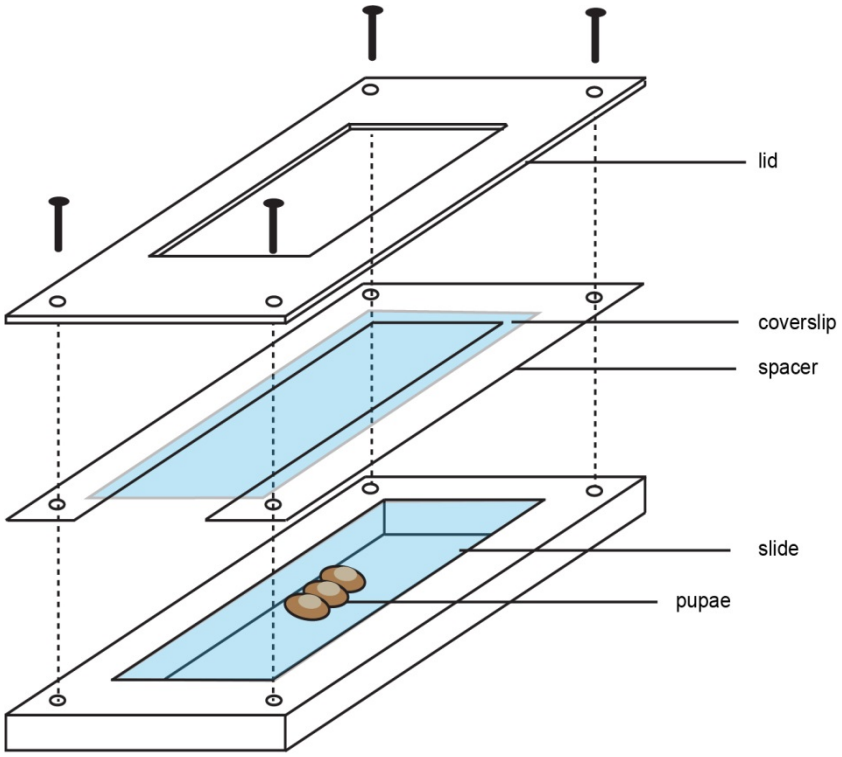

Figure 11. Scheme of the chamber used for imaging pupae

The chamber consists on a base, a lid and a spacer that avoids sample squashing. The rigidity of the materials and the fact that the lid is screwed to the base avoids drifting of pupae and facilitates imaging overnight.

The specimens selected were only imaged when LECs had not started migration and where hexagonally shaped. Imaging of the abdomen of the pupae focused on the second segment, as it is not anatomically distinct from other segments and it is easier to image considering the roundness of the abdomen (Bischoff and Cseresnyés, 2009). Pupae were imaged using a Leica TCS SP8 confocal microscope (Leica Microsystems, Mannheim, Germany) at a temperature of 25 ± 1 °C. After imaging, all the studied flies were checked to see whether they developed into pharate adults or eclosed to verify that the imaging did not affect the development of the abdomen.

2.3 Analysis of the 4D microscopy

All pupae recordings were exported from the confocal software as image sequences comprising single TIF files. Images were processed using ImageJ (Rasband, W.S., ImageJ, U.S. National Institutes of Health, Bethesda, Maryland, USA, https://imagej.nih.gov/ij/, 1997-2016). The spatio-temporal coordinates of the objects of interest were tracked using SIMI Biocell (SIMI Motionsystems, Unterschleissheim, Germany) (Schnabel et al., 1997).

2.3.1 Representation of actin dynamics

To be able to represent the dynamics of the actin cytoskeletonon in a single image, kymographs were used. Kymographs were generated drawing a 20 μm square in a selected region of the cell during migration, approximately 25 min before the lamellipodium disappears, and during apical constriction, around 75 min after the lamellipodium disappears. Kymographs were obtained using the *reslice* tool from ImageJ, followed by a maximum z-projection of the obtained stack. This operation creates an intensity plot along each horizontal line of the given square in all the frames selected for the analysis. The lines are stacked along the y axis to obtain an average intensity plot of the region of interest. The z-projection provides the image that represents the intensity distribution of the region of interest over time.

2.3.2 Localisation of actin foci within a cell

GFP-labelled actin filaments come together creating regions of high fluorescence intensity that can move around the cell, called actin foci and flows. A focus of actin is formed when two or more flows that come from different directions coalesce at a specific region of the cell to then disassemble. The tracking of these actin foci consisted on the manual recording of their (x, y, z, t) coordinates using SIMI Biocell. To establish the position of actin foci within a cell, the coordinates of the anterior, posterior, lateral and medial membranes of the cell were tracked along with the actin focus (Figure 12).

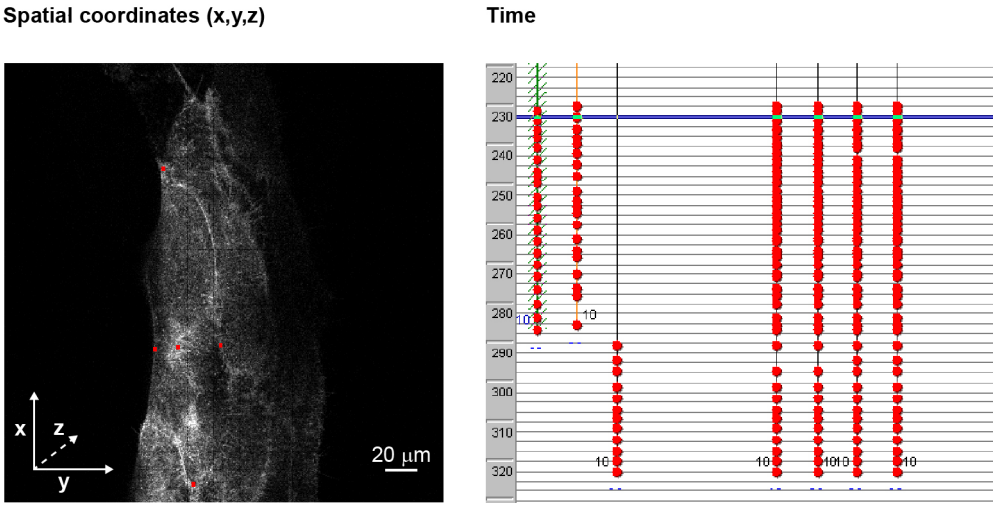

Figure 12. Tracking of the spatial and temporal coordinates of actin foci and membranes

The images from the recordings of LECs behaviour, in this case expressing *UAS.gma*, are analysed with SIMI Biocell. The software allows the tracking of points in the image. It generates a file with the spatial coordinates x, y and z of the tracked point (red dots) and the specific time (frame) in which the point was tracked.

Using the coordinates of the focus and the membranes, the position of the actin foci was expressed by the relative position (RP) parameter, which informs of the position of the actin foci within a cell independent of the cell's size. This parameter was calculated using the distance between the focus and the anterior membrane and the A-P length of the cell (equation 1). The former was obtained by subtracting the X-coordinates of the tracked foci and the anterior membrane. The latter was obtained by subtracting the X-coordinates of the anterior and posterior membranes.

$$RP\ (along\ AP\ axis) = \frac{Distance\ focus\ to\ anterior\ membrane}{A-P\ length\ of\ cell} \qquad (1)$$

To study the position of the actin foci during dorsal repolarisation the RP parameter was calculated along the D-V axis (equation 2).

$$RP\ (along\ DV\ axis) = \frac{distance\ foci\ to\ ventral\ membrane}{D-V\ length} \qquad (2)$$

The distance from the actin focus to the ventral membrane was obtained by subtracting the values of the Y-coordinates of the tracked foci and the anterior membrane. The dorsal-ventral length of the cell was obtained by subtracting the Y-coordinates of the dorsal and ventral membranes.

2.3.3 Periodicity of foci

The study of the periodicity of foci consisted in calculating the time difference between the foci tracked in each recording. The temporal coordinate of a tracked focus was subtracted from the previous foci observed to obtain the frame difference between the two events.

2.3.4 LECs shape analysis

To study the shape of LECs over time, the lengths along the A-P and D-V axis were calculated using the spatial coordinates (Figure 12) obtained every 5 frames (150 seconds). To obtain a single value that informs about the shape of the cell at each time point, the cell shape coefficient was calculated. Equation 3 considers the relation between the A-P length and the D-V length of the cell.

$$Cell\ shape\ coefficient = \frac{A - P\ length}{D - V\ length} \tag{3}$$

This relation takes values close to 1 when the cell is round and close to 0 when the cell is thin and long.

Given a period of time, the percentage of cell shape change along both axes was obtained by subtracting the first and the last value of the A-P and D-V lengths of the cell in relation to the initial value (equation 4).

$$cell\ shape\ change\ (\%) = \frac{AP\ or\ DV\ length(t_{final}) - AP\ or\ DV\ length(t_{initial})}{AP\ or\ DV\ length(t_{initial})} \times 100 \tag{4}$$

2.3.5 Cell apical area analysis over time: correlation of apical cell area size and occurrence of actin foci

The apical area of LECs was measured using the polygon selection tool in ImageJ, by drawing the apical membrane of the cell using as many vertices as needed to have an accurate outline. Area was measured every frame (20-30 seconds) for the entire length of the recording.

The percentage of apical area change in a given period of time was calculated subtracting the initial and the final value of the apical area of the cell in relation to the initial value (equation 5).

$$Area\ change\ (\%) = \frac{Area\ (t_{final}) - Area(t_{initial})}{Area\ (t_{initial})} \times 100 \quad (5)$$

The absolute magnitude of the cell area oscillations was obtained by calculating the difference between the crests and the troughs, or highest and lowest area value, for each fluctuation cycle. According to the equation 6, if the cell reduces its apical area the value will be negative:

$$Area\ difference = A(trough) - A(peak) \quad (6)$$

The percentage of the area that a cell reduces in each fluctuation was calculated using equation 7:

$$percentage\ of\ area = \frac{A(trough) - A(peak)}{A(peak)} \times 100 \quad (7)$$

The number of actin foci per area fluctuation was calculated counting the presence of foci tracked between the crests of each area fluctuation. The time difference between the appearance of a focus and the trough of the apical area fluctuation was calculated by subtracting the time point in which the actin focus accumulated and the time point of the nearest trough for each tracked foci.

2.4 Statistical analysis

R (R core team (2016). A language and environment for statistical computing. R foundation for statistical computing, Vienna, Austria. http://R-project.org/) was used for the statistical analysis of this thesis.

2.4.1 Sample size

Initial data on the localisation and frequency of actin foci was obtained in order to gain knowledge about the underlying variability of data. With some knowledge on how variable the different groups of data were, it was possible to provide a good sample size recommendation to be able to detect true differences between groups. Using the power t-test in R, the estimation of an appropriate sample size was N=7 pupae.

2.4.2 Statistical analysis of the data

Descriptive techniques were used to explore the data previous to analysis. Histograms as well as box and whisker plots were used to summarise and identify the distribution of a given variable and to visually compare two or more groups of data.

When the data of each group were found to be normally distributed (Figure 13A), the two group means were compared using a Two-sample t-test. In the case of having more than two groups, the data were compared using a one-way analysis of variance (ANOVA) test. Analysis of variance was chosen for being a powerful test that can be extended to any number of treatment groups. Also, ANOVA is useful in the case of having a single factor, as the sample sizes do not need to be the same within each group. P-values under 0.05 were considered significant to reject the null hypothesis and establish that the difference between groups was significant. If the differences between means were found to be significant, data were further explored using the *lsmeans* (Lenth, 2016) (version 2.14 package of R). This package was used to calculate the least squared means (LSM), or the means after having controlled for a covariate, the standard error and the upper and lower quantiles that include 95% of the data. After using a one-way ANOVA test, the standard assumption that the residuals, or individual sample effect, follows a normal distribution and that the variance of residuals is constant was checked (Figure 13B).

In the case of not having a normal distribution of data, the Kruskal-Wallis test was used to analyse skewed distributions of data of more than two groups (Figure 13A). This non-parametric test was chosen to compare the medians, as they are better measurements of the central tendency of the data for skewed distributions. A pairwise Wilcoxon-Mann-Whitney test was used to compare individual pairs (Dytham, 2003).

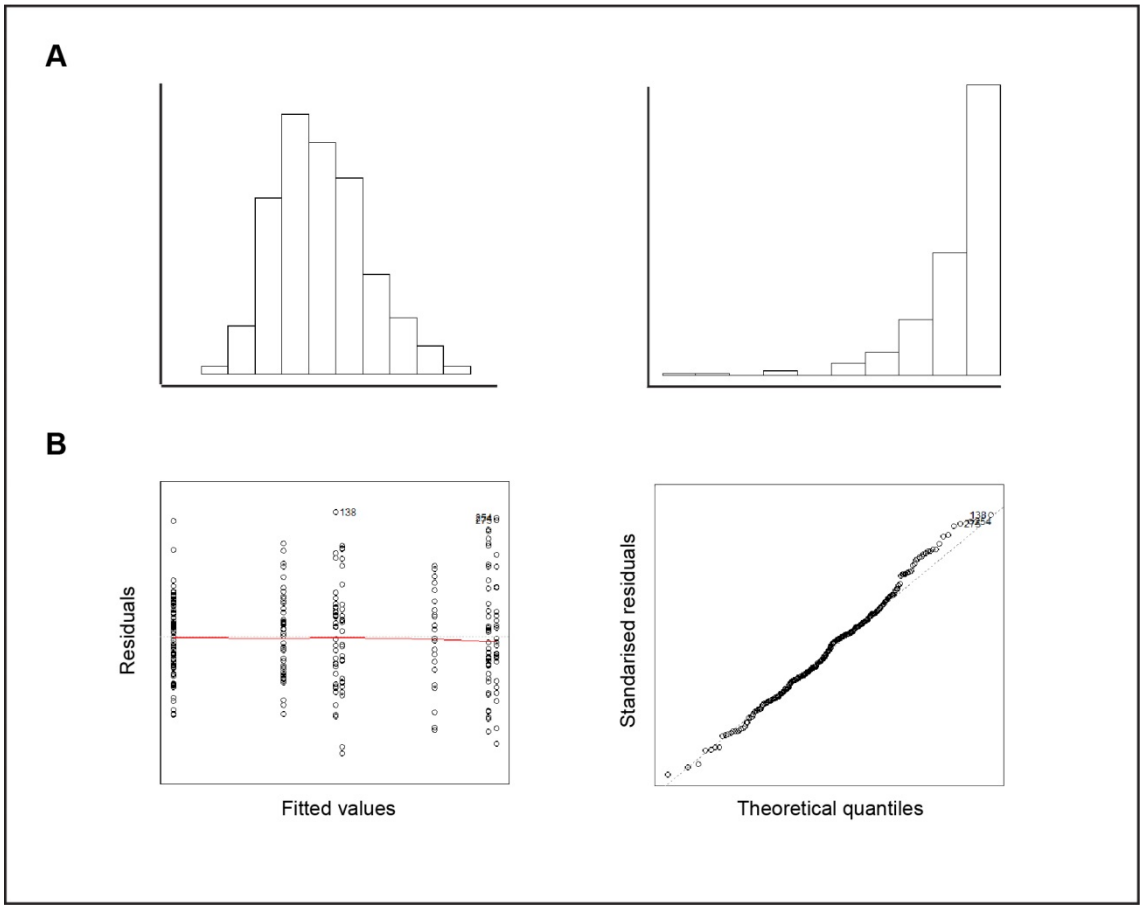

Figure 13. Normal and non-normal distributions and plots for ANOVA assumptions validation.

A) Two distributions of frequencies, a normal (left) and a skewed (right) obtained in different experiments. **B)** Plots to check the assumptions of similar variability and normal distribution in the residuals of an ANOVA test. The variability of the residuals once the group mean has been subtracted should be constant (left plot). Plotting the residual quantiles against the quantiles of a normal distribution with the same variance as the residuals distribution should follow a straight line (right plot).

In order to calculate the standard errors and confidence intervals for the medians, a bootstrap method was used. Bootstrap is a data-based simulation method for statistical inference (Efron, 1979). Using the sample of data obtained experimentally, a sample of the same size is drawn with replacement. Each of these is called a bootstrap sample. The median is calculated for this bootstrap sample. Repeating this process B times generates B bootstrap replicates. The standard deviation of the batch of B replicates generated is an estimate of the standard error of the median (Efron and Tibshirani, 1993). A rough 95% confidence interval can be derived by taking the 25^{th} and 75^{th} percentiles of the bootstrap distribution for the medians. The estimate of the standard error for the median is accurate when using between 50-200 replicates. For the calculation of confidence intervals, much larger values of B are required (Efron & Tibshirani 1993). The estimation of the standard error and confidence interval for the data sets used in this thesis was calculated using a script written in R (suppl. script). Considering that the computational time for these calculations was very low, the number of replications chosen to obtain an accurate estimate was 1000.

3. Characterisation of the spatial and temporal organisation of the actomyosin cytoskeleton of LECs

3.1 Introduction

In the past few years, advances in microscopy and especially the increase in imaging time resolution has led to the discovery of new insights on how cells generate forces to drive morphogenesis. Studies in several tissues have found that, in many cases, cell shape changes are not continuous but pulsatile. The studies conclude that this pulsatile behaviour is caused by the periodic contractile activity of the cytoskeleton (Coravos et al., 2017; Gorfinkiel and Blanchard, 2011).

This pulsatile behaviour of the cytoskeleton was first described in the *C.elegans* oocyte. Following fertilisation of the egg, a cortical actomyosin network undergoes a global flow away from the site of sperm entry (Munro et al., 2004). This cortical flow is generated and driven by the anisotropic tension levels in the egg, which is greater at the anterior pole. This distribution of tension leads the actomyosin flow towards the strongest pulling site, creating a positive feedback and reinforcing the anisotropic distribution of tension. The actomyosin flow helps in polarising the egg for the subsequent asymmetrical divisions (Mayer et al., 2010).

In epithelia, one of the first systems in which oscillations were described was the mesoderm invagination in the *Drosophila* embryo. As introduced in Chapter 1, the classical model where apical constriction is driven by an actomyosin belt underlying the adherens junction (Dawes-Hoang, 2005) was updated, as apical constriction was found to be pulsatile. In the new model, pulsed contractions of the medial actomyosin network drive apical constriction in a ratchet-like manner: cells apically constrict incrementally, alternating phases of constriction and stabilisation (Martin et al., 2009). The biochemical regulation of actomyosin pulses in this new model involves two new molecules, the transcription factors Twist and Snail. Expression of Snail, enhanced by Twist (Leptin, 1991), initiates actomyosin network contractions. The expression of Twist stabilizes the constricted state of the cell and activates the expression of Fog and T48, which are thought to activate Rho1 and promote contractility (Kolsch et al., 2007).

The distribution of the actomyosin cytoskeleton and its regulators is no longer restricted to the AJs, but ventral furrow cells exhibit radially polarised distribution of Rok, Myosin and E-cad (Mason et al., 2013). Twist is required for this polarised distribution and Rok is concentrated in medio-apical foci (Mason et al., 2013), targeting Myosin at the medio-apical domain to phosphorylate and stabilise mini-filaments and promote apical constriction (Martin et al., 2009). As apical constriction starts, E-cad accumulates apically at the AJs and while Myosin spots coalesce, the apical membranes bend inwards (Martin et al., 2009). The distribution of E-cadherin is maintained by Dia-mediated F-actin polarisation, allowing contractile forces generated by the medio-apical actomyosin network to be transmitted across AJs (Mason et al., 2013). Apical constriction is achieved by the gradual accumulation of Myosin at the cell cortex, which allows tension accumulation and transmission across the epithelium (Martin et al., 2010) (Figure 14a)

Another example of pulsatile behaviour was found during the study of *Drosophila* germband extension. During this process, germband cells extend along the anterior-posterior (A-P) axis by shrinking their dorso-ventral (D-V) oriented AJs, producing cell intercalation (Figure 14b) (Blankenship et al., 2006; Irvine and Wieschaus, 1994; Zallen and Wieschaus, 2004). Myosin is enriched along these junctions to increase tension and facilitate changes in cell contacts (Bertet et al., 2004; Rauzi et al., 2008). Myosin is also found at the medial apical side of cells together with actin, exhibiting periodic polarised flows towards the shrinking junctions. These periodic flows of actomyosin lead to a non-continuous junction shrinkage (Rauzi et al., 2010) (Figure 14b). Cell intercalation requires a planar polarised distribution of the cytoskeletal components initiated by F-actin, which accumulates at the D-V oriented junctions prior to intercalation (Blankenship et al., 2006). Active Rho binds Rok, activating and localising the kinase at the D-V oriented junctions. Rok at the same time activates Myosin, which accumulates at the shrinking junctions while Shroom maintains this planar polarised Myosin contractility (De Matos Simões et al., 2014). Actin polymerisation is also required for Myosin localisation and is mediated by the activation of Dia, which controls the total amount of Myosin present apically and inhibits Wasp, required for

cortical Myosin concentration (Bertet et al., 2009). Junctional proteins become enriched at D-V interfaces at the time of intercalation (Blankenship et al., 2006). In particular E-cad polarity is required to orient actomyosin flows towards the shrinking junctions. The uneven distribution of junctional proteins, enriched at the transverse junctions, could control the actomyosin flow pattern by spatially modulating the properties of the actin network, such as crosslinking or viscosity (Rauzi et al., 2010). These actomyosin flows produce individual steps of junction shrinkage and junctional actomyosin accumulation is required for the stabilisation of the junction length (Levayer and Lecuit, 2012) (Figure 14b).

Likewise, the behaviour of epithelial cells during dorsal closure has been found to be pulsatile. After germband retraction, the dorsal side of the *Drosophila* embryo is covered by an extra-embryonic epithelium, the amnioserosa (AS). During dorsal closure, the AS has to be eliminated and the dorsal side covered by the embryonic epithelium. This is achieved by the combined force produced by the apical constriction of AS cells and an actomyosin cable formed around the amnioserosa (Blanchard et al., 2010; Gorfinkiel et al., 2009; Kiehart et al., 2000). The apical constriction of these cells is found to be pulsatile (Solon et al., 2009) and driven by medial actomyosin foci as well (Figure 14c) (Blanchard et al., 2010; David et al., 2010). However, at the beginning of the process, during the slow phase of dorsal closure, AS cells do not show phases of stabilisation between pulses. AS cells apically constrict during the fast phase by decreasing progressively the amplitude of their apical area fluctuations, causing the shortening of their area fluctuation cycle length (Blanchard et al., 2010; Solon et al., 2009). The decrease in amplitude is caused by an increase in apical Myosin, both at cell-cell junctions and medially, which requires the activity of Rok and Dia, both downstream effectors of Rho. The activity of Rho is found to be required for the formation of actomyosin foci and the accumulation at the junctions (Blanchard et al., 2010). The formation of foci also requires Rok, which controls Myosin activity and is required for area oscillation production (Duque and Gorfinkiel, 2016). Dia is required for the stabilisation of active Myosin and actin at the adherens junctions (Homem and Peifer, 2008). The accumulation of actin at the junctions helps in translating the

generated tension by the medio-apical foci into membrane deformation, presumably by stabilisation of E-cad at the junctions (Fischer et al., 2014). At the same time, α-cat regulates the cytoskeletal dynamics by stabilising and promoting actomyosin contractions and stabilises E-cad. This suggests an interdependence between the actin cytoskeleton and the cadherin-catenin complex to generate pulsed apical constriction (Jurado et al., 2016).

Non-stabilised deformations also occur in the *Drosophila* oocyte (He et al., 2010). The *Drosophila* ovary is made of developing egg chambers. Each egg chamber is composed of 16 germline cells surrounded by a monolayer of epithelial follicle cells (Horne-Badovinac and Bilder, 2005; Wu et al., 2008). During oocyte development, the egg chamber grows dramatically, elongating along the A-P axis. To do so, the basal side of each follicle cell depends on an array of polarized actin filaments along the perpendicular axis that act as a corset, forcing follicle cells to grow along A-P (Horne-Badovinac and Bilder, 2005). Periodic constrictions, caused by the transient accumulation of Myosin along the polarised actin meshwork, produce the tension to force growth in a specific direction. The accumulation of Myosin requires the activity of Rho-GTPase and its downstream effector Rok, while cell-cell cohesion requires the activity of E-cad. Interestingly, these Myosin dependent basal contractions do not change cell shape permanently, but generate forces that constrain the shape of the underlying tissue (He et al., 2010).

The pulsatile behaviour of the cytoskeleton in tissue morphogenesis has also been observed in vertebrates. In *Xenopus* gastrulae, the pulsatile behaviour of the cytoskeleton is observed in converging and extending mesoderm cells. Pulsatile actomyosin foci in these cells are polarised along the axis of movement. These foci are the product of coordinated actin polymerization and Myosin-II activity regulated by ROCK and accompany mesoderm cells as they elongate and intercalate (Kim and Davidson, 2011; Skoglund et al., 2008). In mouse, cortical actomyosin waves are observed in the 8-cell blastocyst. These waves are the principal force generator that

produce cell pulsed contractions, which lead to embryo compaction (Maître et al., 2015).

The presence of actomyosin flows and foci in different vertebrate and non-vertebrate systems suggest that pulsatile behaviour is a common developmental mechanism. These pulsatile contractions are always driven by the actomyosin network, turned into net contraction if stabilised by a ratchet mechanism. The ratchet mechanism, either by accumulation of a medio-apical actomyosin network or accumulation at the junctions, provides stiffness to the tissue to resist deformations. The contractile activity of the actomyosin network is controlled by common shared cytoskeletal regulators and by the interaction with junctional components. The polarity of all these components is different in order to drive the different cell deformations. Planar cell polarity (PCP), or the polarisation of cells in the plane of the tissue, is required for cell intercalation (Rauzi et al., 2010), whereas Radial cell polarity (RCP) is necessary for apical constriction (Mason et al., 2013). The study of the temporal organisation of the pulses in all these morphogenetic systems reveals that in all tissues there is an above-threshold frequency of actomyosin foci required for productive tissue contraction (Gorfinkiel and Blanchard, 2011). The periodicity of pulses becomes an important feature for apical constriction as above this threshold -like during the DC slow phase, when the frequency of actomyosin foci is low- contraction is not achieved (Gorfinkiel and Blanchard, 2011).

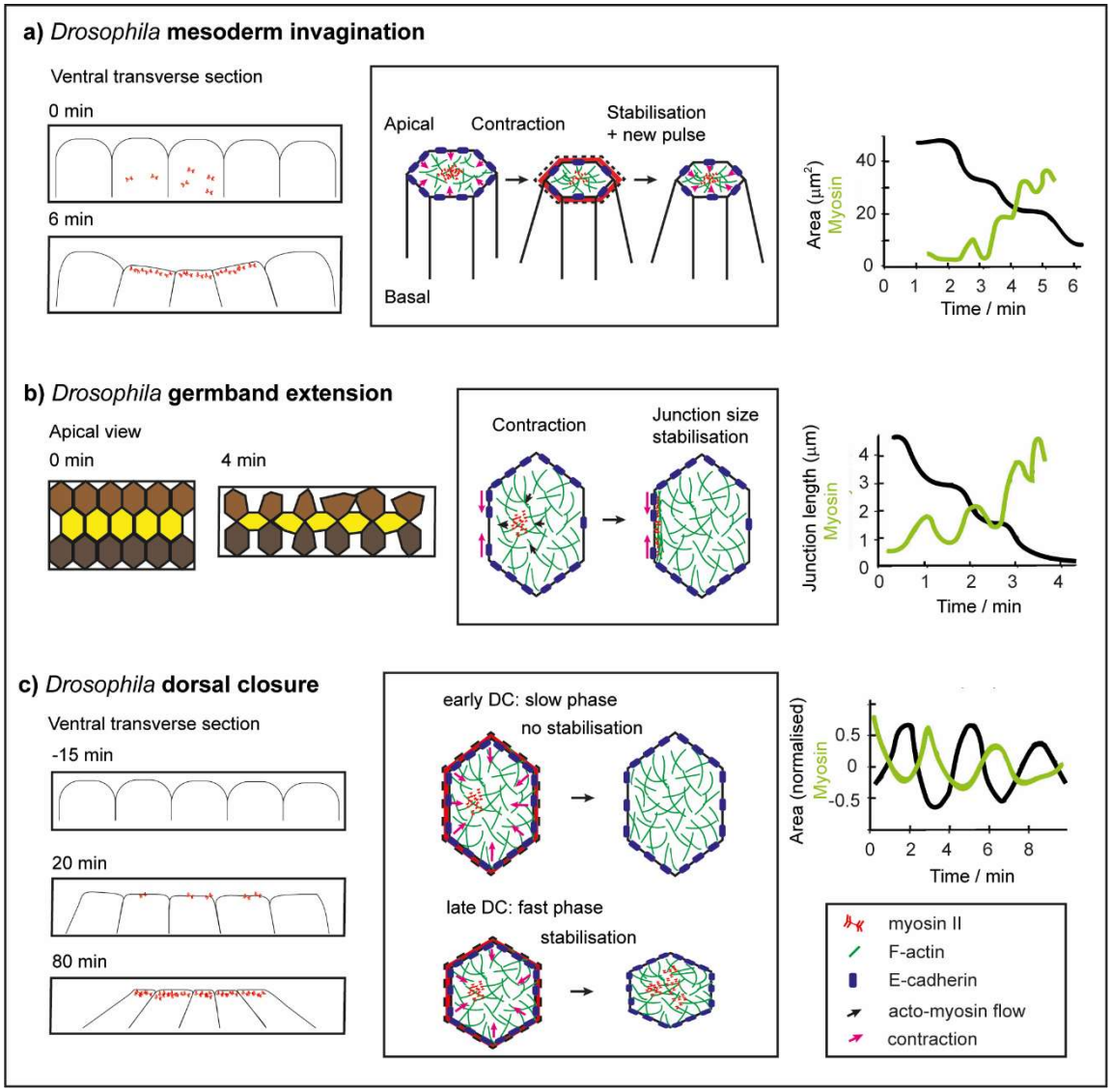

Figure 14. Different epithelial tissues in which cell shape changes are pulsatile and the specific organisation of their actomyosin cytoskeleton.

Left: Schematic drawing of the shape changes cells undergo. Middle: Specific organisation of their cytoskeleton. Right: Modified from (Gorfinkiel and Blanchard, 2011), the graphs show the stepwise contractility of the different cells and the fluorescence intensity levels of a Myosin-GFP reporter in each morphogenetic system. **a)** During mesoderm invagination, presumptive mesoderm cells undergo pulsatile apical constriction to facilitate epithelial sheet bending and invagination. These pulses are powered by medial actomyosin contractions (Martin et al., 2009). **b)** During germband extension, tissue elongation is driven by cell intercalation. Germband cells reduce their dorsal-ventral oriented junctions using polarised flows of actomyosin pulses towards this junctions (Rauzi et al., 2010). **c)** Contractility in amnioserosa cells is based on the repeated assembly and disassembly of apical actomyosin foci, an active-force generation mechanism that contributes to dorsal closure (Blanchard et al., 2010; David et al., 2010).

In the context of the abdominal morphogenesis of *Drosophila*, the mechanism by which cells produce the force to drive this morphogenetic event is poorly understood. During abdominal closure, prior to extrusion, LECs undergo apical constriction and coordinated migrations (Ninov et al. 2007; Bischoff 2012). It has been reported that LEC constriction uses a cell autonomous mechanism that depends on Myosin-II (Ninov et al., 2007). Nevertheless, this morphogenetic event involves the coordination of cell movement and cell shape changes simultaneously to produce a normal adult abdomen. The motivation of this first chapter is to understand what are the cellular mechanisms underlying the coordination of cell migration and cell constriction and more specifically, how is the actomyosin cytoskeleton of LECs spatially and temporally organised during abdominal closure.

3.2 Methods

3.2.1 *Drosophila* stocks

The transgenes used to perform the experiments are listed in Table 1.

Transgene	**Flybase entry**(Gramates et al., 2016)
UAS.gma	Moe$^{GMA.Scer\UAS.T:Avic\GFP-S65T}$(Bloor and Kiehart, 2001)
UAS.LifeAct-Ruby	ABP140$^{Scer\UAS.T:Disc\RFP-Ruby}$
hh.Gal4	Scer\GAL4$^{hh-Gal4}$
tub.Gal80ts	Scer\GAL80$^{ts.\alpha Tub84B}$
	sqh^{AX3}(Jordan and Karess, 1997)
Sqh::GFP	*sqh*$^{RLC.T:Avic\GFP-S65T}$(Royou et al., 2004)
sqh.Rok::GFP	Rok$^{K116A.sqh.T:Avic\GFP}$ (De Matos Simões et al., 2014)

Table 1. Summary of the transgenes used for the experiments performed for this chapter.

The Left column corresponds to the abbreviated nomenclature used throughout the text and the right column to the entry in www.flybase.org.

The following stocks were used to visualise the actin cytoskeleton of LECs: 1) *y,w,hs.FLP;UAS.gma/CyO;hh.Gal4/MRS* : These flies express GMA, a construct that carries the actin binding domain of *Drosophila* Moesin fused to GFP (Bloor and Kiehart, 2001), in the posterior (P) compartment, where Hedgehog is expressed. 2) *y,w,hs.FLP;UAS.LifeAct-Ruby/CyO;hh.Gal4,tub.Gal80ts/MRS*: LifeAct is a 17-amino-acid peptide that stains filamentous (F) and globular (G) actin (Riedl et al., 2008). In this case, this actin-binding protein is fused to Ruby, a red fluorophore. The expression of the LifeAct-Ruby in the P compartment is controlled by repression of *hh.Gal4* expression by the temperature sensitive form of Gal80 (*tub.Gal80ts*). 3) *w; UAS.gma/CyO;hh.Gal4, tub.Gal80ts/+* : Expression of the GMA construct under the control of Gal80ts.

To visualise the organisation of Myosin-II the following stock was used: *w,sqh*[AX3]*; sqh::GFP; sqh::GFP*. These flies express Myosin-II regulatory light chain (MRLC, Spaghetti-squash (Sqh) in *Drosophila*) tagged at the C terminus with GFP under the control of its own promoter. The stock furthermore contains a mutant *sqh* allele, which

produces a loss of function of Myosin. In this case, the only functional Myosin in these flies is the one tagged with GFP, which we can visualise.

To visualise the dynamics of Rho associated kinase (Rok), the following stock was used: *w,sqh.Rok::GFP;+;+*. The stock contains a *rok* transgene fused to GFP expressed under the endogenous *sqh* promoter.

For the co-localisation experiments of Myosin and actin, the pupae recorded had the following genotype: *w,sqh[AX3];UAS.LifeAct-Ruby/sqh::GFP;hh.Gal4,tub.Gal80ts /sqh::GFP*.

For the co-localisation experiments of Rok and actin, the pupae recorded had the following genotype: *w,sqh.Rok::GFP; UAS.LifeAct-Ruby/+;hh.Gal4,tub.Gal80ts/+*.

3.2.2 Expression of UAS-transgenes in the P compartment

Flies carrying *hh.*Gal4 and *tub.*Gal80ts were shifted to 29 °C for 24-30 hours prior to recording.

3.2.3 4D microscopy: Imaging of the cytoskeleton of a single cell

Recordings of single LECs concentrated on a region of two to three LECs from the P compartment of the second segment (A2) of the abdomen of *Drosophila*. The selected region was two cells rows close to the segment midline, where two tendon cells are positioned. These cells are easy to identify, as they do not express Hedgehog and thus are not marked with GFP. This allows the comparable selection of a recording area, which is always at the same position within the P compartment. Also, the size of the recording area was specifically selected to ensure the recording of the whole process (Figure 15). Z-stacks of 5-30 μm with a step size of 1 μm were made every 20-30 seconds with a Leica SP8 confocal at a temperature of 25 ± 1 °C.

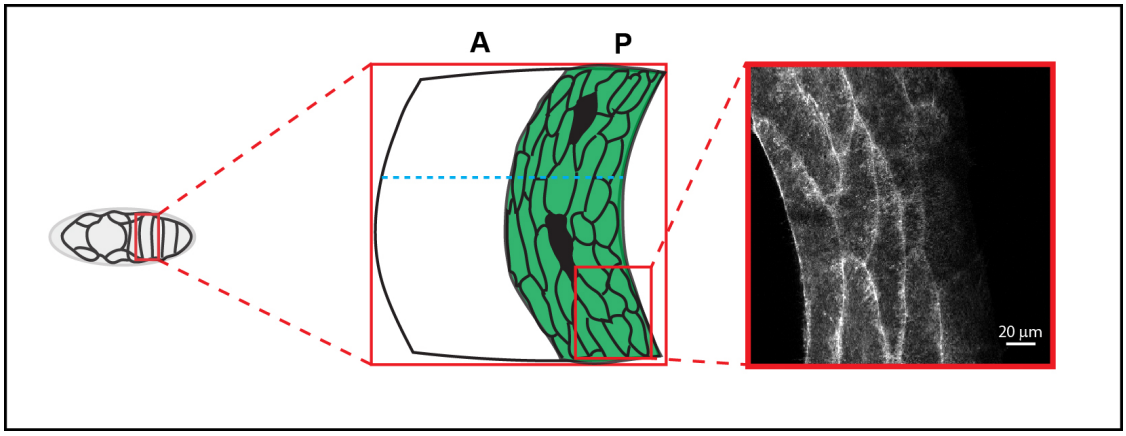

Figure 15. Experimental region of interest

Schematic drawing that shows the region in which a window is made in the pupal case to image LECs. The drawing shows the segment (A2) of the abdominal epidermis and the anterior (A) and posterior (P) compartments. The red square shows the region of interest, lateral to the tendon cells (black) and an image of an actual experiment showing cells from the P compartment expressing the GMA construct. The blue dotted line represents the midline.

3.2.4 4D microscopy analysis

Pupae were mounted and recorded as described in Chapter 2. The recordings of pupae were selected for analysis when, at least one LEC was clearly visible throughout the whole process and the pupae developed into a pharate adult or hatched.

For the analysis of the recordings of pupae expressing actin markers, only one LEC was analysed per pupa recorded. The development of the abdominal epidermis was divided into 4 phases depending on the behaviour of LECs and the behaviour of their actin cytoskeleton: 1) Phase 1, start of posterior migration and presence of a lamellipodium in the direction of movement; Phase 2, appearance of actin foci while migrating posteriorly; Phase 3, disappearance of the lamellipodium, end of migration and the start of apical constriction; Phase 4, repolarisation and protrusion in dorsal direction while constricting apically.

The recordings of pupae in which LECs were visible from the start of the process (phase 1) until the onset of apical constriction (phase 3) were used for analysis. They

are listed in tables S1 to S3 - *UAS.gma* (N=7) (Table S1), *UAS.gma* under the control of Gal80ts (N=5) (Table S2) and *UAS.LifeAct-Ruby* expressing pupae (N=7) (Table S3). The recordings of analysed pupae expressing *UAS.gma* in which the transition to dorsal movement was visible (phase 4) are listed in Table S4. Each table specifies the timing of the external features that defines each phase, such as the presence of the lamellipodium in the direction of movement and the end of migration. Each of these pupae was used for the tracking of the foci, their membranes and the tracking of the apical area over time. The relative position (RP) parameter was calculated as stated in Chapter 2, using equation (1) for migration (phase 2) and apical constriction (phase 3) and equation (2) for dorsal repolarisation (phase 4). The cell shape coefficient was calculated using equation (3) and the magnitude and percentage of apical area fluctuations using equations (6) and (7). All these parameters were calculated for each phase of every individual pupa. The percentage of cell shape changes and the change in apical area were calculated between the start and end of each phase using equations (4) and (5). Individual pupae were compared using the appropriate statistical tests. The values for the RP of foci, cell length and cell shape change presented a normal distribution and the different analysed pupae were compared using parametric tests (t-test when comparing two groups and ANOVA when comparing more than two groups). The values for the periodicity of foci and the magnitude of the apical area fluctuations presented a skewed distribution and pupae were compared using non-parametric tests (Kruskal-Wallis).

The cell shape and apical area fluctuations were analysed in LECs in which delamination was visible, listed in Table S5.

3.2.5 Co-localisation analysis of Actin, Sqh::GFP and Rok foci

The co-localisation of Sqh::GFP, Rok::GFP and actin foci of selected images was analysed using ImageJ. F- and G-Actin were labelled using LifeActin-Ruby. A region of 20 μm^2 was drawn, covering most of the apical area. Intensity plots for each channel, red for the Actin marker and green for Sqh or Rok, were calculated using the plot profile function in ImageJ. This function displays a two-dimensional graph of the

intensities of pixels from the rectangular selection. The X-axis represents distance along the X-axis of the rectangle and the Y-axis is the pixel intensity averaged along the Y-axis.

3.3 Results

This chapter studies the dynamics of the cytoskeleton of LECs during abdominal morphogenesis as a potential mechanism for cells to coordinate the different behaviours they undergo. For that, the chapter consists firstly of the study of the spatial and temporal organisation of the actin cytoskeleton during migration and apical constriction. Then, LEC shape changes and cell apical area reduction during the process are studied in relation to the spatio-temporal organisation of actin. Finally, there is a characterisation of the dynamics of other cytoskeletal components.

3.3.1 Spatial and temporal organisation of the actin cytoskeleton in LECs

The following section studies the spatial and temporal organisation of the actin cytoskeleton of LECs during migration and apical constriction. The actin cytoskeleton of LECs was found to be pulsatile and cells displayed periodic actin flows and foci, the dynamics of which are described in the first part of this section. The second part quantifies the position of these periodic actin foci within the cell and studies the correlation with the change in cell behaviour. The third part studies the quantification of the temporal dynamics of the actin cytoskeleton, quantifying the periodicity of the actin foci.

3.3.1.1 The actin cytoskeleton of LECs show periodic actin foci during abdominal morphogenesis

Live imaging was used to record pupae that express the GMA construct to visualise F-actin over time. The organisation of the actin cytoskeleton was found to be pulsatile, with the presence of periodic foci in the apical side of LECs. Considering the appearance of these foci and the behaviour of LECs, four phases can be differentiated:

1. At the beginning of the morphological process, LECs start to change their shape from hexagonal to a cell that shows a clear lamellipodium (Bischoff 2012) (Figure 16A). This is considered the start of phase 1, an active posterior migration. While migrating, the apical actin cytoskeleton starts flickering with no apparent specific pattern (Movie S1).
2. Later on, while still migrating posteriorly, the LECs apical cytoskeleton begins to show a more organized behaviour. GMA-labelled filaments periodically coalesce at specific foci showing a peak of fluorescence intensity. Interestingly, these foci localise to the back of the moving cell, close to the anterior membrane (Movie S2). These foci are repeatedly observed in approximately the same region, one accumulates laterally and the other medially along the D-V axis (Figure 16A). Although the number of foci during posterior migration can vary, two is the most common case (Table S1). These foci are formed when flows of actin coming from different directions coalesce. After focus formation, actin also flows either towards the lamellipodium (Figure 16B) or from lateral to medial, or vice-versa, to accumulate and form a new focus (Figure 16C) (Movie S2). At the end of the posterior migration this flowing pattern changes and actin flows from lateral and medial regions of the cell towards a single actin focus positioned centrally along the D-V axis, which still localises close to the anterior membrane (Figure 16D) (Movie S3).
3. The disappearance of the lamellipodium marks the end of the posterior migration and the start of phase 3 (Figure 16A). At the onset of this phase, the pattern of actin flowing from different locations to form a single focus continues, but now the flows come from the cell periphery towards a single

focus, localising to the centre of the cell (Figure 16E) (Movie S4). LECs that are closer to the midline round up and apically constrict, showing the presence of this central focus until delamination and death. It takes the cell 2.5 ± 1.1 hours from the start of phase 3 until delamination (N=3).

4. Finally, cells that are 2 or 3 rows away from the midline and are being approached by the histoblasts (hb) undergo dorsal migration. These cells, after entering phase 3, will repolarise creating a lamellipodium in the dorsal direction (Bischoff 2012). During repolarisation, actin focus localisation appears to randomise along the A-P axis to then localize centrally again. Interestingly, these foci localise closer to new back of the cell (i.e. their ventral membrane), showing a repolarisation of the actin cytoskeleton along the D-V axis (Figure 16A) (Movie S5). Eventually, these cells will completely reduce their apical area and delaminate within 3-5 hours from the start of phase 3 (Table S4), taking longer than the cells that do not repolarise.

In order to test a different cytoskeletal marker and check that the foci observed expressing GMA are not artefacts, the same region of interest was recorded in pupae expressing LifeAct-Ruby. LifeAct is a commonly used modified peptide that allows the visualisation of actin dynamics *in vivo* (Riedl et al., 2008b) and can be used as a control for the dynamics of the actin cytoskeleton observed in GMA recordings. Also, it will be necessary for future experiments to assess whether the temperature sensitive repressor Gal80ts has an effect on the dynamics of the cytoskeleton. For that, LECs expressing *UAS.LifeAct-Ruby* or *UAS.gma* together with *tub.Gal80ts* were recorded. With both markers, the four different phases described above could be identified. LECs presented the same spatial and temporal actin dynamics, observing the same flowing pattern from lateral to medial during phase 2 to form periodic foci, the change in the flowing pattern at the end of phase 2 to present a single focus at the back of the cell and finally a centrally localised single focus during phase 3 (Figure S1).

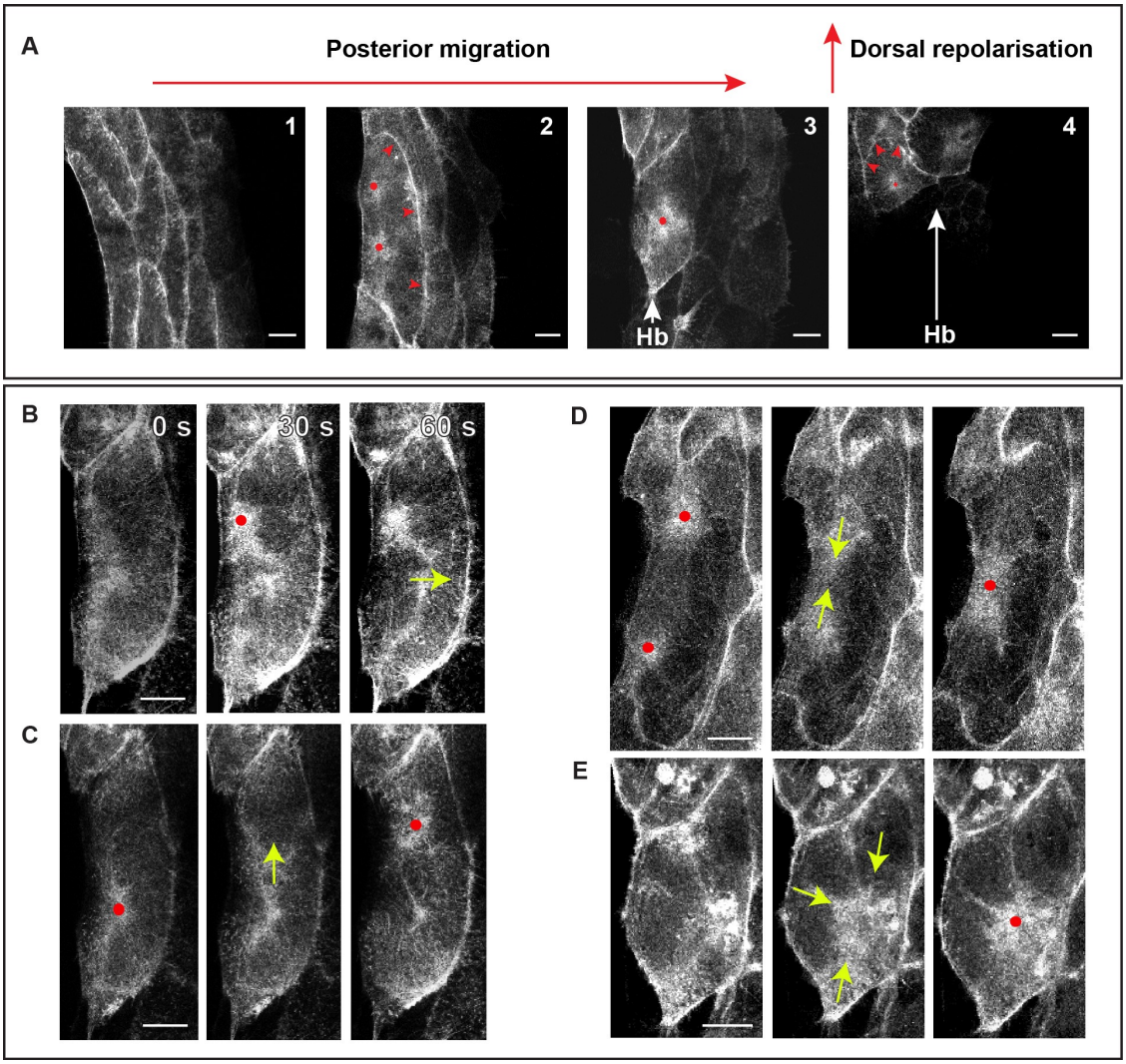

Figure 16. Description of the 4 phases LECs undergo during abdominal morphogenesis and the different actin flow patterns during foci formation.

Images taken from a recording of LECs from the P compartment expressing the GMA construct. Scale bars, 20 μm. The red arrows represent the movement of cells and mark the lamellipodium during the different movements. Red dots mark the localization of foci. Yellow arrows indicate the direction of the flows of actin. While the LECs migrate and apically constrict, the histoblasts (Hb) expand and replace them. **A)** Numbers indicate the different phases. Phase 1: posterior migration, no actin foci; Phase 2: posterior migration, anterior foci; Phase 3: dorsal movement, central foci; Phase 4: Dorsal movement, foci repolarisation. **B)** Actin flows from the foci towards the lamellipodium. **C)** Actin coalesces at a focus localised laterally. Then, actin flows towards a medial region of the cell to accumulate and form a new focus. **D)** Actin flows from the lateral and medial ends of the cell to accumulate at a mid-point. **E)** Central foci formation during phase 3. Actin flows from different directions to coalesce in the centre of the cell, forming a single focus.

3.3.1.2 Quantitative analysis of the localisation of the actin foci within a LEC during abdominal morphogenesis

The visualisation of the cytoskeleton of LECs over time has shown that Actin is highly dynamic, generating transient foci that localise differently over time. In this section a quantitative study of the localisation of foci is performed.

3.3.1.2.1 Localisation of actin foci during posterior migration and apical constriction

The position of the actin foci is analysed by tracking the observed foci during posterior migration (phase 2) and apical constriction (phase 3).

The actin foci tracked during phase 2 localise close to the anterior membrane, whereas the foci tracked during phase 3 localise to the centre of the cell (Figure 17A). After posterior migration, some pupae (N=4) show absence of foci. This could be due to the randomisation of actin dynamics when the cell is transitioning between migration and apical constriction, making the actin foci difficult to track.

To quantify the differences in the position of foci, the relative position (RP) parameter is calculated for every focus observed. The difference in the mean RP value of foci of phases 2 and 3 is statistically significant when combining all analysed cells (N=7, $p<0.001$) (Figure 17B). When the mean RP parameter of the two phases are compared in each individual cell, the difference is statistically significant (Table S6A), showing that the pattern of localisation is reproduced in each individual pupae. Also for the LifeAct-Ruby (N=7) and GMA controls with tub.Gal80ts (N=5), the plots of the position of the foci along the A-P axis show a clear pattern of localisation (Figures S3 and S4). Moreover, the difference in the mean RP values between phase 2 and phase 3 is equally significant for the combined sample (Figure 17B) and for each individual pupa (Table S6B,C).

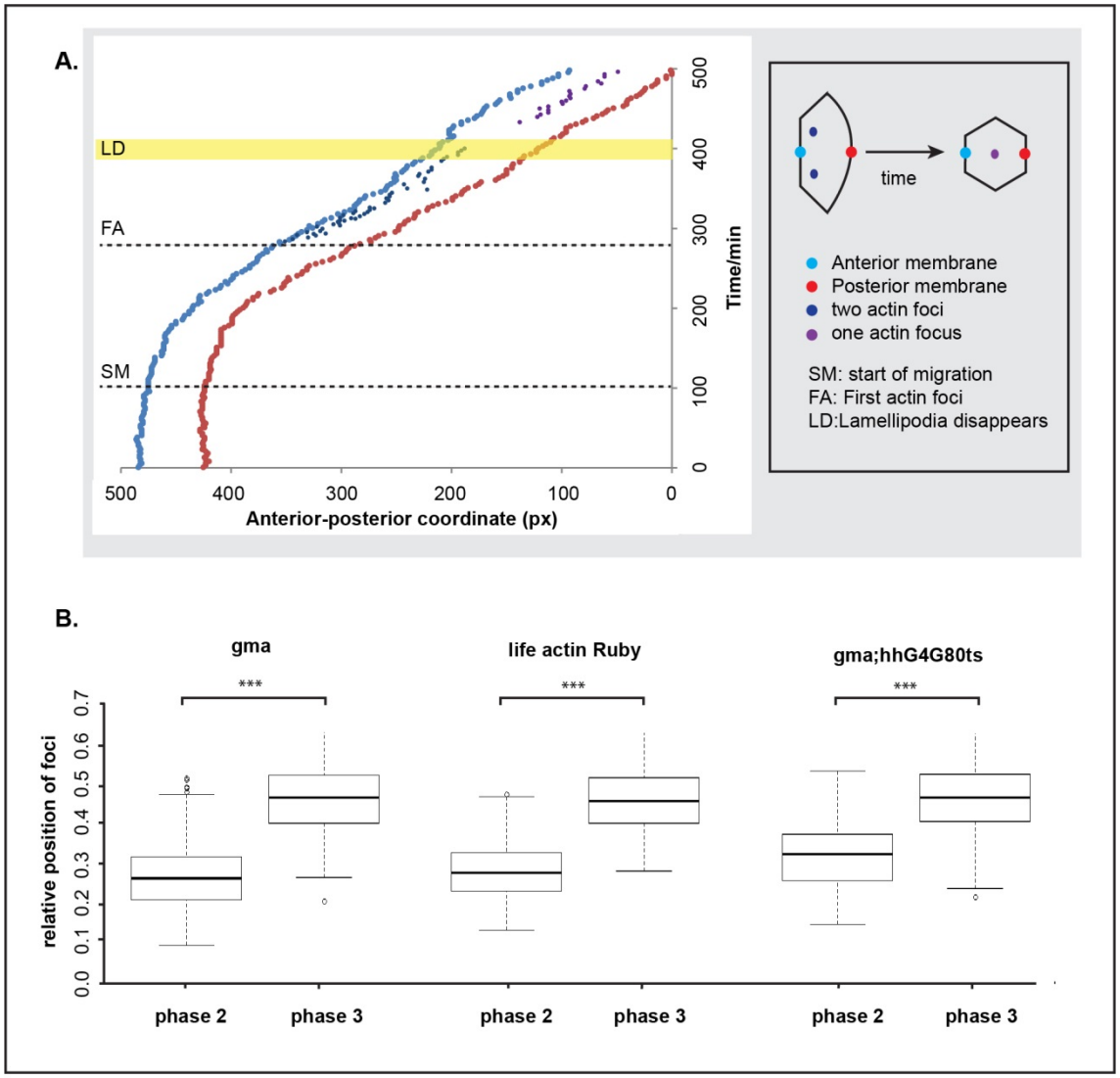

Figure 17. Quantification and statistical analysis of the localization of foci during phases 2 and 3.

A) Plot of the coordinates of the actin foci and the anterior and posterior membranes tracked during phase 2, when the first actin foci appear during posterior migration, and during phase 3, after the lamellipodium has disappeared (N=7). One representative cell is shown to illustrate the general trend found in all cells (suppl. Figure 2). **B)** Boxplots of the relative position (RP) of foci during phase 2 and phase 3 of GMA expressing pupae (N=7), LifeAct-Ruby (N=7) and GMA with *tub.Gal80ts* (N=5). The difference between mean RP of foci during phases 2 and 3 is significant in all genotypes (significance codes: '***' p<0.001). The mean values and their standard errors for the relative position of foci for the GMA recorded pupae are: RP (phase 2)= 0.27±0.01 and RP (phase 3)= 0.46±0.01; for LifeAct-Ruby: RP (phase 2)= 0.29±0.01 and RP (phase 3)= 0.46±0.01; and for GMA;*hhG4G80ts*: RP (phase 2)= 0.31±0.01 and RP (phase 3)= 0.46±0.01.

Looking in more detail, when comparing the mean RP values of the seven different GMA expressing pupae during phase 2, there are statistically significant differences ($p<0.001$) (Figure 18A). These differences are also found in controls (Figure S5). Comparing the mean RP values from the different cells analysed in GMA expressing pupae during phase 3, the variability between pupae is not significant ($p=0.5$) (Figure 18B), whereas it is significant for the controls (Figure S5). The statistically significant differences between RP means can be associated to the intrinsic variability of the system. Although actin foci tend to localise closer to the anterior membrane when migrating posteriorly, foci do not localise at the exact same position along the A-P axis in all cells. One reason for that could be that the shape of cells varies between pupae, with some cells being thinner than others. Also, surrounding cells could affect LEC behaviour and foci position.

Although the position of foci differs in individual cells, in all cells foci localize closer to the anterior membrane, taking RP values around 0.2-0.3 during posterior migration, and in the centre, taking RP values around 0.5 during apical constriction (Figure 18C). This is reflected in the significant difference in RP of the combined sample (Figure 17B).

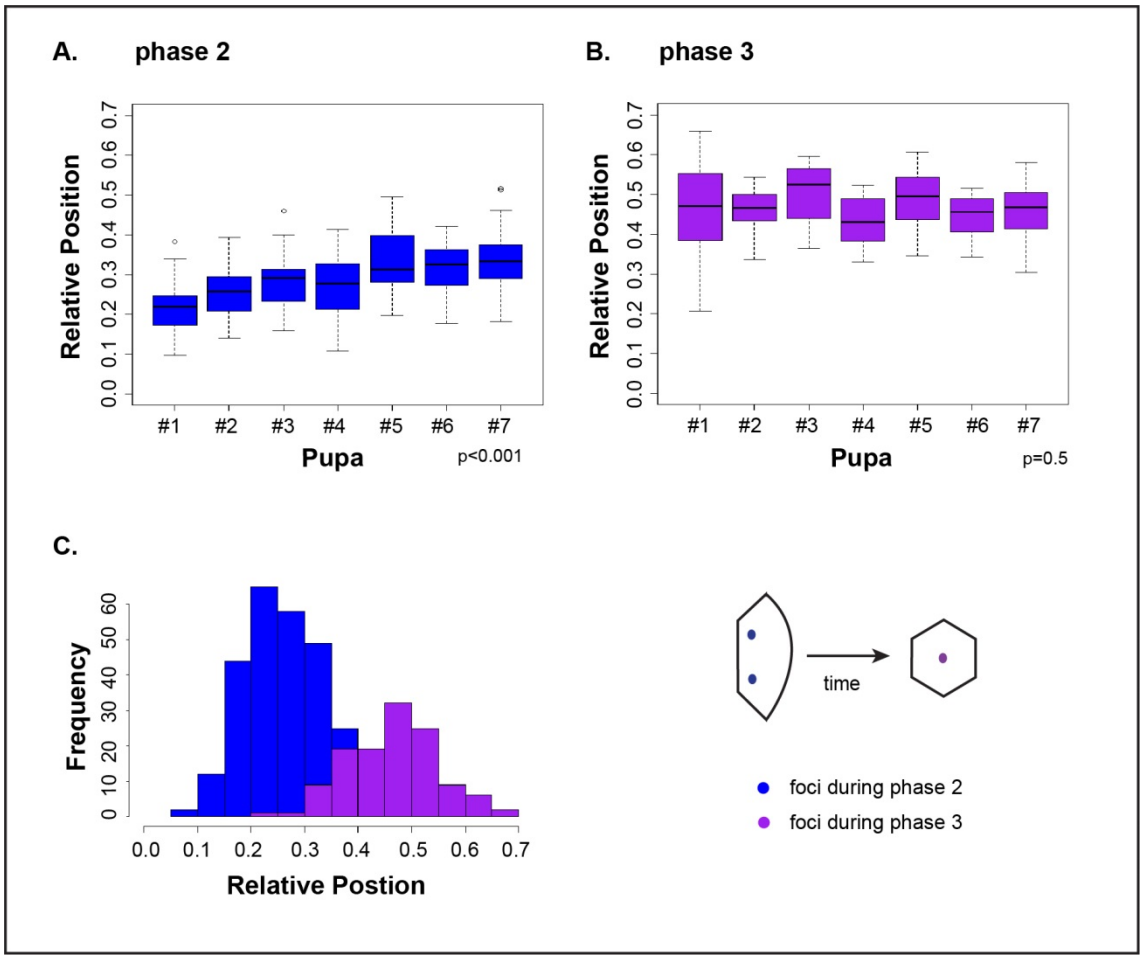

Figure 18. Quantification and statistical analysis of the localization of foci along the anterior-posterior (AP) axis during phases 2 and 3 for individual GMA expressing pupae.

A) The relative position of foci tracked during phase 2 from the different pupae analysed show a statistically significant difference between the means. **B)** There is no statistically significant difference between the mean relative position values of the different pupae analysed during phase 3. **C)** The frequency distribution of the relative position values of all the foci tracked in phase 2 (blue) and phase 3 (purple) show that foci tend to accumulate close to the anterior membrane during migration and to the localise in the centre of the cell. For values of RP of foci during phases 2 and 3 in all the individual pupae see Table S6A.

3.3.1.2.2 Localisation of the actin cytoskeleton during dorsal repolarisation

As shown above (Figure 16A), in dorsally migrating LECs actin foci localise closer to the ventral membrane, i.e. the back of the cell. Tracking of the actin foci throughout dorsal repolarisation allowed the quantification of this phenomenon (Figure 19A). Calculating the RP of foci along the D-V axis before and after repolarisation shows that the foci position in phase 3 and phase 4 is statistically different in all individually analysed pupae (Table S6D) and when all data is regarded as a combined sample (N=3, $p<0.001$) (Figure 19B).

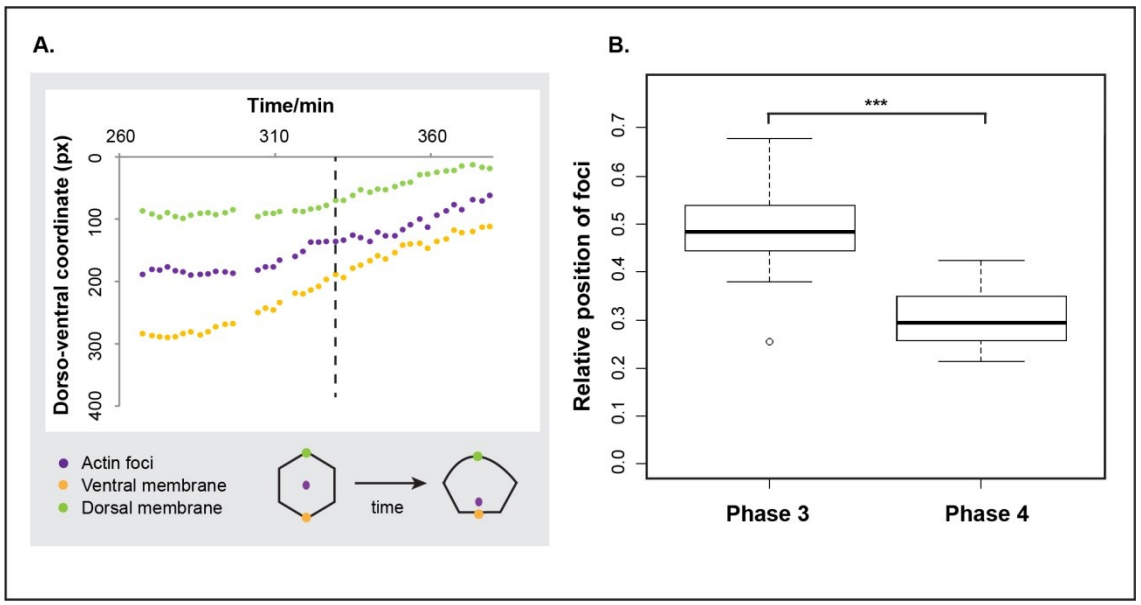

Figure 19. Quantification of the localization of foci during phases 3 and 4.

A) Tracking of actin foci and the dorsal and ventral membranes during phase 3, when LECs have finished posterior migration and phase 4, after LECs have repolarised (N=3). The dashed line indicates the start of repolarisation, when LECs show a lamellipodium in dorsal direction. **B)** Boxplot representing the relative position of foci before (phase 3) and after cell dorsal repolarisation (phase 4). There is a statistically relevant difference between the two means (N=3): RP (phase 3) = 0.49±0.01; RP (phase 4) = 0.30±0.01. Significance code: '***' $p<0.001$.

Detailed analysis of the RPs of foci in individual pupa shows that there is no significant difference in foci position between individuals in phase 3 as well as phase 4 (Figure 20). Overall, the analysis concludes that there is a pattern of localization of foci that coincides with a change in cell behaviour, from a cell that is ready to apically constrict and localises its cytoskeleton in the centre to a cell that migrates dorsally and re-localises these actin accumulations to the back of the migrating cell.

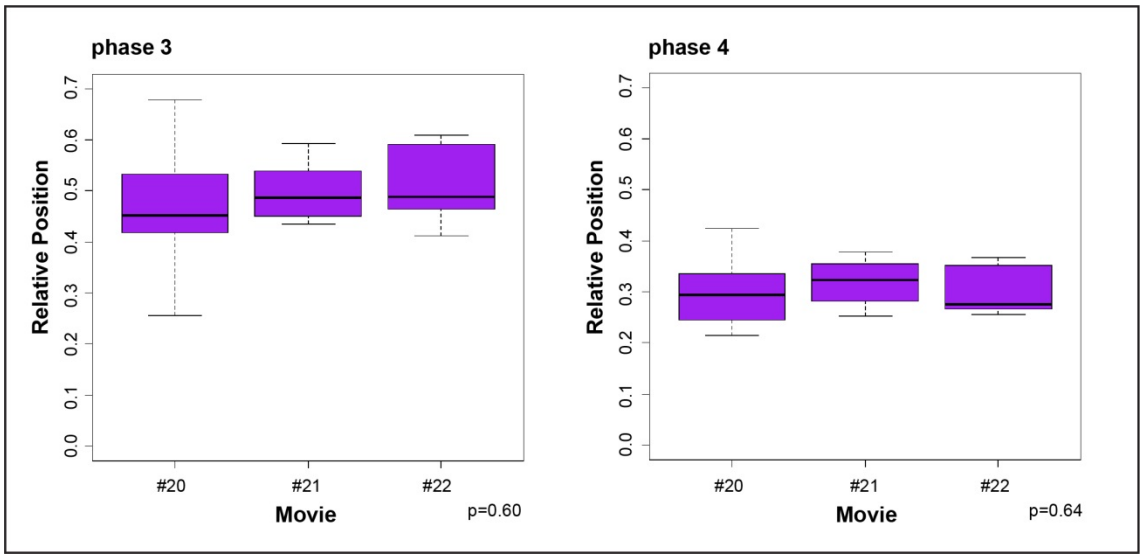

Figure 20. Comparison between the mean relative position of foci during dorsal repolarisation for each individual GMA expressing pupae.

The mean RP values before the cell repolarises (phase 3) and when it is migrating dorsally (phase 4) show no statistically significant differences between the analysed pupae. The p-values for the ANOVA test are indicated under each boxplot. For values of the RP in each individual pupa see Table S6D.

In summary, observing the behaviour of LECs and their actin cytoskeleton during abdominal morphogenesis, there is a change in the polarisation of the actin cytoskeleton that correlates with a change in cell behaviour. These changes are identifiable by the fact that cells show external features that can be used to identify the transition between posterior migration and apical constriction. The analysis of the position of foci within the cell allows the quantification of this change in polarity and the identification of a consistent pattern of localisation of the periodic actin foci. Foci localise in the back of the cell during posterior migration and in the centre during apical constriction. Depending on the position of the cell within the tissue along the D-V axis, LECs undergo dorsal repolarisation and migration towards the midline, which correlates with a repolarisation of the actin cytoskeleton, having foci close to their "new" back (Figure 21).

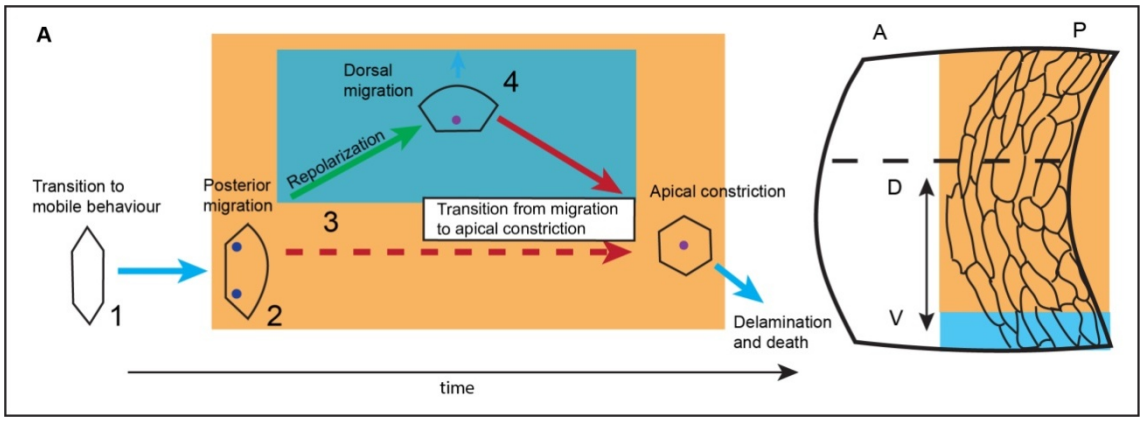

Figure 21. Different cell behaviours LECs undergo depending on their position along the D-V axis and localisation of the actin foci.

LECs transition from stationary to migratory behaviour (1) and migrate posteriorly (2). Cells closer to the midline (orange square) undergo apical constriction after posterior migration (3). Cells positioned more ventral in the tissue along the D-V axis (blue square) undergo repolarisation and extensive dorsal migration (4). Two actin foci accumulate closer to the anterior membrane during phase 2. A single focus localises centrally during phase 3. Central focus during phase 3 repolarises and localises again in the back of the migrating cell during phase 4.

3.3.1.3 Analysis of the periodicity of the actin foci

As mentioned above and similar to many other systems, the temporal organisation of the actin cytoskeleton in LECs is pulsatile or oscillatory. The foci observed during phase 2 and phase 3 assemble and disassemble periodically. This next section analyses the periodicity with which the actin foci are formed.

The values of the period of foci assembly present some variability. This variability is due to the fact that the period between foci is calculated subtracting the time points in which a focus is visible and the previous tracked one. Due to folds in the tissue or the cell morphology, foci are not always tracked creating occasionally high period values. Because of these outlier values, the median of the distribution of periods becomes a more sensible and representative parameter to explore than the mean period.

During posterior migration, interestingly, the two foci present in the back alternate asynchronously with a period of around 90 seconds (Figure 22A). This value is very consistent between the different pupae as there is no statistically significant difference between their medians (N=6, p=0.6).

The period of all tracked foci during phase 2, considering lateral and medial foci separately, as well as phase 3, is approximately 180 seconds (N=7, p=0.13) (Figure 22B). Considering pupae individually, the periodicity of foci presents statistically significant differences in their medians (Figure 22C). Thus, similar to foci position, there is also variability between pupae with respect to their foci periodicity. This variability of medians between 140 and 240 seconds could be explained by the fact that the imaging interval between frames was chosen to be between 20 and 30 seconds. Thus, the time point of full contraction could lie within a time interval of ± 20-30s from the point of tracking (Table S7).

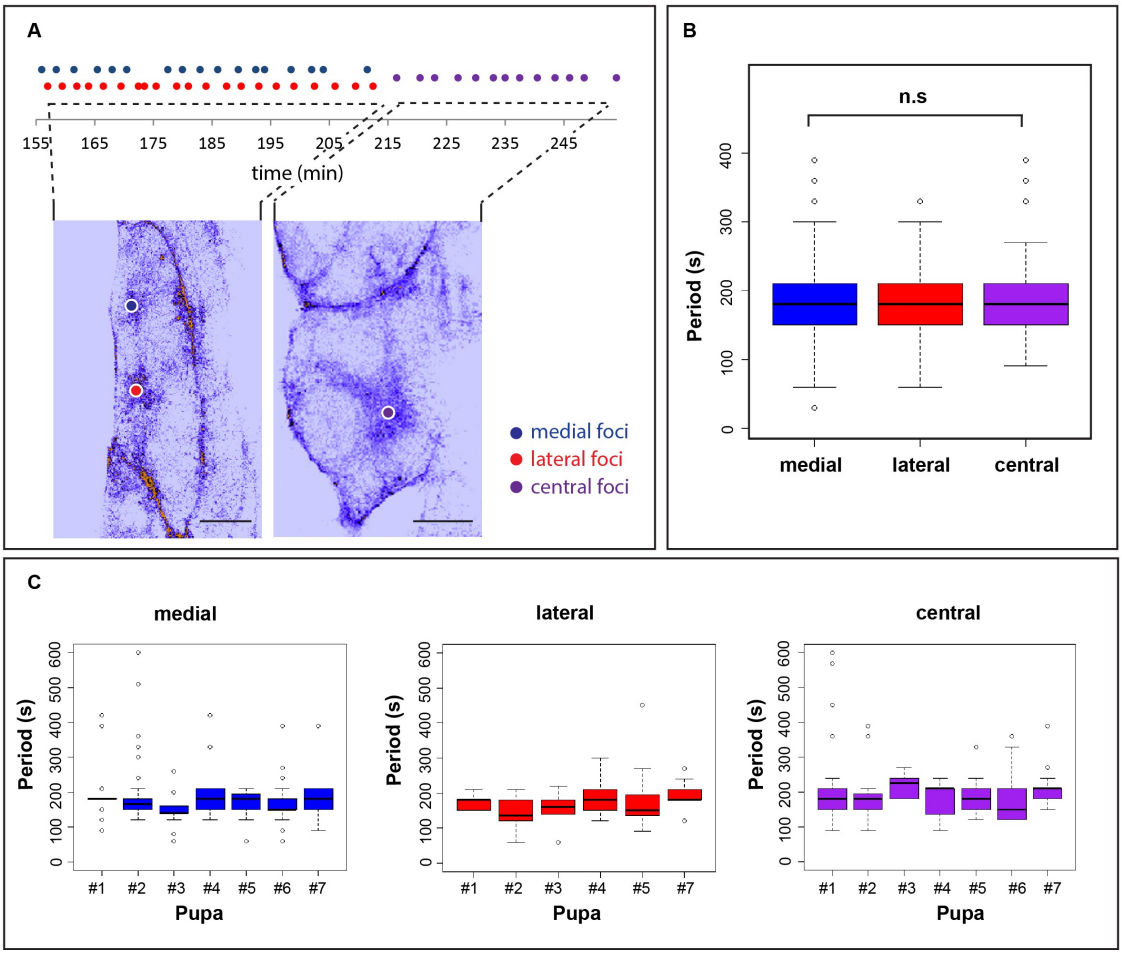

Figure 22. Foci period for the medial, lateral and central foci during phases 2 and 3 respectively.

Scale bars, 20 μm. **A)** In most cases, there are two foci present at the back of the migrating cell, one localising medially and the other laterally. These foci assemble and disassemble periodically, alternating asynchronously. During phase 3, the single focus present at the centre also assembles periodically. **B)** The periodicity of foci assembly is the same for medial (180 ± 0.86 s), lateral (180 ± 7.91 s) and central (180 ± 3.25 s) foci, presenting no statistically significant difference between them (p=0.13). **C)** The periodicity of foci comparing the individual pupae presents statistically significant differences between their medians for both medial (p=0.02) and lateral (p=0.02) foci during phase 2 but not during phase 3, when foci localise centrally (p=0.2). For values of the periodicity of foci for each individual pupa see Table S7.

An interesting question to tackle is, whether foci periodicity changes over the course of development. The change in the periodicity of foci over time could contribute to apical constriction, for example accelerating the rate of assembly previous to delamination to prevent area relaxation. The analysis of the periodicity of actin foci in late phase 3, shortly before delamination, shows that the interval between the actin foci does not increase over time. From the start of phase 3 until LECs have completely constricted their apical area, actin foci assemble with an average period of 180 s (Figure 23B).

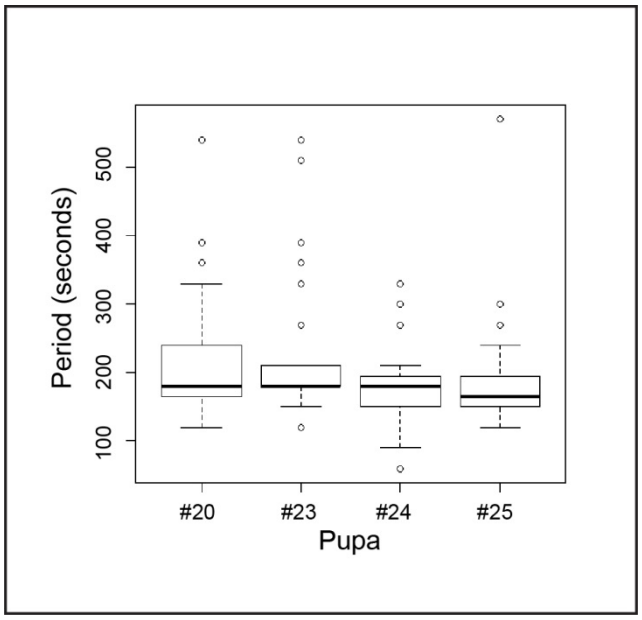

Figure 23. **Period of the actin foci during phase 3 in GMA expressing pupae.**

The period of foci during phase 3 has a median value of 180 seconds, with no statistically significant differences between the different pupae analysed (N=4, p = 0.70).

The same analysis is performed in pupae that express LifeAct-Ruby or GMA with *tub.Gal80ts*, to verify that the periodicity of actin foci is not affected by the overexpression of GMA or *tub.Gal80ts.* The median values for the periodicity of foci in puape expressing GMA together with *tub.Gal80ts*are 150 ± 13.67 seconds for medial, 150 ± 15.80 seconds for lateral and 180 ± 3.13 seconds for central foci. Like in pupae expressing GMA, these medians do not differ (p=0.10) (Table S8). Also, considering pupae individually, the median period values are not significantly different in medially

(p=0.11), laterally (p=0.17) or centrally (p=0.29) localising foci (Table S8). The periodicity of foci from LifeAct-Ruby expressing pupae follows the same pattern. Medial, lateral and central foci assemble every 180 seconds with no statistically significant differences between them (p=0.4) (Table S9). Considering pupae individually, medial foci present significant differences between the median periods of the different pupae (N=7, p=0.001) although they all oscillate around 180 seconds, whereas the periodicity of lateral (N=6, p=0.1) and central (N=7, p=0.1) do not differ between the pupae (Table S9). Again, taking into account the fact that the imaging interval is 20-30 seconds, actin foci in pupae expressing GMA and LifeAct-Ruby together with *tub.Gal80ts* assemble every 180 seconds.

Also the time interval between alternating foci during posterior migration is 90 seconds in LifeAct-Ruby expressing pupae (N=7, p=0.1).

In summary, the study of the temporal dynamics of actin shows that the periodicity of foci assembly is rather constant over time during posterior migration and apical constriction. The observation that both medial and lateral foci accumulate with the same period, 180 seconds, alternating with half of this period, 90 seconds, could be a consequence of the exchange of actin observed between both regions. Interestingly, the periodicity of foci is constant during phase 3, from the first central actin focus until the last one tracked before LEC delamination.

3.3.2 Analysis of LEC shape changes during abdominal morphogenesis

LECs display a very specific spatial organisation of their actin cytoskeleton. This organisation changes over time and correlates with a change in cell behaviour. The next section studies the shape of LECs along the A-P and D-V axes and the behaviour of their apical area during the different phases of the morphogenetic process. The aim is to study the pattern of cell shape changes, which LECs undergo during morphogenesis while they change their behaviour. Moreover, the study of LECs apical area will allow testing of the hypothesis that the pulsed contractions lead to a change in the apical area.

3.3.2.1 Cell shape change correlates with the position of actin foci

To be able to establish any relation between the localisation of the pulsed contractions and the shape of LECs, a first analysis of the shape changes LECs undergo during the process must be done. To estimate cell shape, the length of LECs along their A-P and D-V axis is measured over time. Although cell shape varies between different GMA expressing pupae, (Figure S6), the following trends are observed:

Phase 1. At the onset of morphogenesis, LECs are hexagonally shaped, being thin along the A-P axis and long along the D-V axis. Once LECs start to change their shape and migrate, they become wider and shorter. On average they increase D-V length by 10 % and A-P length by 54% (AP/DV ratio= 0-0.2) (Figure 24A, C).

Phase 2. When the first actin focus starts to assemble, cells are about or already reducing length along the D-V axis, decreasing on average 21 % of their D-V length. Moreover, cells keep increasing length along the A-P axis, in average 48%, so by the end of phase 2, LECs become more round (AP/DV ratio= 0.5) (Figure 24A, C).

Phase 3. LECs continue to become round, mainly by reducing their D-V length (Figure 24A, C). LECs that repolarise, maintain a round shape throughout dorsal migration until delamination. LECs maintain this round shape until delamination (AP/DV ratio=0.8-1.0) (Figure 24B, C).

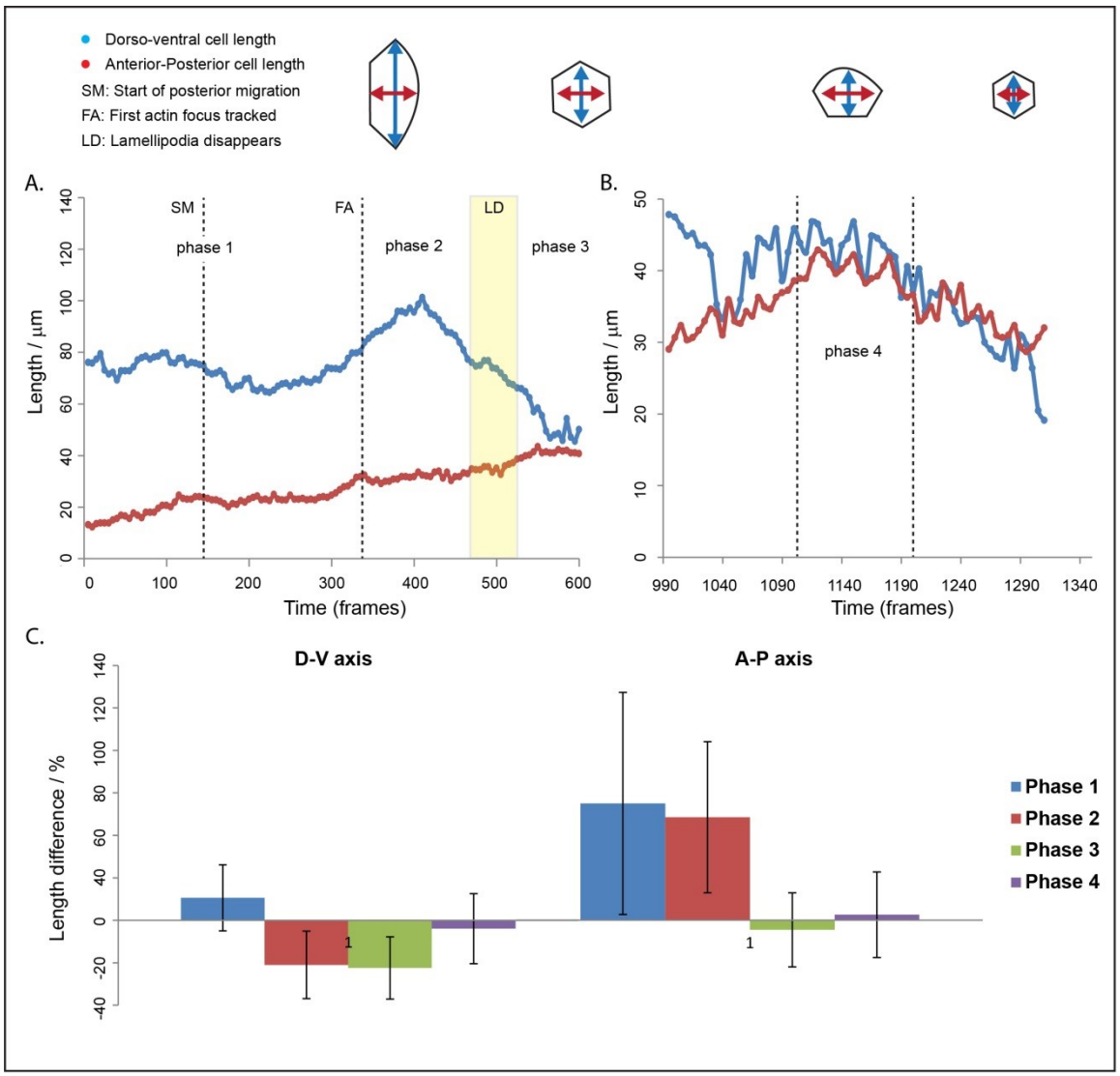

Figure 24. LECs shape changes throughout the different phasesof cell behaviour during abdominal morphogenesis

One representative cell is shown to illustrate the general trend found in all cells (Figure S6). **A)** Plot of the dorsal-ventral (D-V) length (blue line) and the anterior-posterior (A-P) length (red line) over time (N=7). The panel shows phases 1, 2 and 3 and the external features that help to identify each phase. **B)** Plot of the A-P and D-V lengths over time for a cell that enters phase 3, undergoes dorsal repolarisation and delaminates (N=3). **C)** Mean percentage of cell shape change along the A-P and D-V axes between the start and end of phases 1, 2 , 3 (N=7) and 4 (N=4). For values of the percentage of length difference see Tables S10 and S11.

Despite the variability between the different pupae analysed, LECs follow a pattern of shape changes. This pattern consists of a large reduction in the D-V length and an increase in the A-P length of posteriorly migrating LECs. These shape changes happen in the presence of actin foci, localising at the back of the cell while it becomes round. The round shape could be maintained by the presence of the centrally located foci during apical constriction.

Representing the position of foci and the shape of the cells over time helps visualising the relation between the foci localisation and the cell shape changes. Since the appearance of the first actin foci, LECs start to transition from a thin and long state, taking cell shape coefficient values around 0.1-0.4, to and intermediate state, where the cell is double the length along the DV axis. At this point, LECs finish migrating posteriorly and the first central foci appear. Then, the cell becomes progressively more round, taking values closer to 1 by the end of phase 3 (Figure 25A). The same pattern of cell shape changes throughout the process is observed in the GMA expressing pupae with *tub.Gal80ts* (Figure 25B). This shows that the transition from a cell that is actively migrating to a cell that apically constricts is progressive. This change in cell behaviour is related to the localisation of the periodic contractions of the actin cytoskeleton.

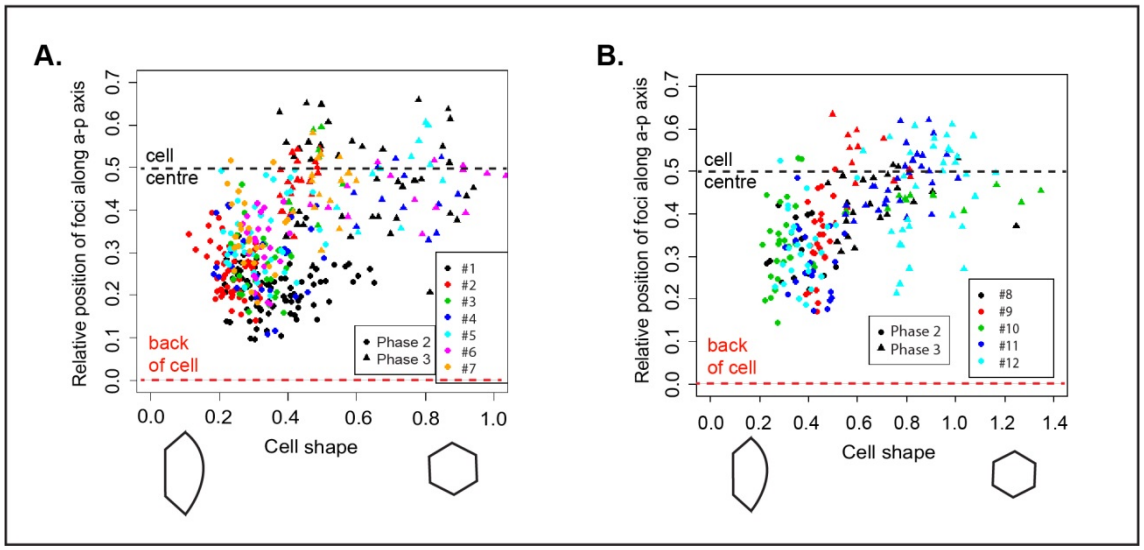

Figure 25. Relation between the relative position (RP) of actin foci and LEC shape.

A) Plot of the relation between actin foci relative position (RP) and cell shape coefficient of the different pupae analysed for cells expressing GMA (N=7) and **B)** for pupae expressing the GMA *tub.Gal80ts* (N=5).

Interestingly, LECs that express LifeAct-Ruby behave differently when they transit from migration to constriction. Actin foci are positioned similar to GMA expressing pupae (Figure 17B), however, LifeAct-Ruby expressing LECs change their shape only little when they constrict. In four out of the seven pupae, the difference in the cell shape coefficient between phases 2 and 3 is only 0.1 (Figure 26A). This suggests that the capacity of these LECs to change their shape might be affected. Unlike the pattern observed in GMA expressing LECs, cells keep approximately the same shape throughout the whole morphogenetic process, not rounding up while reducing their apical area (Figure 26B).

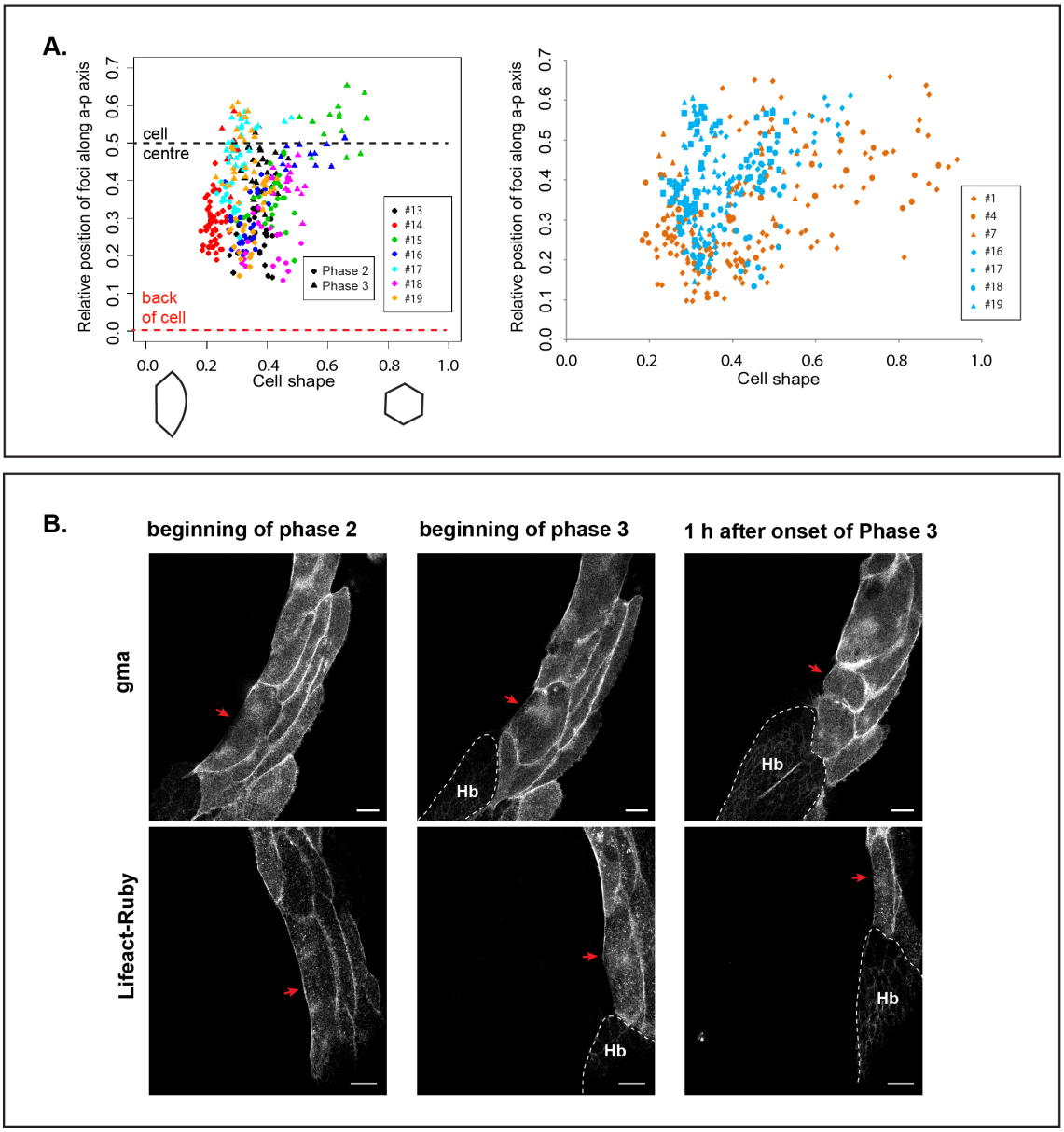

Figure 26. Comparison of LECs shape throughout phases 2 and 3 in LifeAct-Ruby and GMA expressing pupae.

A) (Left) Correlation of foci relative position (RP) and cell shape coefficient of e LifeAct-Ruby expressing LECs (N=7). (Right) Plot comparing GMA (green; N=3) and LifeAct-Ruby (red; N=4) pupae. **B)** Confocal images illustrating cell shape in GMA and LifeAct-Ruby expressing LECs. Scale bars, 20 μm. LifeAct-Ruby cells, as opposed to GMA, do not round up when they constrict (red arrow).

LECs in LifeAct-ruby expressing pupae appear to be less able to change their shape. This could be due to the effects of LifeAct-ruby on actin. It has been shown that LifeAct binds both F-actin and G-actin *in vitro*, with higher affinity for G-actin (Riedl et al., 2008b). Moreover, studies in *Drosophila* germline cells have shown that strong expression of LifeAct affects the cortical actin pool of cells (Spracklen et al., 2014). These defects could be due to G-actin sequestering and altering of the ability of other endogenous actin binding proteins (Spracklen et al., 2014). Thus, LifeAct could affect the cortical actin pool of LECs impairing changes in cell shape. Interestingly, medio-apical actin dynamics is not affected, and thus pulsed contractions appear not to be perturbed. This suggests that, independently from the medio-apical network, the cortical actin network plays an important role in mediating cell shape changes.

In summary, changes in cell shape correlate with the behaviour of the LECs as well as the behaviour of their pulsatile medio-apical cytoskeleton.

3.3.2.2 LECs apical area fluctuates differently through the distinct phases

In many systems it has been shown that pulsed contractions lead to a reduction in apical cell area (Blanchard et al., 2010; Martin et al., 2009; Solon et al., 2009). To gain insights into how LECs apically constrict, it is necessary to study the changes of the apical area of LECs over time and ask whether the apical area is indeed fluctuating. To tackle this question, the apical area of LECs during phases 1, 2 and 3 was measured over time:

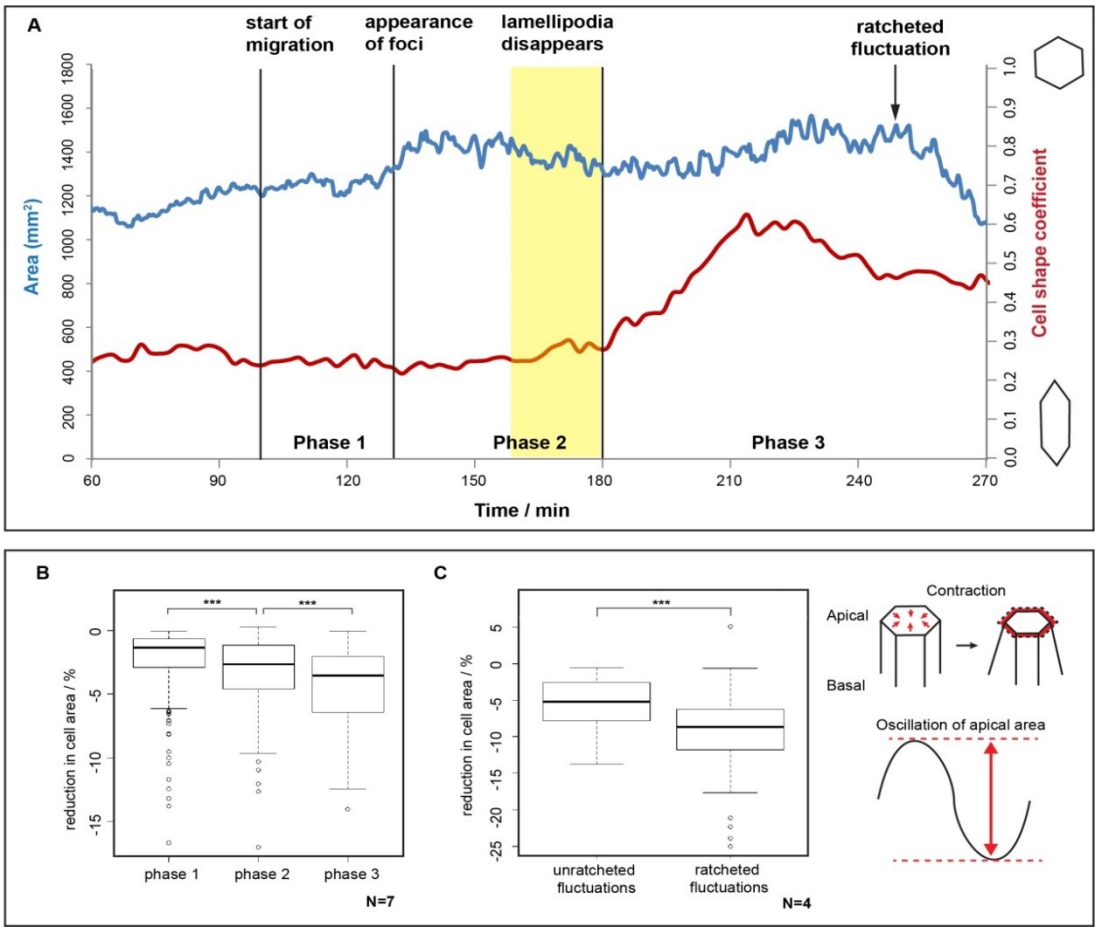

Figure 27. Analysis of the apical area of LECs during abdominal morphogenesis

A) Plots of the cell apical cell area (blue line) and the cell shape coefficient (red line) over time. Pupa #13 is shown as a representative cell to illustrate the general trend found in all cells (Figure S7 to S12). LECs increase their apical area during phase 1 and maintain it during phase 2 and 3. Sometime into phase 3, LECs start to reduce their apical area. During the whole process, the apical area of LECs fluctuates apically. **B)** Percentage of cell area reduction per apical area oscillation for phase 1 (-1.36 ± 0.09 %), phase 2 (-2.64 ± 0.22 %) and phase 3 (-3.55 ± 0.26 %) (N=7) **C)** Percentage of cell area reduction per area oscillation in non-ratcheted (-5.18 ± 0.43 %) and ratcheted (-8.68 ± 0.77 %) oscillations during phase 3 (N=4 pupae).

Phase 1. LECs increase their apical area during early migration (Figure 27A). On average, cells almost double it during this phase (Table 2). The apical area slightly fluctuates, with variations of low magnitude (on average 1.36 % of the apical area) (Figure 27B). These small fluctuations could be caused by the unorganised cytoskeletal activity observed prior to the formation of the first focus.

Phase 2. LECs significantly increase the magnitude of their apical area fluctuations (on average 2.64 % of the apical area) (Figure 27B) (Table S12 and S13). In terms of net apical area variations throughout this phase, LECs in average maintain their apical area as they become roundish (Table 2) (Figure 27A).

Phase 3. Apical area fluctuations are significantly higher in this phase compared to the previous phases considering individual pupae (Table S12 and S13) and combining all samples. On average, cell fluctuates by around 3.55 % of its apical area (Figure 27B). In terms of net apical area reduction, there are quite some variations. Some of the analysed LECs reduce their area around 50% whereas some others maintain it or even slightly increase it. The reason for the variation is that not all cells underwent delamination in the analysed time window (Table 2). Thus, recordings in which cell apical area could be analysed from the onset of phase 3 until delamination are studied. Apical area plots over time from LECs that went from phase 3 until final delamination show a clear change in trend, with apical area being reduced rapidly prior to delamination (Figure 27A) (Figures S13 to S16). This behaviour resembles the ratcheted fluctuations, where phases of constriction are stabilised leading to apical constriction (Martin et al., 2009). This behaviour has been observed before in embryonic cells during *Drosophila* gastrulation, which also show a transition in pulse behaviour, when unratcheted area fluctuations, which do not produce area reduction, transition to ratcheted oscillations (Xie and Martin, 2015). In LECs, throughout phase 3 the apical area oscillations are not translated into net apical area reduction (non-ratcheted phase 3) and only sometime into phase 3, rapid net apical area reduction begins (ratcheted phase 3) (Table 3). The average magnitude of area fluctuations during the non-ratcheted phase 3 amounts to 5.18 % of the apical area, whereas during ratcheted

phase 3 increases to 8.68 %, due to the net apical area reduction in each fluctuation (Figure 27C). The ratcheted fluctuations start when LECs are about 1588 ± 356 μm^2 (N=4), showing medio-apical actin foci until 24 ± 13 minutes before delaminating, when the apical area was only 234 ± 97 μm^2 in average (N=8). At this point, prior to delamination, LECs assemble large amounts of actin at their apical side, making tracking of the apical area impossible.

In summary, LECs during phase 1, 2 and early phase 3 show unratcheted fluctuations, where the reduced area is not stabilised and the cell does not apically constrict. These unratcheted fluctuations increase in magnitude throughout the different phases, being the largest during phase 3. Finally, during late phase 3, ratcheted constrictions produce apical area reduction leading to delamination.

It is worth mentioning that the percentage of apical area reduced per fluctuation during phase 3 (Figure 27B), measured using the pupae in which LEC delamination is not observed, is significantly smaller than the median calculated for the unratcheted phase 3 ($p=0.01$) (Figure 27C), using the set of pupae in which the transition to ratcheted fluctuations was observed. The percentage of area reduced is larger in the second group as LECs are in average smaller. Having the same absolute reduction of area per fluctuation, if LECs are smaller, the percentage of area it reduces will be bigger proportionally (Table S14). The smaller size of LECs from the second group of pupae could be due to the fact that when the area was started to be measured, the cell had already reduced its area without transitioning to ratchet fluctuations.

Movie	Change in area Phase 1 / %	Change in area Phase 2 / %	Change in area Phase 3 / %
#1	7.17	-6.38	-57.82
#2	61.547	6.75	0.58
#3	26.747	-30.10	2.95
#4	76.41	7.21	-39.52
#5	56.91	-3.73	7.53
#6	80.83	5.96	-11.05
#7	22.06	-4.91	-22.38
Average ± SD	47.38 ± 28.68	-3.60 ± 13.08	-17.10 ± 24.31

Table 2. Change in apical area during phases 1, 2 and 3

Change in cell apical area (in %) for each phase in GMA expressing cells (N=7). Values for each individual puape and average and standar deviation (SD) are shown.

Pupae	Difference in area non-ratcheted / %	Difference in area ratcheted / %
#20	63.51	-60.89
#23	6.48	-51.53
#24	-16.32	-76.73
#25	-3.67	-45.58
Average + SD	12.50 ± 35.26	-58.68 ± 13.58

Table 3. Change in apical area during ratecheted and non-ratcheted phase 3.

Change in apical area comparing non-ratcheted and ratcheted phase 3 in GMA expressing LECs (N=4). During non-ratcheted phase 3 almost no apical area is reduced, whereas during ratcheted phase 3, net apical area reduction starts. Values for each individual puape and average and standar deviation (SD) are shown.

3.3.2.3 LECs apical area fluctuations correlate with the presence of actin foci

One interesting question to ask is whether actin foci correlate with individual apical area fluctuations, which one would expect if the fluctuations and the reduction in area were a consequence of the periodic activity of the cytoskeleton. To this end, the number of actin foci per area fluctuation was counted during phase 2 and 3 and cell area fluctuations were studied in detail (Figure 28A). This analysis shows that during phase 2, 51 % of the area fluctuations correlate with the occurrence of one actin focus and during phase 3, 74 % (Figure 28B). Thus, in constricting LECs, more than in migrating LECs, cell area fluctuations correlate with the presence of one focus.

Apart from the fluctuations that correlate with foci, there are other fluctuations during which no foci occurred. 22.40 % of the area fluctuations did not coincide with any actin focus (Figure 28B). Classifying area fluctuations by duration, a high percentage of these area fluctuations are very short, between 60-90 seconds long (Figure 28B). Interestingly, these short area fluctuations did not reduce the apical area much, both during phase 2 and 3 (Figure 28C), producing a similar area reduction than the ones observed during phase 1 ($p=0.6$), when no foci are observed. Other fluctuations are longer, more than 90 seconds. These medium length area fluctuations represent a high percentage of the fluctuations that contain foci (Figure 28B) and also produce stronger area reductions compared to the short fluctuations in both phases 2 and 3 (Figure 28C). These results suggest that the majority of apical cell area fluctuations which occur without any foci are short non-contractile (s.n.c), which might be driven by other cytoskeletal activity, such as flows of actin, or external factors, like forces exerted by neighbours.

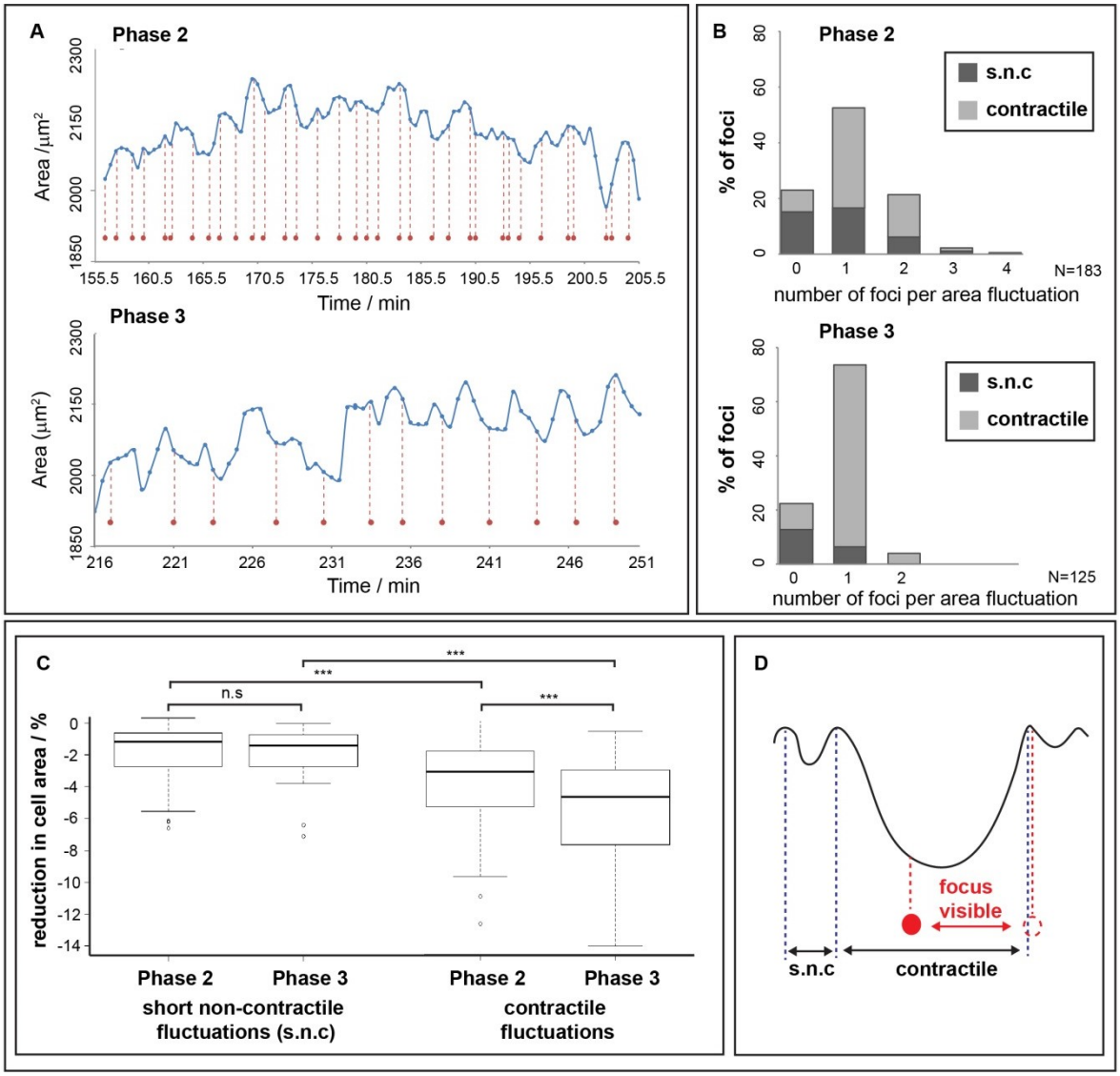

Figure 28. Analysis of the apical area fluctuations of LECs during phase 2 and 3

A) Apical area of LECs expressing GMA over time during phase 2 and 3. There are differences in the magnitude of the area fluctuations. Some of the fluctuations coincide with foci (red dots) and some not. **B)** Number of foci per apical area fluctuation during phase 2 and 3, differentiating between short non contractile (s.n.c) and contractile fluctuations. For values of the percentages see Table S15. **C)** Comparison of the reduction in cell apical area between s.n.c and contractile fluctuations during phases 2 and 3. The medians for the s.n.c area fluctuations are not statistically significant (phase 2= -1.19 ± 0.21 %; phase 3= -1.41 ± 0.37 %, p=0.54). The medians for the contractile fluctuation are significantly different between phases (phase 2= -3.14 ± 0.24 %; phase 3= -4.72 ± 0.50 %, p=0.0001). **D)** The number of actin foci per area fluctuation was calculated counting the foci located between the crests of each area fluctuation. When actin foci assemble, remain visible for 30-60 seconds. This could cause, depending on the time point in which the focus was tracked, the coincidence of a focus with a s.n.c fluctuation, leading a contractile fluctuation without focus associated.

A small proportion of short fluctuations correlates with one or more foci (Figure 28B), contradicting the hypothesis presented above. However, the apical area reduction of these short area fluctuations that coincide with actin foci is similar to the ones that do not (Table 4). Similarly, a few medium length fluctuations do not coincide with any foci (Figure 28B), but produce the same area reduction as the ones that coincide with a focus (Table 4). This suggests that the short non-contractile fluctuations that coincide with foci or contractile fluctuations without any associated foci are a consequence of the fact that the analysis entails an error. Actin foci assemble and remain visible for 30 to 60 seconds. Depending on the time point at which the focus was tracked, it could have coincided with the previous or following fluctuation, coinciding with a short fluctuation and leaving a medium length fluctuation without foci associated (Figure 28D).

	Fluctuations no foci. Area reduction / %	Fluctuations 1 focus. Area reduction / %	Fluctuations 2 foci. Area reduction / %	p-value
Short (phase 2)	-1.25 ± 0.47	-1.20 ± 0.34	-0.89 ± 0.41	0.57
Medium (phase 2)	-2.51 ± 0.44	-3.30 ± 0.40	-3.34 ± 0.81	0.25
Short (phase 3)	-1.23 ± 0.46	-2.04 ± 0.52	None	0.12
Medium (phase 3)	-4.58 ± 0.89	-4.60 ± 0.48	-7.37 ± 2.35	0.30

Table 4. Median percentage of apical area reduction for the area fluctuations observed during phases 2 and 3 respectively, depending on their length and the presence of actin foci.

Study of the magnitude of the cell apical area fluctuations depending on their time length and the presence of foci during phases 2 and 3. The average percentage of apical area reduction is not significantly different between the fluctuations that do not coincide with any focus and the ones that coincide with one or more than one focus in short length (60-90 seconds) and medium length (120-300 seconds) fluctuations during phase 2. Similarly, during phase 3 there is no significant difference either between the short length and medium length fluctuations that do not coincide with any focus and the ones that coincide with one or more than one focus.

Furthermore, during phase 2, a considerable percentage of fluctuations coincide with more than 1 focus (Figure 28B) and are less extensive in average compared to phase 3 (Figure 28C). This agrees with the observation that during migration, two foci accumulate in the back of the cell. If an actin focus represents a contractile event in which tension is generated, the medially or laterally located actin foci might pull the membranes only locally. This could produce the observed weaker and less regular apical area fluctuations.

During apical constriction, the percentage of area fluctuations that coincided with more than 1 focus is very low (Figure 28B). The concentration of the whole medio-apical contractile network in a single central accumulation might pull the membranes more evenly, generating the observed extensive apical area fluctuations.

Moreover, the observation that the single central foci assemble on average 30 ± 15 seconds before the trough of the apical area fluctuation (N=4 pupae, 118 foci) suggests, more clearly than in migration (phase 2), that foci cause apical area fluctuation.

In summary, there are two types of periodic apical area fluctuations during posterior migration and apical constriction of LECs, the short and weak fluctuations, probably produced by the extra-cellular environment and the longer and stronger fluctuations, produced by the actin foci.

3.3.3 Analysis of the spatio-temporal distribution of Myosin and Rho associated kinase (Rok)

Force generation not only depends on the organisation of the actin meshwork but requires specific Myosin localisation, as Myosin on actin filaments is what produces the force that drives many morphogenetic events (Bertet et al., 2004; Blankenship et al., 2006; Dawes-Hoang, 2005; Lecuit and Lenne, 2007; Montell, 2008; Young et al., 1991). In particular, during the pulsed contractions that drive non-continuous cell shape change in many *in vivo* systems, Myosin and Actin co-localise in the periodic medial flows and foci observed in the medio-apical side of cells (Blanchard et al., 2010; Martin et al., 2009; Rauzi et al., 2010).

Visualising the localisation of Myosin using Spaghetti squash-GFP (Sqh-GFP; Myosin-II Regulatory Light Chain) within the whole second segment during abdominal morphogenesis reveals that firstly, LECs accumulate Myosin at the cell cortex before the start of migration (Figure 29A) and maintain a cortical pool of Myosin throughout the whole process. A multicellular cable of Myosin clearly separates the A from the P compartment, forming a straight compartment boundary between LECs (Monier et al., 2010; Umetsu and Dahmann, 2010) (Figure 29A). This distinct accumulation of Myosin at compartment boundaries have been observed in the *Drosophila* wing disc and suggested to actively contribute to compartmentalisation by generating contractile tension (Major and Irvine, 2006). Within each cell, the spatio-temporal organisation of Sqh::GFP becomes highly dynamic during posterior migration at the apical side of LECs. Similar to Actin, Sqh::GFP bundles coalesce to form foci, assembling and disassembling periodically. These multiple Myosin foci also localise in the back of the cell. Furthermore, Sqh::GFP also shows fibre-like structures at back of the cell during posterior migration (Figure 29B). These fibre-like structures resemble the contractile bundles described as stress fibres in sarcomeres (Kreis and Birchmeier, 1980), or the contractile bundles observed in follicle cells, in which Myosin accumulates in parallel fibres at the basal side of cells acting like a corset, with transient foci that assemble and disassemble (He et al., 2010). After lamellipodia disappears, Sqh::GFP periodically accumulates in the centre of the cell, forming a single focus. The stress fibre-like

structures during constriction irradiate from the centre to the membranes (Figure 29C).

The dynamics and localisation of Sqh::GFP is very similar to the one of Actin. To test whether the described F-actin dynamics is produced by the action of Myosin, the spatial distribution of both proteins was studied in LECs co-expressing Sqh::GFP and LifeAct-Ruby. The fluorescence intensity distribution of both markers along the region in which foci accumulate show that Sqh::GFP and LifeAct-Ruby foci co-localise during posterior migration and during apical constriction (Figure 29D).

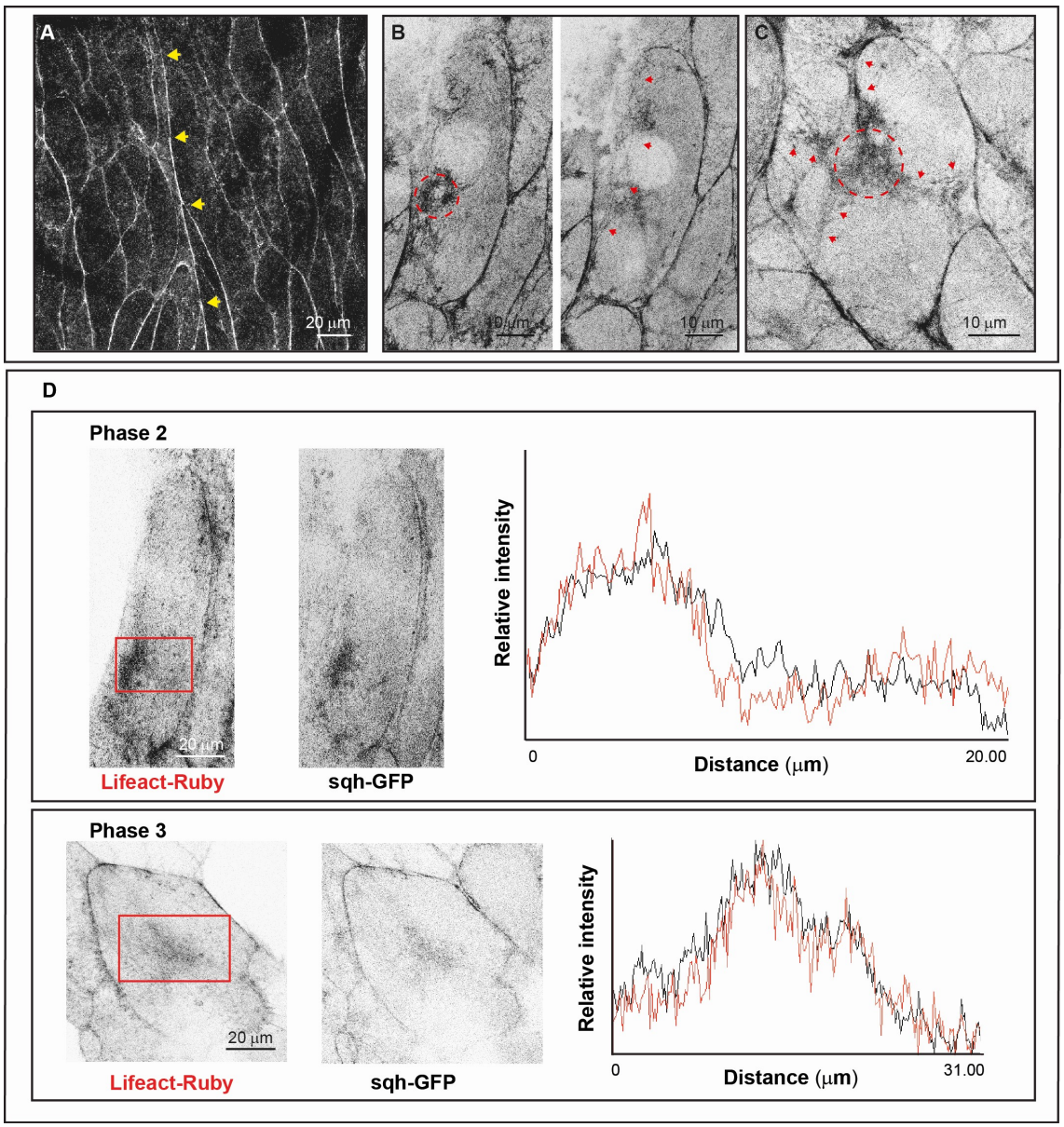

Figure 29. Spatial and temporal organisation of Myosin-II during abdominal morphogenesis.

A) Image showing LECs from the second segment of the abdomen expressing Sqh::GFP to label Myosin. A multicellular cable, marked with yellow arrows, separates the A (left) and P (right) compartments. **B)** Stills from a migrating LEC and a **C)** constricting LEC expressing Sqh::GFP. The red circle outlines the area in which the myosin foci accumulate. Red arrows indicate the stress fibre-like structures. **D)** Images of LECs expressing LifeAct-Ruby to label Actin and Sqh::GFP to label Myosin-II during phases 2 and 3. The plot profiles measured for both markers in the square drawn in the image show that the two proteins co-localise when a focus is formed.

The Rho associated kinase (Rok), which phosphorylates Myosin-II, also displays a similar dynamics and distribution within the cell. Visualising Rok::GFP shows that the kinase constantly localises to the cortex of LECs throughout the whole process, just like Sqh::GFP does. Also the medial pool of Rok::GFP is highly dynamics, showing pulsatile behaviour. Rok::GFP forms transient foci that assemble in the back of the cell during posterior migration and in the centre during apical constriction, with the presence of a single focus. Rok::GFP also co-localises with LifeAct-Ruby foci during phases 2 and 3 (Figure 30).

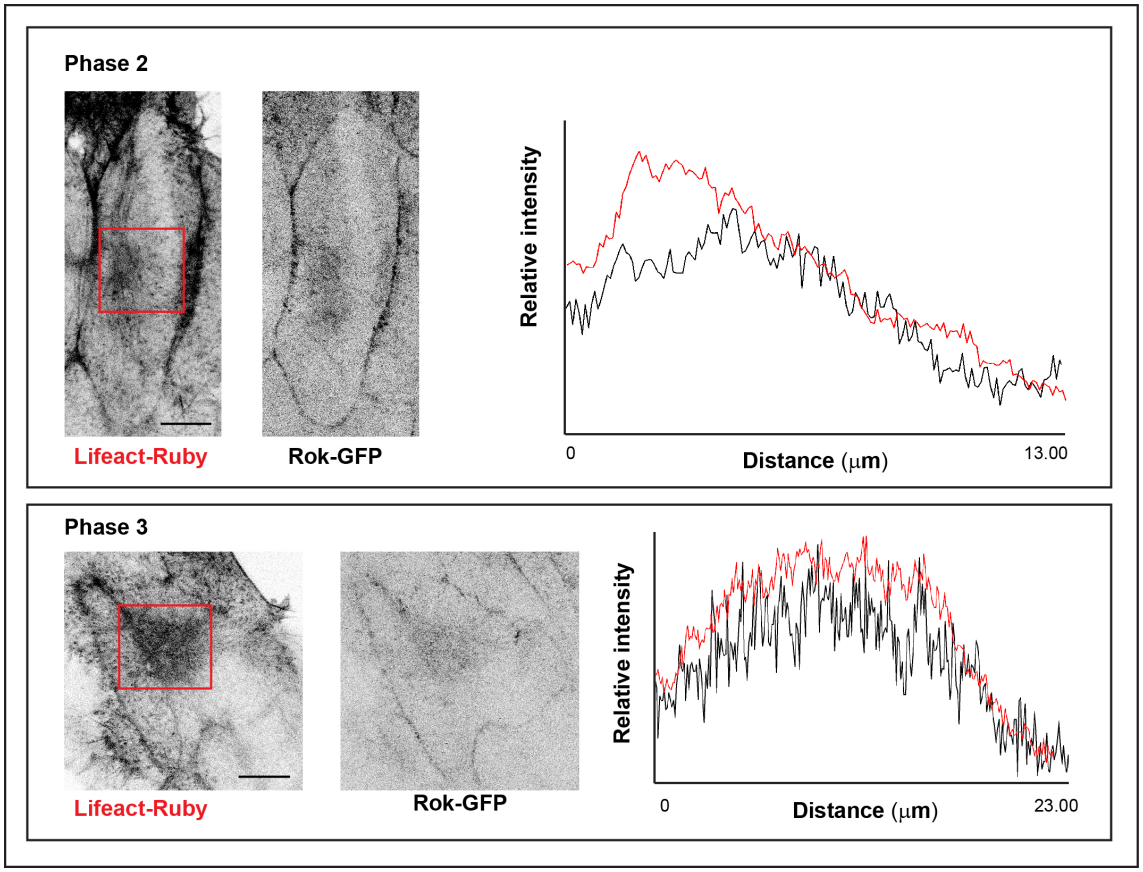

Figure 30. Analysis of the spatial and temporal organisation of Rok during phases 2 and 3.

Images of a LEC expressing LifeAct-Ruby to label Actin and Rok-GFP to label the Rho associated kinase (Rok) during phases 2 and 3. Scale bars, 20 μm. The plot profiles measured for both markers in the square drawn in the image show that the two proteins co-localise when a foci is formed.

The co-localisation of Actin, Myosin-II and Rok suggests that in LECs foci assembly is a consequence of active Myosin pulling on actin filaments, mediated by Rok, as described in other systems.

3.4 Discussion

The morphogenesis of the abdomen of *Drosophila* provides a very good framework to study the role of the cytoskeleton in coordinating cell behaviour. The size of the larval epithelial cells allows a very detailed visualisation of cytoskeletal dynamics when cells coordinate migration with apical constriction. During this coordination of behaviours, the actomyosin cytoskeleton becomes pulsatile, showing periodic accumulations of actin that appear in LECs during posterior migration (Figure 16A). This pulsatile dynamics of the cytoskeleton has been observed previously in many other tissues in *Drosophila*, *C.elegans* and vertebrates (Blanchard et al., 2010; He et al., 2010; Kim and Davidson, 2011; Martin et al., 2009; Munro et al., 2004; Rauzi et al., 2010; Roh-johnson et al., 2012). However, it is the first time that these periodic foci are observed to follow a pattern of localisation within the cell (Figures 17 and 19). The localisation of foci correlates with a pattern of cell shape changes when the cell transitions from migration to apical constriction (Figures 24 and 25). During this transition, the cell apical area fluctuates (Figure 27), coinciding with the presence of the actin foci (Figure 28A, B), until it is completely reduced, prior to delamination.

Pulsed contractions in LECs are a consequence of actomyosin contractility

The periodic contractile activity of the cytoskeleton of LECs appears to be a consequence of the activity of Myosin pulling on actin filaments, as both proteins spatially co-localise in the periodic foci observed during migration and apical constriction (Figure 29D). The fact that pulsed contractions are caused by Myosin has been proposed in all of the *in vivo* systems in which pulsatile behaviour of the cytoskeleton is observed (Blanchard et al., 2010; He et al., 2010; Kim and Davidson, 2011; Martin et al., 2009; Munro et al., 2004; Rauzi et al., 2010). Also, Myosin has been shown to be essential to produce contractility *in vitro* (Bendix et al., 2008). Rok co-localises with Myosin and Actin during the formation of foci (Figure 30).This pulsatile dynamics of Rok have been previously observed in germband cells and proposed to be a consequence of the advection generated by the contractile Myosin speckles moving in the plane of the actin meshwork. This advection generates a positive feedback,

activating more motors and increasing contractility (Munjal et al., 2015). Thus, the co-localisation of Actin, Myosin and Rok suggests that foci are generated by the action of the kinase, activating Myosin. Myosin pulls on the actin cytoskeleton, producing the formation of an Actin, Myosin and Rok focus.

Foci are found to assemble with constant periodicity, with individual foci assembling approximately every 180 seconds. Interestingly, during migration two foci assemble on average every 180 s, alternating every 90 s, and during constriction only one focus assemble every 180 seconds (Figure 22B). Hence, the fact that having two alternating foci or one single focus does not change the fact that each individual focus assembles every 180 s, suggests that foci periodicity seems to depend on network dynamics rather than an external pulse generator that determines when the foci are assembled.

In addition, during migration, there is an exchange of contractile flows between the two assembling foci (Figure 16C). During late migration and constriction, the contractile flows of actomyosin begin in the periphery and move towards a single focus (Figure 16D). Despite requiring further study, the orientation of the actomyosin flows suggests that, although that the periodicity of the contractile events depends on network dynamics, the location of these pulsed contractions might also be determined by an external input.

LECs cytoskeleton change in polarity correlates with cell behaviour

Migrating LECs are planar polarised (PCP) (Bischoff 2012) and so is their actomyosin cytoskeleton, with the contractile network localising anteriorly. The planar polarity of the cytoskeleton changes to a radially polarised (RCP) actomyosin meshwork when migration cease, with foci accumulating at the centre. The polarisation of the contractile network has been described in cells with one type of polarity, with PCP during junctional remodelling (Rauzi et al., 2010) and RCP during apical constriction (Mason et al., 2013), but it is the first time in which a change in polarity has been described. During apical constriction, the data suggests that LECs change from a PCP to a RCP actomyosin network. How LECs establish this change in polarisation needs further investigation. However, this RCP could explain the localisation of the

actomyosin contraction towards the centre. As previously observed in ventral furrow cells, the radially polarised actin cytoskeleton has been proposed to help in localising Rok at the centre of the cells, transported in Myosin flows towards the centre. The actin's cytoskeleton RCP requires the function of Dia (Coravos and Martin, 2016).

Also during dorsal migration, the cytoskeleton repolarises to the "new" back of the cell (Figure 19). The mechanisms that control this repolarisation are not known, but it could be related to a signalling interaction between LECs and histoblasts, as the event appears to rely on the vicinity of both cell types (Bischoff 2012).

Apart from the pulsed contractions, stress fibre-like structures, visible when expressing Sqh::GFP, localise to the back of the migrating LECs (Figure 29B). These stress fibre-like structures, consisting of Sqh::GFP decorating actin bundles, repolarise after migration, irradiating from the centre towards the junctions (Figure 29C). Thus, the change in cytoskeletal polarity is not only evident by the organisation of the pulsed contractions, but also by other cytoskeletal structures.

The change in cytoskeletal polarity correlates with cell shape changes

The results show that LECs follow a pattern of cell shape changes, consisting on the reduction of the D-V length and the increase of the A-P length during behavioural transition. The start of the pulsatile behaviour of the cytoskeleton during migration and the formation of these stress fibre-like structures could facilitate the cell shape changes required for the transition to apical constriction. During migration, the two actomyosin foci accumulating at the back could act as a mechanism to produce tension and the fibre-like structures a mechanism to maintain it, generating the reduction in the D-V length and allowing the expansion along the A-P axis. During constriction, the tension produced by the single central foci would be translated to the junctions through the radially polarised cytoskeletal organisation to maintain a round cell. Although further studies should be done to quantify the tension levels along both cell axes, this mechanism could serve as a structure to increase stiffness and ensure cell shape change.

Also the cortical pool of actomyosin, present throughout the whole process (Figures 29D and 30), could play a role in facilitating cell shape changes.

Pulse contractions correlate with apical area fluctuations

Like in other systems, cell area fluctuations and pulsed contractions of the cytoskeleton correlate. During posterior migration, the apical area fluctuations are weaker and short, probably produced by the presence of two alternating foci. During constriction, when foci localise centrally, the area fluctuations becomes stronger and the periodic foci correlate, more than during migration, with the apical area fluctuations, preceding the through (Figure 28B, C). The increase in actomyosin fluorescence preceding contraction have been observed in other morphogenetic systems (He et al., 2010; Martin et al., 2009; Rauzi et al., 2010) and strongly suggests that actomyosin foci generate apical area fluctuations.

LECs apical area fluctuations go through two phases: unratcheted and ratcheted. During migration and early stages of phase 3, the contraction of the apical area is followed by an almost equal relaxation, the unratcheted phase. At later stages, when LECs are around 1500 μm^2, the ratcheted phase starts and the net apical area is reduced between pulsations, leading to apical constriction.

The mechanisms that control the transition from unratcheted to ratcheted fluctuations in LECs are unknown. In dorsal closure, cells progressively decrease in amplitude coinciding with a decrease in the period between the actomyosin foci when comparing early and late stages of the closure, showing that network dynamics change over development producing apical area reduction over many cell constrictions (David et al., 2010). During abdominal morphogenesis the area fluctuations that coincide with actin foci have cycle lengths that range from 2-5 min. However, neither the fluctuation cycle lengths, nor the periodicity of foci increase in frequency over time. The comparison between different systems in which transient cell contractility is observed suggest that the threshold fluctuation cycle length above which cells start to contract is around 2-3 min, and an increase in the frequency is associated with increased contractility (Gorfinkiel and Blanchard, 2011). The magnitude of LECs fluctuation cycle length is

near the threshold of contractility, which suggests that the area fluctuations could contribute to apical constriction. The absence of a frequency increase over development and the increase of the amplitude of area fluctuations suggests that the mechanism by which LECs increase their contractility is different. In ventral furrow cells, the mechanism by which cells transition to ratcheted fluctuations is thought to consist on a molecular "clutch", that would be engaged coupling the force generating by the pulse contractions to the AJs (Roh-johnson et al., 2012). This molecular "clutch" could be present in LECs and engaged during ratcheted phase 3, transmitting the force generated by the centrally located pulsed contractions. Furthermore, the cortical pool of actomyosin could play a role in apical constriction, as shown in AS cells (Martin et al., 2010), by generating tension and stabilising cell apical area deformations.

In summary, the actomyosin contractile network in LECs is highly dynamic and the change in the polarity of the network underlies a behavioural change. A better understanding of the mechanisms underlying this differential localisation, as well as the contribution of the periodic actomyosin foci and the cortical actomyosin pool to cell migration, apical constriction and the transition between the two behaviours requires further study.

4. Study of the role of Myosin dynamic activation on cytoskeletal organisation and LEC behaviour

4.1 Introduction

Non-continuous cell deformations have been found to drive cell shape changes in many different systems. These deformations require the generation of pulsed contractions, produced by periodic cycles of assembly and disassembly of the actomyosin cytoskeleton of cells. When these deformations are combined with steps of stabilisation, irreversible cell shape changes are achieved (Blanchard et al., 2010; He et al., 2010; Martin et al., 2009; Rauzi et al., 2010). Although operating in many different systems (Coravos et al., 2017; Gorfinkiel and Blanchard, 2011), the functioning details of this ratchet mechanism remain unclear.

One of the components that has been found to be crucial for pulsatility is Myosin regulation (Munjal et al., 2015; Valencia-Expósito et al., 2016). The generation of forces depend on Myosin activity. The studies in apical constriction suggest that Myosin needs to be activated and localised apically and, ultimately, this depends on the presence of the Myosin-II kinase, Rok, which becomes a crucial actor for tissue remodelling (Levayer and Lecuit, 2012; Sawyer et al., 2010). As introduced in Chapter 3, the generation of actomyosin pulses depends on Rok mediated phosphorylation, which associates Myosin monomers into minifilaments to initiate contractility of the network (Blanchard et al., 2010; He et al., 2010; Martin et al., 2009; Rauzi et al., 2010). Nevertheless, not only the activation of Myosin is required for pulsatility of the cytoskeleton and tissue morphogenesis. Myosin also needs to be deactivated. Interestingly, recent studies in *Drosophila* germband extension have found that dephosphorylation of Myosin by the phosphatase, Mbs, apart from being important for generating normal morphogenesis (Kasza et al., 2014), is crucial for pulse disassembly (Munjal et al., 2015). In germband cells, Rok and Mbs spatially co-localise with Myosin periodic foci. Rho 1 also shows transient foci that spatially co-localise with its downstream effectors in these cells (Munjal et al., 2015). Importantly, it has been found that the inhibition of Rok blocks the pulsatile activity of Rho 1, discarding the possible role of Rho1 as an upstream pacemaker (Munjal et al., 2015). As an

alternative, Munjal *et al.* (2015) propose a self-organised model in which biochemical regulation of Myosin and advection drive network oscillatory behaviour. In this model, Rok and Myosin phosphatase are required for the biochemical regulation of Myosin, recruiting and dissociating the motors from the apical side of germband cells, respectively. Advection, the movement of speckles of Myosin along with F-actin in the apical plane, also transports Rok molecules into the assembling focus, activating more Myosin and generating a positive feedback that enhances foci assembly. Advection eventually slows down due to the densification of the actomyosin network, reducing the activation of motors. This creates a negative feedback in which the phosphatase mediated dissociation of motors supersedes advection, leading to pulse disassembly (Figure 31) (Munjal et al., 2015). Live imaging of the Mbs and Rok reporters in amnioserosa cells during dorsal closure also show that both co-localise with the medio-apical foci. These observations suggests that the model proposed above could be a general mechanism for the emergence of the oscillatory behaviour of actomyosin networks (Duque and Gorfinkiel, 2016).

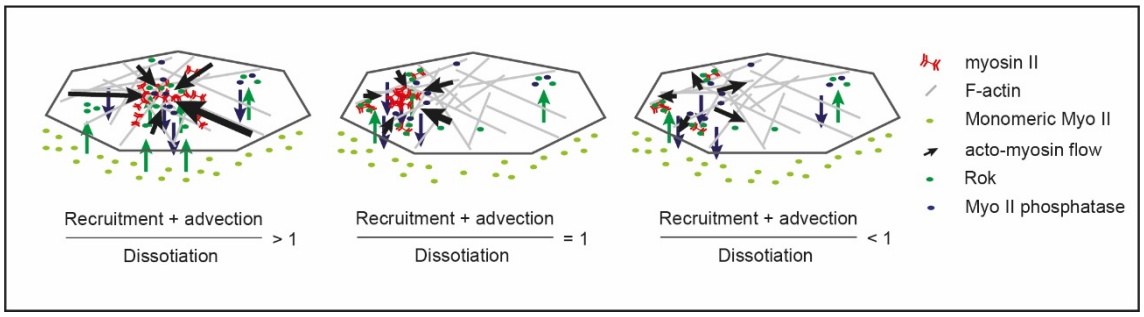

Figure 31. Pulsatility depends on a self-organised biomechanical network in germband cells

Figure modified from Munjal *et al.* 2015. Pulse assembly and disassembly model in germband cells. Pulsatility requires a self-organised system that involves positive and negative biomechanical feedback between Myosin advection and dissociation rates. Advection promotes the recruitment of myosin motors. When the densification of the network reduces advection, and thus recruitment, dissociation supersedes advection, driving pulse disassembly.

During abdominal morphogenesis, LECs show a pulsatile pool of Rok, which co-localises spatially and temporally with the actomyosin foci, suggesting that the same biomechanical mechanism could explain the dynamics of the cytoskeleton in LECs. Interfering with the dynamic phosphorylation of Myosin and studying the spatial and temporal organisation of the cytoskeleton under these conditions can inform us of how the foci are generated and the role of these foci in coordinating cell behaviours.

4.2 Methods

4.2.1 *Drosophila* stocks

Transgene	Flybase entry
UAS.gma	Moe$^{GMA.Scer\UAS.T:Avic\GFP-S65T}$(Bloor and Kiehart, 2001)
UAS.rok-RNAi	*Rok^{KK107802}* (VDRC 104675) (Dietzl et al., 2007)
UAS.MbsN300	Mbs$^{N300.Scer\UAS}$(Lee and Treisman, 2004)
hh.Gal4	Scer\GAL4$^{hh-Gal4}$
	sqh^{AX3}(Jordan and Karess, 1997)
Sqh::GFP	*sqh$^{RLC.T:Avic\GFP-S65T}$*(Royou et al., 2004)
mCD8-GFP	(Lee and Luo, 1999)

Table 5. Summary of the transgenes used for the experiments performed for this chapter.

The left column corresponds to the abbreviated nomenclature used throughout the text and the right column to their entry in www.flybase.org(Gramates et al., 2016).

The RNAi line was obtained from the Vienna *Drosophila* RNAi centre (VDRC) (Dietzl et al., 2007). The following stocks were used to visualise the actin cytoskeleton in LECs that express different UAS-transgenes in the P compartment: 1) *y,w,hs.FLP;UAS.rok-RNAi/UAS.gma;hh.Gal4/+*: These flies express in the P compartment GMA to label the F-actin and Rok-RNAi, to target the knock-down of endogenous Rok messenger RNA. 2) *y,w,hs.FLP;UAS.MbsN300/UAS.gma;hh.Gal4/+*: These flies express in the P compartment GMA and a truncated form of the Myosin phosphatase, which consists of the N-terminal 300 amino acids of Mbs. This truncated form of the phosphatase has been shown to be constitutively active (Lee and Treisman, 2004).

The following stocks were used to visualise the behaviour of LECs that express the UAS-transgenes in all LECs: 1) *y,w,hs.FLP; UAS.rok-RNAi/tub<CD2<Gal4,UAS.FLP,UAS-mCD8-GFP ; + / +* :After heat shock, the recombinase Flippase (FLP) removes CD2 by FLP-out, preferentially in the LECs but not in the diploid histobloasts (Ninov et al., 2007). This activates *tub.Gal4* leading to the expression of *rok-RNAi* and mCD8-GFP. *mCD8-GFP* is a marker that labels the membranes of cells (Lee and Luo, 1999). In

addition *UAS.FLP* is expressed, which increases expression levels (Bischoff 2012). 2) *y,w,hs.FLP; UAS.MbsN300/tub<CD2<Gal4,UAS.FLP,UAS-mCD8-GFP:* These flies express MbsN300, FLP and mCD8-GFP after heat shock.

To perform Chromophore-assisted laser inactivation (CALI) on Myosin-II, the following stock was used: *w,sqh [AX3]; sqh::GFP; sqh::GFP.*

4.2.2 Temporal control of the expression of UAS lines

In order to induce clones in the LECs, a 37.4-37.8 °C heat shock was performed for 15 minutes on 3rd instar larvae 24 hours prior to recording and stored in a 25 °C incubator.

4.2.3 4D microscopy

Recordings of single LECs were performed on the same region described in Chapter 3 (Figure 15). The size of the recording area was specifically selected to ensure the recording of the whole process. Z-stacks of 5-30 μm with a step size of 1 μm were made every 30 seconds with a 512 x 512 pixels resolution. Short higher resolution recordings to see the behaviour of the actin cytoskeleton in detail used a Z-stack of 5-10 μm with a step size of 0.2-0.5μm, made every 10-15 seconds with a 1024 x 1024 pixels resolution and using a 63x objective.

Recordings of the behaviour of all cells from A2 focused on the dorsal side of the abdomen, in a region that included a hemisegment of segment A2. Z-stacks of 15-30 μm with a step size of 2.5μm were made every 150 seconds with a 512 x 512 pixels resolution using a 20x objective.

All pupae were recorded using a Leica SP8 confocal at a temperature of 25 ± 1 °C.

4.2.4 CALI experiments and conditions

To inactivate *in vivo* the function of Sqh::GFP in LECs, Chromophore-assisted laser inactivation (CALI) was used. CALI selectively inactivates engineered proteins bound to a fluorophore, using laser irradiation at a wavelength of light absorbed by the fluorophore but not by other proteins (Jay, 1988). The irradiated fluorophore produces highly reactive free radicals, including reactive oxygen species (ROS) that inactivate the proximate proteins (Jacobson et al., 2015). The inactivation of the protein is very

dependent on the distance between the fluorophore and the target protein, having no significant effect beyond 60 Å (Linden et al., 1992). CALI of Sqh::GFP has been shown to work in embryonic cells in *Drosophila* (Monier et al., 2010).

CALI was used to inactivate Sqh::GFP in LECs of the posterior compartment of A2. CALI was performed using a Leica SP8 confocal with a 50 mW argon laser set at 80% of its power. To study the effect of Myosin inactivation in the ability of cells to apically fluctuate their area, LECs were recorded before and after CALI. For image acquisition, GFP was excited using the 488 nm laser line at 1–3%. For CALI, to excite GFP maximally and to produce high levels of reactive oxygen species, both the 477 nm and 488 nm laser lines were set at 80% (Monier et al., 2010). CALI experiments were performed using the Leica AF LAS software (Leica, Mannheim, Germany) FRAP assistant with the following parameters: pixel time 1.2 µs; scan speed, 400 Hz; number of scans per frame, 1; pinhole, 1 airy unit. Before CALI, the cell was recorded choosing a Z-stack to visualise the apical side of LECs for 40 iterations every 5-9 s. Then, CALI was performed using a loop consisting of 2 high intensity scans to inactivate Sqh::GFP in a ROI placed at the centre of the cell and one image acquisition of the apical side of the cell, using the previous Z-stack settings. The loop was run for 40 iterations with the same time interval used before CALI.

4.2.5 Cuticle preparation

Hoyer's medium

15 g of gum Arabic were added to 25 mL of water in a glass beaker. The solution was heated to 60°C, stirring overnight on a magnetic stirrer. Successively, 100 g of chloral hydrate were added. After chloral hydrate had dissolved, 10 g of glycerol were added. The solution was centrifuged for 30 min at 10,000g and stored at room temperature. Shortly before use, 1 ml was transferred into an Eppendorf tube and centrifuged in a table top centrifuge for at least 15 min to pellet undissolved particles. The supernatant was used for preparation of cuticles. (Modified after: doi:10.1101/pdb.rec12429 Cold Spring HarbProtoc 2011.)

Cuticle preparation and visualisation

After recording, the Rok-RNAi or MbsN300 pupae that presented a dorsal cleft phenotype (unfinished abdominal closure) visible under the stereo-microscope, were dissected. The pupae, kept in 70 % ethanol, were transferred to a Petri dish and the dorsal cuticle of the abdomen was dissected with a razor blade. The section was placed on a drop of Hoyer's medium on a microscope slide. Pictures were obtained using transmitted light imaging with a Leica SP8 confocal.

4.2.6 Analysis of 4D microscopy

4.2.6.1 Analysis of CALI

The effect of Myosin inactivation on LECs pulsatile behaviour was studied by tracking the apical area of cells and calculating the magnitude of area oscillations before and after CALI.

4.2.6.2 Analysis of single LEC recordings

The recordings of pupae were selected for analysis when at least one of the LECs was clearly visible during the process and the pupae developed into a pharate adult or hatched. Only one LEC was analysed per recording.

For the analysis of the recordings of pupae expressing actin markers and Rok-RNAi or MbsN300, the development of the abdominal epidermis could not be divided into the 4 phases established in chapter 3, as in some pupae foci are not observed. Instead, the process was divided into migration and apical constriction. Recordings of pupae used in this chapter are listed in TableS16 (Rok-RNAi) and TableS17 (MbsN300). To study pulsed contractions, kymographs and manual tracking of the spatial-temporal coordinates of actin foci and their membranes was used. The percentage of cell shape change along the A-P and D-V axes was measured and analysed in pupae in which migration was visible from the start until the lamellipodium disappears. The quantification of the percentage of cell length change along the A-P and D-V axes was done using equation (4) during migration and constriction. For migration, the cell shape change was calculated between the start and end of migration; for constriction,

between the start and the first 75 min of constriction. This time intervals were chosen in order to maximise the number of pupae that could be analysed, as some could not be tracked until delamination. The tracking of the apical area of LECs was done 25 minutes before and 75 min after the lamellipodium had disappeared for 30 consecutive minutes. This maximized the number of pupae that could be analysed, providing a representative sample of the apical area of LECs over time during migration and apical constriction without having to manually track the area of LECs for the whole process.

The values for the relative position (RP) of foci, the cell percentage of cell shape change along the A-P and D-V axes and the magnitude of the apical area oscillations were obtained using the equations described in the chapter 2.

4.2.6.3 Quantitative analysis of dorsal closure

The effect of the expression of Rok-RNAi and MbsN300 in the collective behaviour of LECs was studied measuring the time cells took to dorsally migrate and the time of closure (Figure 32).

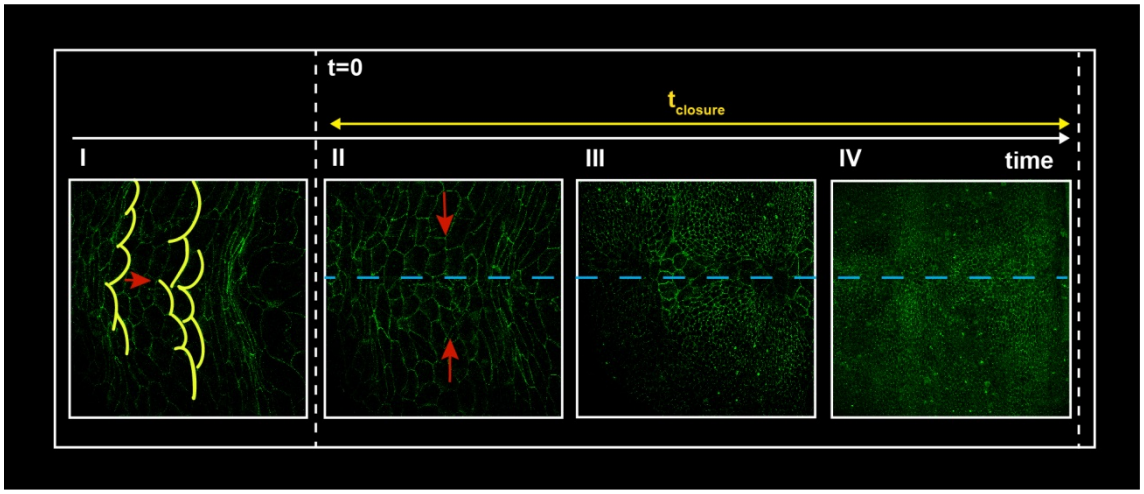

Figure 32. Timing of the collective behaviour of LECs in Rok-RNAi or Mbs-N300 expressing pupae

Confocal images from the dorsal side of the second segment A2. LECs collectively migrate posteriorly (red arrow), protruding in the direction of movement (I). The end of this migration is considered to be the start of dorsal closure (t=0) (II). Histoblasts migrate dorsally (red arrows) and LECs move towards the midline (blue dotted line) and apically constrict, leaving a few rows of immobile LECs left (III), which finally delaminate (IV).The time it takes for the completion of the abdominal closure, $t_{closure}$, was calculated subtracting the time point at which all LECs had delaminated (IV), from the initial time point.

4.3 Results

This chapter studies the behaviour of LECs and the dynamics of their actin cytoskeleton during abdominal morphogenesis when the activation of the motor protein Myosin-II is impaired. Shown to co-localise with the actin foci in LECs and to be important for foci formation in the literature (Duque and Gorfinkiel, 2016; Munjal et al., 2015), the downregulation of Myosin activity can shed light on the mechanisms of foci assembly and their specific localisation in LECs. Also, as a potential force generation mechanism in the development of the abdomen, these experiments can help to understand the role of the pulsed contraction in the coordination of migration and apical constriction, studying the apical area of LECs under these abnormal circumstances.

The strategies selected for interfering with Myosin activation are twofold: 1) Genetically, by downregulating the activity of the Rho associated kinase (Rok) by Rok-RNAi or by over expressing a form of constitutively active Myosin phosphatase, MbsN300; 2) using chromophore-assisted inactivation (CALI) of Sqh::GFP.

4.3.1 Interfering genetically with Myosin activation

The following results section studies the behaviour of LECs and the spatial and temporal organisation of their actin cytoskeleton during migration and apical constriction in Rok-RNAi and MbsN300 expressing pupae. The actin cytoskeleton of Rok-RNAi and MbsN300 expressing LECs was found to be dynamic but cells did not always display periodic actin foci. The dynamics of actin is described in the first part of this section. The second part quantifies the position of periodic actin foci within the cell, when present, in correlation with the change in cell behaviour. The third part presents the quantification of the temporal dynamics of the actin cytoskeleton, studying the periodicity of actin foci.

4.3.1.1 The dynamics of the actin cytoskeleton is affected in Rok-RNAi and MbsN300 expressing LECs

In both genotypes, the transition from stationary to migratory behaviour and the posterior movement are not affected. LECs form a lamellipodium in the direction of movement and migrate posteriorly, comparable to wild-type LECs (Figure 33A, B and C). After posterior migration the lamellipodium disappears, and LECs constrict apically and delaminate (Tables S15 and S16). Like in wild-type (Figure 33D), Rok-RNAi expressing pupae (N=6) show a dynamic actin cytoskeleton, with periodic flows of actin at the apical side of the cell during posterior migration and apical constriction (Figure 33Ei, ii). These flows coalesce and form foci in 75 % of Rok-RNAi pupae (Movie S6). In MbsN300 (N=5), the dynamics of the actin cytoskeleton also show flows of actin during migration and constriction (Figure 33Eiii, iv), although only 20 % of LECs present foci (Movie S7), showing a weak phenotype. 25 % of Rok-RNAi and 80 % of MbsN300 pupae present a strong phenotype, with absence of actin foci (Figure 33Ev) (Movie S8). When present, the foci formed in Rok-RNAi and MbsN300 are more diffuse, with actin filaments accumulating on wide areas on the apical side of LECs, without coalescing into a more condensed region like in wild-type (Figure 33F and G).

In wild-type conditions, images of the apical and basal sides of a LEC and the interface with its direct posterior neighbour reveal that cells crawl by placing the lamellipodia partly on top of their neighbour (Bischoff 2012). In the region of the neighbour, which is below the lamellipodium, flows of actin are observed (Figure 33H). In Rok-RNAi and MbsN300 expressing pupae, the area of overlap is bigger and the flows formed below the lamellipodium are more extensive (Figure 33I) (Movies S9 and S10).

Overall, these results show that both Rok-RNAi and MbsN300 overexpression affect the dynamics of the actin cytoskeleton of LECs, showing more diffuse actin foci or completely inhibited actin dynamics in the stronger phenotypes. Also, LECs generate more extensive lamellipodia on top of neighbours in the direction of movement. The increased overlap between neighbouring LECs could be a consequence of the affected cytoskeletal dynamics, as the organisation of the actomyosin cytoskeleton of cells is

required for cell contact inhibition and the regulation of forward protrusion (Gloushankova et al., 1998). The flows of actin in the back of the neighbouring LECs could be a consequence of the pressure exerted by the lamellipodium of the migrating cell. The fact that cells spread more on top of their neighbours could create larger but thinner overlapping regions in which the response to the pressure from the cell underneath is seen more apically.

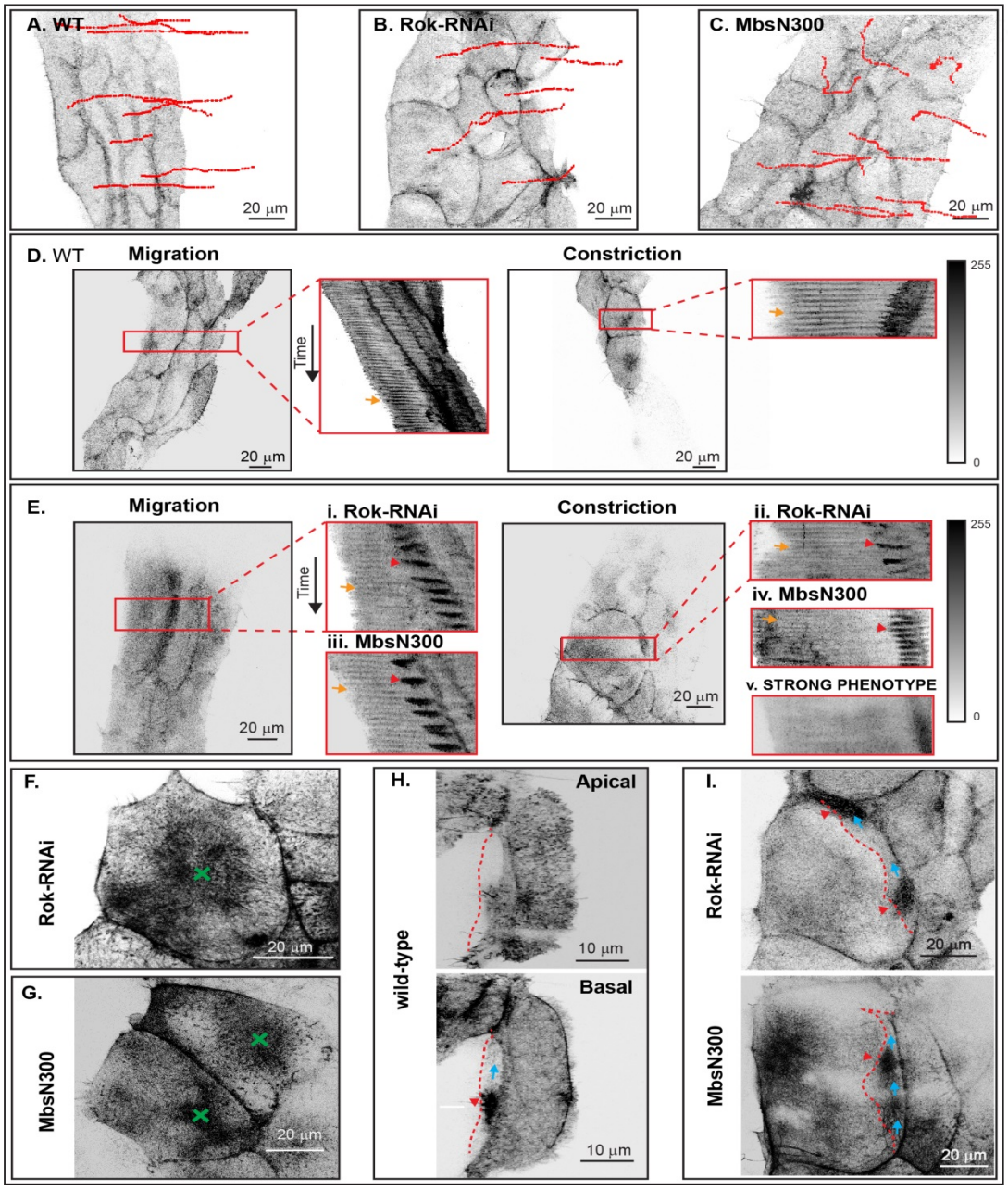

Figure 33. LEC behaviour and actin cytoskeleton dynamics in WT, Rok-RNAi and MbsN300

A) The trajectories show that LECs migrate posteriorly in wild type, Rok-RNAi **(B)** and MbsN300 **(C)**. **D)** Kymographs of the indicated region in migrating and a constricting wild type LEC. Actin foci coalesce periodically creating bands of high intensity (orange arrow). **E)** In Rok-RNAi and MbsN300 expressing LECs, there is some cytoskeletal activity in the weaker but not in the stronger phenotypes. Flows of actin are observed in neighbouring cells underneath the lamellipodium (red arrow). **F)** If present, foci (green cross) are more diffused in Rok-RNAi and MbsN300 **(G). H)** A LEC (not expressing GMA) protrudes on top of its neighbour. In the overlapping region (red dotted line) flows of actin appear basally (red arrow)and flow across the region (blue arrow). **I)** The actin flows in the overlapping region (red dotted line) between Rok-RNAi and MbsN300 expressing LECs are stronger than in wild-type (blue arrow).

4.3.1.2 The localisation of the actin foci does not correlate with the change in behaviour in Rok-RNAi and MbsN300 LECs

In Rok-RNAi and MbsN300 LECs, actin foci did not always localise at the back of the cell during posterior migration or in the centre during apical constriction. The plot of the position of foci over time shows that, in mutants, the localisation is different than in wild type (Figure 34A). As in wild-type, during posterior migration, actin foci localise closer to the anterior membrane. During phase 3, however, actin foci do not localise in the centre of the cell (Movies S6 and S7). Considering all the individual pupae analysed, the localisation of foci does not repolarise along the A-P axis, with most foci localising close to the anterior membrane during phase 3 (Figure S17). Calculating the relative position (RP) of the tracked foci reveals that, in 5 out of the 6 Rok-RNAi expressing pupae, actin foci do not localise differently in phases 2 and 3 (Figure 34B), as is the case in wild-type. In one of the Rok-RNAi pupae and the only MbsN300 expressing pupae analysed that had actin foci, the difference between the two phases exists, but the RP value during phase 3 is around 0.3 and 0.4,indicating that actin foci still do not localise centrally as in wild-type (Table S18).

In summary, the expression of Rok-RNAi or MbsN300 produces an absence or mislocalisation of actin foci.

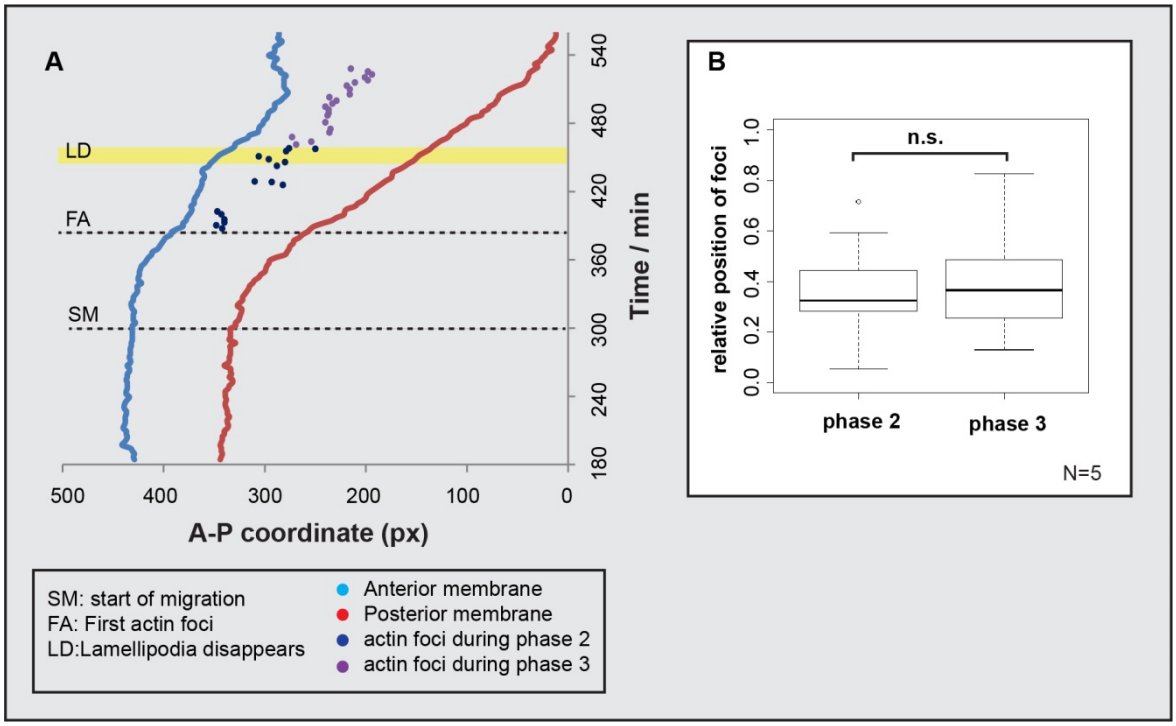

Figure 34. Quantification of the localisation of actin foci during phases 2 and 3 in Rok-RNAi and MbsN300 expressing pupae

A) Plot of the coordinates of the actin foci and the anterior and posterior membranes tracked during phase 2, when the first actin foci appear during posterior migration, and during phase 3, after the lamellipodium has disappeared in a pupae expressing Rok-RNAi. For individual Rok-RNAi and MbsN300 pupae see Figure S17. **B)** Boxplot of the relative position (RP) of foci during phase 2 and phase 3 of the Rok-RNAi expressing pupae that do not follow the wild-type localisation pattern (N=5). The mean values and their standard errors for the relative position of foci during phase 2 is 0.35 ± 0.02 and during phase 3 is 0.39 ± 0.01.

4.3.1.3 The temporal dynamics of the actin cytoskeleton are not affected in Rok-RNAi and MbsN300 expressing pupae

In the weaker phenotypes of Rok-RNAi and MbsN300 expressing LECs, the actin cytoskeleton shows pulsatile behaviour. The actin foci observed in 75 % of Rok-RNAi and 20 % of MbsN300 expressing LECs assemble and disassemble periodically. This next section studies whether the periodicity of foci is affected in Rok-RNAi and MbsN300 expressing pupae.

In all the analysed pupae, only one actin focus can be observed during migration and constriction (Figure 35A). During both phases, the actin foci assemble on average every 180 seconds (Figure 35B). Interestingly, even when most foci mislocalise along the A-P axis compared to wild-type, the periodicity of focus assembly remains similar.

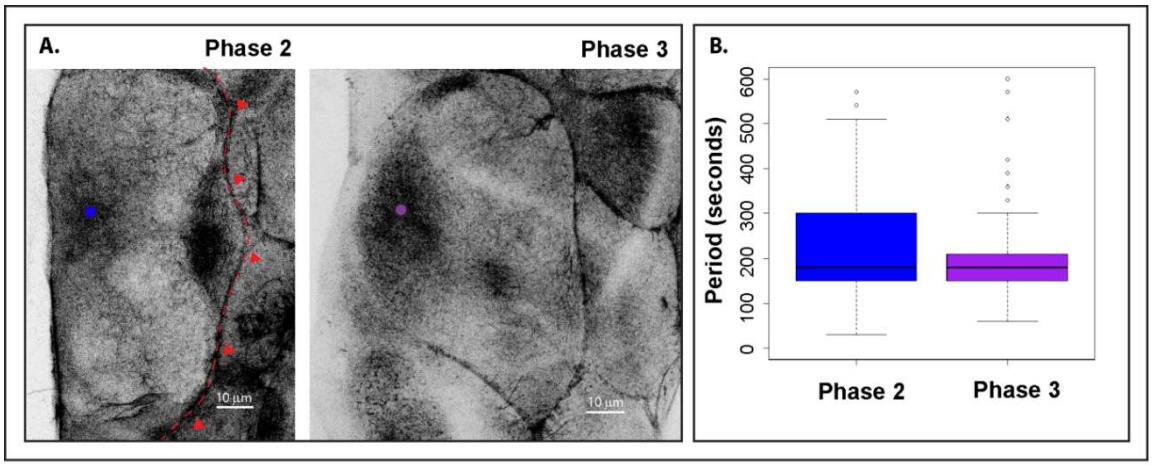

Figure 35. Foci periodicity during phases 2 and 3 of Rok-RNAi/MbsN300 expressing LECs.

A) In all the analysed LECs that show presence of actin foci in pupae expressing Rok-RNAi (N=6) and MbsN300 (N=1)**,** a single focus assembles (blue dot) while the cell protrudes posteriorly to migrate (red arrows) during phase 2. Also during phase 3, a single focus is observed. **B)** Boxplot of the period of foci during phases 2 and 3. Actin foci assemble on average every 180 seconds during migration and constriction.

The period of assembly is surprisingly consistent when comparing individual pupae. The median period of foci is around 180 seconds for each of the analysed pupae during phases 2 and 3, with no statistically significant difference between them (Figure 36A, B). Only in a few pupae the median period is slightly larger. In these pupae only a few foci could be observed (Table S19). The low number of foci, represented as gaps in the plots of the A-P coordinates of foci over time (Figure S17), was due to the diffuse distribution of foci, making the tracking very difficult in some cases. This reduced sample size produced less accurate medians, explaining the disparity of some pupae's average periodicity of foci.

Thus, in Rok-RNAi and MbsN300 LECs, the periodicity of foci is not affected, assembling on average every 180 seconds comparable to wild-type.

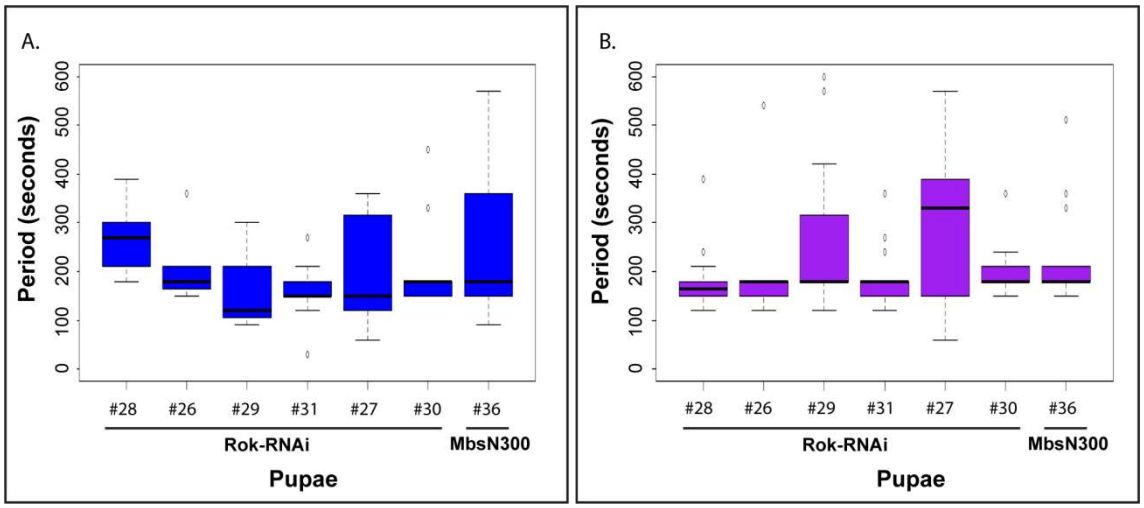

Figure 36. Comparison of the periodicity of foci during phases 2 and 3 between individual Rok-RNAi and MbsN300 expressing pupae.

A) Boxplot of the period of foci during phase 2 for the individual Rok-RNAi and MbsN300 expressing pupae in which foci were observed. The differences in the median periods are not statistically significant (p=0.08). **B)** Boxplot of the period of foci during phase 3 for the individual pupae in which foci are observed. The differences in the median periods are not statistically significant (p=0.06).

4.3.2 Analysis of LEC shape changes in Rok-RNAi and MbsN300 pupae

As discussed in Chapter 3, the correlation between the localisation of actin foci and the shape changes described might be involved in coordinating and facilitating the transition between posterior migration and apical constriction. In addition, the correlation between the presence of a focus and the fluctuation of the apical area suggests that the pulsed contraction of the actomyosin network generates these apical area fluctuations. However, it is still not clear how these periodic pulsed contractions contribute to the development of the abdomen. Rok-RNAi and MbsN300 expressing pupae present an interesting scenario to address the question of whether the affected cytoskeletal dynamics of LECs interferes with their ability to change their shape and coordinate migration and apical constriction.

4.3.2.1 Cell shape changes are affected in Rok-RNAi and MbsN300 producing an increase in the size of LECs

Next, cell shape changes that LECs undergo are studied in Rok-RNAi and MbsN300 expressing pupae by measuring the A-P and D-V lengths over time. Although the individual analysed LECs present some variability (Figure S18 andS19), cell shape changes in Rok-RNAi (N=6) and MbsN300 (N=4) differ markedly from the wild type cell shape pattern (Figure 37A). To quantify these differences, the change in A-P and D-V lengths were calculated for the whole migration phase and the first 75 min of constriction in Rok-RNAi and MbsN300 pupae and compared to wild type. Wild type LECs on average tend to reduce or at least maintain their shape along the D-V axis during posterior migration whereas in Rok-RNAi and MbsN300, LECs D-V length on average increases during the same time window (Figure 37A). There are no significant differences in the behaviour of LECs along the A-P axis between wild type and the mutants during migration and in all cases LECs increase in length along this axis (Figure 37B). During constriction, the increase in A-P length ceases early on in wild-type LECs, whereas both Rok-RNAi and MbsN300 cells in average increase it. The differences in the behaviour of the D-V length of LECs are not significant during this phase (Figure 37B).

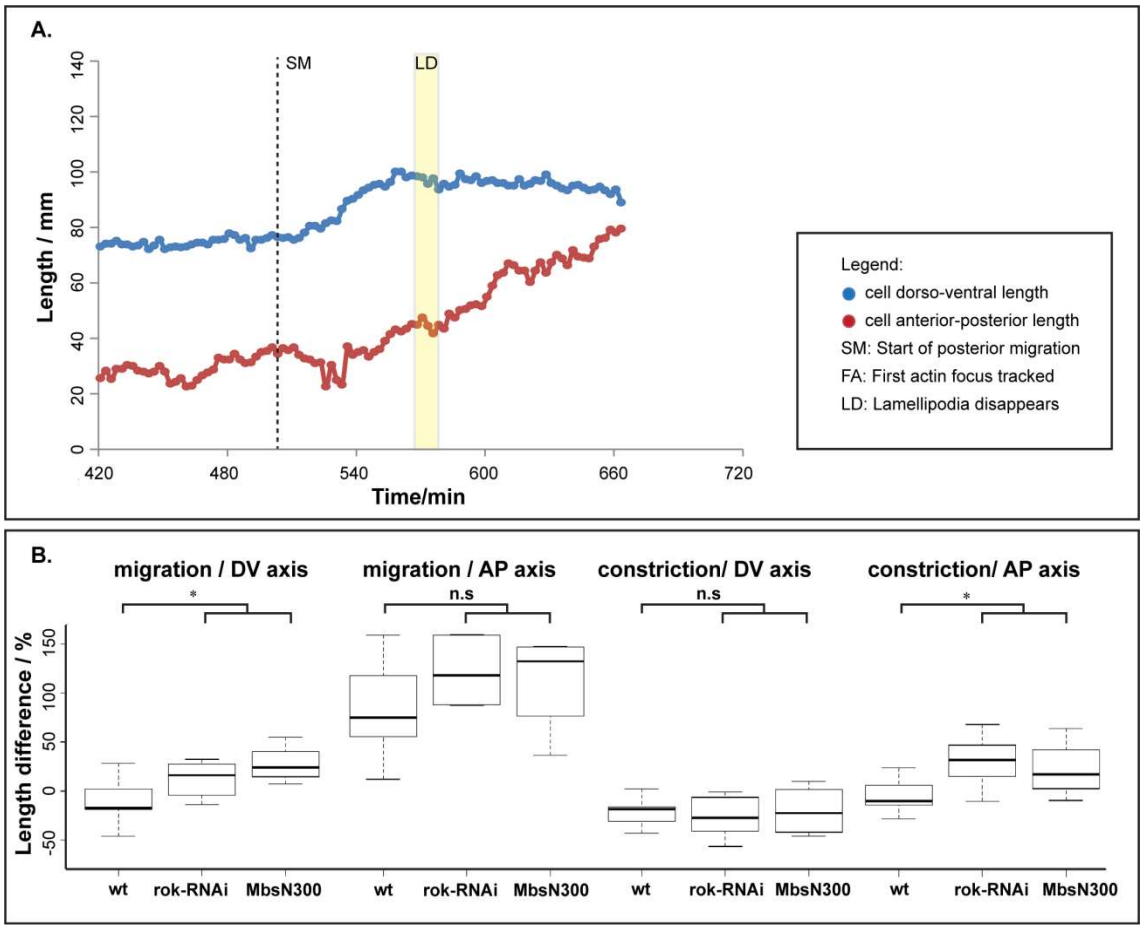

Figure 37. Analysis of the cell shape changes LECs undergo during posterior migration and apical constriction in Rok-RNAi and MbsN300 expressing pupae.

A) Plot of the D-V (blue line) and the A-P (red line) lengths over time of a LEC expressing Rok-RNAi (N=6). The A-P and D-V lengths were measured before the start of migration (SM), during migration and after the disappearance of the lamellipodium (LD). **B)** Significance codes: '*' p<0.05. Boxplots comparing the A-P and D-V length difference (in %) of LECs between the start and the end of posterior migration and the start and 75 min after the start of constriction for wild-type (wt), Rok-RNAi and MbsN300 expressing LECs. For values see Table S20.

These data show that the overexpression of Rok-RNAi and MbsN300 have an impact on cell shape changes, interfering with the capacity of LECs to reduce their D-V length during migration and being unable to maintain their A-P length after the lamellipodia has disappeared. This produces an increase in the size of LECs, being extremely long and wide.

The quantification of the size of LECs during migration and the early stages of constriction reveals that LECs expressing Rok-RNAi or MbsN300 are indeed larger on average than LECs in wild-type. The size of LECs also increases during constriction (Figure 38). This is particularly evident late in phase 3, when cells are close to delamination, 150 min after the lamellipodium has disappeared. Whereas in wild-type a significant reduction in their apical area is observed, in Rok-RNAi the apical area is maintained (p=0.24) and in MbsN300 the area is increased (p<0.0001) (Figure 38).

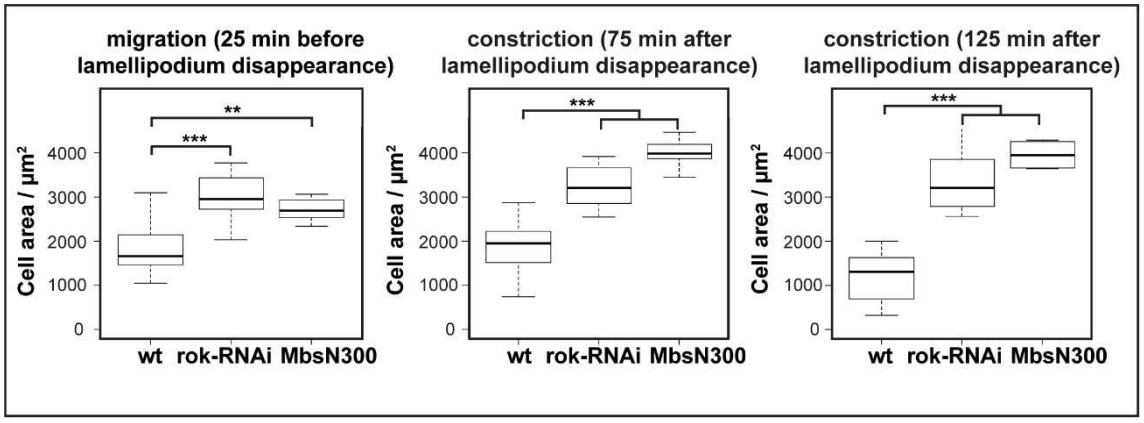

Figure 38. LECs size during posterior migration and apical constriction in Rok-RNAi and MbsN300 compared to wild-type LECs.

The Rok-RNAi (N=8) and MbsN300 (N=5) LECs analysed are significantly larger compared to wild-type LECs (N=14) during posterior migration, 75 min after and 150 min after the start of constriction. The apical area in wild-type LECs decreases when measured 150 frames after the start of constriction in comparison to the earlier stages (p=0.01), whereas in Rok-RNAi the area is maintained (p=0.4) and increased in MbsN300 (p=0.001). Significance codes: '***' p<0.001, '**' p<0.01.For values of LECs size see Table S21.

Despite larger cell areas in late constriction most of the LECs from Rok-RNAi and MbsN300 expressing pupae apically constrict and delaminate, indicating that they take longer to constrict compared to wild-type LECs. This and the increased apical area of LECs throughout morphogenesis suggest that the ability of cells to maintain the apical area is impaired in Rok-RNAi and MbsN300 expressing pupae.

4.3.2.2 Apical area fluctuations are reduced in Rok-RNAi and MbsN300 expressing LECs

The problems in maintaining the apical area of LECs could be linked to the affected dynamics of the cytoskeleton in Rok-RNAi and MbsN300 pupae. To this end, the apical area of LECs expressing Rok-RNAi (N=5) or MbsN300 (N=4) was studied over time. Both mutants show small apical area fluctuations (Figure 39A). The percentage of the apical area reduced in each fluctuation is on average lower in Rok-RNAi and MbsN300 expressing pupae in comparison to wild type during migration and apical constriction (Figure 39B). Although some pupae had a weak phenotype, with the presence of foci, or a strong one, with no actin foci, the average magnitude of area fluctuation was in general reduced (Table S22).

In summary, the impaired cytoskeletal activity in Rok-RNAi and MbsN300 pupae produces a significant reduction in the magnitude of the periodic contractions of the apical area.

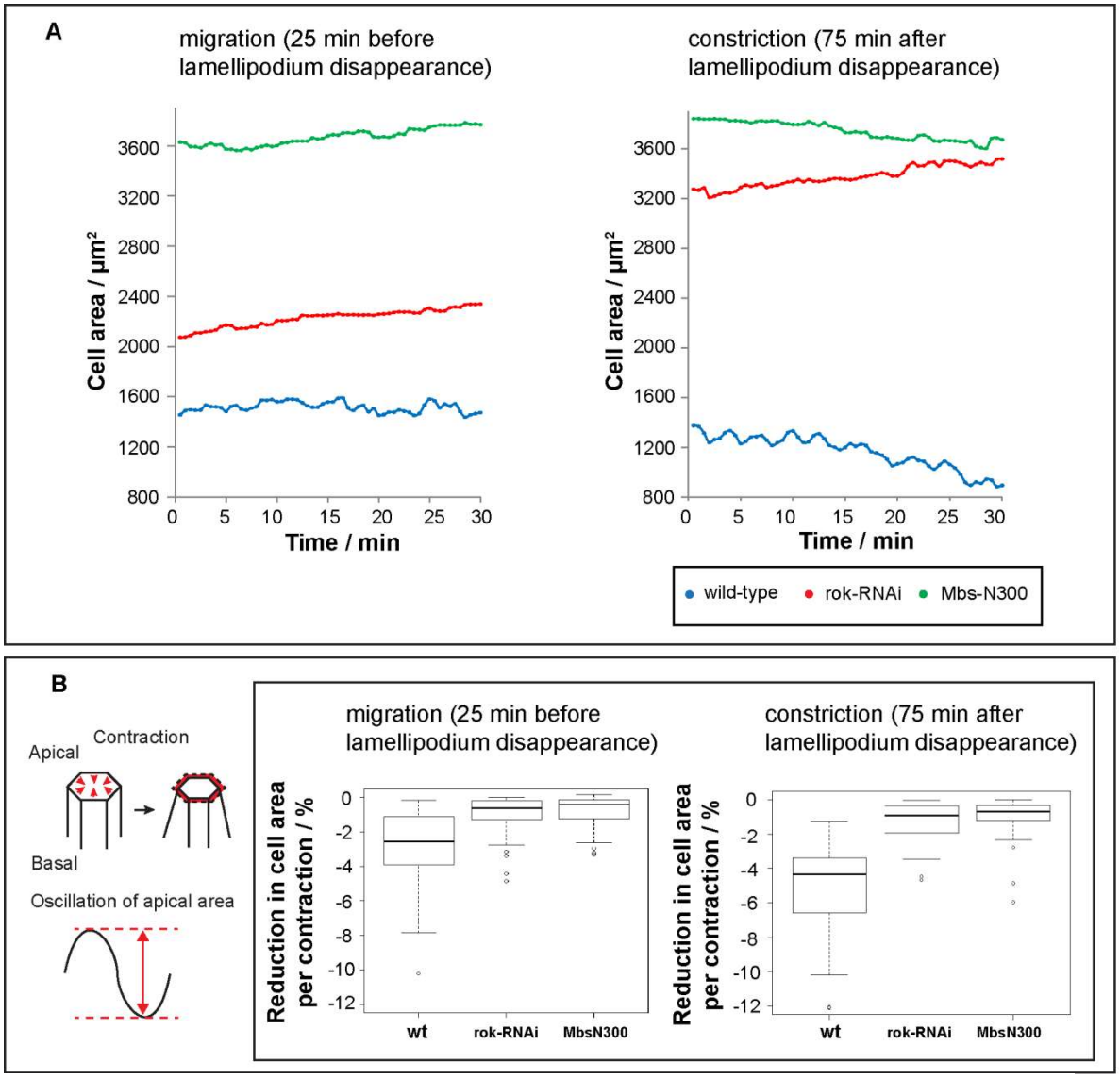

Figure 39. Analysis of the apical area of LECs in Rok-RNAi and MbsN300 expressing pupae.

A) Plots of the apical area of LECs over time show that in Rok-RNAi and MbsN300 expressing pupae, cells are bigger and display smaller area fluctuations than the wild-type LECs. Representative plots shown. **B)** Boxplots comparing the percentage of cell apical area reduction per fluctuation in the different genotypes. The difference between Rok-RNAi (N=5), MbsN300 (N=4) and wild-type is statistically significant during posterior migration (wild-type = -2.55 %; Rok-RNAi = -0.64 %; MbsN300 = -0.40 %); and constriction (wild-type = -4.35 %; rok-RNAi = -0.91 %; MbsN300 = -0.69 %).

4.3.2.3 Abdominal closure is delayed in Rok-RNAi and MbsN300 expressing pupae

To study the effects of the delayed constriction of LECs in the closure of the abdomen, the timing of the process is studied in pupae expressing Rok-RNAi (N=7) or MbsN300 (N=6) in all LECs. By the time abdominal closure is finished in wild-type pupae, there are still remaining LECs that have not delaminated in the Rok-RNAi and MbsN300 expressing pupae (Figure 40A). The dorsal closure time, measured from the start of the LECs dorsal migration until delamination, is significantly higher in Rok-RNAi and MbsN300 compared to wild-type pupae (Figure 40B). Furthermore, in 3% of the Rok-RNAi and 61% and MbsN300 expressing pupae, a dorsal cleft phenotype, or incomplete abdominal closure, is observed (Figure 40C).

In summary, although most LECs reduce their apical area and delaminate, the impaired cytoskeletal dynamics of the ones that express Rok-RNAi and MbsN300 causes a delay in the time they take to complete dorsal closure. In some cases, these LECs do not delaminate, causing the incomplete closure of the abdomen. Hence, this suggests that pulsed contractions, along with the cortical pool of actomyosin, must be important for generating the tension to maintain the apical area of LECs throughout the process and ultimately for delamination. This and the co-operation with other possible force generation mechanisms, like the histoblast expansion, produce the closure of the abdomen.

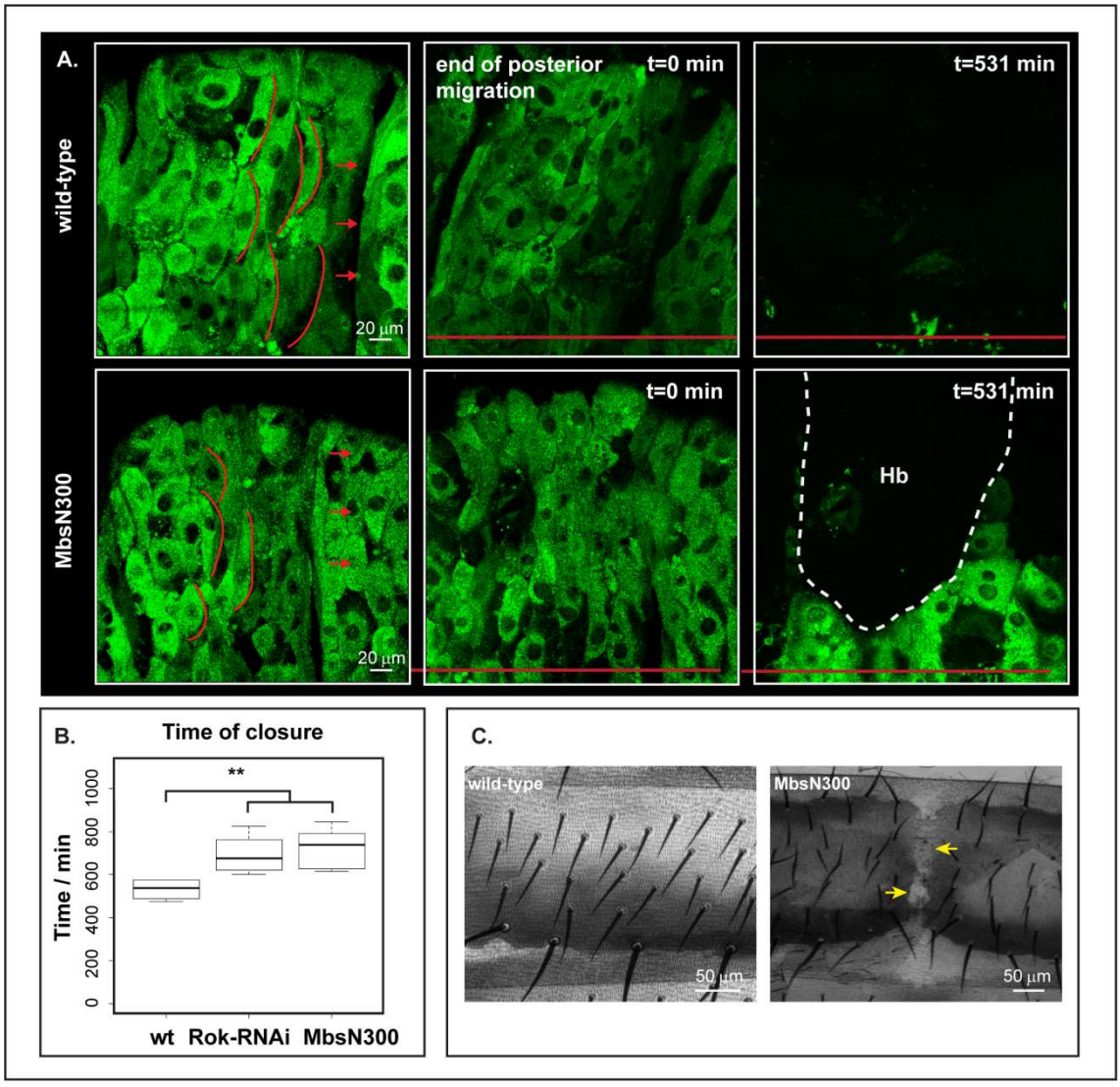

Figure 40. Closure is delayed, and sometimes incomplete, in Rok-RNAi and MbsN300 expressing pupae

A) Confocal images from a representative wild-type and MbsN300 expressing pupae. Red lines indicate the lamellipodium and red arrows the direction of movement. The time of closure is on average 531 min in wild-type (N=4). All the analysed Rok-RNAi (N=7) and MbsN300 (N=6) pupae had not finished closure at this time. **B)** Boxplot comparing the time it takes for LECs to complete abdominal closure in wild-type (531 ± 59 min), Rok-RNAi (724 ± 44 min) and MbsN300 (725 ± 48 min). Significance codes: '**' p<0.01. **C)** Images of the cuticle of the adult second segment of the abdomen in wild-type pupae, where the closure is completed, and MbsN300 pupae as an example of an incomplete closure, with remaining LECs that impede the fusion of the histoblast nests (yellow arrows).

4.3.3 Local inhibition of Myosin-II by Chromophore-assisted laser inactivation (CALI) to study cell area fluctuations

The impaired cytoskeletal dynamics in Rok-RNAi and MbsN300 pupae has an effect on the apical area fluctuations of LECs. Especially during apical constriction, the magnitude is substantially lower than the fluctuation produced by wild-type LECs (Figure 39B). As discussed in Chapter 3, the localisation of pulsed contractions in the centre of LECs could be important for producing extensive apical area fluctuations and along with the cortical pool of actomyosin, could be involved in driving LECs apical constriction. In Rok-RNAi and MbsN300 the medio-apical network dynamics is affected, but the cortical pool might be affected too. To test whether the absence of centrally located pulse contractions produce weaker apical area fluctuations, the activation of Myosin is impaired in the centre of the medio-apical side of cells using chromophore-assisted laser inactivation (CALI). CALI has been shown to work in embryonic cells in *Drosophila* (Monier et al., 2010) and used to inactivate Myosin. Also, once Myosin is inactive at the medio-apical side of LECs, this experiment could test whether the cortical actomyosin pool only can drive apical constriction in LECs.

To test the first hypothesis, CALI is done to inactivate Sqh::GFP in the centre of constricting LECs and the apical area is measured before and after CALI (Figure 41A, B). To control for potential side effects that the high-intensity laser irradiation might have on LEC behaviour, firstly, CALI is done in LECs that only express DE-cad-GFP. The apical area over time before and after laser irradiation does not show apparent differences in cell area fluctuations (Figure 41C). Thus, CALI appears not to affect cells without Sqh::GFP nor does the high laser power induce cell death. Performing the same experiment in Sqh::GFP expressing LECs shows differences in the behaviour of LECs before and after laser irradiation. The net apical area of LECs after CALI increases and the apical area fluctuations are on average significantly reduced (Figure 41D).

These data suggest that CALI on Sqh::GFP expressing LECs results in a dampening of apical area fluctuations. The laser irradiation produces photo-bleaching only at the centre of the cell during the first few repetitions. However, over a few rounds of

irradiation of the area of interest, the fluorescence is progressively lost in the whole apical area of the cell suggesting that CALI could end up affecting the whole medial pool of the irradiated LEC and possibly also the cortical pool. Thus, it is not possible to conclude that the localisation of Sqh::GFP only in the centre of LECs is important for normal apical area fluctuations. Neither it was possible to test whether the cortical actomyosin pool could drive apical constriction on its own. For that, further experiments using CALI should be done on LECs to optimize the technique and ensure that only the medio-apical actomyosin pool of LECs is affected. However, these results show that it is possible to reduce the contractility of a targeted LEC within the tissue.

Moreover, further studies should be done to examine the inhibitory effects of CALI on Myosin. Western blotting could be used to analyse the amount of Sqh::GFP present in laser-irradiated and non-irradiated pupae (Monier et al., 2010). If CALI inhibits Sqh::GFP, the levels of protein should be lower in the pupae in which CALI has been performed.

Despite not being possible to confirm that Sqh::GFP is inactivated, the experiments present CALI as a possible technique to inhibit LECs contractility.

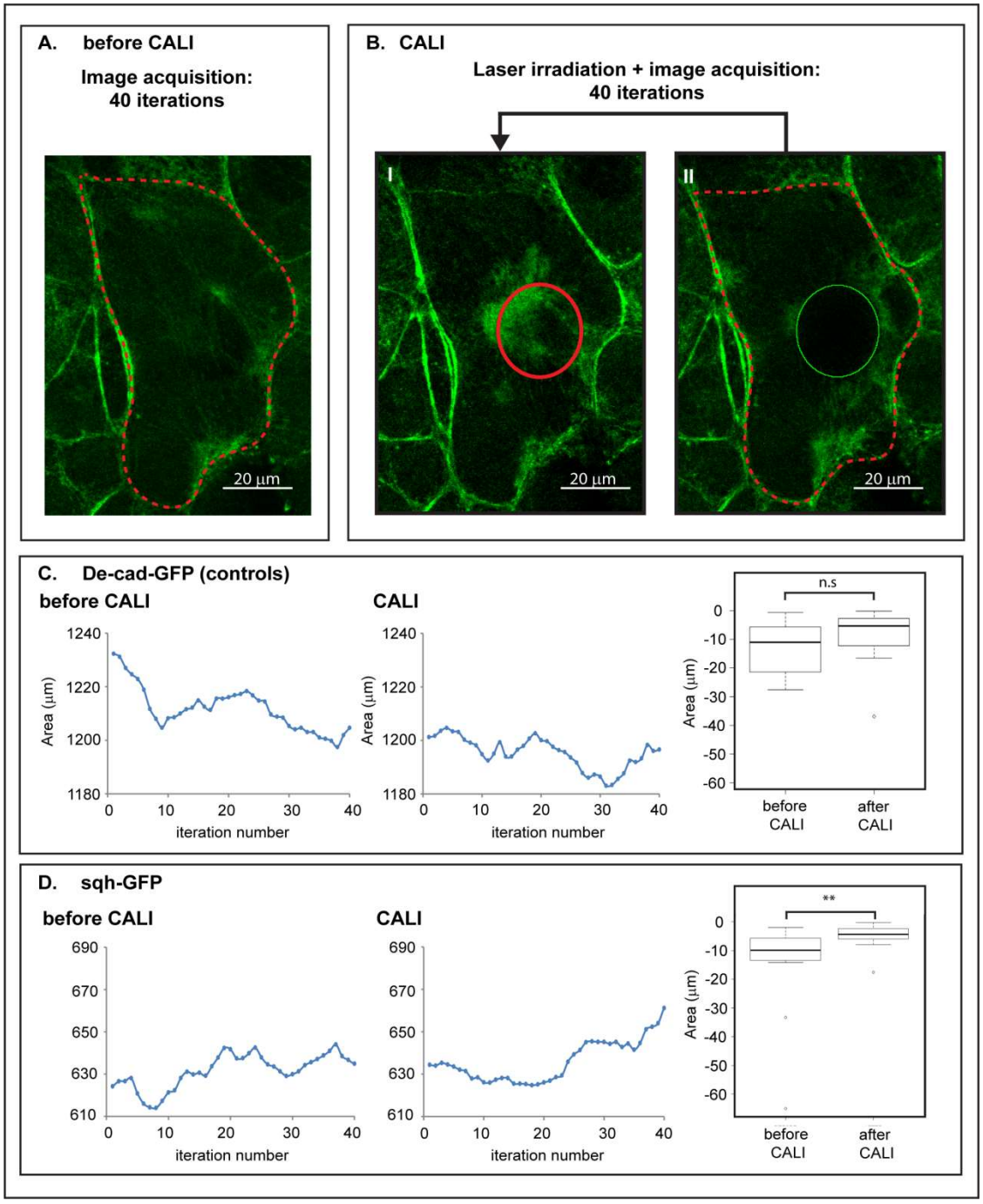

Figure 41. Analysis of the effects of CALI of Sqh::GFP on LECs apical area

A) Confocal images from Sqh::GFP expressing LECs. Before CALI, the apical area of LECs is measured for 40 iterations. **B)** CALI is performed in the centre of LECs (I). After laser irradiation the apical area is measured (II). This process or irradiation and area measurement is repeated for 40 iterations. **C)** In controls, the apical area fluctuates and does not increase after CALI (LEFT). The area reduced per fluctuation is not significantly different before or after irradiation (RIGHT). **D)** In Sqh::GFP expressing LECs, the apical area increases after CALI (LEFT) and the magnitude of the area fluctuations are significantly reduced due to the inactivation of Sqh::GFP (RIGHT).

4.4 Discussion

Interfering with Myosin activation has an effect on pulsed contractions and the ability of LECs to maintain cell size and generate area fluctuations. On a tissue level, the impaired contractility of LECs produces a delay in or incomplete abdominal closure.

The activity of the Myosin kinase and phosphatase are required for the generation of actomyosin pulses

The expression of Rok-RNAi or MbsN300 affects the dynamics of the actomyosin cytoskeleton of LECs (Figure 33E, F). Although the effects of the expression of these constructs have been studied in other systems, the results obtained in LECs differ from what have been found in terms of the temporal and spatial organisation of the cytoskeleton.

Regarding the periodicity of foci, the cycle length of Myosin foci is increased when expressing MbsN300 in amnioserosa cells (Duque and Gorfinkiel, 2016) or partially inhibiting RLC phosphorylation in germ-band cells (Munjal et al., 2015). In contrast, in the weaker phenotypes, LECs present flows of actin that are able to coalesce and form foci, having the same periodicity as in wild-type LECs. In the stronger phenotypes, LEC actomyosin foci are absent.

The spatial dynamics of actomyosin is poorly described in other systems, only mentioning that pulsatility is abolished when blocking the phospho-cycle of Myosin by expressing phosphomimetic or non-phosphorylatable forms of RLC (Munjal et al., 2015; Vasquez et al., 2014). In LECs, the stronger phenotypes could be interpreted as having no pulsed contractions, as the apical side presents some periodic actin flows, but no foci. In the weaker phenotypes, the remaining cytoskeletal activity produces foci that assemble with an abnormal localisation but normal periodicity (Figures 34 and 35). These observations suggest that the function of the kinase and phosphatase, which activate and deactivate Myosin, is not only required for the formation of periodic foci but also for their localisation. Thus, the localisation of foci could depend on the levels of active Myosin on the apical side of LECs.

The activity of the Myosin kinase and phosphatase are required for cell shape changes

The effect of Myosin inactivation on abdominal closure has previously been studied, linking the expression of MbsN300 to abdominal closure defects, producing a proportion of LECs that do not delaminate (Ninov et al., 2007). Revisiting the phenotypes and analysing in great detail the behaviour of LECs and their cytoskeleton has provided the information to explain the causes of these closure defects in MbsN300 and Rok-RNAi expressing pupae.

Interfering with Myosin activation impairs the ability of LECs to undergo the cell shape change pattern described in wild type (Figure 37), producing an increase in LEC size throughout the process (Figure 38). Also, the apical area fluctuations are significantly reduced during migration and apical constriction (Figure 39). Moreover, even though apical constriction occurs in the presence of an impaired medio-apical pool of actomyosin, probably due to the action of other forces such as the cortical actomyosin pool or even the histoblast expansion, abdominal closure is delayed or not completed (Figure 40).

Overall, these data suggest that the actomyosin dynamics observed in wild-type, with the presence of periodic and localised actomyosin foci during migration and constriction, could be important for generating the tension to maintain cell size and coordinate the cell shape changes required for normal abdominal morphogenesis. The results obtained furthermore suggest that, apical constriction and delamination, occurs due to the coordination of pulsed contractions with other intrinsic or extrinsic force generation mechanisms.

The activity of the Myosin kinase and phosphatase impacts on the interaction of lamellipodia and neighbouring cell

The effect on Myosin activation could also explain the presence of more extensive basolateral flows of actin that can be observed in the back of LECs that overlaps with the region occupied by neighbouring lamellipodia (Figure 33H, I).

In wild-type LECs, these flows are small as the overlapping region is very narrow. These flows of actin could be a response of the neighbouring cell to the pressure exerted by the migrating LEC. In Rok-RNAi and MbsN300 expressing LECs, the overlapping region is larger as cells might have problems resisting the pushing of the lamellipodia of the neighbouring cells. This could increase the overlapping region between neighbours and thus the response of the cell to the pressure, producing flows that are more visible.

5. Reverse genetic candidate screen to find RhoGEFs that regulate specific aspects of LEC behaviour

5.1 Introduction

As already presented, Rho GTPases are one of the main cytoskeletal regulators. In particular, the Rho signalling pathway plays an important role during the morphogenesis of the abdomen (Bischoff 2012). Interfering with two of their downstream effectors, Rok and Mbs, has shown their importance in the generation of pulses through the regulation of Myosin phospho-cycle. Their function is especially important for maintaining the apical area of LECs and for producing the cell shape changes that facilitate the transition between migration to apical constriction, prior to delamination. However, not much is known about the spatial and temporal activation of the Rho signalling pathway to coordinate the reorganisation of the actin cytoskeleton during the transition between behaviours. The activity of Rho, important for contractility (Ridley and Hall, 1992), along with other Rho-GTPases important for the establishment of polarity or the generation of the lamellipodium, like Rac or Cdc42 (Nobes and Hall, 1995; Ridley et al., 1992), have to be spatially and temporally regulated in order to coordinate migration and constriction in LECs (Greenberg and Hatini, 2012).

The proteins that regulate Rho GTPase activity are the Rho Guanine nucleotide exchange factors (RhoGEFs) and Rho GTPase activating proteins (RhoGAPs), which respectively activate and deactivate the corresponding GTPases (Figure 3) (Etienne-Manneville and Hall, 2002). In *Drosophila*, there are some well-studied examples of how these Rho GAPs and GEFs target specific Rho-GTPases to regulate their function. In *Drosophila* gastrulation, RhoGEF2 has an important role in regulating Rho1, with RhoGEF2 mutant embryos failing to generate the ventral furrow as apical constriction never occurs (Barrett et al., 1997; Häcker and Perrimon, 1998; Kolsch et al., 2007). Both Sqh and the Myosin-II heavy chain zipper (Zip) become re-localised from the basal side of the cell to the apical side of ventral furrow cells along with RhoGEF2 (Nikolaidou and Barrett, 2004). RhoGEF2 is also involved in localisation of F-actin, functioning in parallel with Abl (Fox and Peifer, 2007). In other systems, RhoGEF2

functions along with other RhoGEFs and GAPs to drive cell shape changes. For instance, cell invagination during *Drosophila* spiracle formation requires apical constriction mediated by the restricted localisation of Rho1. Rho regulators are differentially distributed, with the activators RhoGEF64C and RhoGEF2 apically localised and the inactivator RhoGAPCv-c occupying the complementary basolateral domain (Simoes et al., 2006). RhoGEF2 also regulates via Rho1 the organisation of the actomyosin ring during blastoderm cellularisation (Barmchi et al., 2005), although not all the processes that require the formation of actomyosin rings are regulated by the same GEF. RhoGEF2 is not required for cytokinesis (Nikolaidou and Barrett, 2004), but the formation of the ring is regulated by the RhoGEF Pebble through the activation of Rho1 (Prokopenko et al., 1999). Pebble is also involved in the migration of mesodermal cells (Leptin, 1999). During gastrulation, mesodermal cells invaginate, undergo epithelial-mesenchymal transition and then migrate laterally over the inner surface of the ectoderm (Leptin, 1999). Pebble has been found to localise to the cell cortex of mesoderm cells and regulate their migration through the interaction with Rac GTPase (van Impel et al., 2009). Thus, RhoGEFs and GAPs can function alone or co-ordinately in more than one process to regulate the function of different Rho-GTPases, depending on the morphogenetic system.

In order to elucidate the molecular mechanisms involved in regulating LEC behaviour, several GEFs present in *Drosophila* are knocked down in LECs during abdominal morphogenesis. The visualisation of abdominal closure under these knockdowns provides information about the role of each GEF in regulating cell behaviour. The aim is to find genes that control specific aspects of migration or apical constriction, providing more information about the signalling network that controls LEC behaviour and gain insights on how the transition between behaviours might happen. Also, the knockdown of the genes associated with specific LEC behaviour might impair posterior migration or apical constriction separately, which would allow the study of their role in abdominal closure.

5.2 Methods

5.2.1 *Drosophila* stocks

The RNAi lines to knockdown the 15 different GEFs analysed in this chapter were obtained from the Bloomington *Drosophila* stock centre (BDSC) and are specified in (Table 6).

Gene name	Annotation symbol	BDSC stock number
Ephexin (Exn)	CG33373	33373
-	CG43658	32341
-	CG30456	34380
RhoGEF3	CG43976	42526
RhoGEF4	CG8606	42550
Pebble	CG8114	36841
Trio	CG18214	43549
Sif	CG34418	25789
C-dep	CG44193	31168
RhoGEF2	CG9635	34643
RhoGef64C	CG32239	31130
Sos	CG7793	34833
-	CG15611	31158
-	CG33275	31221
vav	CG7893	39059

Table 6. List of the RhoGEFs analysed in an RNAi screen performedin LECs during abdominal morphogenesis.

The table specifies the gene annotation symbol according to the nomenclature in Flybase (Gramates et al. 2016) and the BDSC RNAi stock number used for the experiments. Some of the genes do not have an associated name.

To visualise the behaviour of LECs expressing the RNAi constructs, the following genotypes were used: *y,w,hs.FLP;**UAS.RhoGEF-RNAi**/tub<CD2<Gal4,UAS.FLP,UAS-mCD8-GFP,* if the RNAi-transgene was inserted on the second chromosome or *y,w,hs.FLP; tub<CD2<Gal4,UAS.FLP,UAS-mCD8-GFP/+*;**UAS.*RhoGEF-RNAi***/+, if the RNAi-transgene was inserted on the third chromosome. After initiation of recombinase

(FLP) expression, these flies express the RNAi-transgene and mCD8-GFP, a marker that labels the membranes of cells.

5.2.2 Control of the expression of RNAi in LECs

In order to induce clones in the larval epithelial cells, a 37.4-37.8 °C heat shock was performed on 3rd instar larvae for 15 minutes 24 hours prior to recording and stored in a 25 °C incubator.

5.2.3 4D microscopy

Focusing on the dorsal side of the abdomen, the behaviour of LECs in the A and P compartments was recorded by zooming in on a region that included a hemisegment of segment A2. A Z-stack of 15-30 μm with a step size of 2.5 μm was made every 150 seconds with a 512 x 512 pixels resolution using a 20x objective.

All pupae were recorded using a Leica SP8 confocal microscope at a temperature of 25 ± 1 °C.

5.2.4 Analysis of 4D microscopy

5.2.4.1 Analysis of the RNAi knockdown experiments

For each cross, at least 3 pupae were prepared and recorded. The recordings were analysed by checking: 1) if all the LECs, except for the cells close to the anterior segment boundary which initially protrude anteriorly, protruded in posterior direction; 2) if LECs moved in posterior direction 3) if the shape and size of LECs was increased or reduced in relation to wild-type recordings.

5.2.4.2 Analysis of the trajectories of LECs

In order to quantify posterior migration, the trajectories of LECs were calculated over time. SIMI Biocell was used to track the coordinates of the centre of LECs. To generate the trajectory and velocity plots, each coordinate was later connected with a straight 'beeline' using a programme written in C# using Microsoft Visual Studio 2005 with the Microsoft .NET 2.0 framework (Bischoff and Cseresnyés, 2009). The colour of trajectory plots represents the velocity of the cell.

5.2.4.3 Duration of abdominal closure

The duration of abdominal closure was calculated by measuring the time difference between the start of LEC posterior migration and the complete delamination of all LECs present in A2.

5.3 Results

In this first section, 15 of the 20 RhoGEFs present in *Drosophila* were depleted by RNAi in LECs and the role of these genes in abdominal morphogenesis was examined. The data obtained suggest that abdominal morphogenesis is achieved through the expression of different RhoGEFs that specifically regulate different aspects of the behaviour of LECs. The analysis identified a role for several RhoGEFs (Table 7) which, depending on their phenotype, could be classified in genes that regulate aspects of the posterior migration and the apical constriction of LECs.

5.3.1 GEFs involved in the regulation of posterior migration

In contrast to wild-type, where LECs protrude and move in a posterior direction (Figure 42A), the knockdown of GEF CG43658 and GEF CG30456 interfered with the directionality of LEC migration. Similar to the effect of Dachsous (Ds) knockdown, a molecule involved in the establishment of planar cell polarity in LECs (Bischoff 2012), some LECs started to create protrusions and move in different directions (Figure 42B, C). Despite the problems of some cells to protrude in the right direction, some others were observed to polarise correctly and the overall tissue moved towards the posterior, probably because not all LECs were affected.

The knockdown of other GEFs completely impaired the ability of LECs to migrate. RhoGEF4, Trio, Sif and Pebble RNAi knockdowns produced phenotypes in which LECs did not protrude or migrate posteriorly. These phenotypes were observed with different frequencies, with Pebble producing the most consistent phenotype (Table 7). The expression of Pebble-RNAi inhibited posterior migration in 87.5 % of cases. LECs remained static and only moved dorsally, meeting at the midline, constricting and delaminating (Figure 42D). Examining the recordings, it becomes clear that the migratory behaviour of LECs is impaired. Comparable to the function of Pebble described in mesoderm cells (van Impel et al., 2009), this GEF appears to regulate some aspect of the migratory behaviour of LECs. Interestingly, Pebble-RNAi produces a delayed abdominal closure. From the start of migration until delamination, LECs take on average 617 ± 24 min in wild-type pupae whereas in Pebble-RNAi expressing pupae, the time LECs take is on average715 ± 24 min, being significantly higher compared to

wild-type (p=0.02). With these data it is not possible to conclude that the delay is due to the absence of posterior migration, but certainly Pebble is required for normal abdominal closure.

5.3.2 GEFs involved in the regulation of apical constriction

After posterior migration, the size of RhoGEF2-RNAi expressing LECs increased. LECs of RhoGEF2-RNAi expressing pupae spread extensively before reducing their apical areas (Figure 42E). Despite this, LECs apically constricted and delaminated and the time of closure was not affected, being similar to wild-type (p=0.70). The ability of LECs to protrude and migrate was not affected either, suggesting that RhoGEF2 is involved in the regulation of LEC shape changes during abdominal morphogenesis.

In summary, the loss-of-function screening identified several GEFs that had an effect on cell polarity, cell migration or apical constriction. These specific phenotypes indicate that these GEFs regulate crucial aspects of the individual behaviour of LECs through the controlled temporal activation of Rho GTPases.

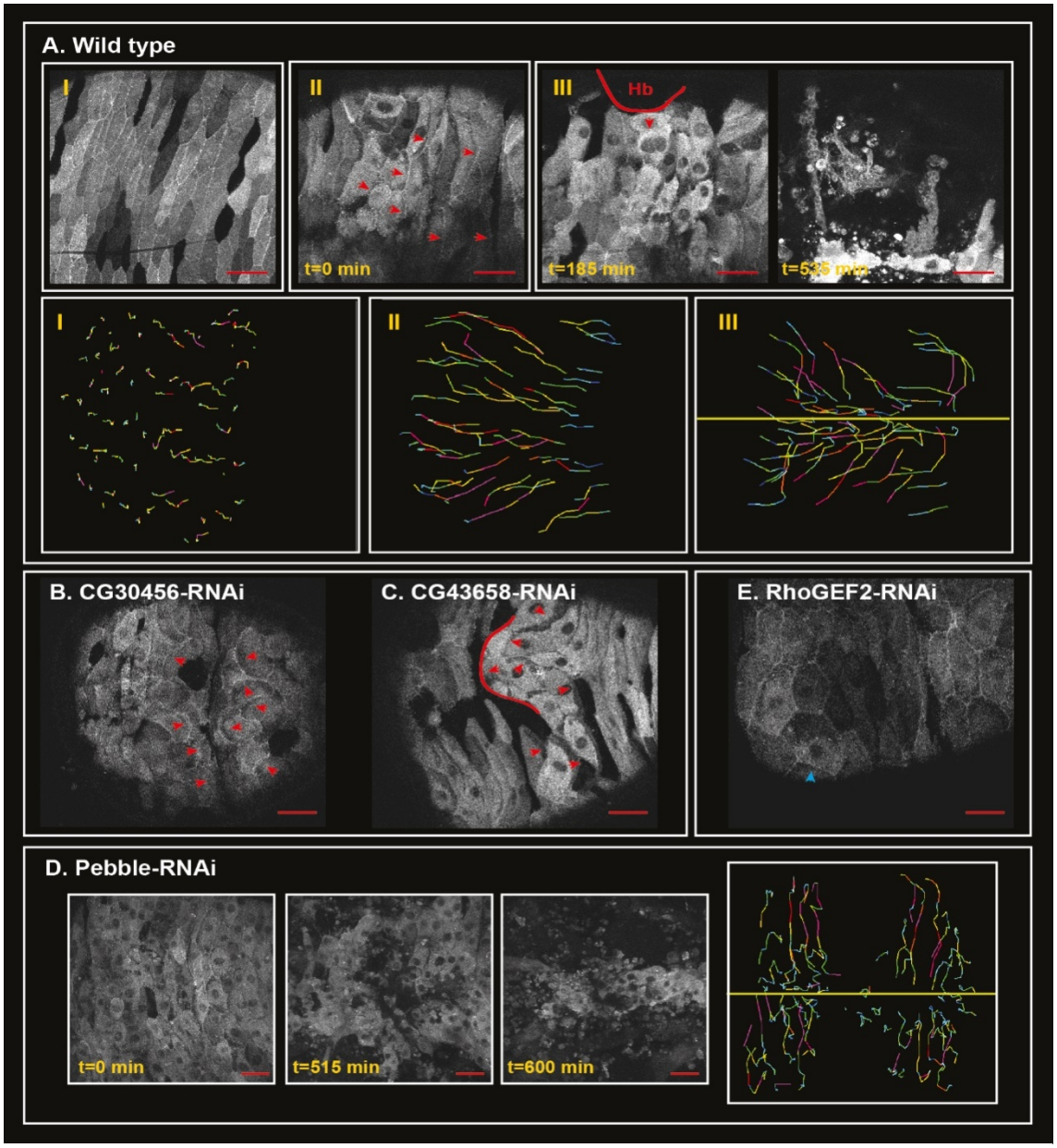

Figure 42. Phenotypes found in the knockdown of the different GEFs during abdominal morphogenesis

Images of LECs from A2 expressing the membrane marker mCD8-GFP. Red arrows indicate the direction of protrusion and the yellow line the midline. Scale bars, 50 μm. Anterior is to the left. **A)** In wild-type, LECs transition from stationary (I) to migratory behaviour, protruding in the posterior direction (II). The trajectories show that after migrating posteriorly, LECs repolarise and move towards the midline. **B)** In the knockdown of GEF CG30456 and **C)** CG43658, LECs protrude in the wrong direction. Sometimes LECs migrate anteriorly, deforming the segment boundaries. **D)** The knockdown of Pebble impairs the posterior migration of LECs. The trajectories show that LECs close to the midline (yellow line) do not move while the other cells move dorsally until they meet the midline and die. **E)** In the knockdown of RhoGEF2, after posterior migration some cells spread extensively (blue arrow).

Gene name	BDSC number	RNAi Phenotype	Frequency of the phenotype
Ephexin (Exn)	CG33373	NP	-
-	CG43658	Some LECs show wrong polarity during migration	50 % (N=4)
-	CG30456	Some LECs show wrong polarity during migration	33.3 % (N=3)
RhoGEF3	CG43976	NP	-
RhoGEF4	CG8606	LECs do not migrate posteriorly	33.3 % (N=3)
Pebble	CG8114	LECs do not migrate posteriorly	87.5 % (N=8)
Trio	CG18214	LECs do not migrate posteriorly	33.3 % (N=9)
Sif	CG34418	LECs do not migrate posteriorly	40 % (N=10)
C-dep	CG44193	NP	-
RhoGEF2	CG9635	After posterior migration, some LECs show extensive spreading	80 % (n=5)
RhoGef64C	CG32239	NP	-
Sos	CG7793	NP	-
-	CG15611	NP	-
-	CG33275	NP	-
vav	CG7893	NP	-

Table 7. Summary of the RNAi-phenotypes of the RhoGEFs analysed in this study.

For each gene, the table describes the loss-of-function phenotypes induced by RNAi and the frequency with which the phenotype was observed. NP indicates no phenotype.

5.4 Discussion

The RNAi screen of different RhoGEFs has identified a number of genes required for abdominal morphogenesis. Most of the RhoGEFs identified had a role in regulating the protrusive activity and the migration of LECs. In the case of RhoGEFs CG43658 and CG30456, the protrusions were randomly oriented (Figure 42B, C) and in the case of Pebble, LECs did not migrate posteriorly (Figure 42D). Studies in several systems suggest that the response to polarity cues to stabilise the direction of movement is controlled by Cdc42 (Etienne-Manneville and Hall, 2002). Macrophage cell migration in response to a gradient of a chemotactic is dependent on Cdc42 and Rac (Allen et al., 1998). When Cdc42 was inhibited, the macrophage failed to polarise, whereas inhibition of Rac blocked all cell movement (Allen et al., 1998). Thus, in LECs, RhoGEF Pebble could interact directly with Rac to regulate cell migration, as described in Mesodermal cells (van Impel et al., 2009) and CG43658 and CG30456, regulate the activity of Cdc42 to orient and maintain the polarized morphology of LECs. Although the mechanism that regulates the function of these GEFs is unknown, they could be activated in response to the existing PCP and in interaction with the molecules that maintain it.

The lack of further study on sif, trio or RhoGEF4 does not allow determining whether the lack of posterior migration is produced by the random polarisation of LECs or the absence of protrusive activity. However, GEF Trio is responsible for lamellipodia formation in a Rac1-dependent manner during fibronectin-mediated spreading and migration (van Rijssel et al., 2012) and also mediates the migration of granule cells during cerebellum development (Dai et al., 2010). The *still life* (sif) knockdown shows reduced locomotor activity during the formation of neural circuits in *Drosophila* and encodes a guanine-nucleotide exchange factor for Rac (Singh et al., 1997). These findings raise the possibility that these GEFs are regulators of cell migration or even lamellipodia formation through the interaction with Rac.

The only gene that had a role in apical constriction was RhoGEF2. As shown in other systems, RhoGEF2 is implicated in controlling the activity of Rho and their downstream

effectors (Barrett et al., 1997; Häcker and Perrimon, 1998; Kolsch et al., 2007; Nikolaidou and Barrett, 2004). The knock-down of Rho1 activity by RNAi also produces the extensive spreading of LECs before constriction (Bischoff, 2012), suggesting that in LECs RhoGEF2 could control specific aspects of Rho1 function.

The results obtained highlight the abdominal morphogenesis as a potential system to study the mechanisms of collective cell migration and polarity and expand the list of genes involved in the control of protrusion orientation in the abdomen. The identification of these genes function in abdominal morphogenesis provides the first steps into novel insights into the regulation of Rho, Rac and Cdc42 signalling cascades and downstream effectors in shaping the morphology of the adult abdomen.

6. General discussion

During morphogenesis of the adult abdominal epidermis, the LEC's contractile actomyosin network becomes pulsatile. Foci assemble with constant periodicity at the medio-apical side of LECs, from LECs migration to apical constriction and delamination. Considering the results obtained, I propose a model based on the regulated activation and deactivation of Myosin and the polarity of the meshwork to explain the formation of foci and their specific localisation, presenting future experiments to further explore the hypothesis. Alternatively, I discuss the importance of the integrity of the actin meshwork and the possible role of actin turnover in localising actomyosin foci. Finally, I discuss the role of the periodic contractions of the actomyosin network and, in general, non-continuous apical constriction in coordinating cell behaviour and driving abdominal closure.

Generation and localisation of actomyosin foci in LECs

My data suggest that pulsed contractions of the actomyosin cytoskeleton of LECs require the activation of Myosin, mediated by the activity of Rok and MBS (Figure 29D and 30), as shown in other systems (Duque and Gorfinkiel, 2016; Munjal and Lecuit, 2014). As introduced in Chapter 4, Munjal *et al.* (2015) propose a self-organised model in which biochemical regulation of Myosin and advection drive network oscillatory behaviour. Although this model can explain the formation of foci in LECs, it does not explain why foci would preferentially localise in specific regions of the cell.

Other studies may help in understanding how this preferential localisation of pulsed contractions happens. In ventral furrow cells, the actin cytoskeleton is radially polarised. This polarisation of the actin filaments on the medio-apical side of these cells involve a differential localisation of the proteins that specifically bind the barbed, or plus, ends and the capped, or minus, ends of actin filaments. The results show that plus ends are enriched at the adherens junctions while minus ends co-localise with Myosin in the medial region (Coravos and Martin, 2016). This polarisation of the actin meshwork help in localising Rok during apical constriction, transported in Myosin flows towards the centre of the cell (Coravos and Martin, 2016). Following this idea, the

periodic assembly of foci at specific locations within the cell could depend on the orientation of the actin meshwork, as Myosin acts on actin in a manner that depends on the actin filament orientation (Reymann et al., 2012).

Considering the model proposed in Munjal et al. (2015) and the observation that a polarised actin meshwork localise pulsed contractions (Coravos and Martin, 2016), I propose a model in which the specific polarisation of LECs cytoskeleton, planar polarised during migration and radially polarised during constriction, could localise the pulsed contractions in the back and in the centre of the cell, respectively.

Furthermore, taking into account the results obtained with the expression of Rok-RNAi and MbsN300 in LECs, the proper regulation of Myosin activation is required for the localisation of actomyosin foci. In Rok-RNAi and MbsN300 strong phenotypes, pulsed contractions are not present in the apical side of LECs (Figure 33). However, in the weaker phenotypes, foci are more diffused and mislocalise (Figure 34). Assuming that the organisation of the actin meshwork is not affected, the diffused foci could be explained following the model proposed by (Munjal et al., 2015). The low concentration of Myosin in Rok-RNAi or MbsN300 LECs would not generate the force required to contract the network, producing, when present, diffuse foci that dissociate due to the low rates of phosphorylation or high rates of dephosphorylation. Nonetheless, despite being diffuse, foci cannot localise properly during apical constriction. Hence, the model suggested here also proposes that, along with the polarisation of the actin meshwork, the correct localisation of foci within the cell requires the activation of a certain amount of molecular motors.

As observed *in vitro*, Myosin molecules work cooperatively. When a group of motors pull in one direction, they enhance others to join and pull (Jülicher and Prost, 1995; Plaçais et al., 2009). This concept of cooperativity can help in understanding the results obtained in LECs. The levels of active Myosin available in the cell would be in general lower in Rok-RNAi and MbsN300 expressing LECs. In the weaker cases, the amount of active Myosin would initiate the contractile event. However, not enough Myosin molecules would be active to join and propagate this contractile event. Thus, pulsed

contractions would be generated, assembling every 180 seconds as observed (Figure 35), but would localise near the point of initiation, at the back of the cell during migration and near the apical cortex during constriction (Figure 43). Foci would dissociate due to the lack of active Myosin. In the stronger cases, the contractile flows would not be propagated or even initiated.

Interestingly, in Rok-RNAi and MbsN300 expressing LECs, only one focus is observed during posterior migration (Figure 35). This suggests that the regulation of Myosin phospho-cycle could also be important for the network dynamics that generates and localises the two alternating foci observed in LECs during migration (Figure 43).

In summary, I propose a model in which the threshold for the initiation of pulsatility and the proper localisation of the actin foci depends on: **(1)** the polarisation of the cytoskeleton during migration (PCP) and during constriction (RCP); **(2)** the amount of phosphorylated Myosin present on the medio-apical side of LECs. Hence, in addition to the model proposed in Munjal et al. (2015), the proper regulation of Myosin phosphor-cycle is required, along with the polarity of the actin cytoskeleton and the signals that regulate it, for generating the localised pulsed contractions.

To support the hypothesis presented above, Myosin activation could be impaired in LECs using CALI (Monier et al., 2010). Instead of expressing an RNAi construct or a mutant form of Myosin to interfere with Myosin activation in the whole cell, the optimisation of CALI in LECs would allow the inactivation of Myosin in specific regions of the cell during migration and apical constriction to study the behaviour of the actomyosin network and the formation of foci when a certain amount of Myosin within the cell has been deactivated.

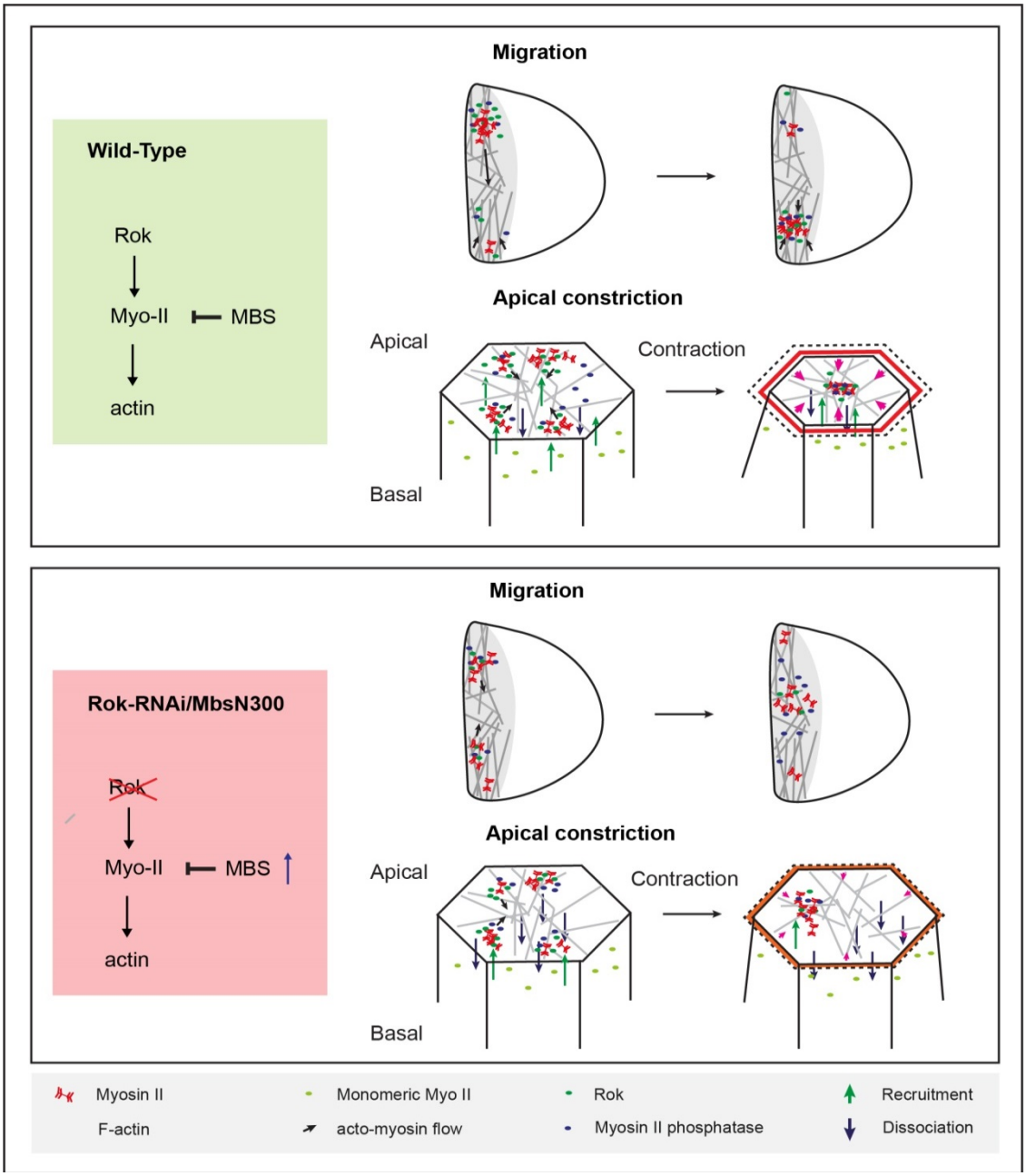

Figure 43. Model of Pulse assembly in wild-type and Rok-RNAi/MbsN300 LECs

Pulse assembly requires a self-organized system that involves the activation of enough Myosin to propagate the contractile events. The formation of two foci would be determined by a planar polarised actin network during migration. The formation of a single central focus would be promoted by a radially polarised actin meshwork during constriction. When the levels of active myosin are not sufficient, in the weaker cases the contractile events cannot be propagated and foci assemble near the site of initiation. In the stronger cases, focus assembly does not occur. In both cases, the abnormal actomyosin dynamics generate weak forces (pink arrows) that translate into smaller contractions of the apical area, especially during constriction.

Actomyosin dynamics could also depend on the regulation of actin polymerisation

An alternative hypothesis to explain the obtained results is that foci do not localise due to a disrupted apical actin meshwork. Such a meshwork would possibly fail to cover the whole apical side of cells, not allowing contractile gradients to converge towards different regions of the cell. Recent studies in mesodermal cells during *Drosophila* gastrulation have shown that the role of F-actin turnover in apically constricting cells is required for connecting actomyosin to the adherens junctions (AJs) and for the stability and balance of force generation (Jodoin et al., 2015). When perturbing F-actin turnover by gene depletion or drug treatment, such as injection of latrunculin A or B, Myosin-II no longer contracted the apical meshwork centrally, but the actomyosin network was fragmented in adjacent medio-apical networks that came back together. This resulted in imbalanced force generation and a deformation of adjacent cells (Jodoin et al., 2015). This phenotype has some similarities with the phenotype obtained in apically constricting LECs that express Rok-RNAi or MbsN300, with foci that no longer localise centrally, producing less extensive apical area fluctuations, suggesting that the apical tension levels are affected. This alternative hypothesis, though, would need further investigation in order to assess whether Rok-RNAi or MbsN300 has an effect on the integrity of the apico-medial actin meshwork or on F-actin turnover specifically.

The studies on the role of F-actin turnover are not only important to understand the phenotype observed in Rok-RNAi or MbsN300 constricting LECs, but it could also be useful to understand the actomyosin dynamics observed during migration. The fact that two alternating foci are present in wild-type migrating LECs, which are no longer present in Rok-RNAi or MbsN300 expressing LECs, suggests that these multiple contractile events depend on the dynamics of the actomyosin network. In mesodermal cells, Myosin-II accumulation condense the actin meshwork into a focus following dispersion (Mason et al., 2013; Vasquez et al., 2014). Disrupting F-acting disassembly by depleting the expression of *Capulet* (Capt), a protein that promotes actin depolymerisation during oocyte development (Baum and Perrimon, 2001; Baum et al.,

2000), the expression of *Slingshot* (Ssh), the phosphatase required for removing the inhibitory phosphorylation of Cofilin (Niwa et al., 2002) or by injecting phalloidin show that inhibition of F-actin disassembly prevents foci from dispersing and produces an accumulation of actin on the apical surface (Jodoin et al., 2015). Expressing Capt-RNAi or Ssh-RNAi in LECs could allow the study of the temporal and spatial dynamics of the actomyosin foci when the meshwork is full of F-actin and thus denser. This, along with the results obtained interfering with myosin activation, would shed light on which are the most important features of the actomyosin network required for the formation of the two actomyosin foci and in general the cytoskeletal dynamics observed in wild-type.

The polarisation of the cytoskeleton could depend on the localised activation of Rho GTPases

During migration, the actomyosin cytoskeleton is planar polarised, probably due to the fact that LECs are also planar polarised. This planar polarisation depends on PCP signalling (Bischoff 2012). The asymmetrical distribution of the cytoskeleton could depend on the localised activation of the small GTPases. Rac1, active at the front of the migrating cell, has been shown to exclude Rho from the front and polarise the cytoskeleton in many cell types (Cao et al., 2015; Ohta et al., 2006; Sander et al., 1999). The results obtained in the RNAi screen presented in Chapter 5 suggest that RhoGEF Pebble, and possibly Sif, Trio and RhoGEF4, could regulate the function of Rac; CG43658 and CG30456, the activity of Cdc42 and RhoGEF2 the activity of Rho. Furthermore, these RhoGEFs could mediate the localisation and activation of the Rho GTPases in LECs. Rho GEFs and GAPs are not only proposed to activate and deactivate Rho GTPases at certain moments, but also to be differentially distributed in specific regions of the cell to promote localized activation (Greenberg and Hatini, 2012; Simoes et al., 2006). The different GEFs identified in chapter 5 could control the formation and orientation of protrusions through the interaction and localisation of Cdc42 and Rac1 at the cell front and the regulation of contractility through the interaction and

localisation of Rho1 at the back. This asymmetrical distribution of the Rho GTPases could explain the planar polarised cytoskeleton.

How LECs change from planar to radial cell polarity (RCP) during the transition between migration and apical constriction is not known. The studies in ventral furrow cells suggest that the RCP of actin and Rok requires the activity of Rho, among others (Coravos and Martin, 2016). Following the mutually exclusive model for Rho GTPases suggested for migration (Cao et al., 2015; Ohta et al., 2006; Sander et al., 1999), the change in the orientation of the meshwork, from PCP to RCP, could be linked to a break in the asymmetrical distribution of Rac and Rho and the reorganisation of Rho GTPase spatial distribution. One possible way to start testing this hypothesis would be to express photo-activatable Rac (Wang et al., 2010) in LECs, localising its expression at the front of the cell during apical constriction to observe any change in cellular behaviour, such as the formation of membrane protrusions or even the initiation of cell migration.

Although requiring further investigation, the results obtained in the RNAi screen provide new candidate proteins to study and a step forward to understand the molecular mechanisms of LECs behaviour coordination.

The actomyosin contractile network facilitates LEC behaviour coordination and is required for normal abdominal closure

The change in the localisation of foci correlates with a pattern of cell shape changes, consisting of the reduction of the length along the D-V axis and the increase in the length along the A-P axis, i.e LECs become rounder, during the transition between behaviours (Figure 24). The presence of actin foci during apical constriction coincide with the periodic fluctuation of LEC's apical area, which is maintained throughout migration and after lamellipodium disappearance and is eventually reduced before delamination (Figure 27). Like in many other systems, LECs apically constrict in a ratchet-like manner (Blanchard et al., 2010; Martin et al., 2009; Rauzi et al., 2010; Solon et al., 2009; Xie and Martin, 2015).

The downregulation of Rok or the overexpression of MBS impairs the medio-apical cytoskeletal dynamics (Figure 33E, F), producing abnormal LEC shape (Figure 37) and increased LEC size throughout migration and constriction (Figure 38). Despite the effects on the medio-apical contractile network, most LECs apically constrict and delaminate, although the morphogenetic process is delayed.

The actomyosin cortical pool could also facilitate cell shape changes and drive apical constriction

The observation that in the absence of medio-apical pulsed contractions, apical constriction occurs suggests that the reduction of the apical area of LECs could be generated by other force generation mechanisms. One of the mechanisms that could drive apical constriction is the cortical actomyosin pool.

A possible strategy to study the role of the cortical pool of actomyosin would be to explore the role of MLCK. Overexpression of a constitutively active form of MLCK (MLCK-CA) in embryos results in the absence of a junctional actin population and affects contractility in AS cells, while maintaining a medial pool of actomyosin that can generate tensile forces (Fischer et al., 2014). Also, the role for actin architecture in stabilizing and strengthening adhesion is crucial (Cavey and Lecuit, 2009), and in AS cells, the absence of actin at the cell-cell junctions produced by the overexpression of MLCK affects E-cad stabilisation (Fischer et al., 2014). Thus, in AS cells overexpressing MLCK, the absence of a junctional actin population prevents the translation of the medial contractile activity generated by actomyosin foci into a rapid contraction (Fischer et al., 2014). If the translation of the force generated by the medio-apical contractile network was impaired in LECs expressing MLCK-CA but they still delaminated, this experiment would shed light on how the cortex contribute to the process.

Junctional proteins could modulate actomyosin dynamics to allow pulsatile contractions

Studies in other systems have shown interdependence between adherens junction proteins and actomyosin dynamics. In germband extension, the orientation of actomyosin flows towards the shrinking junctions depends on the uneven distribution of E-cad, enriched at the transverse junctions (Rauzi et al., 2010). In AS cells, the expression of a mutant form of MBS has been found to affect cell adhesion, decreasing E-cad levels and affecting the formation and maintenance of the interfaces between AS cells after delamination (Duque and Gorfinkiel, 2016). Also in AS cells, the expression of different α-catenin mutants affects actomyosin foci periodicity, increasing the time between consecutive foci, affecting AS cells area fluctuations (Jurado et al., 2016).

Further studies exploring the role of AJ components in LEC behaviour would be crucial to understand the dynamics of the cytoskeleton observed during LEC behaviour coordination and their interdependence with the cadherin-catenin system to generate cell shape changes.

Continuous vs non-continuous apical constriction

Although this thesis has not focused on the study of this particular finding, during abdominal closure two types of apical constriction are observed: continuous (i.e. without pulsed contractions) and non-continuous (i.e. with pulsed contractions). At the beginning of the morphogenetic event, before LECs start to migrate towards the posterior, some LECs delaminate undergoing continuous constriction (Bischoff lab, unpublished). However, after the start of LEC migration, and before delamination, LECs undergo pulsed contractions generated by their actomyosin cytoskeleton. Further experiments would be required to identify the force generation mechanisms used by the early delaminating LECs and what role this early delamination plays in abdominal closure. Although unable to conclude anything on the role of the continuous apical constriction in LECs, considering the results obtained in this thesis I suggest that one possible role for pulsed contractions is their contribution to abdominal closure by

maintaining cell size and facilitating the cell shape changes required for the transition between migration and constriction. The early appearance of the periodic accumulations, generating non-ratcheted area fluctuations could be a mechanism to deal with the local forces that are created during cell shape change and migration (Mason and Martin, 2011) and a way to maintain tissue integrity.

Thus, the periodic contractions of the actomyosin network in LECs could be one of the force generation mechanisms that contribute to abdominal closure. Like in dorsal closure, the morphogenesis of the abdomen seems to require the coordination of multiple force generation mechanisms (Kiehart et al., 2000), which include the cortical pool of actomyosin and/or the histoblasts pushing.

7. Concluding remarks

With the primary aim to understand how LEC behaviour is coordinated during abdominal morphogenesis of *Drosophila*, this thesis investigated the spatial and temporal dynamics of the actomyosin cytoskeleton and the role of the Myosin regulators in regulating these dynamics during LECs migration and apical constriction. Also, a reverse genetic screen of different RhoGEFs was performed to identify upstream signals that regulate specific aspects of LECs behaviour to gain more insights into how genes required for abdominal morphogenesis.

The results obtained showed that the actomyosin network of LECs was pulsatile, generating periodic actomyosin foci. The correct regulation of Myosin phospho-cycle and the polarity of the cytoskeleton seem to be crucial for generating and positioning the contractile activity. The change in polarity of the actomyosin network, from planar polarised during migration to radial polarised during constriction, is crucial for generating a change in LECs behaviour. What regulates this change in polarity requires further investigation.

The emergence of the contractile activity also correlates with the beginning of LECs shape change, although the medio-apical contractile network is not required for apical constriction per se. The results obtained suggest that the contractile actomyosin network, along with the cortex, could be the cellular force generation mechanism, which contribute to abdominal closure.

8. References

Aelst, L. Van and Symons, M. (2002). Role of Rho family GTPases in epithelial morphogenesis. *Genes and Development* **16**, 1032–1054.

Affolter, M. and Caussinus, E. (2008). Tracheal branching morphogenesis in Drosophila: new insights into cell behaviour and organ architecture. *Development* **135**, 2055–2064.

Allen, W. E., Zicha, D., Ridley, A. J. and Jones, G. (1998). A role for Cdc42 in macrohage chemotaxis. *The Journal of cell biology* **141**, 1147–1157.

Aman, A. and Piotrowski, T. (2011). Cell-cell signaling interactions coordinate multiple cell behaviors that drive morphogenesis of the lateral line. *Cell Adhesion and Migration* **5**, 499–508.

Amano, M., Ito, M., Fukata, Y., Chihara, K., Nakano, T., Matsuura, Y. and Kaibuchi, K. (1996). Phosphorylation and Activation of Myosin by Rho-associated. *The Journal of biological chemistry* **271**, 20246–20249.

Arata, M., Sugimura, K. and Uemura, T. (2017). Difference in Dachsous levels between migrating cells coordinates the direction of collective cell migration. *Developmental Cell* **42**, 479–497.

Bae, Y. K., Trisnadi, N., Kadam, S. and Stathopoulos, A. (2012). The role of FGF signaling in guiding coordinate movement of cell groups. *Cell Adhesion and Migration* **6**, 397–403.

Bainbridge, S. P. and Bownes, M. (1981). Staging the metamorphosis of Drosophila melanogaster. *Journal of embryology and experimental morphology* **66**, 57–80.

Barmchi, M. P., Rogers, S. and Häcker, U. (2005). DRhoGEF2 regulates actin organization and contractility in the Drosophila blastoderm embryo. *Journal of Cell Biology* **168**, 575–585.

Barrett, K., Leptin, M. and Settleman, J. (1997). The Rho GTPase and a putative RhoGEF mediate a signaling pathway for the cell shape changes in Drosophila gastrulation. *Cell* **91**, 905–915.

Barzik, M., Kotova, T. I., Higgs, H. N., Hazelwood, L., Hanein, D., Gertler, F. B. and Schafer, D. A. (2005). Ena/VASP proteins enhance actin polymerization in the presence of barbed end capping proteins. *Journal of Biological Chemistry* **280**, 28653–28662.

Bastock, R. and Strutt, D. (2007). The planar polarity pathway promotes coordinated cell migration during Drosophila oogenesis. *Development* **134**, 3055–3064.

Baum, B. and Perrimon, N. (2001). Spatial control of the actin cytoskeleton in Drosophila epithelial cells. *Nature cell biology* **3**, 883–890.

Baum, B., Li, W. and Perrimon, N. (2000). A cyclase-associated protein regulates actin and cell polarity during Drosophila oogenesis and in yeast. *Current Biology* **10**, 964–973.

Bendix, P. M., Koenderink, G. H., Cuvelier, D., Dogic, Z., Koeleman, B. N., Brieher, W. M., Field, C. M., Mahadevan, L. and Weitz, D. A. (2008). A Quantitative Analysis of Contractility in Active Cytoskeletal Protein Networks. *Biophysical Journal* **94**, 3126–3136.

Bernstein, E., Caudy, A. A., Hammond, S. M. and Hannon, G. J. (2001). Role for a bidentate ribonuclease in the initiation step of RNA interference. *Nature* **409**, 363–366.

Bertet, C., Sulak, L. and Lecuit, T. (2004). Myosin-dependent junction remodelling controls planar cell intercalation and axis elongation. *Nature* **429**, 667–671.

Bertet, C., Rauzi, M. and Lecuit, T. (2009). Repression of Wasp by JAK/STAT signalling inhibits medial actomyosin network assembly and apical cell constriction in intercalating epithelial cells. *Development* **136**, 4199–4212.

Bier, E. and Bodmer, R. (2004). Drosophila, an emerging model for cardiac disease. *Gene* **342**, 1–11.

Bischoff, M. (2012a). Lamellipodia-based migrations of larval epithelial cells are required for normal closure of the adult epidermis of Drosophila. *Developmental Biology* **363**, 179–190.

Bischoff, M. (2012b). Lamellipodia-based migrations of larval epithelial cells are required for normal closure of the adult epidermis of Drosophila. *Developmental biology* **363**, 179–90.

Bischoff, M. and Cseresnyés, Z. (2009). Cell rearrangements, cell divisions and cell death in a migrating epithelial sheet in the abdomen of Drosophila. *Development (Cambridge, England)* **136**, 2403–2411.

Blanchard, G. B., Murugesu, S., Adams, R. J., Martinez-Arias, A. and Gorfinkiel, N. (2010). Cytoskeletal dynamics and supracellular organisation of cell shape fluctuations during dorsal closure. *Development (Cambridge, England)* **137**, 2743–52.

Blankenship, J. T., Backovic, S. T., Sanny, J. S. S. P., Weitz, O. and Zallen, J. A. (2006). Multicellular rosette formation links Planar Cell Polarity to tissue morphogenesis. *Developmental Cell* **11**, 459–470.

Bloor, J. W. and Kiehart, D. P. (2001). zipper Nonmuscle myosin-II functions downstream of PS2 integrin in *Drosophila* myogenesis and is necessary for myofibril formation. *Developmental biology* **239**, 215–228.

Boguslavsky, S., Grosheva, I., Landau, E., Shtutman, M., Cohen, M., Arnold, K., Feinstein, E., Geiger, B. and Bershadsky, A. (2007). P120 Catenin Regulates Lamellipodial Dynamics and Cell Adhesion in Cooperation With Cortactin. *Proc Natl Acad Sci U S A* **104**, 10882–10887.

Brand, A. H. and Perrimon, N. (1993). Targeted gene expression as a means of altering cell fates and generating dominant phenotypes. *Development (Cambridge, England)* **118**, 401–15.

Bresnick, A. R. (1999). Molecular mechanisms of nonmuscle myosin-II regulation. *Current Opinion in Cell Biology* **11**, 26–33.

Broach, J. R. and Hicks, J. B. (1980). Replication and recombination functions associated with the yeast plasmid, 2μ circle. *Cell* **21**, 501–508.

Cao, X., Kaneko, T., Li, J. S., Liu, A. D., Voss, C. and Li, S. S. C. (2015). A phosphorylation switch controls the spatiotemporal activation of Rho GTPases in directional cell migration. *Nature Communications* **6**, 1–14.

Carmona-Fontaine, C., Matthews, H. K., Kuriyama, S., Moreno, M., Dunn, G. A., Parsons, M., Stern, C. D. and Mayor, R. (2008). Contact inhibition of locomotion in vivo controls neural crest directional migration. *Nature* **456**, 957–61.

Cavey, M. and Lecuit, T. (2009). Molecular Bases of Cell–Cell Junctions Stability and Dynamics. *Cold Spring Harbor Laboratory Press* 1–18.

Cavey, M., Rauzi, M. and Lecuit, T. (2008). A two-tiered mechanism for stabilization and immobilization of E-cadherin. *Nature* **453**,.

Chen, J., Godt, D., Gunsalus, K., Kiss, I., Goldberg, M. and Laski, F. A. (2001). Cofilin/ADF is required for cell motility during Drosophila ovary development and oogenesis. *Nature Cell Biology* **3**, 204–209.

Chung, S. and Andrew, D. J. (2008). The formation of epithelial tubes. *Journal of Cell Science* **121**, 3501–3504.

Clay, M. R. and Halloran, M. C. (2013). Rho activation is apically restricted by Arhgap1 in neural crest cells and drives epithelial-to-mesenchymal transition. *Development* **140**, 3198–3209.

Coravos, J. S. and Martin, A. C. (2016). Apical Sarcomere-like Actomyosin Contracts Nonmuscle Drosophila Epithelial Cells. *Developmental Cell* **39**, 346–358.

Coravos, J. S., Mason, F. M. and Martin, A. C. (2017). Actomyosin Pulsing in Tissue Integrity Maintenance during Morphogenesis. *Trends in Cell Biology* **27**, 276–283.

Corrigall, D., Walther, R. F., Rodriguez, L., Fichelson, P. and Pichaud, F. (2007). Hedgehog Signaling Is a Principal Inducer of Myosin-II-Driven Cell Ingression in Drosophila Epithelia. *Developmental Cell* **13**, 730–742.

Costa, M., Raich, W., Agbunag, C., Leung, B., Hardin, J. and Priess, J. R. (1998). A Putative Catenin–Cadherin System Mediates Morphogenesis of the of the Caenorhabditis elegans Embryo Michael. *The Journal of cell biology* **141**, 297–308.

Dai, Y., Zhu, N., Lv, N., Zhang, C., Qiao, Y., Zhao, L. and Gao, X. (2010). Trio Is a Key Guanine Nucleotide Exchange Factor Coordinating Regulation of the Migration and Morphogenesis of Granule Cells in the Developing Cerebellum. *The Journal of biological chemistry* **285**, 24834–24844.

David, D. J. V., Tishkina, A. and Harris, T. J. C. (2010). The PAR complex regulates pulsed actomyosin contractions during amnioserosa apical constriction in Drosophila. *Development* **137**, 1645–1655.

Dawes-Hoang, R. E. (2005). Folded Gastrulation, Cell Shape Change and the Control of Myosin Localization. *Development* **132**, 4165–4178.

De Matos Simões, S., Mainieri, A. and Zallen, J. A. (2014). Rho GTPase and Shroom direct planar polarized actomyosin contractility during convergent extension. *Journal of Cell Biology* **204**, 575–589.

Dietzl, G., Chen, D., Schnorrer, F., Su, K.-C., Barinova, Y., Fellner, M., Gasser, B., Kinsey, K., Oppel, S., Scheiblauer, S., et al. (2007). A genome-wide transgenic RNAi library for conditional gene inactivation in Drosophila. *Nature* **448**, 151–6.

Drees, F., Pokutta, S., Yamada, S., Nelson, J. W. and Weis, W. I. (2012). α-Catenin Is a Molecular Switch that Binds E-Cadherin-β-Catenin and Regulates Actin-Filament Assembly Frauke. *Cell* **123**, 903–915.

Duque, J. and Gorfinkiel, N. (2016). Integration of actomyosin contractility with cell-cell adhesion during dorsal closure. *Development* **143**, 4676–4686.

Dytham, C. (2003). *Choosing and Using Statistics. A Biologist's Guide*. Second Edi. Blackwell Publishing.

Efron, B. (1979). Bootstrap Methods: Another Look at the Jackknife. *The Annals of Statistics* **7**, 1–26.

Efron, B. and Tibshirani, R. J. (1993). *An Introduction to the Bootstrap*. Hall/CRC, Chapman &.

Escudero, L. M., Bischoff, M. and Freeman, M. (2007). Myosin II Regulates Complex Cellular Arrangement and Epithelial Architecture in Drosophila. *Developmental Cell* **13**, 717–729.

Etienne-Manneville, S. and Hall, A. (2002). Rho GTPases in cell biology. *Nature* **420**, 629–635.

Ewald, A. J., Brenot, A., Duong, M., Chan, B. S. and Werb, Z. (2009). Collective Epithelial Migration and Cell Rearrangements Drive Mammary Branching Morphogenesis. *Dev Cell* **14**, 570–581.

Fire, A., Xu, S., Montgomery, M. K., Kostas, S. A., Driver, S. E. and Mello, C. C. (1998). Potent and specific genetic interference by double-stranded RNA in Caenorhabditis elegans. *Nature* **391**, 806–811.

Fischer, S. C., Blanchard, G. B., Duque, J., Adams, R. J., Arias, A. M., Guest, S. D. and Gorfinkiel, N. (2014). Contractile and mechanical properties of epithelia with perturbed actomyosin dynamics. *PLoS ONE* **9**,.

Fox, D. T. and Peifer, M. (2007). Abelson kinase (Abl) and RhoGEF2 regulate actin organization during cell constriction in Drosophila. *Development (Cambridge, England)* **134**, 567–78.

Friedl, P. and Gilmour, D. (2009). Collective cell migration in morphogenesis, regeneration and cancer. *Nature reviews. Molecular cell biology* **10**, 445–457.

Gilmour, D., Rembold, M. and Leptin, M. (2017). From morphogen to morphogenesis and back. *Nature* **541**, 311–320.

Gloushankova, N. a, Krendel, M. F., Alieva, N. O., Bonder, E. M., Feder, H. H., Vasiliev, J. M. and Gelfand, I. M. (1998). Dynamics of contacts between lamellae of fibroblasts: essential role of the actin cytoskeleton. *Proceedings of the National Academy of Sciences of the United States of America* **95**, 4362–4367.

Gorfinkiel, N. and Blanchard, G. B. (2011). Dynamics of actomyosin contractile activity during epithelial morphogenesis. *Current Opinion in Cell Biology* **23**, 531–539.

Gorfinkiel, N., Blanchard, G. B., Adams, R. J. and Martinez Arias, A. (2009). Mechanical control of global cell behaviour during dorsal closure in Drosophila. *Development* **136**, 1889–1898.

Gramates, L. S., Marygold, S. J., Santos, G. dos, Urbano, J.-M., Antonazzo, G., Matthews, B. B., Rey, A. J., Tabone, C. J., Crosby, M. A., Emmert, D. B., et al. (2016). FlyBase at 25: looking to the future. *Nucleic Acids Research* **44**, 663–671.

Greenberg, L. and Hatini, V. (2012). Systematic expression and loss-of-function analysis defines spatially restricted requirements for Drosophila RhoGEFs and RhoGAPs in leg morphogenesis. **76**, 211–220.

Grevengoed, E. E., Fox, D. T., Gates, J. and Peifer, M. (2003). Balancing different types of actin polymerization at distinct sites: Roles for Abelson kinase and Enabled. *Journal of Cell Biology* **163**, 1267–1279.

Grünert, S., Jechlinger, M. and Beug, H. (2003). Diverse cellular and molecular mechanisms contribute to epithelial plasticity and metastasis. *Nature reviews. Molecular cell biology* **4**, 657–665.

Gumbiner, B. M. (1996). Cell adhesion: The molecular basis of tissue architecture and morphogenesis. *Cell* **84**, 345–357.

Haas, P. and Gilmour, D. (2006). Chemokine Signaling Mediates Self-Organizing Tissue Migration in the Zebrafish Lateral Line. *Developmental Cell* **10**, 673–680.

Häcker, U. and Perrimon, N. (1998). DRhoGEF2 encodes a member of the Dbl family of oncogenes and controls cell shape changes during gastrulation in Drosophila. *Genes and Development* **12**, 274–284.

Halbleib, J. M. and Nelson, W. J. (2006). Cadherins in development: Cell adhesion, sorting, and tissue morphogenesis. *Genes and Development* **20**, 3199–3214.

Hammond, S. M., Bernstein, E., Beach, D. and Hannon, G. J. (2000). An RNA-directed nuclease mediates post-transcriptional gene silencing in Drosophila cells. *Nature* **404**, 293–296.

Hartman, M. A. and Spudich, J. A. (2012). The myosin superfamily at a glance. *J. Cell Sci.* **125**, 1627–1632.

Hartshorne, D. J., Ito, M. and Erdödi, F. (1998). Myosin light chain phosphatase: Subunit composition, interactions and regulation. *Journal of Muscle Research and Cell Motility* **19**, 325–341.

He, L., Wang, X., Lam Tang, H. and Montell, D. J. (2010). Tissue elongation requires oscillating contractions of a basal actomyosin network. *Nature cell biology* **28**, 1133–1142.

Heasman, S. J. and Ridley, A. J. (2008). Mammalian Rho GTPases: New insights into their functions from in vivo studies. *Nature Reviews Molecular Cell Biology* **9**, 690–701.

Hildebrand, J. D. (2005). Shroom regulates epithelial cell shape via the apical positioning of an actomyosin network. *Journal of cell science* **118**, 5191–203.

Homem, C. C. F. and Peifer, M. (2008). Diaphanous regulates myosin and adherens junctions to control cell contractility and protrusive behavior during morphogenesis. *Development* **135**, 1005–1018.

Horne-Badovinac, S. and Bilder, D. (2005). Mass transit: Epithelial morphogenesis in the Drosophila egg chamber. *Developmental Dynamics* **232**, 559–574.

Irvine, K. D. and Wieschaus, E. (1994). Cell intercalation suring Drosophila germband extension and its regulaton by pair-rule segmentation genes. *Development* **120**, 827–841.

Jacobson, K., Rajfur1, Z., Vitriol, E. and Hahn, K. (2015). Chromophore-assisted laser inactivation in cell biology Ken. *Trends in Cell Biology* **27**, 316–324.

Jay, D. G. (1988). Selective destruction of protein function by chromophore-assisted laser inactivation. *Proceedings of the National Academy of Sciences* **85**, 5454–5458.

Jodoin, J. N., Coravos, J. S., Chanet, S., Vasquez, C. G., Tworoger, M., Kingston, E. R., Perkins, L. A., Perrimon, N. and Martin, A. C. (2015). Stable Force Balance between Epithelial Cells Arises from F-Actin Turnover. *Developmental Cell* **35**, 685–697.

Jordan, P. and Karess, R. (1997). Myosin light chain-activating phosphorylation sites are required for oogenesis in Drosophila. *Journal of Cell Biology* **139**, 1805–1819.

Jülicher, F. and Prost, J. (1995). Cooperative molecular motors. *Physical Review Letters* **75**, 2618–2621.

Jurado, J., de Navascués, J. and Gorfinkiel, N. (2016). α-Catenin stabilises Cadherin-Catenin complexes and modulates actomyosin dynamics to allow pulsatile apical contraction. *Journal of Cell Science* jcs.193268.

Kasza, K. E., Farrell, D. L. and Zallen, J. A. (2014). Spatiotemporal control of epithelial remodeling by regulated myosin phosphorylation. *Proceedings of the National Academy of Sciences of the United States of America* **111**, 11732–7.

Khalil, A. A. and Friedl, P. (2010). Determinants of leader cells in collective cell migration. *Integrative Biology* **2**, 568.

Kiehart, D. P., Galbraith, C. G., Edwards, K. A., Rickoll, W. L. and Montague, R. A. (2000). Multiple forces contribute to cell sheet morphogenesis for dorsal closure in Drosophila. *Journal of Cell Biology* **149**, 471–490.

Kim, H. Y. and Davidson, L. A. (2011). Punctuated actin contractions during convergent extension and their permissive regulation by the non-canonical Wnt-signaling pathway. *Journal of Cell Science* **124**, 635–646.

Kinoshita, N., Sasai, N., Misaki, K. and Yonemura, S. (2008). Apical Accumulation of Rho in the Neural Plate Is Important for Neural Plate Cell Shape Change and Neural Tube Formation. *Molecular biology of the cell* **19**, 308–317.

Knowles, B. A. and Cooley, L. (1994). The specialized cytoskeleton of the Drosophila egg chamber. *Trends in Genetics* **10**, 241–245.

Kobielak, A., Pasolli, A. and Fuchs, E. (2008). Mammalian formin-1 participates in adherens junctions and polymerization of linear actin cables Agnieszka. *Nature cell biology* **6**, 21–30.

Koleske, A. J., Gifford, A. M., Scott, M. L., Nee, M., Bronson, R. T., Miczek, K. A. and Baltimore, D. (1998). Essential roles for the Abl and Arg tyrosine kinases in neurulation. *Neuron* **21**, 1259–1272.

Kolsch, V., Seher, T., Fernandez-Ballester, G. J., Serrano, L. and Leptin, M. (2007). Control of Drosophila Gastrulation by Apical Localization of Adherens Junctions and RhoGEF2. *Science* **315**, 384–386.

Krause, M., Bear, J. ., Loureiro, J. . and Gertler, F. . (2002). The Ena/VASP enigma. *Journal of Cell Science* **115**, 4721–4726.

Kreis, T. E. and Birchmeier, W. (1980). Stress fiber sarcomeres of fibroblasts are contractile. *Cell* **22**, 555–561.

Lawrence, P. A. (2001). Morphogens: how big is the big picture? *Nature cell biology* **3**, E151-4.

Lecuit, T. and Le Goff, L. (2007). Orchestrating size and shape during morphogenesis. *Nature* **450**, 189–192.

Lecuit, T. and Lenne, P. (2007). Cell surface mechanics and the control of cell shape , tissue patterns and morphogenesis. *Nature reviews. Molecular cell biology* **8**, 633–644.

Lee, T. and Luo, L. (1999). Mosaic analysis with a repressible cell marker for studies of gene function in neuronal morphogenesis. *Neuron* **22**, 451–61.

Lee, A. and Treisman, J. (2004). Excessive Myosin Activity in Mbs Mutants Causes Photoreceptor Movement Out of the Drosophila Eye Disc Epithelium. *Molecular biology of the cell* **15**, 3285–3295.

Lenth, R. V. (2016). Least-Squares Means: The *R* Package **lsmeans**. *Journal of Statistical Software* **69**,.

Leptin, M. (1991). twist and snail as positive and negiative regulators during Drosphila mesoderm development. *Genes & Development* **5**, 1568–1576.

Leptin, M. (1999). Gastrulation in Drosophila: The logic and the cellular mechanisms. *EMBO Journal* **18**, 3187–3192.

Levayer, R. and Lecuit, T. (2012). Biomechanical regulation of contractility: Spatial control and dynamics. *Trends in Cell Biology* **22**, 61–81.

Li, S., Yamauchi, A., Marchal, C. C., Jason, K., Quilliam, L. A. and Dinauer, M. C. (2018). Chemoattractant-Stimulated Rac Activation in Wild-Type and Rac2-Deficient Murine Neutrophils: Preferential Activation of Rac2 and Rac2 Gene Dosage Effect on Neutrophil Functions.

Linden, K. G., Liao, J. C. and Jay, D. G. (1992). Spatial specificity of chromophore assisted laser inactivation of protein function. *Biophysical journal* **61**, 956–62.

Llense, F. and Martín-Blanco, E. (2008). JNK Signaling Controls Border Cell Cluster Integrity and Collective Cell Migration. *Current Biology* **18**, 538–544.

Madhavan, M. M. and Madhavan, K. (1980). Morphogenesis of the epidermis of adult abdomen of Drosophila. *Journal of embryology and experimental morphology* **60**, 1–31.

Magie, C. R., Pinto-santini, D. and Parkhurst, S. M. (2002). Rho1 interacts with p120ctn and α-catenin, and regulates cadherin-based adherens junction components in Dr osophila. *Development* **3782**, 3771–3782.

Maître, J. L., Niwayama, R., Turlier, H., Nedelec, F. and Hiiragi, T. (2015). Pulsatile cell-autonomous contractility drives compaction in the mouse embryo. *Nature Cell Biology* **17**, 849–855.

Major, R. J. and Irvine, K. D. (2006). Localization and requirement for myosin II at the dorsal-ventral compartment boundary of the Drosophila wing. *Developmental Dynamics* **235**, 3051–3058.

Mandaravally Madhavan, M. and Schneiderman, H. A. (1977). Histological analysis of the dynamics of growth of imaginal discs and histoblast nests during the larval development of Drosophila melanogaster. *Wilhelm Roux's Archives of Developmental Biology* **183**, 269–305.

Martin, A. C. (2010). Pulsation and stabilization: Contractile forces that underlie morphogenesis. *Developmental Biology* **341**, 114–125.

Martin, A. C., Kaschube, M. and Wieschaus, E. F. (2009). Pulsed contractions of an actin-myosin network drive apical constriction. *Nature* **457**, 495–9.

Martin, A. C., Gelbart, M., Fernandez-Gonzalez, R., Kaschube, M. and Wieschaus, E. F. (2010). Integration of contractile forces during tissue invagination. *Journal of Cell Biology* **188**, 735–749.

Mason, F. M. and Martin, A. C. (2011). Tuning cell shape change with contractile ratchets. *Current Opinion in Genetics and Development* **21**, 671–679.

Mason, F. M., Tworoger, M. and Martin, A. C. (2013). Apical domain polarization localizes actin-myosin activity to drive ratchet-like apical constriction. *Nature cell biology* **15**, 926–36.

Matthews, H. K., Marchant, L., Carmona-Fontaine, C., Kuriyama, S., Larrain, J., Holt, M. R., Parsons, M. and Mayor, R. (2008). Directional migration of neural crest cells in vivo is regulated by Syndecan-4/Rac1 and non-canonical Wnt signaling/RhoA. *Development* **135**, 1771–1780.

Mayer, M., Depken, M., Bois, J. S., Jülicher, F. and Grill, S. W. (2010). Anisotropies in cortical tension reveal the physical basis of polarizing cortical flows. *Nature* **467**, 617–621.

Mayor, R. and Theveneau, E. (2014). The role of the non-canonical Wnt–planar cell polarity pathway in neural crest migration. *Biochemical Journal* **457**, 19–26.

McGuire, S. E. (2003). Spatiotemporal Rescue of Memory Dysfunction in Drosophila. *Science* **302**, 1765–1768.

Mitchison, T. J. and Cramer, L. P. (1996). Actin-based cell motility and cell locomotion. *Cell* **84**, 371–379.

Mitonaka, T., Muramatsu, Y., Sugiyama, S., Mizuno, T. and Nishida, Y. (2007). Essential roles of myosin phosphatase in the maintenance of epithelial cell integrity of Drosophila imaginal disc cells. *Developmental biology* **309**, 78–86.

Monier, B., Pélissier-Monier, A., Brand, A. H. and Sanson, B. (2010). An actomyosin-based barrier inhibits cell mixing at compartmental boundaries in Drosophila embryos. *Nature cell biology* **12**, 60-65–9.

Montell, D. J. (2008). Morphogenetic Cell Movements : Mechanical Properties. **322**, 1502–1505.

Montell, D. J., Rorth, P. and Spradling, A. C. (1992). slow border cells, a locus required for a developmentally regulated cell migration during oogenesis, encodes Drosophila C EBP. *Cell* **71**, 51–62.

Montell, D. J., Yoon, W. H. and Starz-Gaiano, M. (2012). Group choreography: Mechanisms orchestrating the collective movement of border cells. *Nature Reviews Molecular Cell Biology* **13**, 631–645.

Montgomery, M. K., Xu, S. and Fire, A. (1998). RNA as a target of double-stranded RNA-mediated genetic interference in Caenorhabditis elegans. *Proceedings of the National Academy of Sciences* **95**, 15502–15507.

Munjal, A. and Lecuit, T. (2014). Actomyosin networks and tissue morphogenesis. *Development (Cambridge, England)* **141**, 1789–93.

Munjal, A., Philippe, J.-M., Munro, E. and Lecuit, T. (2015). A self-organized biomechanical network drives shape changes during tissue morphogenesis. *Nature* **524**, 351–355.

Munro, E., Nance, J. and Priess, J. R. (2004). Cortical flows powered by asymmetrical contraction transport PAR proteins to establish and maintain anterior-posterior polarity in the early C. elegans embryo. *Developmental Cell* **7**, 413–424.

Murphy, A. M. and Montell, D. J. (1996). Cell Type-specific Roles for Cdc42 , Rac , and RhoL. *The Journal of cell biology* **133**, 617–630.

Niederman, R. and Pollard, T. D. (1975). Human platelet myosin: II. In vitro assembly and structure of myosin filaments. *Journal of Cell Biology* **67**, 72–92.

Nikolaidou, K. K. and Barrett, K. (2004). A Rho GTPase Signaling Pathway Is Used Reiteratively in Epithelial Folding and Potentially Selects the Outcome of Rho Activation. *Current Biology* **14**, 1822–1826.

Ninov, N., Chiarelli, D. A. and Martin-Blanco, E. (2007). Extrinsic and intrinsic mechanisms directing epithelial cell sheet replacement during Drosophila metamorphosis. *Development* **134**, 367–379.

Nishimura, T. and Takeichi, M. (2008). Shroom3-mediated recruitment of Rho kinases to the apical cell junctions regulates epithelial and neuroepithelial planar remodeling. *Development (Cambridge, England)* **135**, 1493–502.

Nishimura, T. and Takeichi, M. (2009). *Chapter 2 Remodeling of the Adherens Junctions During Morphogenesis*. 1st ed. Elsevier Inc.

Niwa, R., Nagata-Ohashi, K., Takeichi, M., Mizuno, K. and Uemura, T. (2002). Control of actin reorganization by slingshot, a family of phosphatases that dephosphorylate ADF/cofilin. *Cell* **108**, 233–246.

Nobes, C. D. and Hall, A. (1995). Rho, Rac, and Cdc42 GTPases regulate the assembly of multimolecular focal complexes associated with actin stress fibers, lamellipodia, and filopodia. *Cell* **81**, 53–62.

Ohta, Y., Hartwig, J. H. and Stossel, T. P. (2006). FilGAP, a Rho- and ROCK-regulated GAP for Rac binds filamin A to control actin remodelling. *Nature Cell Biology* **8**, 803–814.

Plaçais, P. Y., Balland, M., Guérin, T., Joanny, J. F. and Martin, P. (2009). Spontaneous oscillations of a minimal actomyosin system under elastic loading. *Physical Review Letters* **103**, 1–4.

Pollard, T. D. and Borisy, G. G. (2003). Cellular motility driven by assembly and disassembly of actin filaments. *Cell* **112**, 453–465.

Pollard, T. D., Blanchoin, L. and Mullins, R. D. (2000). Molecular mechanisms controlling actin filament dynamics in nonmuscle cells. *Annual Review of Biomole Structure* **29**, 545–76.

Prokopenko, S. N., Brumby, A., O'Keefe, L., Prior, L., He, Y., Saint, R. and Bellen, H. J. (1999). A putative exchange factor for Rho1 GTPase is required for initiation of cytokinesis in Drosophila. *Genes and Development* **13**, 2301–2314.

Quintin, S., Gally, C. and Labouesse, M. (2008). Epithelial morphogenesis in embryos: asymmetries, motors and brakes. *Trends in Genetics* **24**, 221–230.

Raftopoulou, M. and Hall, A. (2004). Cell migration: Rho GTPases lead the way. *Developmental Biology* **265**, 23–32.

Rauzi, M., Verant, P., Lecuit, T. and Lenne, P.-F. (2008). Nature and anisotropy of cortical forces orienting Drosophila tissue morphogenesis. *Nature Cell Biology* **10**, 1401–1410.

Rauzi, M., Lenne, P.-F. and Lecuit, T. (2010). Planar polarized actomyosin contractile flows control epithelial junction remodelling. *Nature* **468**, 1110–4.

Reymann, A.-C., Boujemaa-Paterski, R., Martiel, J.-L., Guerin, C., Cao, W., Chin, H. F., De La Cruz, E. M., Thery, M. and Blanchoin, L. (2012). Actin Network Architecture Can Determine Myosin Motor Activity. *Science* **336**, 1310–1314.

Ridley, A. J. (2003). Cell Migration: Integrating Signals from Front to Back. *Science* **302**, 1704–1709.

Ridley, A. J. (2011). Life at the leading edge. *Cell* **145**, 1012–1022.

Ridley, A. J. and Hall, A. (1992). The small GTP-binding protein rho regulates the assembly of focal adhesions and actin stress fibers in response to growth factors. *Cell* **70**, 389–399.

Ridley, A. J., Paterson, H. F., Johnston, C. L., Diekmann, D. and Hall, A. (1992). The small GTP-binding protein rac regulates growth factor-induced membrane ruffling. *Cell* **70**, 401–410.

Riedl, J., Crevenna, A. H., Kessenbrock, K., Yu, J. H., Bista, M., Bradke, F., Jenne, D., Holak, T. a, Werb, Z., Sixt, M., et al. (2008a). Lifeact: a versatile marker to visualize F-actin. *Nat Methods* **5**, 1–8.

Riedl, J., Crevenna, A. H., Kessenbrock, K., Yu, J. H., Neukirchen, D., Bista, M., Bradke, F., Jenne, D., Holak, T. a, Werb, Z., et al. (2008b). Lifeact: a versatile marker to visualize F-actin. *Nature methods* **5**, 605–607.

Roffers-Agarwal, J., Xanthos, J. B., Kragtorp, K. A. and Miller, J. R. (2008). Enabled (Xena) regulates neural plate morphogenesis, apical constriction, and cellular adhesion required for neural tube closure in Xenopus Julaine. *Am J Hypertens* **314**, 393–403.

Roh-johnson, M., Shemer, G., Higgins, C. D., Mcclellan, J. H., Werts, A. D., Tulu, U. S., Gao, L., Betzig, E. and Kiehart, D. P. (2012). Triggering a Cell Shape Change by Exploiting Pre-Existing Actomyosin Contractions. **335**, 1232–1235.

Roseland, C. R. and Schneiderman, H. A. (1979). Regulation and metamorphosis of the abdominal histoblasts of Drosophila melanogaster. *Wilhelm Roux's Archives of Developmental Biology* **186**, 235–265.

Royou, A., †, Field, C., ‡, Sisson, J. C., †, Sullivan, W., †, And, Karess, R., et al. (2004). Reassessing the Role and Dynamics of Nonmuscle Myosin II during Furrow Formation in Early Drosophila Embryos. *Molecular biology of the cell* **15**, 3751–3737.

Sander, E. E., Ten Klooster, J. P., Van Delft, S., Van Der Kammen, R. A. and Collard, J. G. (1999). Rac downregulates Rho activity: Reciprocal balance between both GTPases determines cellular morphology and migratory behavior. *Journal of Cell Biology* **147**, 1009–1021.

Sawyer, J. M., Harrell, J. R., Shemer, G., Sullivan-Brown, J., Roh-Johnson, M. and Goldstein, B. (2010). Apical constriction: A cell shape change that can drive morphogenesis. *Developmental Biology* **341**, 5–19.

Schnabel, R., Hutter, H., Moerman, D. and Schnabel, H. (1997). Assessing Normal Embryogenesis in *Caenorhabditis elegans* Using a 4D Microscope: Variability of Development and Regional Specification. *Developmental Biology* **184**, 234–265.

Simoes, S., Denholm, B., Azevedo, D., Sotillos, S., Martin, P., Skaer, H., Hombria, J. C.-G. and Jacinto, A. (2006). Compartmentalisation of Rho regulators directs cell invagination during tissue morphogenesis. *Development* **133**, 4257–4267.

Singh, H., Sone, M., Suzuki, E., Kuroda, S., Kaibuchi, K., Nakagoshi, H., Saigo, K., Nabeshima, Y. and Hama, C. (1997). Still life, a Protein in Synaptic Terminals of Drosophila Homologous to GDP-GTP Exchangers. *Science* **275**, 543–547.

Skoglund, P., Rolo, A., Chen, X., Gumbiner, B. M. and Keller, R. (2008). Convergence and extension at gastrulation require a myosin IIB-dependent cortical actin network. *Development* **135**, 2435–2444.

Sokol, N. S. and Cooley, L. (2003). Drosophila filamin is required for follicle cell motility during oogenesis. *Developmental Biology* **260**, 260–272.

Solon, J., Kaya-Çopur, A., Colombelli, J. and Brunner, D. (2009). Pulsed Forces Timed by a Ratchet-like Mechanism Drive Directed Tissue Movement during Dorsal Closure. *Cell* **137**, 1331–1342.

Souza-schorey, C. D. (2005). Disassembling adherens junctions : breaking up is hard to do. *Trends in Cell Biology* **15**, 19–26.

Spracklen, A. J., Fagan, T. N., Lovander, K. E. and Tootle, T. L. (2014). The pros and cons of common actin labeling tools for visualizing actin dynamics during Drosophila oogenesis. *Developmental Biology* **393**, 209–226.

Stramer, B., Wood, W., Galko, M. J., Redd, M. J., Jacinto, A., Parkhurst, S. M. and Martin, P. (2002). Live imaging of wound inflammation in Drosophila embryos reveals key roles for small GTPases during in vivo cell migration. *Journal of Cell Biology* 567–573.

Struhl, G. and Basler, K. (1993). Organizing activity of wingless protein in Drosophila. *Cell* **72**, 527–540.

Sun, C. X., Magalhães, M. A. O. and Glogauer, M. (2007). Rac1 and Rac2 differentially regulate actin free barbed end formation downstream of the fMLP receptor. **179**, 239–245.

Sweeton, D., Parks, S., Costa, M. and Wieschaus, E. (1991). Gastrulation in Drosophila: the formation of the ventral furrow and posterior midgut invaginations. *Development (Cambridge, England)* **112**, 775–89.

Szczur, K., Xu, H., Atkinson, S., Zheng, Y. and Filippi, M. (2018). Rho GTPase CDC42 regulates directionality and random movement via distinct MAPK pathways in neutrophils. **108**, 4205–4214.

Tada, M. and Heisenberg, C.-P. (2012). Convergent extension: using collective cell migration and cell intercalation to shape embryos. *Development* **139**, 3897–3904.

Tahinci, E. and Symes, K. (2003). Distinct functions of Rho and Rac are required for convergent extension during Xenopus gastrulation. *Developmental Biology* **259**, 318–335.

Theveneau, E., Marchant, L., Kuriyama, S., Gull, M., Moepps, B., Parsons, M. and Mayor, R. (2010). Collective Chemotaxis Requires Contact-Dependent Cell Polarity. *Developmental Cell* **19**, 39–53.

Tomlinson, a (1985). The cellular dynamics of pattern formation in the eye of Drosophila. *Journal of embryology and experimental morphology* **89**, 313–31.

Turner, F. R. and Mahowald, A. P. (1976). Scanning electron microscopy of Drosophila embryogenesis. *Developmental Biology* **50**, 95–108.

Umetsu, D. and Dahmann, C. (2010). Compartment boundaries: Sorting cells with tension. *Fly* **4**, 36–40.

Valencia-Expósito, A., Grosheva, I., Míguez, D. G., González-Reyes, A. and Martín-Bermudo, M. D. (2016). Myosin light-chain phosphatase regulates basal actomyosin oscillations during morphogenesis. *Nature Communications* **7**, 1–11.

van Impel, A., Schumacher, S., Draga, M., Herz, H.-M., Grosshans, J. and Müller, H. A. J. (2009). Regulation of the Rac GTPase pathway by the multifunctional Rho GEF Pebble is essential for mesoderm migration in the Drosophila gastrula. *Development (Cambridge, England)* **136**, 813–22.

van Rijssel, J., Hoogenboezem, M., Wester, L., Hordijk, P. L. and van Buul, J. D. (2012). The N-terminal DH-PH domain of trio induces cell spreading and migration by regulating lamellipodia dynamics in a Rac1-dependent fashion. *PLoS ONE* **7**, 1–13.

Vasquez, C. G., Tworoger, M. and Martin, A. C. (2014). Dynamic myosin phosphorylation regulates contractile pulses and tissue integrity during epithelial morphogenesis. *Journal of Cell Biology* **206**, 435–450.

Verheyen, E. M. and Cooley, L. (1994). Profilin mutations disrupt multiple actin-dependent processes during Drosophila development. *Development (Cambridge, England)* **120**, 717–728.

Wang, X., He, L., Wu, Y. I., Hahn, K. M., Montell, D. J., Hill, C. and Hill, C. (2010). Light-mediated activation reveals a key role for Rac in collective guidance of cell movement in vivo. *Nature cell biology* **12**, 591–597.

Welch, M. D. and Mullins, R. D. (2002). Cellular Control of Actin Nucleation. *Annual Review of Cell and Developmental Biology* **18**, 247–288.

Wheeler, A. P. and Ridley, A. J. (2004). Why three Rho proteins? RhoA, RhoB, RhoC, and cell motility. *Experimental Cell Research* **301**, 43–49.

Wood, W., Jacinto, A., Grose, R., Woolner, S., Gale, J., Wilson, C. and Martin, P. (2002). Wound healing recapitulates morphogenesis in Drosophila embryos. *Nature Cell Biology* **4**, 1–7.

Wu, X., Tanwar, P. S. and Raftery, L. A. (2008). Drosophila follicle cells: morphogenesis in an eggshell. *Semin Cell Dev Biol.* **19**, 271–282.

Xie, S. and Martin, A. C. (2015). Intracellular signalling and intercellular coupling coordinate heterogeneous contractile events to facilitate tissue folding. *Nature communications* **6**, 7161.

Xu, N., Keung, B. and Myat, M. M. (2008). Rho GTPase controls invagination and cohesive migration of the Drosophila salivary gland through Crumbs and Rho-kinase. *Developmental Biology* **321**, 88–100.

Yamada, S. and Nelson, W. J. (2007). Localized zones of Rho and Rac activities drive initiation and expansion of epithelial cell–cell adhesion. *Journal of Cell Biology* **178**, 517–527.

Yang, L., Wang, L., Geiger, H., Cancelas, J. A., Mo, J. and Zheng, Y. (2007). Rho GTPase Cdc42 coordinates hematopoietic stem cell quiescence and niche interaction in the bone marrow.

Young, P. E., Pesacreta, T. C. and Kiehart, D. P. (1991). Dynamic changes in the distribution of cytoplasmic myosin during Drosophila embryogenesis. *Development* **111**, 1–14.

Zallen, J. A. and Wieschaus, E. (2004). Patterned gene expression directs bipolar planar polarity in Drosophila. *Developmental Cell* **6**, 343–355.

Zamore, P. D., Tuschl, T., Sharp, P. A. and Bartel, D. P. (2000). RNAi: double-stranded RNA directs the ATP-dependent cleavage of mRNA at 21 to 23 nucleotide intervals. *Cell* **101**, 25–33.

Zhang, L., Luo, J., Wan, P., Wu, J., Laski, F. and Chen, J. (2011). Regulation of cofilin phosphorylation and asymmetry in collective cell migration during morphogenesis. *Development* **138**, 455–464.

9. Supplementary material

9.1 Supplementary Script

```
bootFun <- function(inputData, reps){

bootStat <- numeric(reps)

for (i in 1:reps){ # resample for each bootstrap

    bootInd <- sample (1:length(inputData), length(inputData), replace=T)
    #resample

    bootData <- inputData[bootInd] # store each sample

    bootStat[i] <- median(bootData) # calculate the median for each of those
    generated samples

bootSE<- sd(bootStat) # standard deviation of the distribution of the estimated
median, which is the estimate of the standard error

bootCI<- quantile (bootStat, probs=c(0.025, 0.975)) # 95% CI based on upper and lower
quantiles (2 values each time)

bootMed <- median(bootStat) # overall median

bootMean <- mean(bootStat) # overall mean

output <- data.frame(meanEst=bootMean, medEst=bootMed, lower95CI=bootCI[1],
upper95CI = bootCI[2], stdErr = bootSE) #store all the values in output

output #show output
```

9.2 Supplementary Figures

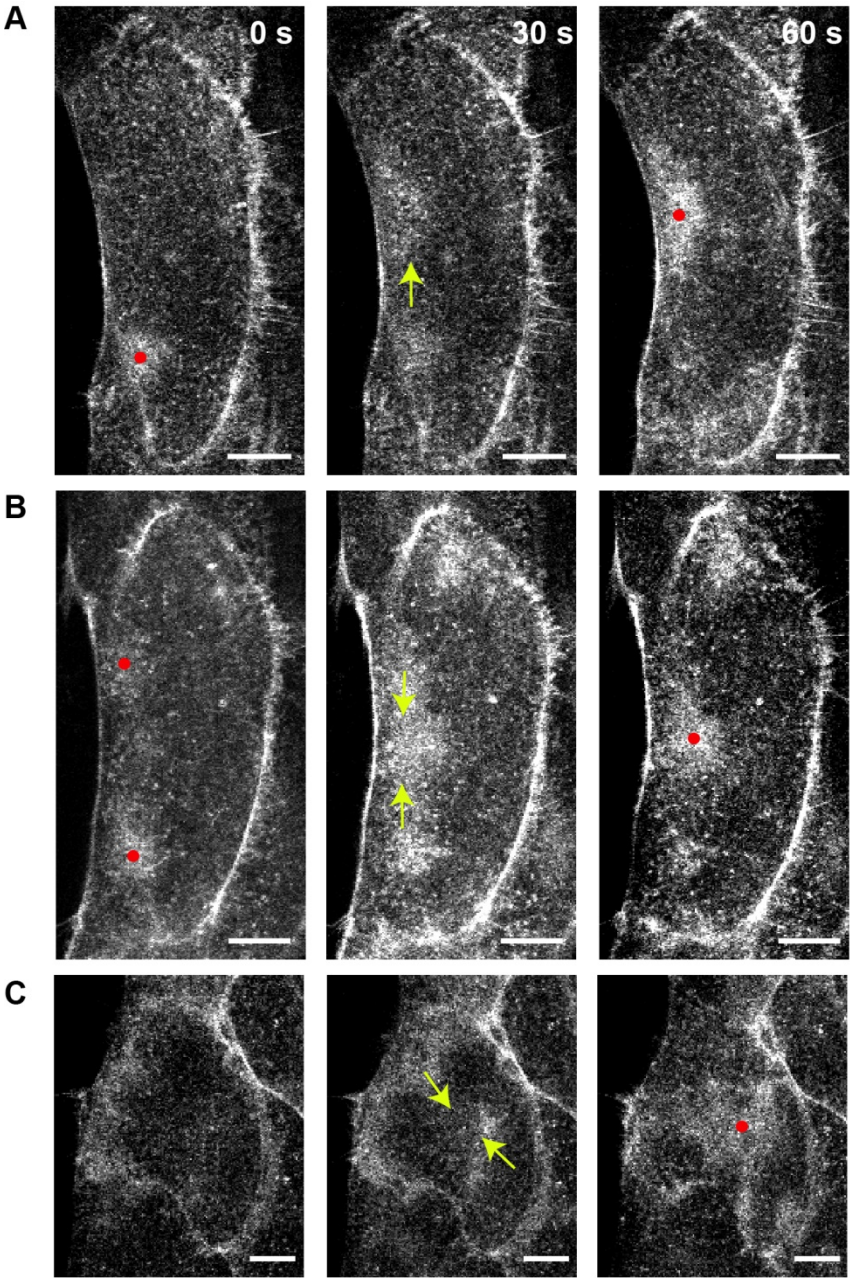

Figure S1. Actin flow patterns in LECs expressing LifeAct-Ruby

Consecutive captions taken from the recordings of pupae expressing LifeAct-Ruby with *tub.Gal80ts*. Scale bars, 20 μm. Red dots indicate the localization of the actin foci and yellow arrows the flow of actin. **A)** During migration, actin coalesces in a focus that localises laterally. Then, actin flows towards a medial region to form a new focus. **B)** During late migration, actin flows from the lateral and medial ends of the cell to accumulate at a mid-point. **C)** During constriction, actin flows from different directions to coalesce in the centre of the cell, forming a single focus.

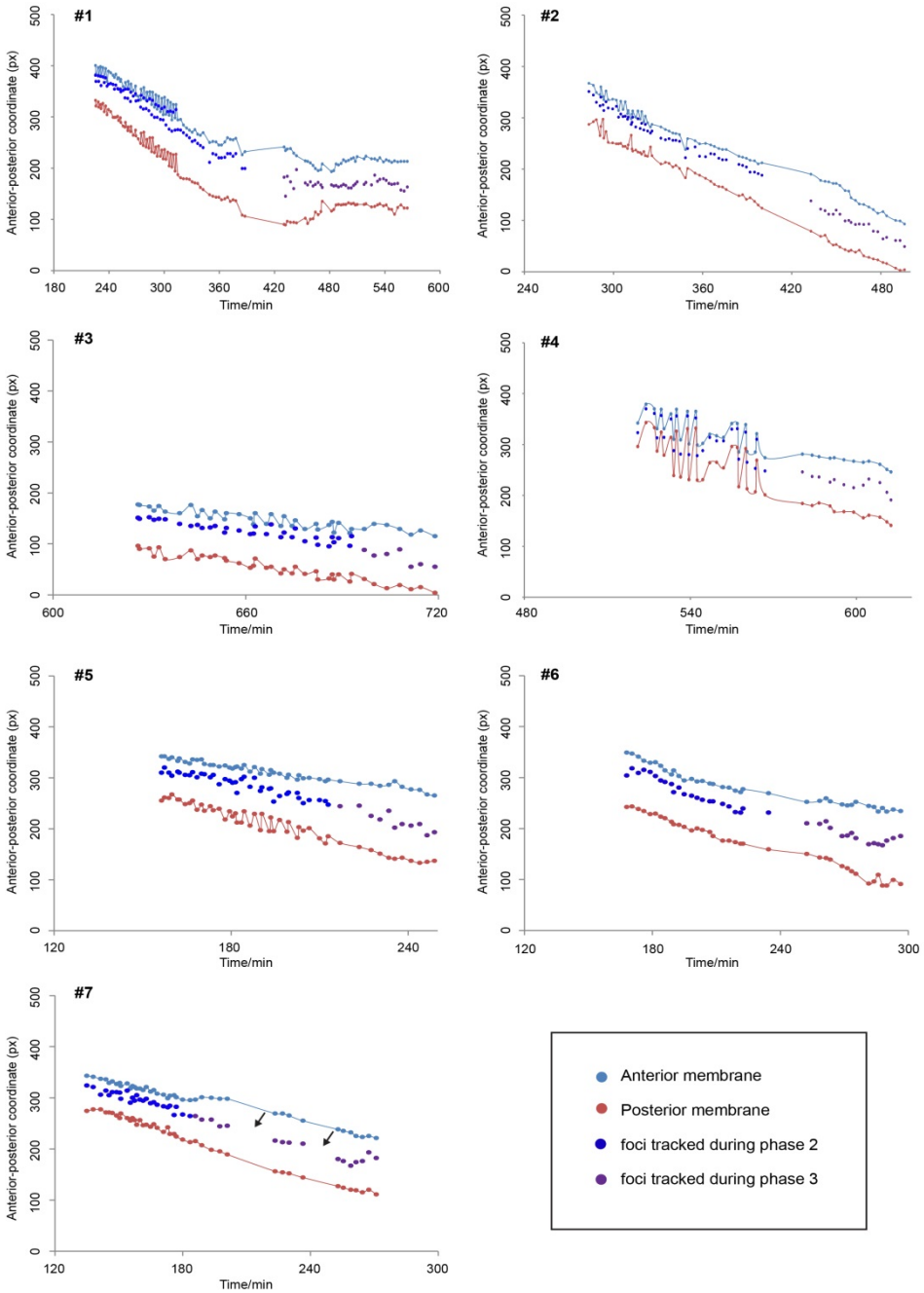

Figure S2. Quantification of the localisation of foci during phase 2 and 3

Spatial coordinates of actin foci and anterior and posterior membranes tracked for the seven GMA expressing LECs analysed. During phase 2 (migration), foci localise at the back of the cell, and during phase 3 (constriction), foci localise centrally. During phase 2, the anterior and posterior membrane coordinates are tracked in line with where the focus assembles, along the anterior-posterior (AP) axis. In some LECs, the AP length at the medial and lateral ends, where the two foci assemble, can be very different. This creates strong fluctuations in the representation of the AP coordinates over time. In some LECs, foci cannot be tracked during phase transition due to the randomisation of actin dynamics. The time gaps between tracked foci (black arrows) are bits of the recording in which foci could not be tracked.

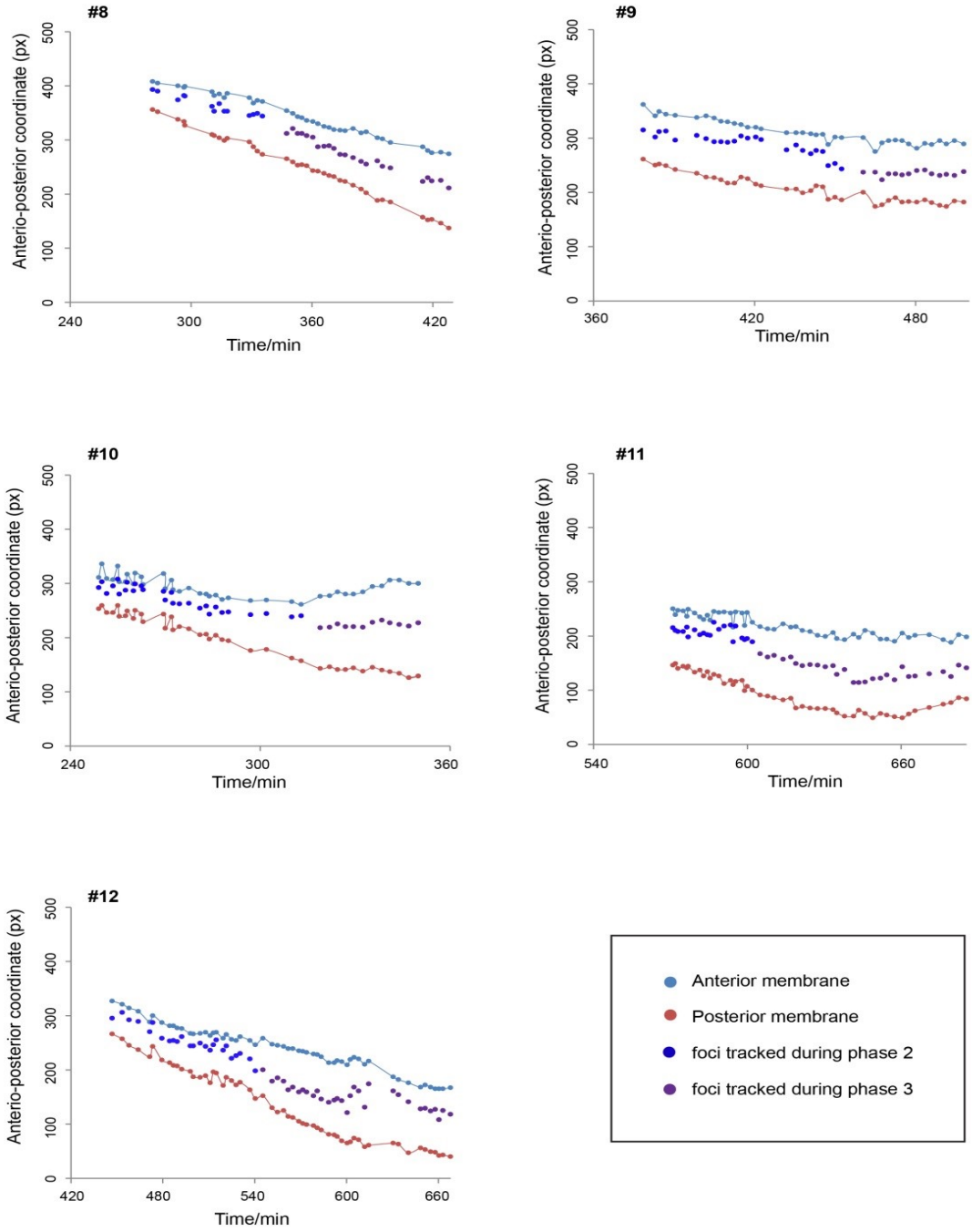

Figure S3. Quantification of the localisation of foci during phases 2 and 3 in LECs expressing GMA with *tub.Gal80ts*.

Spatial coordinates of actin foci and anterior and posterior membranes tracked for the five GMA expressing LECs with *tub.Gal80ts* analysed. In all cases, during phase 2 foci localise at the back and during phase 3 foci localise in the centre.

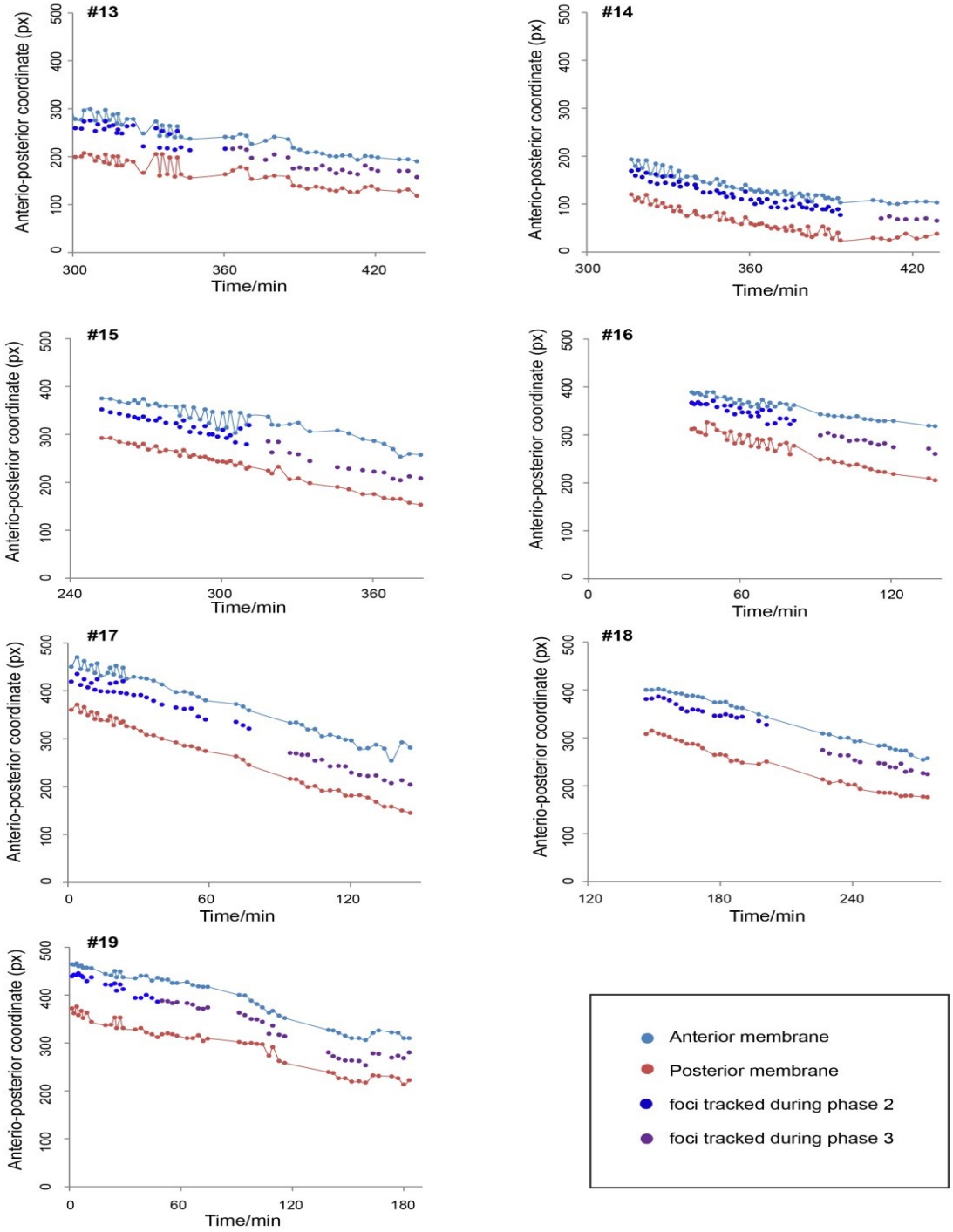

Figure S4. Quantification of the localisation of foci during phase 2 and 3 in LECs expressing LifeAct-Ruby with *tub.Gal80ts*

Spatial coordinates of actin foci and anterior and posterior membranes tracked for the 7 LifeAct-Ruby expressing LECs with *tub.Gal80ts* analysed. Like in GMA expressing LECs, during phase 2 foci localise at the back and during phase 3 foci localise in the centre.

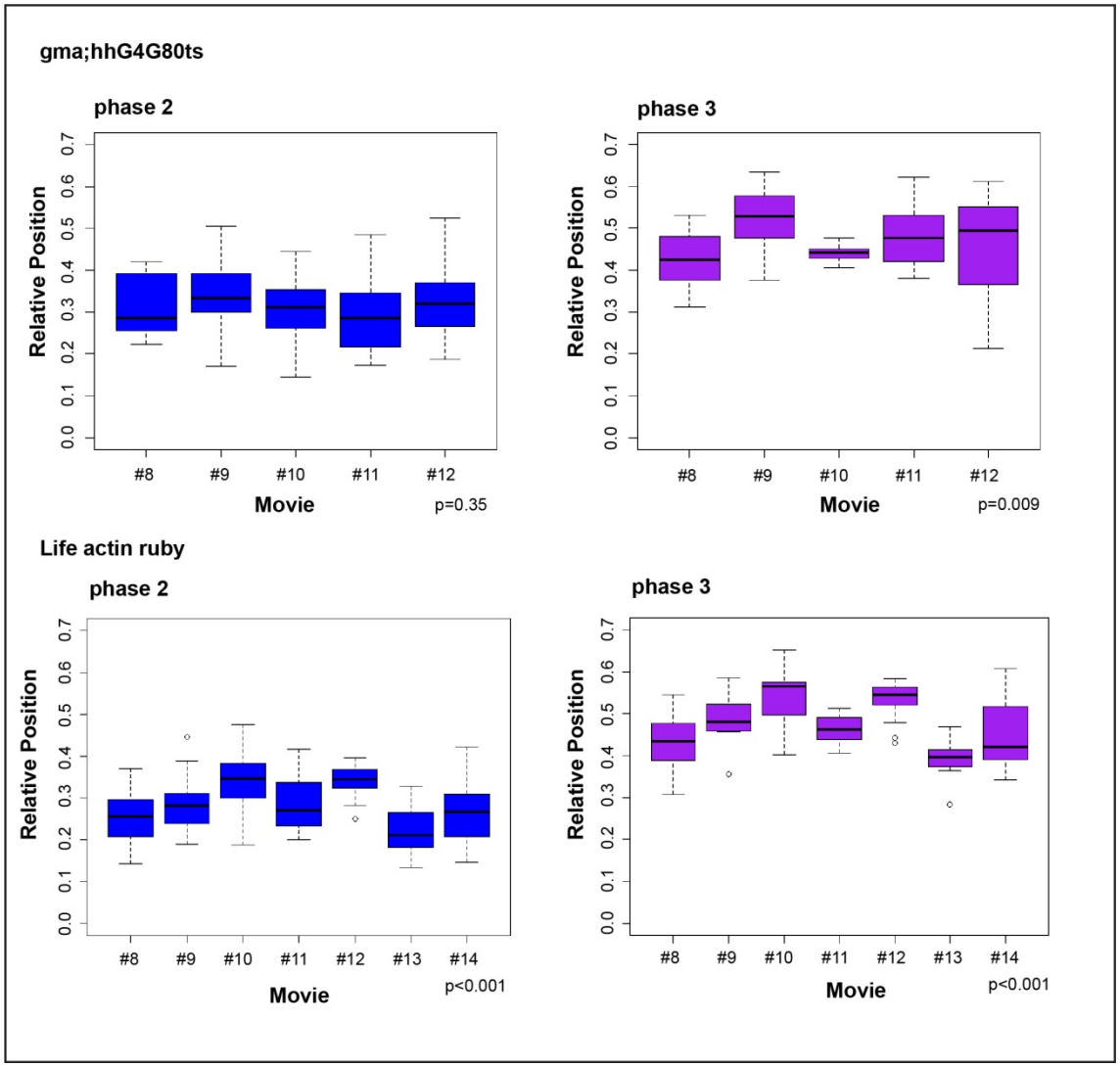

Figure S5. Statistical analysis of the localization of foci during phase 2 and 3 in LECs expressing GMA and LifeAct-Ruby with *tub.Gal80ts*.

The mean relative position (RP) of foci during phases 2 and 3 for the GMA (N=5) and LifeAct-Ruby (N=7) expressing LECs show in most cases statistically significant differences. Despite the differences, foci during phase 2 take values between 0.2-0.4 and during phase 3, close to 0.5. The p-values for the ANOVA test are indicated under each boxplot.

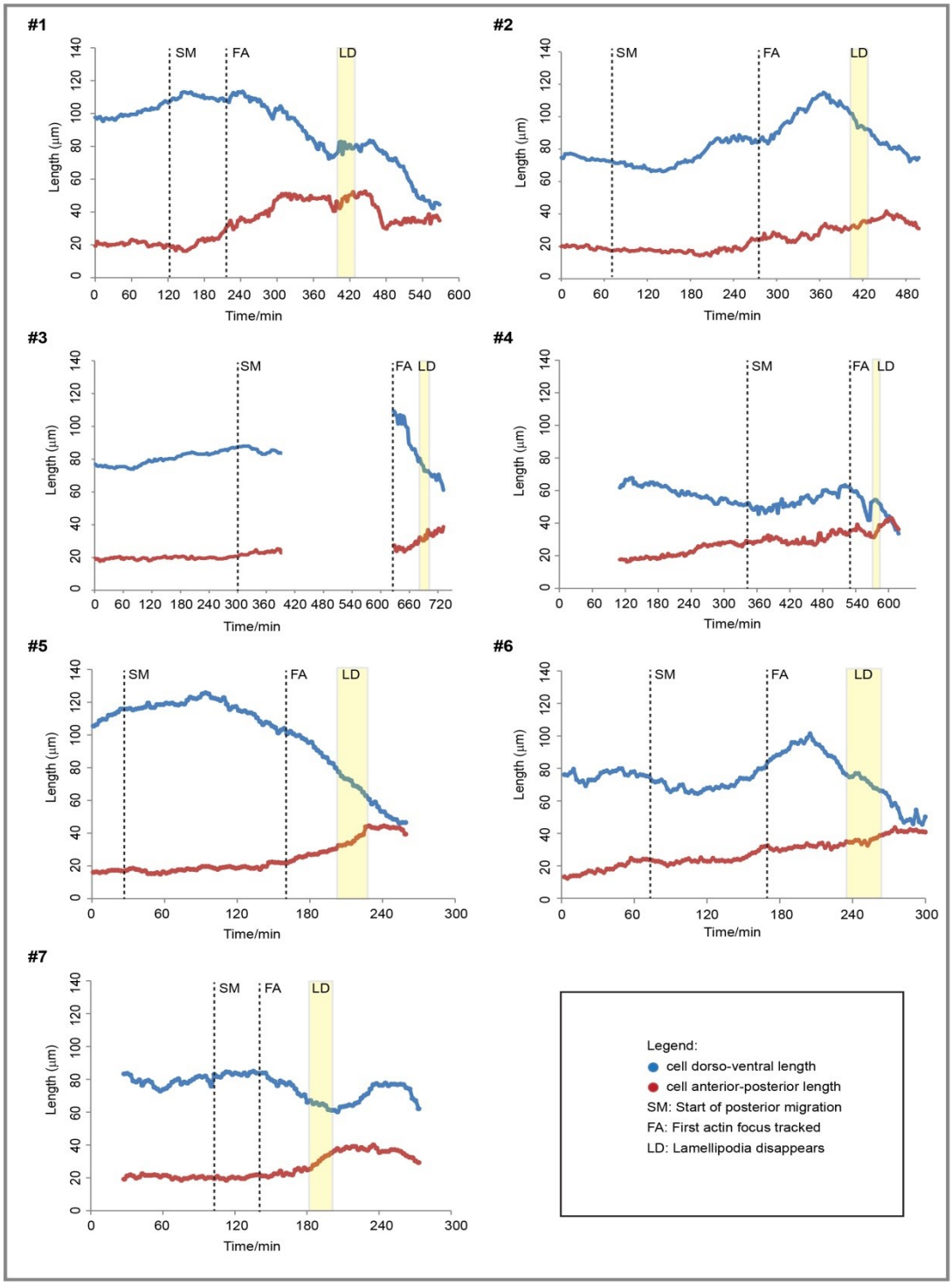

Figure S6. LECs shape changes throughout the different phasesof cell behaviour during abdominal morphogenesis.

Plots of the dorsal-ventral and the anterior-posterior lengths over time for the seven GMA expressing pupae analysed. Each plot includes phase 1, when migration starts, phase 2, when the first actin focus appears and phase 3, after lamellipodium has disappeared. In pupae #3 the analysis is incomplete due to the cell moving out of the field of view of the recording.

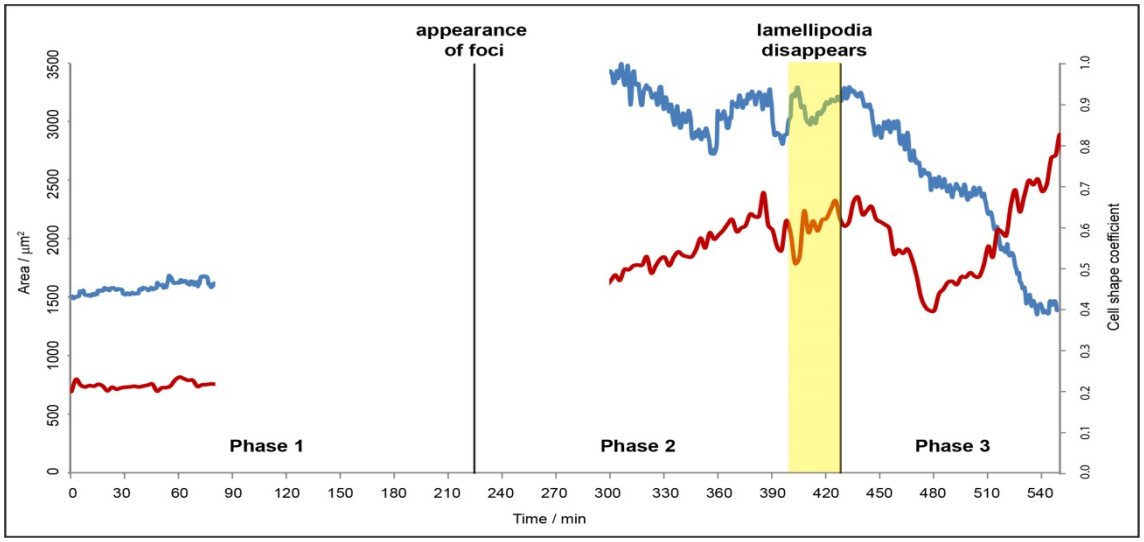

Figure S7. Apical area and cell shape during abdominal morphogenesis of pupa #1

Plot of the cell apical area (blue line) and the cell shape coefficient (red line) over time. The plot is incomplete due to the cell moving out of the field of view of the recording.

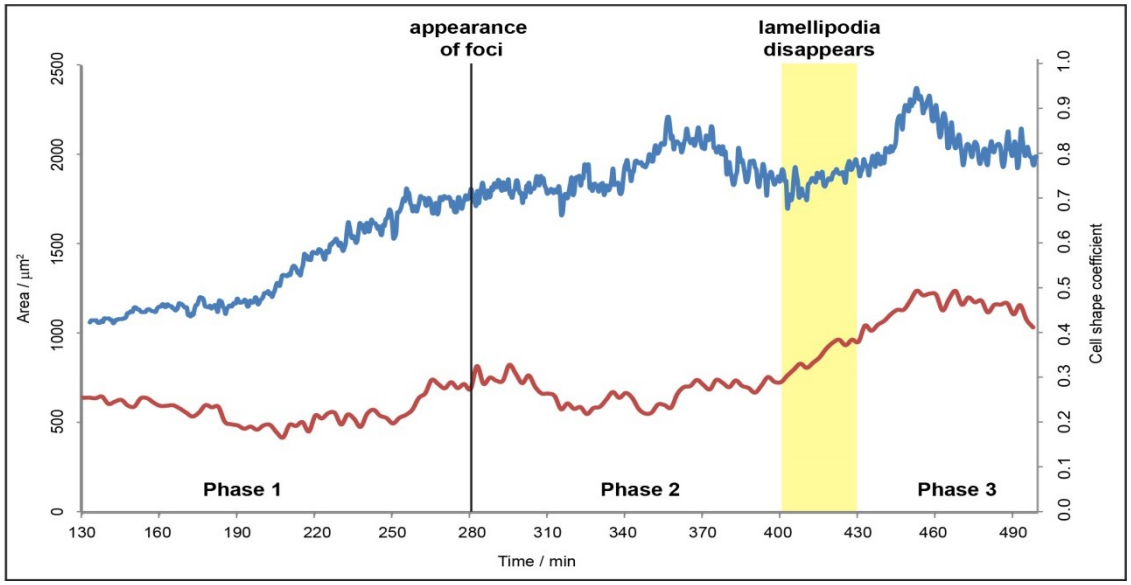

Figure S8. Apical area and cell shape during abdominal morphogenesis of pupa #2

The recording stopped before the cell's transition to apical constriction (blue line).

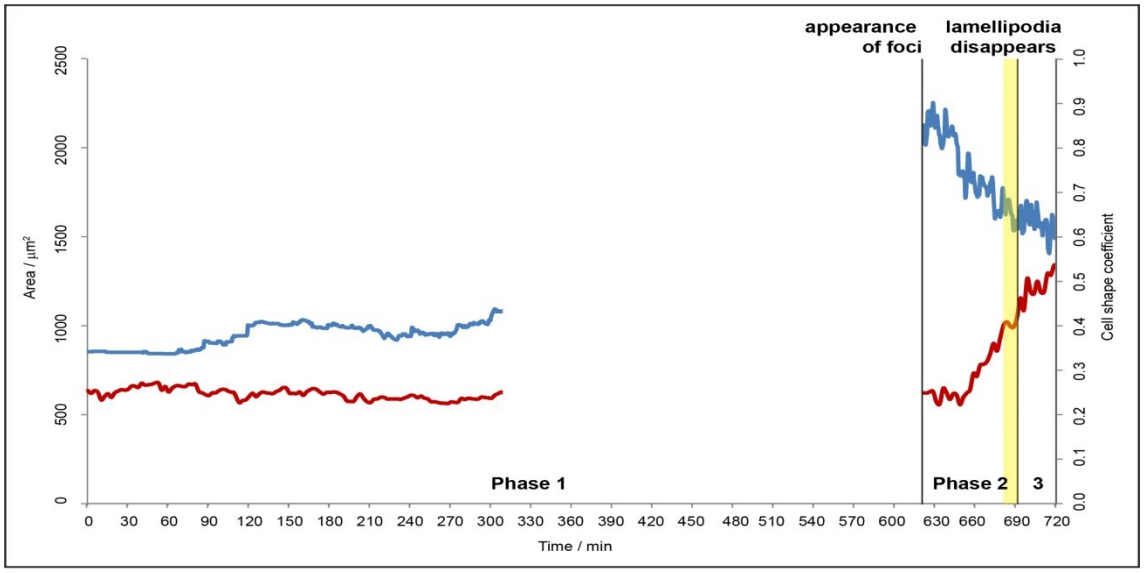

Figure S9. Apical area and cell shape during abdominal morphogenesis of pupa #3

The plot is incomplete due to the cell moving out of the field of view of the recording.

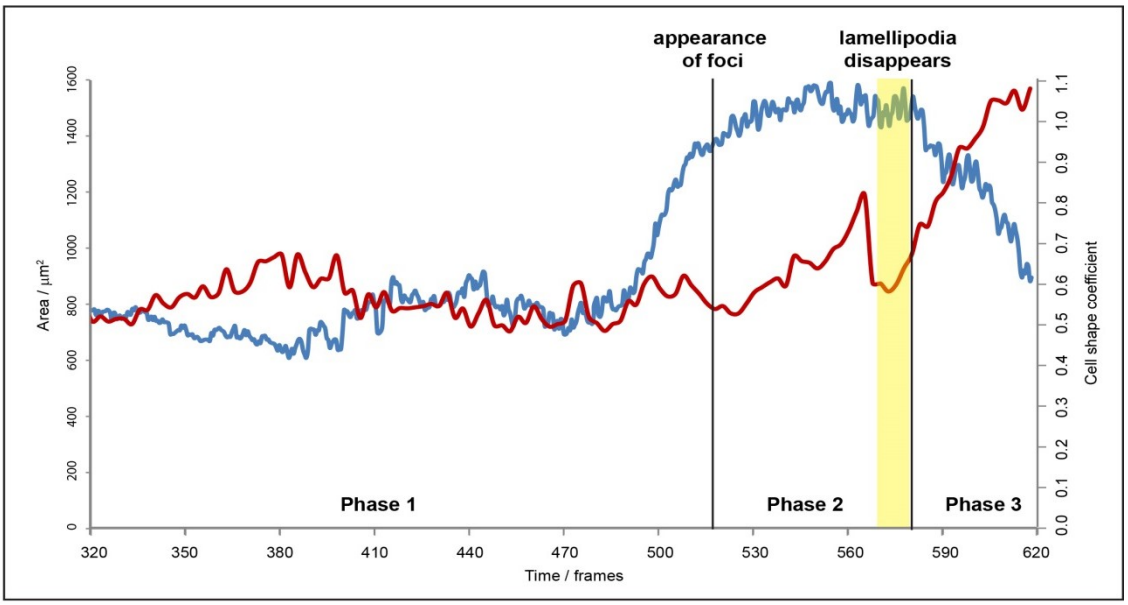

Figure S10. Apical area and cell shape during abdominal morphogenesis of pupa #4

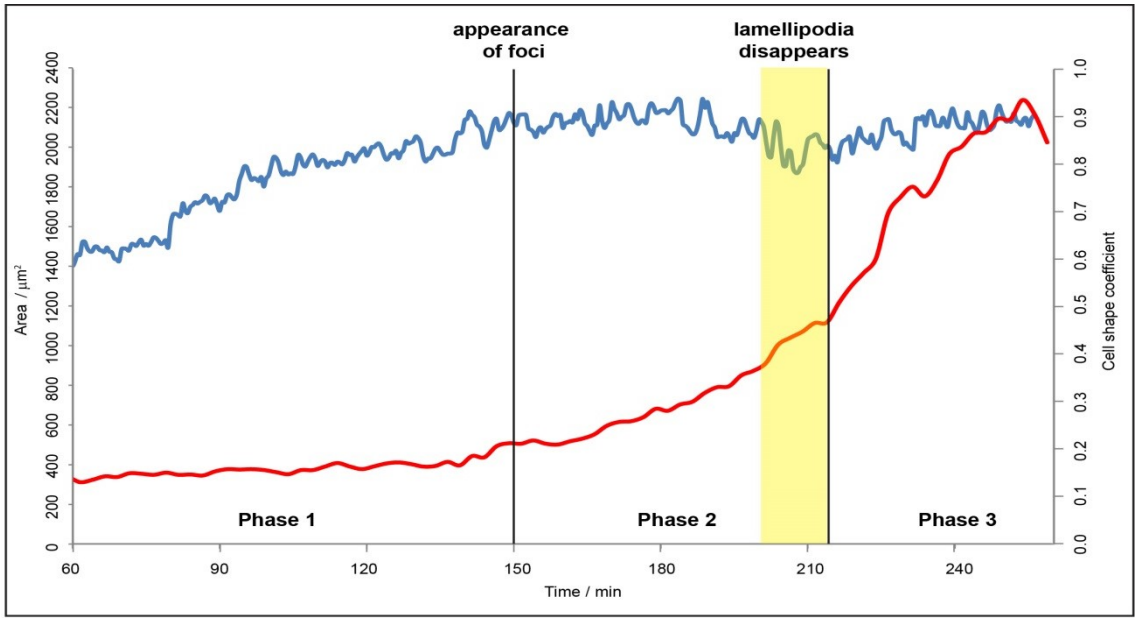

Figure S11. Apical area and cell shape during abdominal morphogenesis of pupa #5

The recording stopped before the cell's transition to apical constriction (blue line).

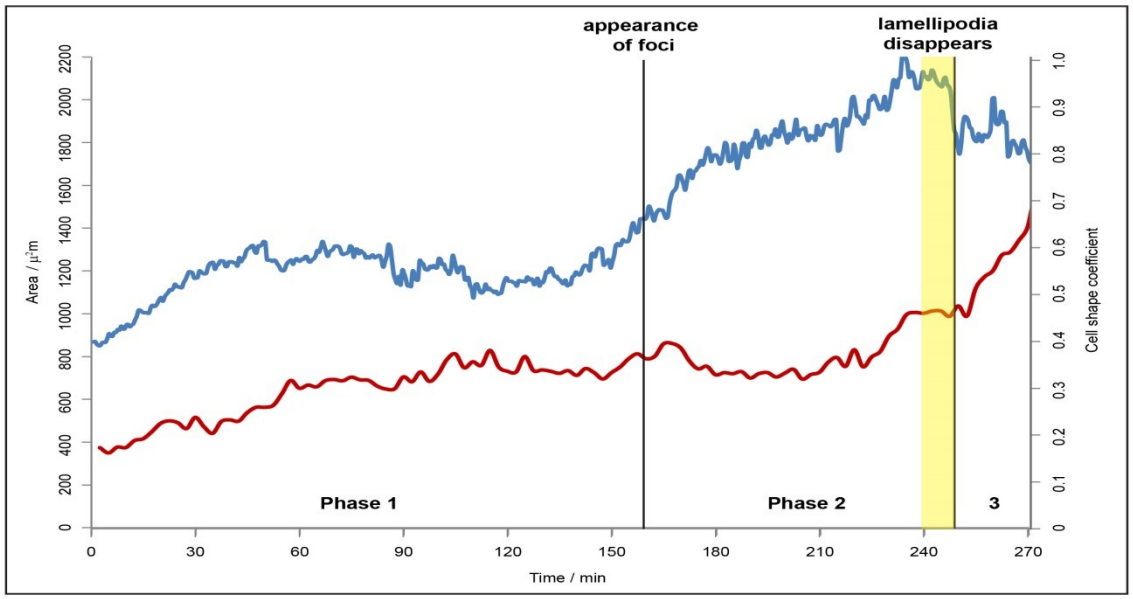

Figure S12. Apical area and cell shape during abdominal morphogenesis of pupa #6

The recording stopped before the cell's transition to apical constriction (blue line).

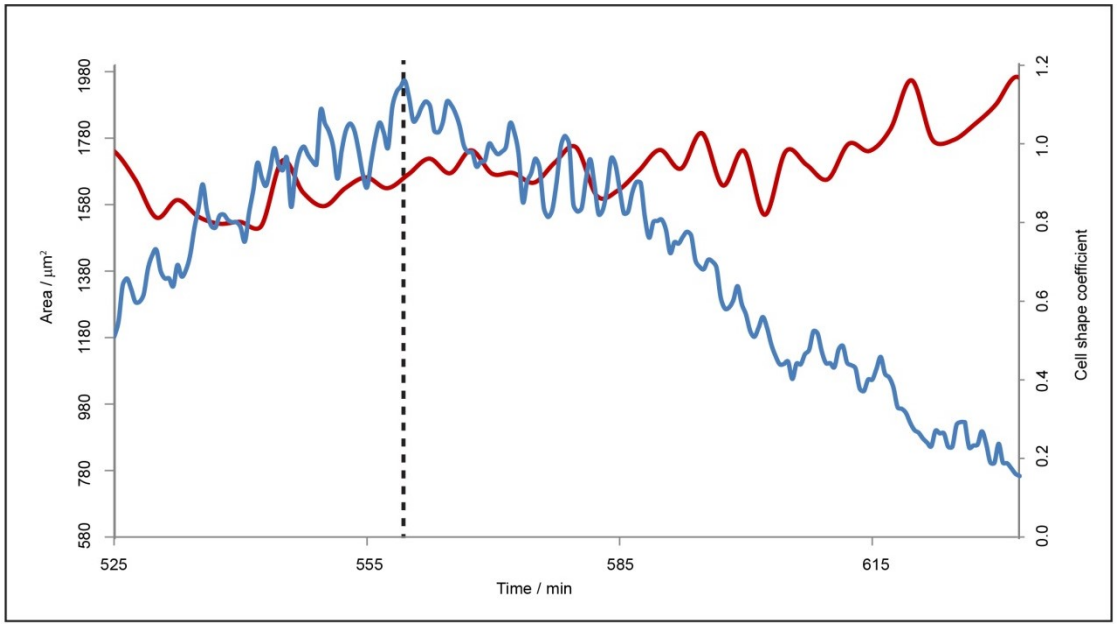

Figure S13. Apical area and cell shape during phase 3 of pupa #20

Plot of the cell apical area (blue line) and the cell shape coefficient (red line) over time of a LEC that was tracked since the start of constriction until delamination. The cell fluctuates maintaining or increasing the net apical. Sometime into phase 3 (dotted vertical line), rapid net apical area reduction begins. The cell is round throughout the whole phase.

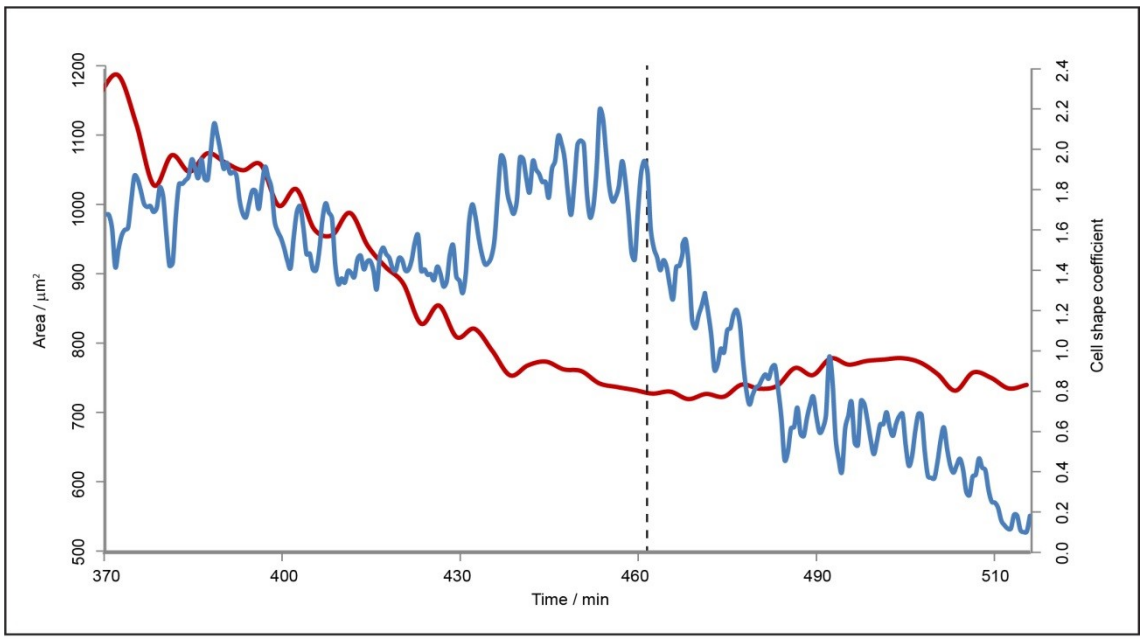

Figure S14. Apical area and cell shape during phase 3 of pupa #23

See legend Figure S13.

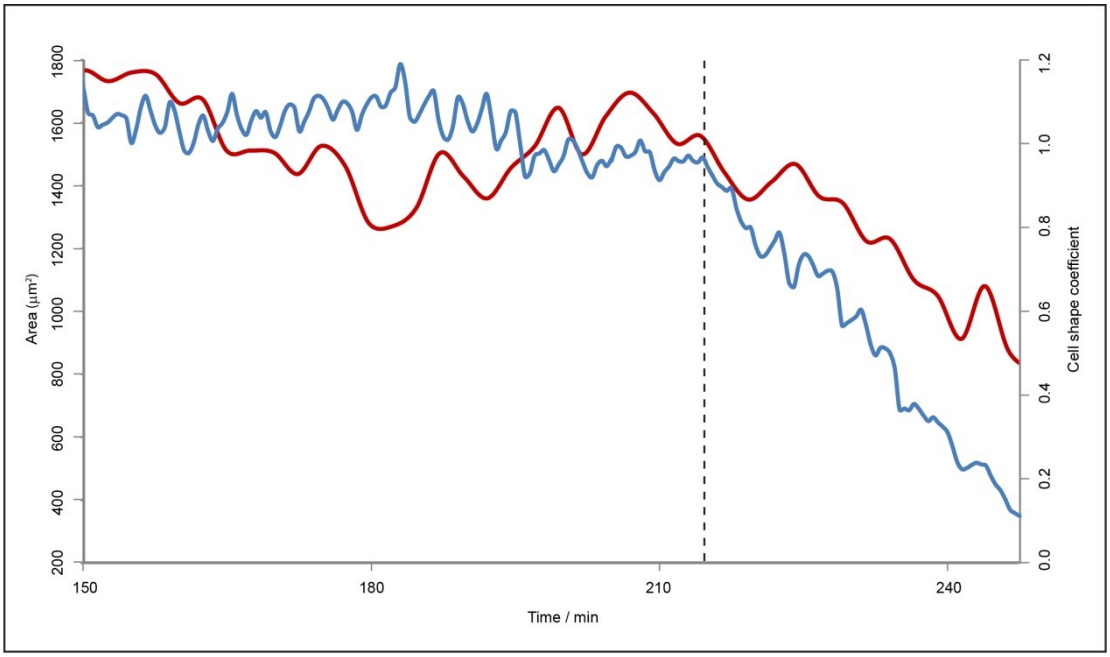

Figure S15. Apical area and cell shape during phase 3 of pupa #24

See legend Figure S13.

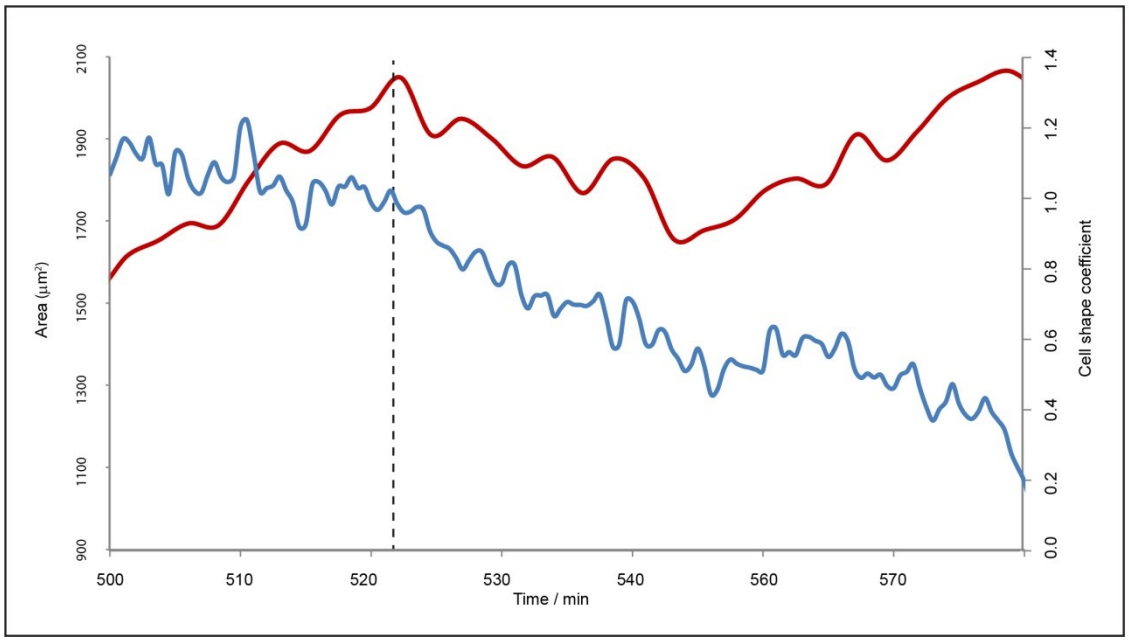

Figure S16. Apical area and cell shape during phase 3 of pupa #25

See legend Figure S13.

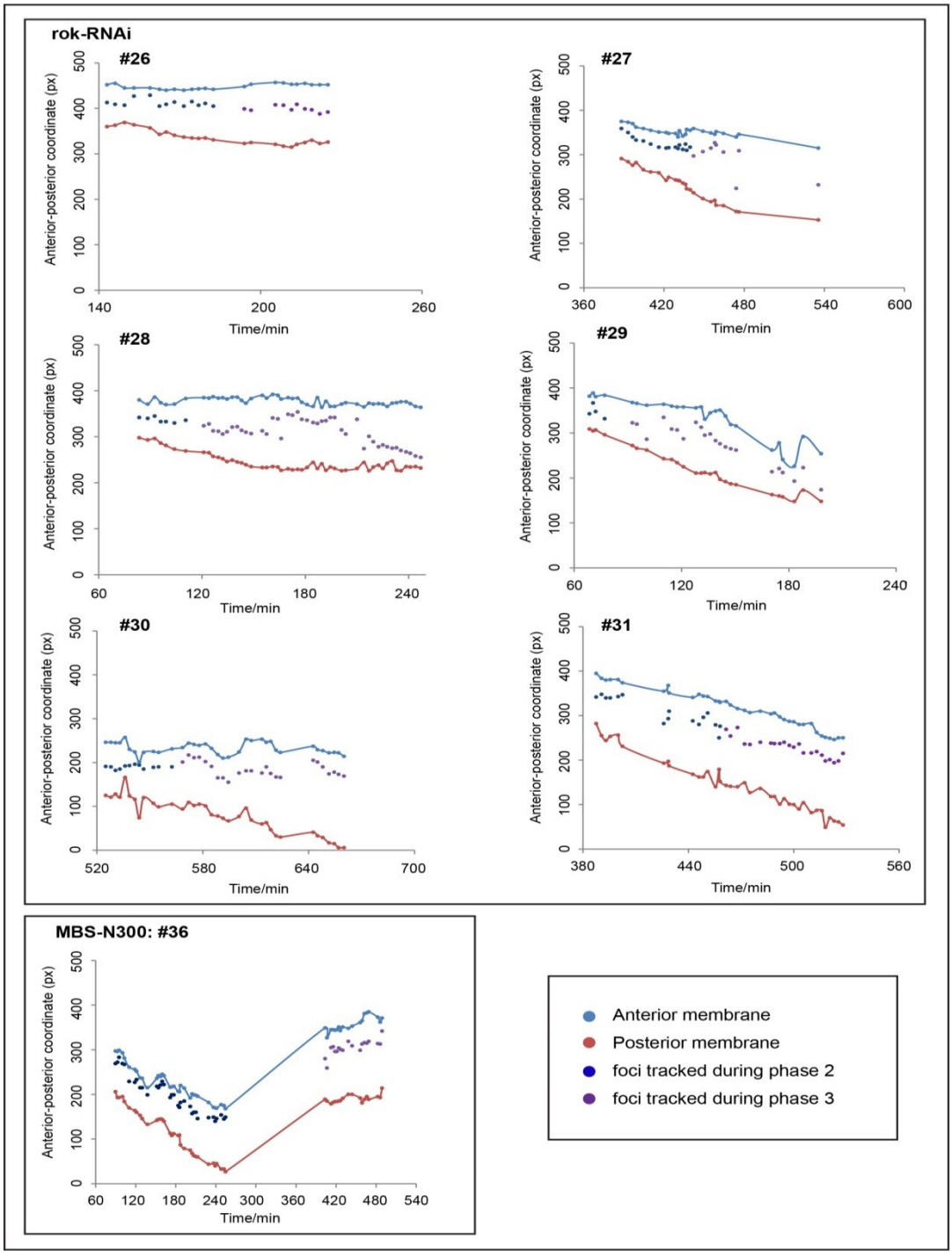

Figure S17. Quantification of the localisation of foci during phase 2 and 3 in LECs expressing Rok-RNAi or MbsN300.

Spatial coordinates of actin foci and anterior and posterior membranes tracked during posterior migration and apical constriction. The anterior and posterior membrane coordinates are tracked in line with where the focus assembles, along the anterior-posterior (AP) axis. In some LECs, the shape of the cell produces that depending on where the two foci assemble, the A-P length can be very different. The time gaps between tracked foci are bits of the recording in which foci could not be tracked.

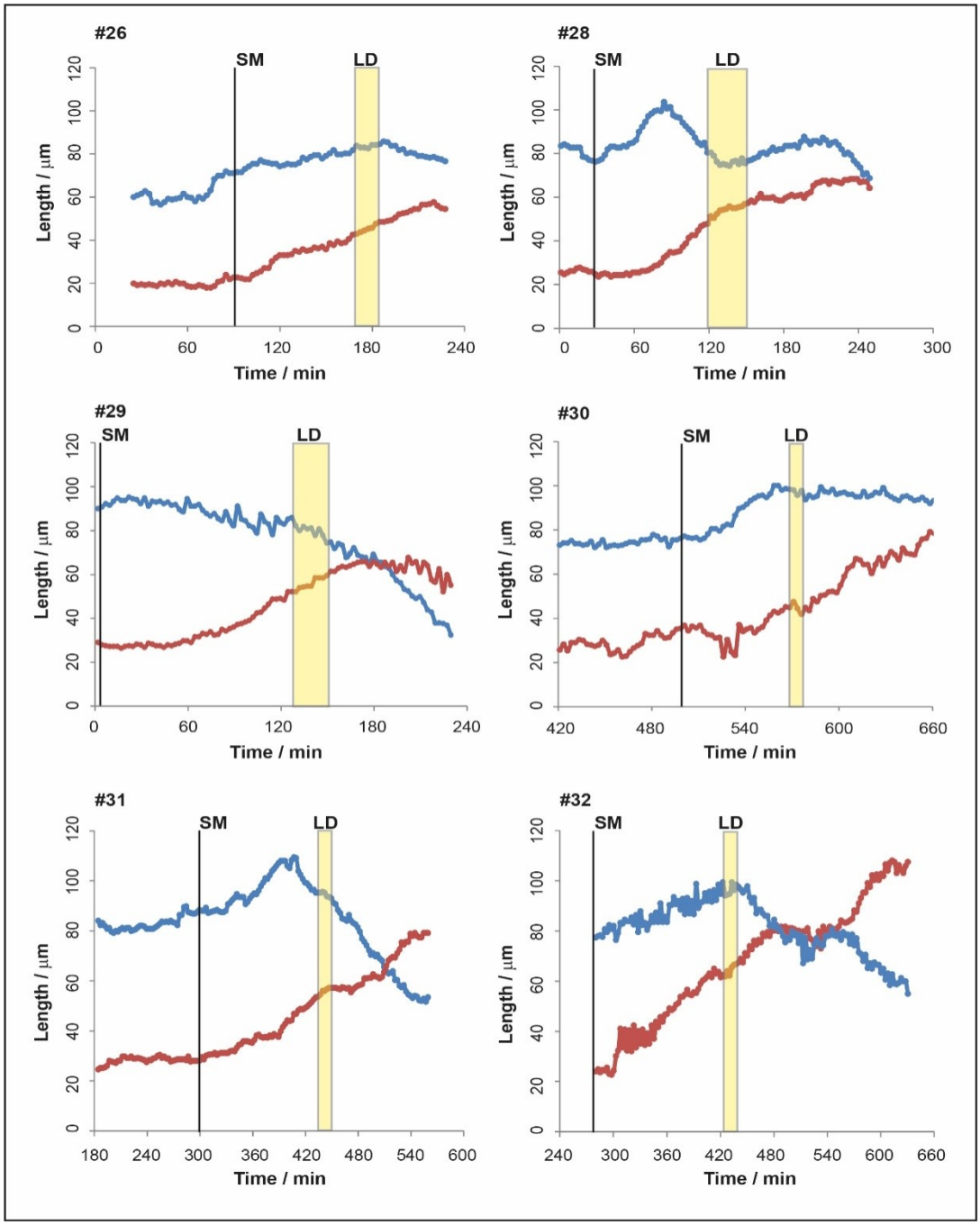

Figure S18. LECs shape changes throughout the different phasesof cell behaviour during abdominal morphogenesis of pupae expressing Rok-RNAi.

Plots of the dorsal-ventral (D-V) (blue line) and the anterior-posterior (A-P) (red line) lengths over time. Each plot indicates the start of posterior migration (SM) and the disappearance of the lamellipodium (LD).

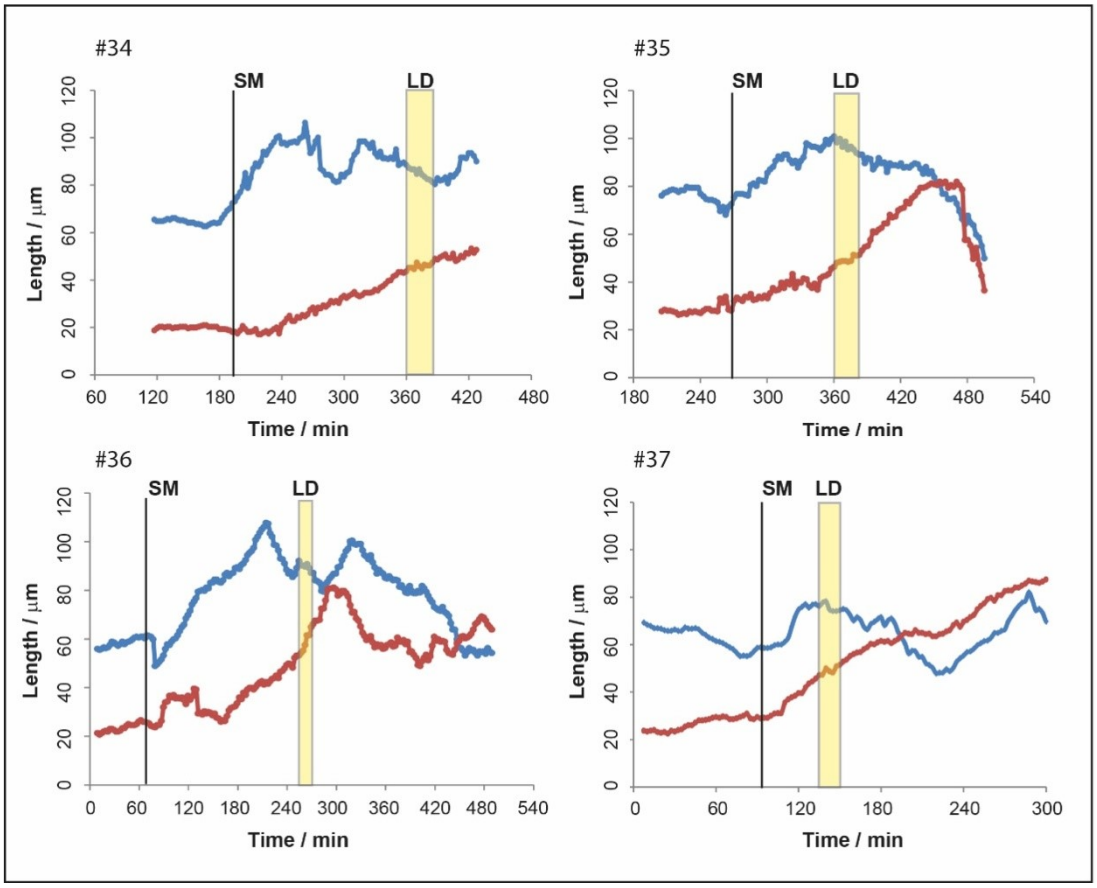

Figure S19. LECs shape changes throughout the different phasesof cell behaviour during abdominal morphogenesis of pupae expressing Mbs-N300.

Plots of the dorsal-ventral (D-V) (blue line) and the anterior-posterior (A-P) (red line) lengths over time. Each plot indicates the start of posterior migration (SM) and the disappearance of the lamellipodium (LD).

9.3 Supplementary tables

GMA

Pupa		Time/min
#1	Formation of the lamellipodia	1-125
	Posterior migration	125-375
	Tracking of the first actin focus	225
	Two foci present at the back of the migrating cell	225-300
	One focus present at the back of the migrating cell	300-375
	Transition of behaviour: lamellipodia disappears	400-430
	Apical constriction	430-650(SD)
	First central focus	430.5
#2	Formation of the lamellipodia	1-75
	Posterior migration	75-430
	Tracking of the first actin focus	283.5
	Two foci present at the back of the migrating cell	283.5-325
	One focus present at the back of the migrating cell	325-400
	Transition of behaviour: lamellipodia disappears	400-430
	Apical constriction	430-500 (ND)
	First central focus	433
#3	Formation of the lamellipodia	1-300
	Posterior migration	300-695
	Tracking of the first actin focus	626.5
	Two foci present at the back of the migrating cell	626.5-680
	One focus present at the back of the migrating cell	680-695
	Transition of behaviour: lamellipodia disappears	685-695
	Apical constriction	695-725 (ND)
	First central focus	697
#4	Formation of the lamellipodia	1-385
	Posterior migration	385-580
	Tracking of the first actin focus	521
	Two foci present at the back of the migrating cell	521-547
	One focus present at the back of the migrating cell	547-580
	Transition of behaviour: lamellipodia disappears	570-580
	Apical constriction	580-665 (SD)
	First central focus	581.5
#5	Formation of the lamellipodia	1-25
	Posterior migration	25-215
	Tracking of the first actin focus	157
	Two foci present at the back of the migrating cell	157-185
	One focus present at the back of the migrating cell	-
	Transition of behaviour: lamellipodia disappears	200-215
	Apical constriction	215-260 (ND)
	First central focus	217
#6	Formation of the lamellipodia	1-75
	Posterior migration	75-250
	Tracking of the first actin focus	168
	Two foci present at the back of the migrating cell	-
	One focus present at the back of the migrating cell	168-235
	Transition of behaviour: lamellipodia disappears	240-250
	Apical constriction	250-335.5 (ND)
	First central focus	252.5
#7	Formation of the lamellipodia	1-100
	Posterior migration	100-180
	Tracking of the first actin focus	135
	Two foci present at the back of the migrating cell	-
	One focus present at the back of the migrating cell	135-160
	Transition of behaviour: lamellipodia disappears	160-180
	Apical constriction	180-330 (SD)
	First central focus	180

Table S1. Table listing all analysed recordings of pupae expressing GMA.

Table showing for each fully analysed recording the important external features used to identify the different phases LECs undergo, the length of posterior migration and apical constriction, the number of foci during posterior migration and the time gap between the last foci observed before the lamellipodium disappears and the first central foci after. In some of the recordings cell delamination was observed (SD) and in some others not (ND) due to the recording settings.

GMA with tub.Gal80ts

Pupa		Time/min
#8	Formation of the lamellipodia	0-225
	Posterior migration	125-347.5
	Tracking of the first actin focus	281
	Two foci present at the back of the migrating cell	281-310
	One focus present at the back of the migrating cell	310-345
	Transition of behaviour: lamellipodia disappears	330-345
	Apical constriction	345-428 (ND)
	First central focus	347.5
#9	Formation of the lamellipodia	0-310
	Posterior migration	310-460
	Tracking of the first actin focus	378.5
	Two foci present at the back of the migrating cell	-
	One focus present at the back of the migrating cell	378.5-452.5
	Transition of behaviour: lamellipodia disappears	450-460
	Apical constriction	460-498 (ND)
	First central focus	460.5
#10	Formation of the lamellipodia	0-100
	Posterior migration	100
	Tracking of the first actin focus	249
	Two foci present at the back of the migrating cell	249-289.5
	One focus present at the back of the migrating cell	290-313
	Transition of behaviour: lamellipodia disappears	300-315
	Apical constriction	315-350 (ND)
	First central focus	319
#11	Formation of the lamellipodia	0-440
	Posterior migration	440-605
	Tracking of the first actin focus	571
	Two foci present at the back of the migrating cell	571-602
	One focus present at the back of the migrating cell	-
	Transition of behaviour: lamellipodia disappears	585-605
	Apical constriction	605-685.5 (ND)
	First central focus	605
#12	Formation of the lamellipodia	0-325
	Posterior migration	325-545
	Tracking of the first actin focus	447
	Two foci present at the back of the migrating cell	-
	One focus present at the back of the migrating cell	447-540.5
	Transition of behaviour: lamellipodia disappears	525-545
	Apical constriction	545-568 (ND)
	First central focus	545.5

Table S2. Table listing all analysed recordings of LECs expressing GMA with *tub.Gal80ts*

Table showing for each fully analysed recording the important external features and length of the different phases LECs undergo. See Table S1.

LifeAct-Ruby with tub.Gal80ts

Pupa		Time/min
#13	Formation of the lamellipodia	0-190
	Posterior migration	190-400
	Tracking of the first actin focus	299.5
	Two foci present at the back of the migrating cell	299.5-341.5
	One focus present at the back of the migrating cell	342-360
	Transition of behaviour: lamellipodia disappears	335-360
	Apical constriction	360-436.5 (ND)
	First central focus	363.5
#14	Formation of the lamellipodia	0-100
	Posterior migration	100-375
	Tracking of the first actin focus	316.5
	Two foci present at the back of the migrating cell	316.5-393.5
	One focus present at the back of the migrating cell	394-405
	Transition of behaviour: lamellipodia disappears	395-405
	Apical constriction	405-429 (ND)
	First central focus	405.5
#15	Formation of the lamellipodia	0-225
	Posterior migration	225-300
	Tracking of the first actin focus	252.5
	Two foci present at the back of the migrating cell	252.5-315
	One focus present at the back of the migrating cell	--(not clear)*
	Transition of behaviour: lamellipodia disappears	300-315
	Apical constriction	315-379 (SD)
	First central focus	318.5
#16	Formation of the lamellipodia	0-5
	Posterior migration	5-90
	Tracking of the first actin focus	41
	Two foci present at the back of the migrating cell	41-85
	One focus present at the back of the migrating cell	--
	Transition of behaviour: lamellipodia disappears	75-90
	Apical constriction	90-137.5 (SD)
	First central focus	95
#17	Formation of the lamellipodia	--
	Posterior migration	0-75
	Tracking of the first actin focus	1.5
	Two foci present at the back of the migrating cell	1.5-25
	One focus present at the back of the migrating cell	25-75
	Transition of behaviour: lamellipodia disappears	60-75
	Apical constriction	75-145.5 (SD)
	First central focus	94.5
#18	Formation of the lamellipodia	--
	Posterior migration	0-225
	Tracking of the first actin focus	146.5
	Two foci present at the back of the migrating cell	146.5-207.5
	One focus present at the back of the migrating cell	208-222.5
	Transition of behaviour: lamellipodia disappears	210-225
	Apical constriction	225-274 (SD)
	First central focus	226.5
#19	Formation of the lamellipodia	--
	Posterior migration	0-50
	Tracking of the first actin focus	1.5
	Two foci present at the back of the migrating cell	1.5-18.5
	One focus present at the back of the migrating cell	19-46
	Transition of behaviour: lamellipodia disappears	40-50
	Apical constriction	50-183
	First central focus	53

Table S3. Table listing all analysed recordings of LECs expressing the LifeAct-Ruby with *tub.Gal80ts*

Table showing for each fully analysed recording the important external features and length of the different phases LECs undergo. See Table S1.

Pupa		Time/min
#20	Phase 3: round cell	400-700 (SD)
	Phase 4: lamellipodia in dorsal direction	550-607.5
#21	Phase 3: round cell	225- 415(SD)
	Phase 4: lamellipodia in dorsal direction	335.5-358
#22	Phase 3: round cell	500-650 (ND)
	Phase 4: lamellipodia in dorsal direction	550-650

Table S4. Table listing all analysed recordings of LECs expressing GMA in which dorsal repolarisation is visible

For each recording, the table specifies the duration of phase 3, from the end of posterior migration until delamination or until the cell drifts out of the plane of focus, and phase 4, during which LECs show a lamellipodium in dorsal direction. In some of the pupae recording I could observe cell delamination (SD) and for others not (ND).

Pupa		Time/min
(#20)	Phase 3 (until delamination)	425-700
	non-ratcheted	425-559.5
	ratcheted	559.5-700
(#23)	Phase 3 (until delamination)	225-550
	non-ratcheted	250-447.5
	ratcheted	447.5-550
(#24)	Phase 3 (until delamination)	125-280
	non-ratcheted	125-214.5
	ratcheted	214.5-280
(#25)	Phase 3 (until delamination)	485-600
	non-ratcheted	485-521.5
	ratcheted	521.5-600

Table S5. Table listing all analysed recordings of LECs expressing GMA in which phase 3 is visible until delamination.

For each recording, the table specifies the duration of phase 3, since the end of posterior migration until the cell delaminates. The table also specifies the duration of the non-ratcheted and ratcheted phases within phase 3.

A. GMA

Pupa	Phase 2: RP mean ± SE	Phase 3: RP mean ± SE	Reproduces the pattern? T-test
#1	0.21 ± 0.01	0.48 ± 0.01	YES. p<0.001
#2	0.25 ± 0.01	0.46 ± 0.02	YES. p<0.001
#3	0.28 ± 0.01	0.50 ± 0.03	YES. p<0.001
#4	0.28 ± 0.01	0.43 ± 0.02	YES. p<0.001
#5	0.34 ± 0.01	0.49 ± 0.02	YES. p<0.001
#6	0.31 ± 0.01	0.45 ± 0.02	YES. p<0.001
#7	0.34 ± 0.01	0.46 ± 0.02	YES. p<0.001

B. GMA with tub.Gal80ts

Pupa	Phase 2: RP mean ± SE	Phase 3: RP mean ± SE	Reproduces the pattern? T-test
#8	0.31±0.04	0.42±0.02	YES. p<0.001
#9	0.34±0.03	0.52±0.02	YES. p<0.001
#10	0.31±0.01	0.44±0.02	YES. p<0.001
#11	0.29±0.03	0.48±0.01	YES. p<0.001
#12	0.32±0.03	0.46±0.01	YES. p<0.001

C. LifeAct-Ruby with tub.Gal80ts

Pupa	Phase 2: RP mean ± SE	Phase 3: RP mean ± SE	Reproduces the pattern? T-test
#13	0.25±0.01	0.43±0.01	YES. p<0.001
#14	0.28±0.01	0.48±0.01	YES. p<0.001
#15	0.34±0.01	0.54±0.01	YES. p<0.001
#16	0.28±0.01	0.46±0.01	YES. p<0.001
#17	0.35±0.01	0.50±0.01	YES. p<0.001
#18	0.22±0.01	0.39±0.01	YES. p<0.001
#19	0.23±0.01	0.44±0.01	YES. p<0.001

D. GMA. Dorsal repolarisation

Pupa	Phase 3: RP mean ± SE	Phase 4: RP mean ± SE	Reproduces the pattern? T-test
#20	0.47±0.02	0.30±0.01	YES. p<0.001
#21	0.50±0.01	0.32±0.01	YES. p<0.001
#22	0.51±0.03	0.30±0.03	YES. p<0.001

Table S6. The difference between the mean relative position of foci of phases 2 and 3 is statistically relevant for all the recordings realised expressing different markers

The first 3 tables (**A,B** and **C**) correspond to the different markers used to study actin dynamics. The tables compare the mean relative position (RP) of foci along the A-P axis during phases 2 and 3 for each individual pupa. The last of the tables (**D**) corresponds to the comparison of the mean RP values of phase 3 and 4 along the D-V axis for the pupae in which dorsal repolarisation is visible. Each table contains the p-value obtained in the T-test to compare means. The difference was found to be statistically significant in all cases.

pupa	Median period medial foci ± SE / seconds	Median period lateral foci ± SE / seconds	Median period central foci ± SE / seconds
#1	180 ± 0.15	180 ± 0.3	180 ± 6.50
#2	165 ± 13.90	180 ± 13.93	180 ± 8.02
#3	140 ± 10.90	140 ± 10.99	225 ± 21.47
#4	180 ± 14.86	180 ± 14.98	210 ± 32.51
#5	180 ± 10.88	180 ± 10.91	180 ± 16.30
#6	150 ± 13.28	-	150 ± 29.19
#7	180 ± 15.16	180 ± 15.19	210 ± 15.09
Combined sample	180 ± 0.85	180 ± 7.91	180 ± 3.25

Table S7. Period of foci during phase 2, treating the medial and lateral foci independently, and during phase 3 for the GMA expressing pupae.

Median period and standard error (SE) for each individual pupa and for the sample combining all. The medial, lateral and central foci are regarded as separate samples. Despite the variability in individual pupae, the periodicity of foci is very constant, assembling on average every 180 seconds.

pupa	Median period medial foci ± SE / seconds	Median period lateral foci ± SE / seconds	Median period central foci ± SE / seconds
#8	150 ± 16.51	-	165 ± 18.68
#9	150 ± 11.08	-	150 ± 14.79
#10	150 ± 22.15	165 ± 51.32	180 ± 11.42
#11	180 ± 26.69	150 ± 18.62	180 ± 5.60
#12	210 ± 33.96	-	180 ± 17.11
Combined sample	150 ± 15.16	150 ± 15.56	180 ± 3.50

Table S8. Period of foci during phase 2, treating the medial and lateral foci independently, and during phase 3 for the pupae expressing GMA with *tub.Gal80ts*.

Median period and standard error (SE) for each individual pupa and for the sample combining all. The medial, lateral and central foci are regarded as separate. Despite the variability in individual pupae, the periodicity of foci is very constant. Considering that the imaging interval is 30 seconds, laterally and medially located foci assemble on average with the same period as phase 3, 180 seconds.

pupa	Median period medial foci ± SE / seconds	Median period lateral foci ± SE / seconds	Median period central foci ± SE / seconds
#13	180 ± 37.61	180 ± 12.78	180 ± 12.63
#14	150 ± 13.37	180 ± 13.07	180 ± 20.50
#15	210 ± 16.08	225 ± 15.79	270 ± 27.77
#16	180 ± 12.50	165 ± 15.86	180 ± 7.33
#17	180 ± 2.98	180 ± 25.74	195 ± 14.40
#18	150 ± 4.26	-	150 ± 19.81
#19	150 ± 37.37	180 ± 10.20	210 ± 11.16
Combined sample	180 ± 2.36	180 ± 4.28	180 ± 3.17

Table S9. Period of foci during phase 2, treating the medial and lateral foci independently, and during phase 3 for the pupae expressing LifeAct-Ruby with *tub.Gal80ts*.

Median period and standard error (SE) for each individual pupae and for the sample combining all.

Phase1		Phase2		Phase3	
D-V length / %	A-P length / %	D-V length / %	A-P length / %	D-V length / %	A-P length / %
10.57 ± 15.55	54.55 ± 51.91	-21.01 ± 15.91	48.08 ± 35.34	-22.40 ± 14.65	-4.51 ± 17.30

Table S10. LECs shape change along the anterior-posterior and dorsal-ventral axes.

Mean percentage of cell shape change along the A-P and D-V axes between the start and end of each phase(N=7).

Phase 4		Delamination	
D-V length / %	A-P length / %	D-V length / %	A-P length / %
-1.42 ± 7.65	2.54 ± 20.05	-32.86 ± 48.90	-46.13 ± 29.74

Table S11. LECs shape change along the anterior-posterior and dorsal-ventral axes during repolarisation and delamination.

Mean percentage of cell shape change along the A-P and D-V axes between the start and end of dorsal repolarisation (phase 4) (N=4).

pupa	Apical area reduction ± SE Phase 1/ μm^2	Apical area reduction ± SE Phase 2/ μm^2	Apical area reduction ± SE Phase 3/ μm^2	Kruskal-Wallis test / p-value
#1	-26.44 ± 7.67	-53.33 ± 7.96	-90.16 ± 18.10	> 0.0001
#2	-14.54 ± 2.61	-57.63 ± 21.27	-92.33 ± 12.25	> 0.0001
#3	-6.90 ± 3.02	-53.52 ± 39.06	-135.15 ± 22.30	> 0.0001
#4	-21.90 ±3.02	-50.08 ± 6.24	-99.78 ± 17.75	> 0.0001
#5	-16.47 ± 2.24	-35.64 ± 11.39	-71.27 ± 7.13	> 0.0001
#6	-20.90 ± 3.80	-51.49 ± 10.89	-61.63 ± 28.07	0.0001
#7	-12.66 ± 2.33	-40.10 ± 7.36	-50.07 ± 8.36	> 0.0001
Average ± SE	-16.80 ± 1.07	-49.37 ± 4.44	-74.46 ± 5.98	> 0.0001

Table S12. Extent of the apical area fluctuations (in μm^2) during phase 1, 2 and 3.

Median apical area reduction per fluctuation, standard error (SE) and analysis of variance comparing all phases for the analysed GMA expressing pupae. All the analysed pupae increase the magnitude of their apical area fluctuations when foci appear (phase 2) and when foci localise central (phase 3).

pupa	Apical area reduction ± SE Phase 1/ %	Apical area reduction ± SE Phase 2/ %	Apical area reduction ± SE Phase 3/ %	Kruskal-Wallis test / p-value
#1	-2.20 ± 0.48	-2.85 ± 0.43	-4.36 ± 0.87	0.0004
#2	-0.88 ± 0.15	-1.78 ± 0.65	-3.27 ± 0.53	> 0.0001
#3	-0.68 ± 0.16	-2.98 ± 1.79	-7.94 ± 1.26	> 0.0001
#4	-2.76 ± 0.37	-3.27 ± 0.37	-8.16 ± 1.22	> 0.0001
#5	-0.91 ± 0.13	-1.66 ± 0.53	-3.45 ± 0.35	> 0.0001
#6	-1.90 ± 0.31	-2.77 ± 0.52	-3.40 ± 1.41	0.08
#7	-1.07 ± 0.19	-2.85 ± 0.50	-3.45 ± 0.50	> 0.0001

Table S13. Extent of apical area fluctuation (in %) during phases 1, 2 and 3 for the analysed pupae expressing the GMA construct.

Median percentage of apical area reduction, standard error (SE) and analysis of variance comparing all phases for the analysed GMA expressing pupae. Most of the cases the Kruskal-Wallis tests indicate differences in the median values, indicating the tendency to increase apical area fluctuations when foci appear (phase 2) and again when foci localise central (phase 3).

	Phase 3	Non-racthet phase 3
Average apical area reduction ± SE / μm^2	-74.46 ± 5.98	-75.76 ± 6.65
Average cell size ± SD / μm^2	1967 ± 642	1501 ± 413
Average apical area reduction ± SE / %	-3.55 ± 0.26	-5.18 ± 0.43

Table S14. Relation between the percentage of apical area reduction per fluctuation and cell size.

The differences in the percentage of apical area reduction between incomplete phase 3 and complete phase 3 (visible until delamination), is due to the differences in cell size and not to the magnitude of apical area fluctuations.

	Number of foci	Total fluctuations / %	s.n.c fluctuations /%	contractile fluctuations / %
Phase 2	No foci	22.40	15.17	7.86
	1 focus	51.36	16.85	35.95
	2 foci	23.50	6.18	15.16
	3 foci	2.18	1.12	1.12
	4 foci	0.55	-	0.55
Phase 3	No foci	22.40	12.8	9.6
	1 focus	73.60	6.4	67.2
	2 foci	4	-	4

Table S15. Number of foci per apical area fluctuation during phases 2 and 3.

Percentage of area fluctuations depending on their correlation with the presence of actin foci. Fluctuations are sorted between short non contractile (s.n.c) and contractile. There are more area fluctuations that coincide with two or more foci during phase 2. During both phases, a great percentage of the fluctuations that do not coincide with foci are short and weak whereas the ones that coincide with foci are mostly longer and stronger.

Pupae		Time/min
#26	Migration	95-185
	Lamellipodia disappears	170-185
	Constriction (and repolarisation)	185-400 (SD)
#27	Migration	350-450
	Lamellipodia disappears	425-450
	Constriction	450-630 (SD)
#28	Migration	25-150
	Lamellipodia disappears	120-150
	Constriction	150-250 (ND)
#29	Migration	0.5-150
	Lamellipodia disappears	130-150
	Constriction	150-265 (SD)
#30	Migration	500-580
	Lamellipodia disappears	570-580
	Constriction	580-700 (ND)
#31	Migration	300-450
	Lamellipodia disappears	430-450
	Constriction	450-610 (SD)
#32	Migration	315-440
	Lamellipodia disappears	420-440
	Constriction	440-630 (ND)
#33	Migration	0.5-80
	Lamellipodia disappears	55-80
	Constriction	80-303.5 (ND)

Table S16. Table listing all analysed recordings of LECs expressing GMA with Rok-RNAi.

Table showing the length of posterior, the timing of the disappearance of the lamellipodium and the length of apical constriction for each analysed recording. Due to the length of the recording, in some of the recordings cell delamination was observed (SD) and in some others not (ND).

Pupae		Time/min
#34	Migration	190-380
	Lamellipodia disappears	365-380
	Constriction (and repolarisation)	380-450 (ND)
#35	Migration	275-385
	Lamellipodia disappears	360-385
	Constriction	385-510 (SD)
#36	Migration	75-275
	Lamellipodia disappears	250-275
	Constriction	275-515 (SD)
#37	Migration	100-150
	Lamellipodia disappears	135-150
	Constriction	150-300 (ND)
#38	already migrating	0.5-125
	Lamellipodia disappears	120-125
	Constriction	125-245 (ND)

Table S17. Table listing all analysed recordingsof LECs expressing GMA with MbsN300.

Table specifying for each recording the length of posterior, the timing of the disappearance of the lamellipodium and the length of apical constriction. In some of the recordings cell delamination was observed (SD) and in some others not (ND).

Pupa	RP mean phase 2 ± SE	RP mean phase 3 ± SE	Reproduces the pattern? P-value
#26	0.34 ± 0.02	0.41 ± 0.02	YES, p=0.02
#27	0.29 ± 0.03	0.32 ± 0.04	NO, p=0.65
#28	0.43 ± 0.07	0.48 ± 0.03	NO, p=0.49
#29	0.46 ± 0.07	0.45 ± 0.03	NO, p=0.88
#30	0.38 ± 0.03	0.28 ± 0.02	INVERTED, p=0.02
#31	0.33 ± 0.02	0.31 ± 0.02	NO, p=0.51
#36	0.23 ± 0.01	0.31 ± 0.01	YES, p=0.0004

Table S18. Relative position of foci during phases 2 and 3 for the Rok-RNAi and MbsN300 pupae

Mean relative position (RP) of foci along the A-P axis during phases 2 and 3 for each individual pupae expressing Rok-RNAi (#26-#31) or Mbs-N300 (#36). The table includes the standard error (SE) for each median. The p-value obtained in the T-test indicates the difference between means and whether the pupae reproduces the pattern of localisation of foci described in wild-type.

Pupae	Median period phase 2 ± SE (seconds)	Number of foci tracked	Median period phase 3 ± SE (seconds)	Number of foci tracked
#28	270 ± 39	6	165 ± 14	42
#26	180 ± 13	12	180 ± 15	9
#29	120 ± 85	3	180 ± 31	20
#31	150 ± 13	16	180 ± 15	21
#27	150 ± 43	16	330 ± 102	7
#30	180 ± 20	11	180 ± 8	22
#36	180 ± 27	32	180 ± 14	16

Table S19. Period of foci during phases 2 and 3 in the Rok-RNAi and MbsN300 expressing pupae

Median period of foci during phase 2 and 3 for each individual pupae expressing Rok-RNAi (#26-#31) or MbsN300 (#36).The table includes the standard error (SE) for each median.

	Migration		Constriction (first 75 min)	
Genotype	DV length difference / %	AP length difference / %	DV length difference / %	AP length difference / %
WT	-9.49 ± 7.96	83.90 ± 17.22	-22.39 ± 7.76	-4.51 ± 9.19
Rok-RNAi	12.64 ± 8.60	120.99 ± 18.60	-27.13 ± 8.37	30.52 ± 9.92
MbsN300	27.73 ± 10.54	111.14 ± 22.79	-20.97 ± 10.26	22.25 ± 12.16

Table S20. Cell length changes along A-P and D-V axes in wild-type and Rok-RNAi/MbsN300

Average percentage and standard deviation of length difference along the A-P and D-V axes in wild-type (N=7), Rok-RNAi (N=6) and MbsN300 (N=4) expressing pupae. During migration, wild-type LECs reduce their length along the D-V whereas Rok-RNAi and MbsN300 LECs do not. Along the A-P, all genotypes behave similarly. During the first 75 min of constriction, wild-type LECs reduce or maintain their length along the A-P axis whereas Rok-RNAi and MbsN300 LECs substantially increase it. Along the D-V axis, all genotypes behave similarly.

Genotype	Area migration (25 min before l.d.) / μm^2	Area constriction (75 min afterl.d.) / μm^2	Area constriction (150 min afterl.d.) / μm^2
WT	1781 ± 141	1521 ± 139	1229 ± 161
Rok-RNAi	3005 ± 234	2874± 230	3367± 261
MbsN300	2713 ± 275	3874 ± 271	3960 ± 332

Table S21. Cell length changes along A-P and D-V axes in wild-type and Rok-RNAi/MbsN300

Average value and standard deviation of LEC size in wild-type (N=14), Rok-RNAi (N=8) and MbsN300 (N=5) expressing pupae measured during migration, 75 min after the lamellipodium has disappeared (l.d) and 150 min after l.d, close to delamination. The area in wild-type decreases over time. In Rok-RNAi and MbsN300 LECs are significantly larger and the area is maintained or increased over the same time window.

		Migration (25 min before lamellipodia disappearance)		Constriction (75 min after lamellipodia disappearance)	
Genotype	Pupae	Reduction in cell area/ μm^2	Reduction in cell area/ %	Reduction in cell area/ μm^2	Reduction in cell area/ %
Wild-type	#1	-96.53 ± 28.03	-3.15 ± 0.80	-101.322 ± 23.26	-3.45 ± 0.83
	#2	-52.20 ± 17.66	-2.54 ± 0.80	-140.328 ± 22.59	-6.05 ± 1.01
	#6	-18.66 ± 6.74	-1.50 ± 0.50	-74.2775 ± 10.25	-3.73 ± 0.50
	#7	-48.54 ± 11.61	-3.50 ± 0.83	-82.941 ± 22.34	-6.16 ± 1.56
Rok-RNAi	#28	-19.18 ± 9.03	-0.75 ± 0.34	-27.13 ± 8.37	-0.96 ± 0.43
	#26	-6.26 ± 2.65	-0.28 ± 0.12	-20.97 ± 10.26	-0.73 ± 0.17
	#29	-13.33 ± 7.32	-0.67 ± 0.72	-34.92 ± 15.78	-1.84 ± 0.38
	#33	-18.88 ± 8.28	-0.50 ± 0.22	-25.53 ± 5.98	-1.18 ± 0.35
	#31	-25.16 ± 15.12	-0.81 ± 0.27	-45.74 ± 9.35	-0.45 ± 0.21
MbsN300	#34	-9.21 ± 3.96	-0.33 ± 0.17	-35.24 ± 10.04	-0.57 ± 0.22
	#36	-34.90 ± 12.12	-1.24 ± 0.40	-17.80 ± 7.93	-0.72 ± 0.12
	#37	-13.49 ± 4.68	-0.81 ± 0.24	-18.43 ± 7.14	-0.96 ± 0.54
	#38	-5.33 ± 4.15	-0.14 ± 0.12	-33.13 ± 6.11	-0.62 ± 0.21

Table S22. Extent of area reduction per fluctuation in wild-type, Rok-RNAi and MbsN300 expressing pupae

Apical area that cells reduce per fluctuation (in μm^2) and the percentage of cell area it represents during migration and constriction. In Rok-RNAi and MbsN300 pupae, the absence or mislocalisation of produce in general smaller apical area fluctuations compared to wild-type.

10. Supplementary movies

To notice all the details in the complex movies please use the arrow keys to play the movies. In all movies, anterior is to the left. Scale bars are indicated.

Movie S1. LEC expressing GMA recorded during phase 1, the start of posterior migration. While migrating, the apical actin cytoskeleton starts flickering with no apparent specific pattern. Frame from this movie shown in Figure 16A.

Movie S2. LECs expressing GMA recorded during phase 2, while still migrating posteriorly. GMA-labelled filaments periodically coalesce at specific foci (red dots) that localise to the back of the moving cell, closer to the anterior membrane. Actin also flows either from lateral to medial, or vice-versa, between the two assembling foci. Frames from this movie shown in Figure 16A, C.

Movie S3. LECs expressing GMA recorded during late phase 2. At the end of the posterior migration the flowing pattern changes and actin flows from lateral and medial regions of the cell towards a single actin focus (red dot) which still localises close to the anterior membrane. Frames from this movie shown in Figure 16D.

Movie S4. LECs expressing GMA recorded during phase 3, after the lamellipodium has disappeared. Actin flows from the cell periphery towards a single focus (red dot), localising to the centre of the cell. Frames from this movie shown in Figure 16E.

Movie S5. LEC expressing GMA recorded during phase 4. LECs are being approached by the histoblasts. LECs repolarize and actin foci localise closer to new back of the cell (i.e. their ventral membrane). Frames from this movie shown in Figure 16A.

Movie S6. LEC expressing GMA and Rok-RNAi recorded during apical constriction. This cell presents a weak phenotype, with foci assembling close to the membranes (red dots), in contrast wild-type centrally localised foci during constriction.

Movie S7. LEC expressing GMA and MbsN300 recorded during apical constriction. This cell presents a weak phenotype, with foci forming close to the membranes (red dots).

Movie S8. LECs expressing GMA and MbsN300 recorded during apical constriction. These LECs present a strong phenotype, with no foci being formed on their medio-apical side.

Movie S9. LEC expressing GMA and Rok-RNAi. During posterior migration, in the region of the neighbour, which is below the lamellipodium, periodic flows of actin are observed (red arrow).

Movie S10. LEC expressing GMA and MbsN300 recorded during posterior migration, flows of actin below the lamellipodium are observed (red arrow).